

Università degli Studi di Salerno
Department of Chemistry and Biology
Ph.D. in Chemistry

**Olefin Metathesis Reactions Promoted by Ru-Catalysts with
a *Syn* Substituted N-heterocyclic Carbene Backbone**



Supervisor:
Prof. P. Longo

PhD student:
Alessandra Perfetto
Matr: 8880700107

Co-tutor:
Dott. F. Grisi

Coordinator:
Prof. G. Guerra

Intern supervisor:
Prof. A. Spinella

External supervisors:
Dott. M. Scalone (F. Hoffmann-La Roche Ltd, Basel)
Prof. G. Paolucci (University of Venice)

XII cycle **Years 2011-2014**

*A noi due,
alla famiglia che formeremo
in Gesù Cristo*

*.....sono debitore al mio mestiere anche
di ciò che fa maturo l'uomo:
il successo e l'insuccesso,
riuscire e non riuscire,
le due esperienze della
vita adulta necessarie per crescere.
Per il chimico che lavora in laboratorio
ci vogliono tutte e due;
il chimico militante le conosce entrambe:
sbagliare e correggersi,
incassare colpi e renderli,
affrontare un problema e risolverlo
oppure uscirne sconfitto
e subito ricominciare la battaglia...*

Primo Levi

List of abbreviation

RCM= Ring Closing Metathesis

CM= Cross Metathesis

ROMP= Ring Opening Metathesis Polymerization

Et₂O= diethyl ether

DCM= dichloromethane

DEDAM= diethyldiallyl malonate

NHC= *N*-heterocycle carbene

COD= 1,5-cyclooctadiene

DMCOD= 1,5-dimethyl-1,5-cyclooctadiene

Ewg= electron withdrawing group

Edg= electron donating group

IR= Infra red

TCDE = C₂D₂Cl₄ tetra chloro ethane

FeMe₈= octamethylferrocene

SAR= structure-activity relationship

N₂= nitrogen

Ar= Argon

Abstract

The development of efficient catalytic systems dedicated to the formation of C–C double bonds from simple to highly functionalized alkenes represents a great challenge in modern organic synthesis. In addressing this challenge, olefin metathesis has become an extremely versatile tool¹ simplifying synthetic routes to numerous and valuable natural and unnatural products dramatically.² Breakthroughs made in the last two decades have applied mechanistic understanding in the design of innovative and well-defined homogeneous pre-catalysts, increasing the appeal of this highly atom efficient reaction methodology.

Ruthenium based metathesis catalysts have received considerable attention because of their tolerance to oxygen, moisture and many functional group, but even more because it is possible to control catalyst activity by fine tuning of the steric and electronic properties of the ligands.¹

Major improvements in Ru-based pre-catalysts were achieved through the incorporation of *N*-heterocyclic carbene (NHC) as ancillary ligand. In general, *N*-aryl bulk was found to increase activity, whereas increased backbone substitution decreased activity but increased catalyst lifetime.³ The development of this class of complexes has broadened the scope and the utility of the olefin metathesis reaction in both organic synthesis and polymer science.

The research group in which I developed my PhD thesis, recently focused on the investigation of NHC ligand symmetry in ruthenium based complexes underlining the pivotal role played by NHC backbone substitution in the design of highly active pre-catalyst for the RCM of hindered di-olefins.⁴

¹ Selected reviews on olefin metathesis: (a) Handbook of Metathesis; Grubbs, R. H., Ed.; Wiley-VCH: Weinheim, Germany, **2003**; Vol. 1–3. (b) Vougioukalakis, G. C.; Grubbs, R. H. *Chem. Rev.* **2010**, *110*, 1746. (c) Kotha, S.; Dipak, M. K. *Tetrahedron* **2012**, *68*, 397.

² For recent reviews on olefin metathesis in total synthesis, see: Furstner, A. *Chem. Commun.* **2011**, *47*, 6505.

³ Chung, C. K.; R. H. Grubbs *Organic Letters* **2008**, *10*, 2693.

⁴ Costabile, C; Mariconda, A.; Cavallo, L.; Longo, P.; Bertolasi, V.; Ragone, F.; and Grisi, F.; *Chemistry a European Journal*, **2011**, *31*, 8618

This thesis was aimed to furnish a deeper understanding of the effect of *syn* backbone substitution on catalyst activity by creating a properly designed catalyst library. In particular, besides testing their activity toward many different metathesis reactions, we performed conformational studies of these newly synthesized complexes (via NMR and DFT calculations).

Chapter one presents a brief introduction on the topic.

Chapter two is aimed at providing an overview focused on the advantage of using *N*-heterocyclic carbene as ligands for ruthenium complexes.

In **chapter three**, a series of ruthenium olefin metathesis catalysts bearing *N*-heterocyclic carbene (NHC) ligands with varying degrees of backbone and *N*-aryl substitution were prepared and fully characterized.

In **chapter four** the catalytic behaviour of these newly synthesized complexes was explored toward the ring closure of standard di-olefins to gain five and fourteen membered rings.

In **chapter five** we extended the scope of the best performing catalysts (identified through the RCM studies of Chapter 4) to other classes of metathesis reactions like ring opening metathesis polymerization and cross metathesis.

Finally in **chapter six** the comparison of the electrochemical behaviour of the complexes developed in our group and the commercially available ones is reported.

Index

Chapter 1.....	1
<i>Introduction to olefin metathesis: Ruthenium</i>	
<i>Catalyst development.....</i>	1
Importance & basic concepts.....	1
Brief history toward the design of commercially available Ruthenium complexes.....	3
Chapter 2.....	15
<i>Ligand substituent effects on ruthenium based complexes</i>	15
Introduction	15
Insight on metathesis mechanism and catalyst decomposition pathways.....	16
Key aspect of catalytic activity comparison.....	17
Our interest	19
Symmetrically 1, 3-disubstituted imidazol and imidazolin 2-ylidene ligand	19
Asymmetrically 1, 3-disubstituted imidazol and imidazolin 2-ylidene ligand	31
Chapter 3.....	37
<i>Synthesis of new Ruthenium based catalysts with a Syn Substituted N-heterocyclic Carbene Backbone</i>	37
Abstract.....	37
Introduction	37
Modification of NHC backbone	39
Introduction.....	39
Synthetic strategy toward complexes 74 and 77	40
Solution Structure studies.....	44

Computational studies	54
2D NMR studies	56
Modification of NHC backbone and <i>N</i> -aryl substituents.....	57
Introduction	57
Synthetic strategy toward complexes 76 and 77	57
Solution Structure studies	58
Modification of NHC backbone and <i>N</i> -aryl substituents.....	61
Introduction	61
Synthetic strategy toward complexes 78 and 79	61
Solution Structure studies	63
Conclusion.....	65
Experimental Procedure	66
Synthesis.....	67
Determination of the thermodynamic parameters for the equilibrium between the major and minor forms of anti-75 (75B-75C).....	102
2D EXSY determination of exchange rate constant between 8B and 8C isomers.....	103
Crystal structure details	105
Chapter 4.....	115
<i>Screening of new Ru-Based catalysts in ring closing metathesis</i>	115
Abstract.....	115
Introduction.....	115
Results and discussion.....	117
RCM standard tests on malonate derivatives.....	117
RCM standard tests on <i>N</i> -tosyl ammine derivatives...	130
RCM of \pm Linalool (g).....	137
RCM of 4-(allyloxy)-4,4-diphenylbut-1-yne (h).....	149
RCM of toward macrocycles with different steric hindrance.....	152

Conclusion.....	156
Experimental Procedures	157
Chapter 5.....	161
<i>Screening of selected new Ru-Based catalysts in ring opening metathesis polymerization and cross metathesis.....</i>	161
Abstract	161
Ring opening metathesis polymerization.....	161
Cross metathesis	172
Experimental procedures	176
Chapter 6.....	179
<i>Electrochemical behavior of II Generation Grubbs and Grubbs Hoveyda type complexes.....</i>	179
Abstract.....	179
Introduction.....	179
Results and discussion.....	189
Experimental Procedures.....	199

Chapter 1

Introduction to olefin metathesis: ruthenium catalyst development.

Importance & basic concepts

Olefin metathesis is one of the most versatile methods for forming carbon–carbon bonds; its applications range from natural product and pharmaceutical synthesis, to polymers and materials.¹

The name metathesis (from the Greek word “μεταθεση” which means change of position) was given for the first time to this reaction by Calderon in 1967² just few years after the first observation of metathesis phenomena (mid 1950s).³ A widely accepted idea is that metathesis revolutionized synthetic chemistry⁴ attracting a vast amount of interest both in academia and in industry⁵.

The olefin metathesis established mechanism was originally proposed by Chauvin and Hérisson in 1970.⁶ According to this mechanism, this metal catalyzed transformation proceeds through metallacyclobutane intermediates, generated by the coordination of the olefin(s) to a metal alkylidene, via a series of alternating [2 + 2]-cycloadditions and cycloreversions¹ (Scheme 1. 1).

¹ Grubbs, R. H. *Handbook of Metathesis*; Wiley-VCH: Weinheim, Germany, **2003**

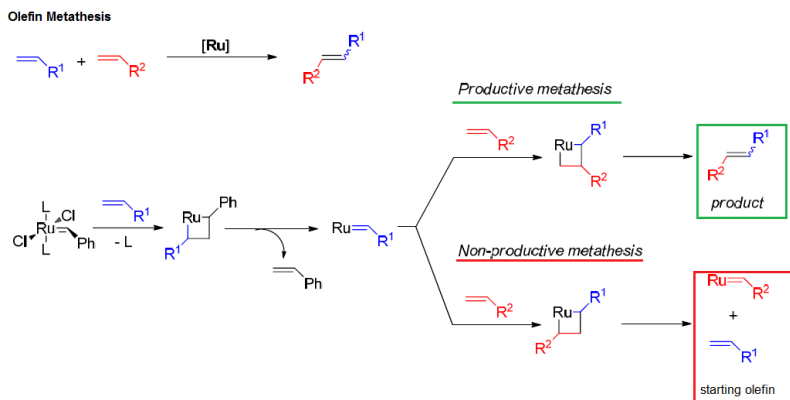
² (a) Calderon, N.; Chem, H. Y.; Scott, K. W. *Tetrahedron Lett.* **1967**, *34*, 3327. (b) Calderon, N. *Acc. Chem. Res.* **1972**, *5*, 127.

³ (a) Anderson, A. W.; Merckling, N. G. (Du Pont de Nemours & Co.) U.S. Patent 2,721,189, 1955. Also see: (b) Truett, W. L.; Johnson, D. R.; Robinson, I. M.; Montague, B. A. *J. Am. Chem. Soc.* **1960**, *82*, 2337.

⁴ For the 2005 Nobel Prize in Chemistry Lectures, see: (a) Chauvin, Y. *Angew. Chem., Int. Ed.* **2006**, *45*, 3740. (b) Schrock, R. R. *Angew. Chem., Int. Ed.* **2006**, *45*, 3748. (c) Grubbs, R. H. *Angew. Chem., Int. Ed.* **2006**, *45*, 3760.

⁵ Ivin, K. J.; Mol, J. C. *Olefin Metathesis and Metathesis Polymerization*; Academic Press: San Diego, CA, 1997.

⁶ Hérisson, J.-L.; Chauvin, Y. *Makromol. Chem.* **1971**, *141*, 161.



Scheme 1. 1: olefin metathesis mechanism

Since the metathetical cycle is based on reversible individual steps an equilibrium mixture of olefins is obtained. For the metathesis to be productive and useful, it is necessary to shift the equilibrium in one direction.

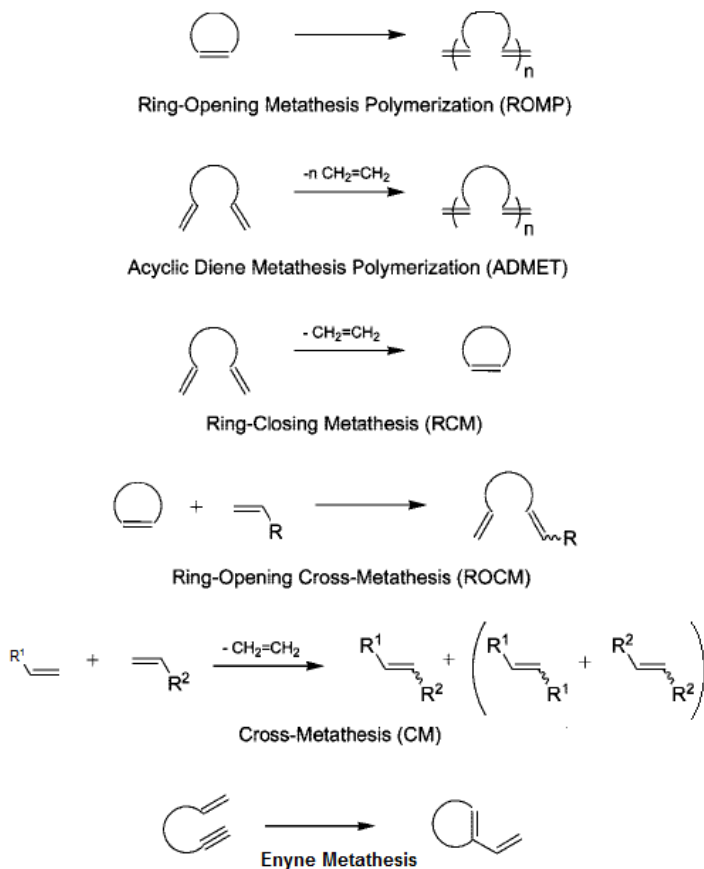
For this reason most of the consolidated protocols exploit a driving force, such as the formation of ethylene or the release of ring strain, to favour the formation of a single product.⁷

As illustrated in Scheme 1. 2 metathesis transformations can be categorized by the starting material and the outcome of the reaction.

- Ring Closing Metathesis: consists in the cyclization of α - ω di-olefins with concomitant elimination of gaseous alkenes;
- Acyclic Diene Metathesis polymerization: provides the polymerization of terminal dienes.
- Enyne Metathesis: involves reaction between the unsaturated bonds of an alkene and an alkyne;
- Cross Metathesis: provides the synthesis of new E/Z alkenes by mutual exchange of alkylidene groups between two different alkenes.
- Ring Opening Metathesis Polymerization: it is a chain growth polymerization whose driving force comes from the opening of a strained cycle.

⁷ Wiberg, K. B. *Angew. Chem., Int. Ed. Engl.* **1986**, 25, 312.

- Ring Opening Cross Metathesis: it is a class of cross metathesis which also provides a ring opening metathesis event, since one the of its substrate is a cyclic alkene.



Scheme 1. 2: types of metathesis transformations

Brief history toward the design of commercially available ruthenium complexes

The first metathesis reactions were catalyzed by ill-defined, multi component systems consisting of transition-metal halides and main group co-catalysts such as $WCl_6/EtAlCl_2$, $WCl_6/BuSn_4$, or metals on solid supports, such as MoO_3/SiO_2 .^{1,3}

The use of these systems was anyway limited just to organic synthesis mainly because of the harsh conditions required and the long initiation period.

The isolation of the first well-defined metal carbene complexes in the 1970s gave rise to great advances in catalyst design, leading to titanium,⁸ tungsten,⁹ molybdenum¹⁰ complexes. Among them, the molybdenum based ones resulted the most active; nevertheless their poor stability rendered them difficult to use in many cases¹¹

Many of these stability problems (moisture, oxygen and functional group sensitivity) were overcome by the development of ruthenium based systems in late 1980.^{4c,11,12}

It is worth to note that ruthenium based complexes took long to come “*in auge*” for metathesis applications if we consider that the use of $\text{RuCl}_3(\text{H}_2\text{O})_n$ in ROMP reactions was known since 1960.¹³

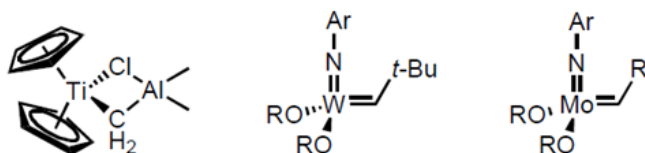


Figure 1. 1: Well defined transition metal olefin metathesis catalyst

For the sake of completeness, in Figure 1. 1 well defined catalysts for olefin metathesis based on different transition metals are reported. This thesis will deal just with ruthenium based systems.

⁸(a) Tebbe, F. N.; Parshall, G. W.; Reddy, G. S. *J. Am. Chem. Soc.* **1978**, *100*, 3611.

(b) Tebbe, F. N.; Parshall, G. W.; Ovenall, D. W. *J. Am. Chem. Soc.*, **9** **1979**, *101*, 5074.

⁹(a) Quignard, F.; Leconte, M.; Basset, J. M. *J. Mol. Catal.* **1986**, *36*, 13. (b) Wengrovius, J. H.; Schrock, R. R.; Churchill, M. R.; Missert, J. R.; Youngs, W. J. *J. Am. Chem. Soc.* **1980**, *102*, 4515. (c) Kress, J. R. M.; Russell, M. J. M.; Wesolek, M. G.; Osborn, B. P. *J. Chem. Soc., Chem. Commun.* **1980**, 431. (d) Schrock, R. R.; DePue, R. T.; Feldman, J.; Schaverien, C. J.; Dewan, J. C.; Liu, A. H. *J. Am. Chem. Soc.* **1988**, *110*, 1423. (e) Couturier, J.-L.; Paillet, C.; Leconte, M.; Basset, J.-M.; Weiss, K. *Angew. Chem., Int. Ed. Engl.* **1992**, *31*, 628.

¹⁰(a) Schrock, R. R.; Murdzek, J. S.; Bazan, G. C.; Robbins, J.; DiMare, M.; O'Regan, M. *J. Am. Chem. Soc.* **1990**, *112*, 3875. (b) Bazan, G. C.; Oskam, J. H.; Cho, N.-H.; Park, L. Y.; Schrock, R. R. *J. Am. Chem. Soc.* **1991**, *113*, 6899. (c) Schrock, R. R.; Hoveyda, A. H. *Angew. Chem. Int. Ed. Engl.* **2003**, *42*, 4592.

¹¹Armstrong, S. K. *J. Chem. Soc., Perkin Trans. 1* **1998**, 371. (b) Trnka, T. M.; Grubbs, R. H. *Acc. Chem. Res.* **2001**, *34*, 18.

¹²Grubbs, R. H. *Tetrahedron* **2004**, *60*, 7117.

¹³(a) Michelotti, F. W.; Keaveney, W. P. *J. Polym. Sci.* **1965**, *A3*, 895. (b) Rinehart, R. E.; Smith, H. P. *Polym. Lett.* **1965**, *3*, 1049.

It is important to underline that catalyst activity is not only influenced by the central metallic core (as will be discussed later in detail for ruthenium), but also small adjustments in the ligand environment can cause large changes in catalytic behavior.

Unlike their early transition metal counterparts, ruthenium ill-defined systems result quite stable to oxygen, moisture and many functional groups.

As previously mentioned a turning point in the development of catalytic systems was the Chauvin proposed metathesis mechanism which was furthermore demonstrated by Grubbs.¹⁴ Chauvin suggested that the active specie was a metal alkylidene.^{6,15} He introduced the new idea of synthesizing a metal-alkylidene complex to promote metathesis reactions and the first of these synthesis (based on Ru as core metal) was accomplished in 1992 by Nguyen and co-workers¹⁶ (complex **1** Figure 1. 2) furnishing the first active well defined ruthenium pre-catalyst complex, whose activity was studied in the ROMP of norbornadiene.

Despite its low activity and long initiation period the system showed an high functional group tolerance; so the goal was the design of more active ruthenium based complexes to overcome (or at least to match) the activity observed with the early metal systems. Therefore many efforts were addressed in order to improve catalyst **1** activity by modifying ancillary ligands (since it was clear that ruthenium presence was fundamental to confer superior stability to the catalyst).

Subsequent variation showed that larger and more basic phosphine ligands conferred greater metathesis activity, in this order: PCy₃ > P(*i*-Pr)₃ >> PPh₃ (Cy = cyclohexyl; Ph = phenyl; *i*-Pr = *iso*-propyl).¹⁷ Catalyst **2**, bearing PCy₃ ligands was the first well-defined ruthenium carbene active toward *acyclic* olefins, in addition to performing ROM polymerization. This was the first time that

¹⁴ (a) Grubbs, R. H.; Burk, P. L.; Carr, D. D. *J. Am. Chem. Soc.* **1975**, *97*, 3265. (b)

Grubbs, R. H.; Carr, D. D.; Hoppin, C.; Burk, P. L. *J. Am. Chem. Soc.* **1976**, *98*, 3478.

¹⁵ (a) France, M. B.; Paciello, R. A.; Grubbs, R. H. *Macromolecules* **1993**, *26*, 4739. (b) France, M. B.; Grubbs, R. H.; McGrath, D. V.; Paciello, R. A. *Macromolecules* **1993**, *26*, 4742.

¹⁶ Nguyen, S. T.; Johnson, L. K.; Grubbs, R. H.; Ziller, J. W. *J. Am. Chem. Soc.* **1992**, *114*, 3974.

¹⁷ (a) S. T. Nguyen, R. H. Grubbs, J. W. Ziller, *J. Am. Chem. Soc.*, **1993**, *115*, 9858; (b) G. C. Fu, S. T. Nguyen, R. H. Grubbs, *J. Am. Chem. Soc.*, **1993**, *115*, 9856.

researchers could perform the ring closing metathesis of functionalized hydrocarbons thanks to the increased catalyst stability by enhanced phosphine basicity.¹⁶

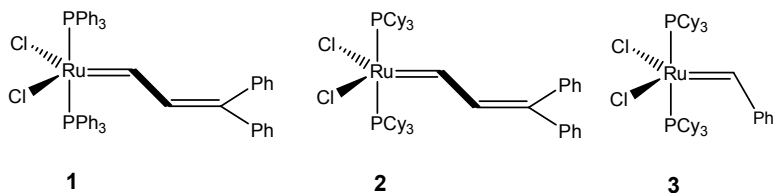


Figure 1. 2: well defined metathesis active ruthenium alkylidene complexes

Pursuing the goal of increasing catalyst activity, in 1995 Schwab and co-workers modified complex **2** replacing the vinyl carbene with a benzylidene, and using, as phosphine unit, the more sigma donating tricyclohexylphosphine. This complex not only displayed good activity but also improved functional group tolerance over **1** and **2** greatly expanding the substrate scope.¹⁸

Complex **3** known as First Generation Grubbs' catalyst (CAS: 172222-30-9; price per gram about 100 Euros)¹⁹ is actually commercially available and still used both in academic and industry environment.²⁰ Its properties, in addition to its resistance to decomposition in the presence of air or moisture led to a surge of interest in olefin metathesis, particularly in RCM and ene-yne metathesis.¹

Between end of 1990 and beginning of 2000 the research in the field of metathesis raised exponentially; in particular many efforts were addressed in the modification of the first generation Grubbs complex to overcome thermal stability issue and to further improve catalyst lifetime and turnover.

A great intuition which gave rise to spectacular progress in Ru-alkylidene catalyst design, was the introduction of carbenes as ancillary ligands. Ligands of this type show high propensity for acting as typical σ -donors and strong Lewis base, yet displaying a

¹⁸ (d) Schwab, P.; France, M. B.; Ziller, J. W.; Grubbs, R. H. *Angew. Chem., Int. Ed.* **1995**, *34*, 2039. (e) Schwab, P.; Grubbs, R. H.; Ziller, J. W. *J. Am. Chem. Soc.* **1996**, *118*, 100.

¹⁹ Prices from sigma Aldrich official website: www.sigmaaldrich.com

²⁰ G. C. Vougioukalaki and R. H. Grubbs *Chem. Rev.* **2010**, *110*, 1746

slight π -back bonding tendency. Finally *N*-heterocyclic carbene (NHCs) are able to generate rather stable metal-carbon bonds.²¹ Hermann was the first to propose a modification of Grubbs catalyst consisting in the replacement of the two phosphines by imidazolin-2-ylidene ligands (Figure 1. 3). Compounds **4-7** show high tolerance toward functional groups while being active in ROMP and RCM.²²

Even though the activity of the upper mentioned complexes turned out to be lower than that of the original first generation Grubbs' catalyst,^{21,23} these results suggested that NHCs could have been indeed interesting ligands for ruthenium based olefin metathesis catalysts. The origin of this lower reactivity probably derives from the fact that NHC ligands are less labile than phosphines therefore the catalytically active $14e^-$ species are formed more slowly.

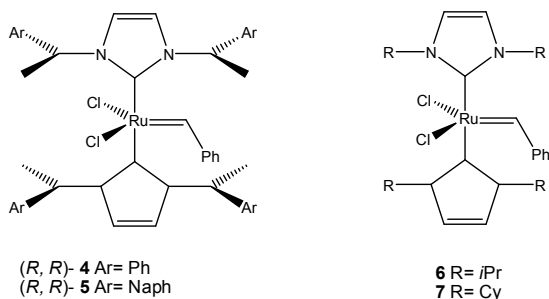


Figure 1. 3: Catalysts bearing two NHC ligands

The calculation of Ru-C (NHC) bond strength corroborates this hypothesis since it was found to be 20-40 Kcal/mol stronger than R_3P-Ru bond strengths.²⁴ This results justified the raising stability of NHC-Ruthenium complexes with respect to the di-phosphine ones.

²¹(a) Hermann, W. A.; Köcher, C. *Angew. Chem., Int. Ed.* **1997**, *36*, 2163. (b) Huang, J.; Schanz, H.-J.; Stevens, E. D.; Nolan, S. P. *Organometallics* **1999**, *18*, 2370. (c) Jafarpour, L.; Nolan, S. P. *Adv. Organomet. Chem.* **2001**, *46*, 181.

²²(a) Weskamp, T.; Schattenmann, W. C.; Spiegler, M.; Hermann, W. A. *Angew. Chem., Int. Ed.* **1998**, *37*, 2490. (b) Weskamp, T.; Kohl, F. J.; Wolfgang, A.; Hermann, W. A. *J. Organomet. Chem.* **1999**, *582*, 362.

²³(a) Achermann, L.; Fürstner, A.; Weskamp, T.; Kohl, F. J.; Hermann, W. A. *Tetrahedron Lett.* **1999**, *40*, 4787. (b) Scholl, M.; Ding, S.; Lee, C. W.; Grubbs, R. H. *Org. Lett.* **1999**, *1*, 953.

²⁴Weskamp, T.; Schattenmann, W. C.; Spiegler, M.; Hermann, W. A. *Angew. Chem., Int. Ed.* **1999**, *38*, 262.

So we could say that the development of complexes **4-7** provided an important evidence to the stabilizing effect of NHC ligands.

Mindful of the above mentioned stabilizing effect, independently and almost simultaneously, the groups of Nolan²⁵, Grubbs,²⁶ Fürstner and Herrmann²⁷ pursued the idea of combining a labile phosphine group for rapid metathesis initiation, with a non-labile NHC ligand, resulting in heteroleptic complexes.

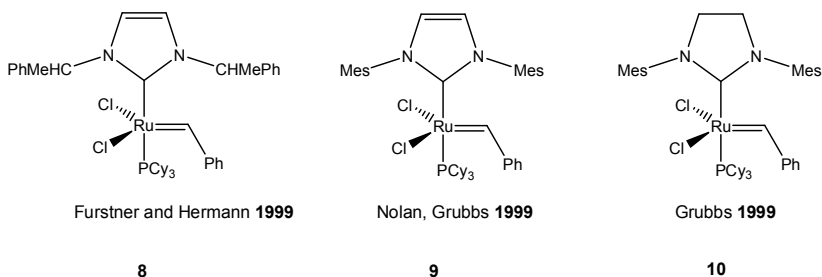


Figure 1. 4: Second generation Grubbs catalysts

The newly synthesized mixed phosphine/NHC complexes displayed superior catalyst activity with respect to their bis NHC and bis phosphine analogues²⁸

Among them complex **10**, incorporating a more powerfully σ -donating carbene, owing to lack of aromaticity in the NHC ring, resulted as the most active catalyst. This complex represented a good compromise between high activity of early group transition metals and high air, moisture and functional-group tolerance of late group transition metals. Its high efficiency allowed for the first time (for ruthenium based complexes), the formation of tri- and tetrasubstituted alkenes, and the reaction of 'deactivated' electron-deficient olefins (such as vinyl carbonyl species). Complex **10** was also employed in cross metathesis reactions affording for the first time, the cross reaction to a trisubstituted olefin.²⁹

This class of catalysts has been named second generation Grubbs'. In particular complex **10** is currently commercially available and it is

²⁵ Huang, J.; Stevens, E. D.; Nolan, S. P.; Petersen, J. L. *J. Am. Chem. Soc.* **1999**, *121*, 2674.

²⁶ Scholl, M.; Trnka, T. M.; Morgan, J. P.; Grubbs, R. H. *Tetrahedron Lett.* **1999**, *40*, 2247.

²⁷ Achermann, L.; Fürstner, A.; Weskamp, T.; Kohl, F. J.; Herrmann, W. A. *Tetrahedron Lett.* **1999**, *40*, 4787.

²⁸ Samojlowic, C.; Bieniek, M. and Grela, K. *Chem. Rev.* **2009**, *109*, 3708.

²⁹ Chatterjee, A. K.; Grubbs, R. H. *Org. Lett.* **1999**, *1*, 1751.

the second most used catalyst for metathesis reactions (CAS 301224-40-8; cost: about 400 Euros per gram).¹⁹

The remarkable performances of these catalysts can be reasonably explained considering that the non-labile, bulky NHC ligand provides to the metal center a considerable steric protection, and acting as a good-donor, stabilizes both the pre-catalyst and the coordinatively unsaturated, catalytically relevant intermediate.

NHC-PCy₃ based complexes similarly to the first-generation Grubbs' catalysts **3**, are susceptible to oxidative decomposition; that is a typical decomposition pattern for phosphine based systems.¹

Another important issue, which has just been mentioned before, is related to the complex thermal stability. Decomposition in solution is indeed accelerated at high temperature. In an attempt to solve this problem, the alkylidene ligand has been replaced by a phenylindenyliidene moiety.³⁰ Complexes **11-13** have been widely used in natural product synthesis,³¹ their thermal stability is due to a slower initiation rate that requires higher temperature with respect to the Ru-benzylidene analogues.

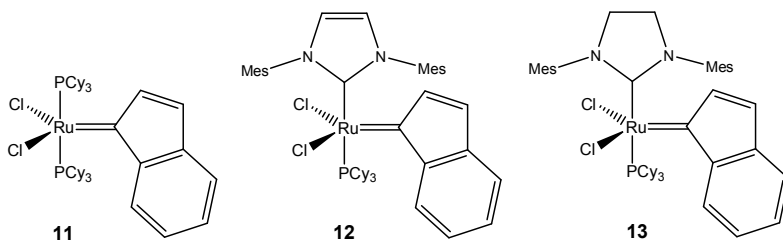


Figure 1. 5: Indenyliidene phosphine based complexes

A notable improvement in terms of catalyst longevity and thermal stability was reached by Hoveyda and co-workers which replaced for the first time one phosphine of complex **3** with a chelating

³⁰ For a review, see: Dragutan, V.; Dragutan, I.; Verpoort, F. *Platinum Met. Rev.* **2005**, *49*, 33, and references cited herewith.

³¹ (a) Jafarpour, L.; Schanz, H.-J.; Stevens, E. D.; Nolan, S. P. *Organometallics* **1999**, *18*, 5416. (b) Fürstner, A.; Guth, O.; Düffels, A.; Siedel, G.; Liebl, M.; Gabor, B.; Mynott, R. *Chem. Eur. J.* **2001**, *7*, 4811.

alkylidene ligand (complex **14** Figure 1. 6).³² The introduction of an ether moiety bestows on **14** a particular stability. Mindful of the beneficial effect of eliminating a phosphine group in favor of a chelating alkylidene, in 2000 the groups of Hoveyda³³ and Blechert³⁴ simultaneously reported the phosphine-free, NHC-bearing catalysts **15** and **16**. These so-called “Hoveyda” or “Hoveyda-Grubbs” complexes, in addition to being extremely robust, demonstrate improved activity toward electron deficient alkenes (for instance acrylonitriles, fluorinated alkenes, vinyl phosphine oxides and sulfones).²⁷

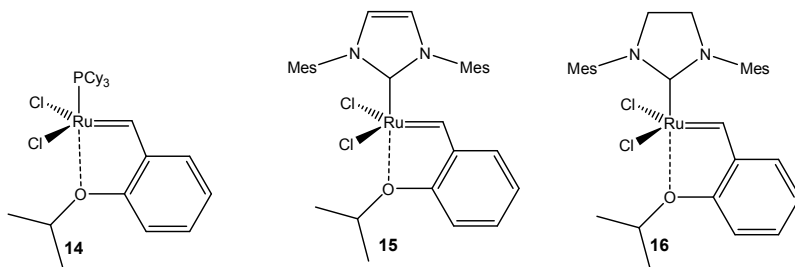


Figure 1. 6: Grubbs-Hoveyda type complexes

Moreover, metathesis reactions involving vinyl chlorides and trisubstituted alkenes catalyzed by ether based complexes showed improved yields with respect to those obtained with the corresponding benzylidene or indenylidene catalysts.²⁷ Hoveyda type complexes displayed an interesting combination of properties which render them attractive for scaled up uses: air and moisture stability, good turnover at low loading, easy of handling, and moreover the possibility to be linked to a solid support (easy automatization and re-use)

Catalyst **14** and **16** are today commercially available under the name respectively of: First generation Grubbs Hoveyda catalyst (203714-71-0; price is about 400 Euros per gram) and Second

³²(a) Harrity, J. P. A.; La, D. S.; Cefalo, D. R.; Visser, M. S.; Hoveyda, A. H. *J. Am. Chem. Soc.* **1998**, *120*, 2343. (b) Kingsbury, J. S.; Harrity, J. P. A.; Bonitatebus, P. J., Jr; Hoveyda, A. H. *J. Am. Chem. Soc.* **1999**, *121*, 791.

³³ Garber, S. B.; Kingsbury, J. S.; Gray, B. L.; Hoveyda, A. H. *J. Am. Chem. Soc.* **2000**, *122*, 8168.

³⁴ Gessler, S.; Randl, S.; Blechert, S. *Tetrahedron Lett.* **2000**, *41*, 9973.

generation Grubbs Hoveyda catalyst (301224-40-8; price is again about 400 Euros per gram)¹⁹

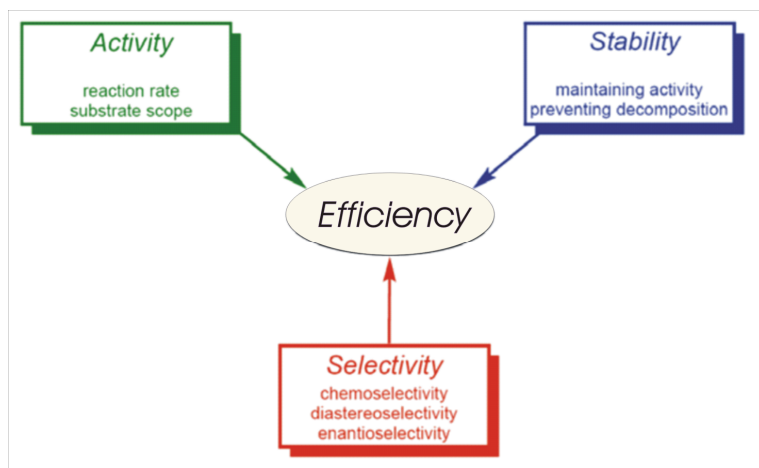
All the developments reported in this brief overview on metathesis history give idea of how powerful and promising this method is. Over these years metathetical processes like ring closure or cross metathesis became the key step in total synthesis of natural products or complex molecules. Despite these advances, a complete control of catalyst efficiency parameters is still missing. Anyway it is worth to note that complete control and perfect balance of catalyst crucial parameters (activity, selectivity and stability) represents one of the major challenges for chemists which deal with catalyst design.

Ritter and co-workers³⁵ in 2006 have described best the above mentioned parameters:

- Activity is tied to both the initiation and propagation rates of a given catalyst in olefin metathesis. As such, it is reaction dependent and can be quantified through kinetic experiments.³⁶
- Stability is directly related to activity and refers to the lifetime of a catalyst and its ability to perform productive metathesis events over extended periods of time. Stability can be measured qualitatively by monitoring loss in catalyst activity throughout the course of a reaction.
- Selectivity describes the ability of a catalyst to react with a certain type of substrate (chemoselectivity) or to provide control over product formation (enantioselectivity and diastereoselectivity).

³⁵ Ritter, T.; Hejl, A.; Wenzel, A. G.; Funk, T. W.; Grubbs, R. H. *Organometallics* **2006**, *25*, 5740.

³⁶ Sanford, M. S.; Love, J. A.; Grubbs, R. H. *J. Am. Chem. Soc.* **2001**, *123*, 6543



Scheme 1. 3: key parameters to design an efficient catalyst

With that in mind, the development of more efficient catalysts for a variety of applications remains a very important goal in which research is still ongoing.

Other important issues concern catalyst economic and environmental sustainability as well as the developing of a technology applicable on big scale; so many efforts have been addressed to lower the catalyst loading and to anchor and re-use it. This in order to match two requirements: reduce the cost needed for the catalyst (lowering its loading by using a more active and stable complexes) and avoid metal impurities. Indeed, we have to consider that besides the economic reason strictly related to the cost of ruthenium, the increasing catalyst loading could also potentially increase the level of residual ruthenium impurities in the final products, which becomes especially undesirable when reaction products are intended for pharmaceutical use (because of metal toxicity).³⁷ On the whole, all these issues have a direct influence on the operational cost of a process. With these aspects in mind, the next challenge in all metathesis transformations is to substantially decrease the catalyst loading, thereby reducing both reaction cost and the challenges in product purification.

³⁷Governmental recommendations for residual ruthenium are now routinely less than 10 ppm. For recent guidelines, see: (a) Zaidi, K. *Pharmacoepial Forum* **2008**, *34*, 1345. (b) Criteria given in the EMEA Guideline on the Specification Limits for Residues of Metal Catalysts, available at: www.emea.europa.eu/pdfs/human/swp/444600.pdf

Mechanistic and decomposition pathway studies have played an important role in the evolution and improvement of ruthenium based olefin metathesis catalyst leading to an enormous variety of complex structurally designed to allow structure-reactivity relationship studying.

The first part of this thesis was focused on the study of the effect of NHC backbone substitution on catalyst activity to reach top performances at low metal loadings.

Chapter 2

Ligand substituent effects on ruthenium based complexes

Introduction

As seen in chapter 1 two among the best performing catalysts for metathesis transformations identified in the late 1990s and early 2000s were both characterized by an NHC as ancillary ligand (second generation Grubbs **10** complex and Grubbs Hoveyda **16** complex). These two complexes have been the starting point of extensive investigations in which ligand properties have been changed one by one and the effect of these modifications have been carefully examined by experimental and theoretical studies.

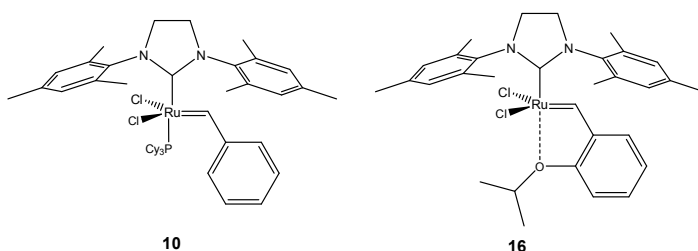


Figure 2. 1 Commercially available second generation Grubbs and Grubbs-Hoveyda catalysts

This chapter is thought to provide an overview on the effect of NHC structural modifications on complex activity toward metathesis reactions both for ether and phosphine based complexes.

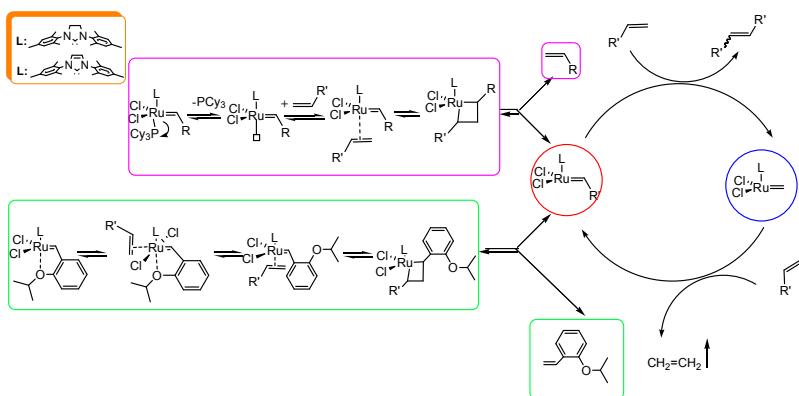
Since detailed investigation on catalyst decomposition pathways and metathesis mechanism has played a fundamental role in the design of improved catalysts, a suitable way to approach the topic is to provide insights into these two crucial aspects.

Insight on metathesis mechanism and catalyst decomposition pathways

As for the first feature it is important to underline that the initiation steps of metathesis reactions involving the phosphine and ether based complexes are different.

Indeed the widely accepted mechanism for the II generation Grubbs complex is based on the dissociation of the labile phosphine in order to generate a 14 electron ruthenium intermediate which then coordinates the incoming olefin.

For ether based Hoveyda complex the experimental evidences support the hypotheses of an interchange associative step as initiation of the catalytic cycle.



Scheme 2.1: Mechanism of metathesis catalyzed by common ruthenium pre-catalysts.

As just mentioned understanding the decomposition pathways of existing ruthenium-based metathesis catalysts is crucial for the development of new, more efficient catalysts.

A rational design of ligand environments could reduce secondary reactions which involve the loss of the active species (alkylidene). It is worth to note that all the decomposition pathways that take place in typical metathesis reaction conditions include at least one of these events: loss of phosphine and metallation (C-H activation).

In particular the first step in the decomposition pathway for phosphine based complexes foresees at first the labile ligand loss

and afterwards the metallation reaction. The key step for Hoveyda systems in the crumbling process is the C-H activation.

Due to the weaknesses of these complexes many efforts were addressed to design catalyst which minimize or completely avoid these decomposition routes.

In 2008 Grubbs formulated the hypothesis that restricting rotation of the *N*-aryl groups would prevent catalyst decomposition. Actually, the addition of substituents on the backbone of the NHC ligand, allowed for the first time the access to a stable ruthenium complexes bearing an *N,N'*-diphenyl-substituted NHC with saturated backbone. The synthesis of this class of complexes has long been elusive¹

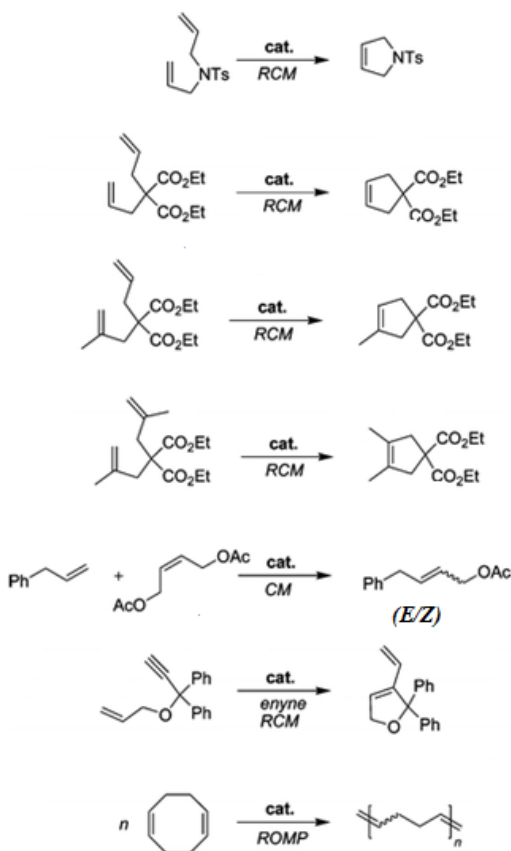
Key aspect of catalytic activity comparison

For the sake of clarity it is important to underline some crucial aspects on catalyst activity comparison :

1. The catalytic behavior of different complexes (of the same class) has to be tested toward the same reaction, performed in the same conditions (same loading, temperature, and solvent). A standard system of characterization for ruthenium based olefin metathesis catalyst has been introduced² in 2006 by Ritter and Co-workers. The reactions were selected on the basis of their ability to provide the maximum amount of information describing catalyst activity, stability, and selectivity, while being operationally simple. In scheme 2.1 are reported some of the benchmark reactions to operate ring closure, ring opening and cross metathesis on small molecules.

¹ Chung, C. K.; R. H. Grubbs *Organic Letters* **2008**, *10*, 2693 (coincide con rif 20 cambia sotto)

² Ritter, T.; Hejl, A.; Wenzel, A. G.; Funk, T. W.; and Grubbs, R. H. *Organometallics* **2006**, *25*, 5740



Scheme 2. 2: Some of the benchmark transformations in olefin metathesis

2. Different type of complexes are often tested at different temperatures and in different solvents toward the same reaction. Different experimental conditions do not allow an unaffected and direct comparison between complexes belonging to different classes.
3. When the aim of a study is the observation of ligand modification effect on catalyst activity it is appropriate to change ligand characteristics one by one and then to examine the catalytic behavior of the obtained complexes as reported below.

Our interest

Since significant effect on catalyst activity arises from NHC steric and electronic modifications recently our interest in catalyst design moved in this direction; in particular we focused on the effect of these variations in the backbone positions (R') and in the substituents of the nitrogen atoms both for phosphine and ether based complexes.

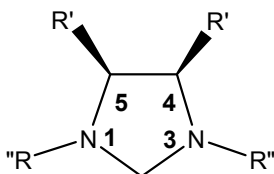


Figure 2. 2: NHC possible modification sites

NHC-Ru based complexes can be classified in many ways. Among them, two important categories are identified:

1. Symmetrically 1, 3-disubstituted imidazol and imidazolin 2-ylidene ligands
2. Asymmetrically 1, 3-disubstituted imidazol and imidazolin 2-ylidene ligands

This overview will mainly focus on the first category because of major pertinence with my PhD project.

Symmetrically 1, 3-disubstituted imidazol and imidazolin 2-ylidene ligand

In order to establish a structure-activity relationship (SAR) in the last fifteen years a considerable number of differently substituted NHCs were used as ancillary ligand in Ru based complexes and the catalytic behavior of the so-obtained derivatives was explored. Typically, imidazol- and imidazolin-2-ylidene ligands with aliphatic substituents were either not formed or resulted unstable and displayed reduced catalytic activities. For example, Grubbs and Louie described the preparation of **17a**³ which was obtained

³ Louie, J.; Grubbs, R. H. *Angew. Chem., Int. Ed.* **2001**, *40*, 247.

quantitatively as a bright blue solid. Unfortunately it resulted inactive in the RCM of the diethyl diallylmalonate (**a**), even using harsh reaction conditions. The same reaction, in the presence of **17b** proceeded in high yield.

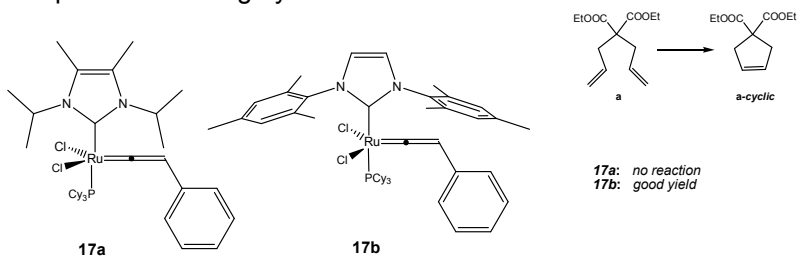


Figure 2. 3: Selected 1,3 disubstituted NHC-Ru complexes

Similarly, Verpoort and Ledoux reported on the low stability of Grubbs benzylidene complexes **18a** and **18b**, which prevented their isolation. This lack of stability was attributed to steric effects resulting in a weakened NHC-metal bond.⁴ Fortunately, the sterically less demanding Hoveyda-type complexes could be substituted with NHC ligands bearing two aliphatic *N*-substituents, yielding **18c** and **18d** as solids, respectively olive and bright green (Figure 2. 4).⁵² Compared with the standard Hoveyda catalyst **16**, a slightly decreased Ru-C (NHC) bond length (1.972 vs 1.981 Å) was noted in **18c**. This may be indicative of a stronger σ -donation of the NHC ligand caused by the aliphatic *N*-groups. Although more active in the ROMP of *cis,cis*-cycloocta-1,5-diene [COD, (**m**)], in the RCM of DEDAM (**a**) and in the CM of acrylonitrile,⁵³ these modified complexes displayed lower activity than the parent Hoveyda complex **16**. It should be noted, however that in the CM reaction these complexes led to slightly higher *Z* selectivity.

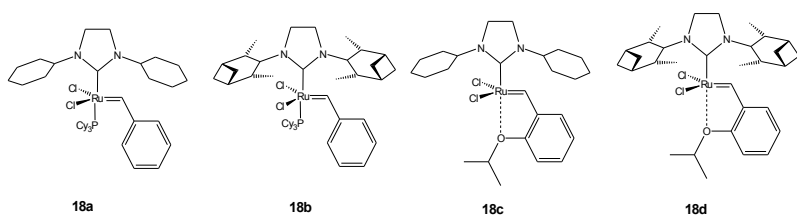


Figure 2. 4: 1,3-dialkyl substituted NHC-Ru complexes

⁴ Ulman, M.; Grubbs, R. H. *J. Org. Chem.* **1999**, *64*, 7202.

In 2000, Nolan and co-workers carried out the synthesis of complex **19** (Figure 2. 5), bearing two *ortho* bulky aryl groups (2,6-diisopropylphenyl), in order to study the influence of the bulkiness of the NHCs on the catalytic activity of the corresponding complexes.⁵ When **19** was employed to modulate the ring closing metathesis of the diethyldiallyl malonate, it was observed a complete cyclization in about 15 minutes while **10** took about 17 minutes to yield the 92% of product.

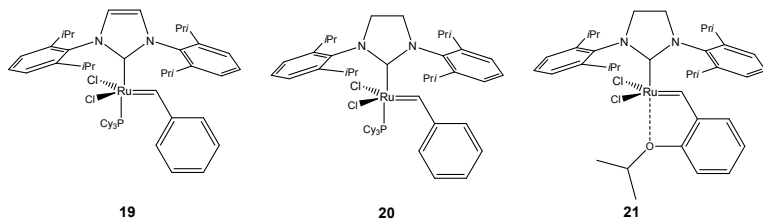


Figure 2. 5 Ruthenium catalyst **19-21** bearing sterically demanding *N*-heterocycle carbenes

In the following three years the groups of Fürstner,(2001),⁶ Mol (2002)⁷ and Wagener (2003)⁸ reported the synthesis and the catalytic activity evaluation of complexes **20** and **21** (Figure 2. 5), which are the saturated phosphine-containing and phosphine-free analogues of **19**. At room temperature, catalyst **20** shows effective turnover numbers 6 times higher than those of **10**,⁵ along with remarkable higher initiation rates. This increased activity has been paid by a parallel increase of the decomposition rate⁸ especially when utilized in challenging transformations.⁹ Phosphine-free catalyst **21** instead demonstrates increased thermal stability and improved ADMET polymerization efficiency compared to complex **20**.⁸

Parallel work in Fürstner's group led to the preparation of complex **22** (Figure 2. 6)⁶ characterized by an unsaturated NHC with two chlorine atoms on the backbone. This kind of substitution has little

⁵ Jafarpour, L.; Stevens, E. D.; Nolan, S. P. *J. Organomet. Chem.* **2000**, *606*, 49.

⁶ Fürstner, A.; Ackermann, L.; Gabor, B.; Goddard, R.; Lehmann, C. W.; Mynott, R.; Stelzer, F.; Thiel, O. R. *Chem.sEur. J.* **2001**, *7*, 3236.

⁷ Dinger, M. B.; Mol, J. C. *Adv. Synth. Catal.* **2002**, *344*, 671.

⁸ Courchay, F. C.; Sworen, J. C.; Wagener, K. B. *Macromolecules* **2003**, *36*, 8231.

⁹ Ritter, T.; Hejl, A.; Wenzel, A. G.; Funk, T. W.; Grubbs, R. H. *Organometallics* **2006**, *25*, 5740.

effect on the reactivity of the resulting complex, despite the obvious electronic alteration of the ligand.

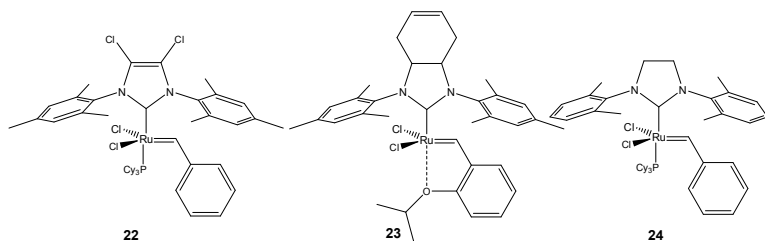


Figure 2. 6: modified NHC ruthenium based complexes.

The synthesis of complexes **23**¹⁰ and **24**,¹¹ presented in Figure 2. 6, were published in 2005. Complex **23**, which bears an internal double bond as part of the NHC ligand backbone, represents a good starting material for the preparation of further functionalized NHC-Ru catalysts applicable under various process conditions, for example, in immobilized or biphasic liquid catalysis.¹⁰

Indeed, the unsaturated backbone in **23** remains intact even raising the temperature, most probably because of the low metathesis reactivity of unstrained cycloolefins such as cyclohexenes. The reactivity of this complex toward the cyclization *N,N*-diallyl tosylamine was slightly lower than that of the second-generation Grubbs Hoveyda complex **16**. (Figure 2. 1). The Grubbs second generation like complex **24** was easily purified by simple hexane washings (avoiding undesirable column chromatography step, which often favors complexes decomposition) and displayed comparable performance in the self-CM of acrylonitrile to its commercially available analogous **10**.¹¹

In 2006 the reporting of the first fluorinated *N*-aryl substituted complex paved the way for *N*-aryl halide substitution. The ring closing metathesis of the less encumbered malonate derivative DEDAM (**a**) was performed much faster by complex **25** with respect to its analogue **10**. The opposite trend was observed for the corresponding Hoveyda **26**. This contradictory behavior of **25** and **26** was ascribed to an unprecedented fluorine-ruthenium interaction

¹⁰ Weigl, K.; Köhler, K.; Dechert, S.; Meyer, F. *Organometallics* **2005**, *24*, 4049.

¹¹ (a) Bai, C. X.; Lu, X. B.; He, R.; Zhang, W. Z.; Feng, X. J. *Org. Biomol. Chem.* **2005**, *3*, 4139. (b) Bai, C. X.; Zhang, W. Z.; He, R.; Lu, X. B.; Zhang, Z. Q. *Tetrahedron Lett.* **2005**, *46*, 7225. (c) Zhang, W. Z.; He, R.; Zhang, R. *Eur. J. Inorg. Chem.* **2007**, 5345

(Ru-F distance = 3.2 Å) observed in the solid-state structure of **26** (Figure 11) via X-ray diffraction.¹² The absence of an analogous interaction for complex **25** was explained by steric congestion between the NHC and the large tricyclohexylphosphine which does not allow fluorine approach to establish the coordination.

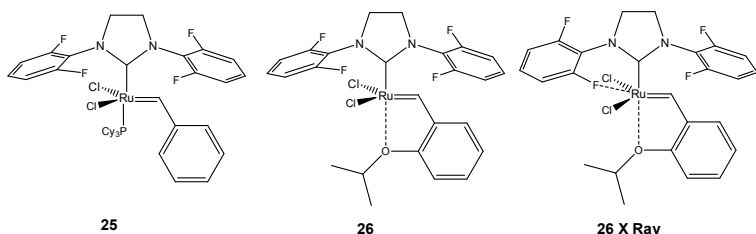


Figure 2. 7 Fluorinated ruthenium based II generation Grubbs and Grubbs Hoveyda complexes.

The chloride analogues of **25** and **26** were prepared, but resulted not suitable for catalysis purpose due to their low stability.¹³

Despite all these improvements, an highly active (while robust) system for challenging ring closing metathesis to tetrasubstituted olefins was still missing; to improve reactivity in this direction, Grubbs¹⁴ group synthesized some new complexes (**27-31**). His guidelines in the design of these new derivatives originated from earlier observations:¹⁵

- *N*-aryl substitution prevents the decomposition pathways via C-H activation (since it hinders *N*-C_{aryl} rotations);
- reduced bulk at the *ortho* position of the *N*-aryls exerts increased efficiency in the conversion of sterically demanding substrates,

Among these new catalysts (**27-31**), **31** was identified as the most efficient in the ring closing reactions that afford tetrasubstituted olefins. Unfortunately, however, the difficult preparation of catalyst

¹² Ritter, T.; Day, M. W.; Grubbs, R. H. *J. Am. Chem. Soc.* **2006**, *128*, 11768.

¹³ (a) Fournier, P. A.; Savoie, J.; Stenne, B.; Bédard, M.; Grandbois, A.; Collins, S. K. *Chem. Eur. J.* **2008**, *14*, 8690. (b) Grandbois, A.; Collins, S. K. *Chem.sEur. J.* **2008**, *14*, 9323.

¹⁴ Berlin, J. M.; Campbell, K.; Ritter, T.; Funk, T. W.; Chlenov, A.; Grubbs, R. H. *Org. Lett.* **2007**, *9*, 1339.

¹⁵ (a) Van Veldhuizen, J. J.; Campbell, J. E.; Giudici, R. E.; Hoveyda, A. H. *J. Am. Chem. Soc.* **2005**, *127*, 6877. (b) Funk, T. W.; Berlin, J. M.; Grubbs, R. H. *J. Am. Chem. Soc.* **2006**, *128*, 1840.

31 rendered its large-scale production uneconomical and imposed significant drawbacks regarding its commercialization.¹⁶

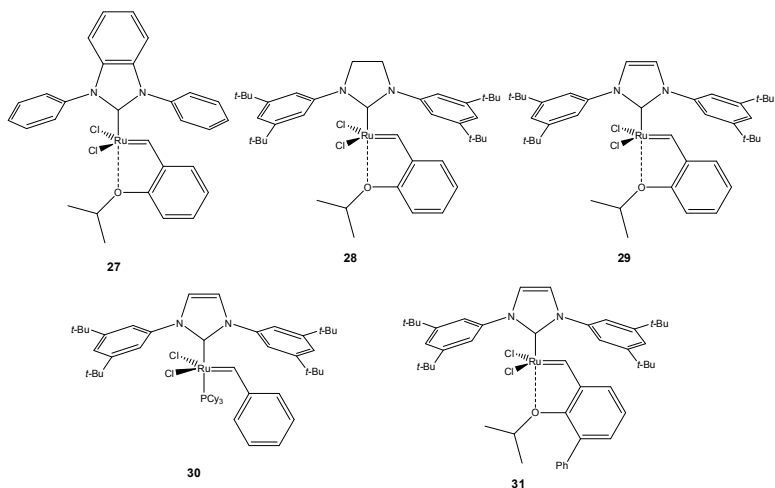


Figure 2. 8: Ruthenium based pre-catalysts 27-31

An interesting NHC architecture has been proposed by Blechert et al. in 2007¹⁷. The corresponding phosphine¹⁸ and phosphine free Ru complexes show some promising catalytic results in diastereoselective ring rearrangement metathesis reactions (dRRM) but should be handled in inert atmosphere, due to their strong tendency toward deactivation.

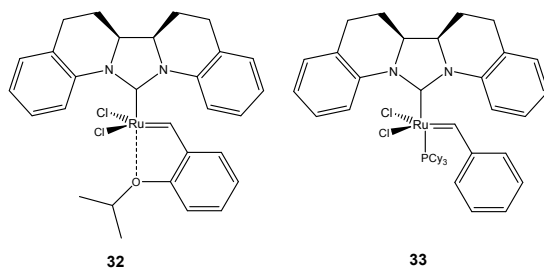


Figure 2. 9: ruthenium based catalysts 32-33 bearing bulk NHC ligands

¹⁶Stewart, I. C.; Ung, T.; Pletnev, A. A.; Berlin, J. M.; Grubbs, R. H.; Schrodi, Y. *Org. Lett.* **2007**, *9*, 1589.

¹⁷Vehlow, K.; Gessler, S.; Blechert, S. *Angew. Chem., Int. Ed.* **2007**, *46*, 8082

¹⁸Stewart, I. C.; Benitez, D.; O'Leary, D. J.; Tkatchouk, E.; Day, M. W.; Goddard, W. A., III; Grubbs, R. H. *J. Am. Chem. Soc.* **2009**, *131*, 1931.

An interesting application of metathesis catalysis is related to the availability of chiral catalysts which deliver enantiomerically enriched molecules. In addition to furnish products of high enantiomeric purity, a chiral catalyst can offer higher level of efficiency that are not achievable through their achiral variant. Chirality can be introduced by subtle modifying backbone or nitrogen positions. (NHC 4,5 and 1,3 positions respectively). One of the first-ruthenium based catalysts bearing chiral monodentate NHC was reported by Grubbs in 1999 (**34a**). Its catalytic activity was evaluated toward the enantioselective desymmetrization of achiral trienes (3-allyloxy-2,4-dimethylpenta-1,4-dienes), also known as asymmetric ring-closing metathesis (ARCM). Replacement of the mesityl flaps with *o*-isopropylaryl groups (**34c**) led to improved enantioselectivity.¹⁹

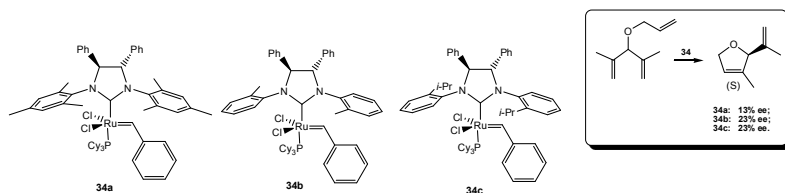


Figure 2. 10: ruthenium complexes **34a** **34c** bearing chiral monodentate NHC ligands.

A key observation that highlights on which positions of the NHC ring is more appropriate to introduce chirality in order to induce stereoselectivity in alkene metathesis arose from the synthesis of the first symmetrical di-hydro NHC ligands containing *N*-(*S*)-phenylethyl substituents²⁰.

¹⁹Seiders, T. J.; Ward, D; Grubbs R. H. *Org. Lett.* **2001**, *20*, 3225

²⁰Grisi, F.; Costabile, C.; Gallo, E.; Mariconda, A.; Tedesco, C.; Longo, P. *Organometallics* **2008**, *27*, 4649.

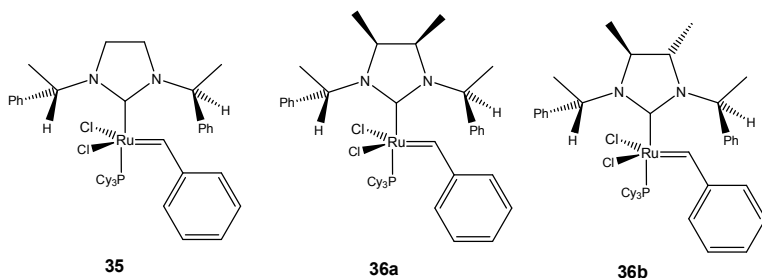


Figure 2. 11 Ruthenium based complexes bearing chiral monodentate NHCs 35, 36a, 36b.

In fact the investigation on catalytic behavior of these complexes led to the observation that **36b** was the only complex able to afford modest enantioselectivity in the challenging AROCM reported below (33% ee, Figure 2. 12), while **35** and **36a** led essentially to racemic product.

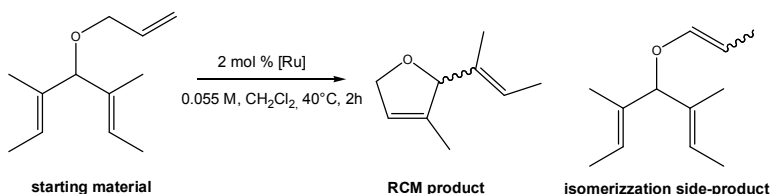


Figure 2. 12 ARCM of the prochiral triene

This evidence confirms the significance of chiral substitution on the backbone in transferring the asymmetric information to the active site of the catalysts while chiral *N*-substituents play a minor role. Separable isomers were instead obtained by Dorta and co-workers²¹ by exchange of a phosphine in favor of the oxygen chelating ligand. He had indeed observed the formation of not separable isomers for phosphine based complexes by raising the bulk of *N*-aryl groups. The variable temperature NMR analysis revealed the synthetic nature of these isomers which were not convertible one into the other by heating the sample (because of the high rotation barrier around C-N bond). So, to enhance the possibility of separating such complexes and at the same time

²¹ a) L. Vieille-Petit, X. Luan, M. Gatti, S. Blumentritt, A. Linden, H. Clavier, S. P. Nolan, R. Dorta, *Chem. Commun.* **2009**, 3783 ; b) M. Gatti, L. Vieille-Petit, X. Luan, R. Mariz, E. Drinkel, A. Linden, R. Dorta, *J. Am. Chem. Soc.* **2009**, *131*, 9498; c) L. Vieille-Petit, H. Clavier, A. Linden, S. Blumentritt, S. P. Nolan, R. Dorta, *Organometallics* **2010**, *29*, 775.

ensure high catalytic activity he had the smart idea of exploiting a ligand exchange procedure which allows the transformation of phosphine system into an Hoveyda one. By using this synthetic route he prepared complex **39** from an *anti/syn* mixture of complex **37**, isolating after careful chromatography workup complex *anti* **39** and *syn* **39** (1:1 ratio) in 63% overall yield. The same reaction performed on 4:1 *anti/syn* mixture of **38** led just to the isolation of the first isomeric derivative after chromatographic step (yield 62% for *anti* **40**).

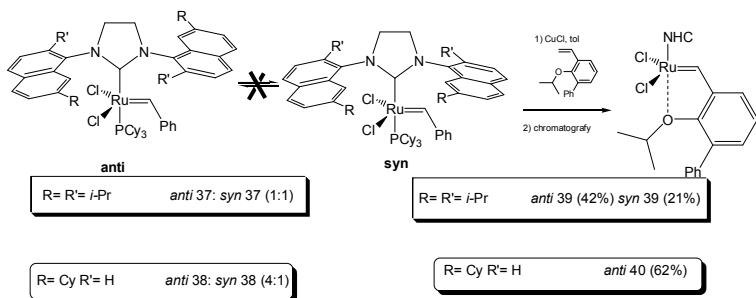


Figure 2. 13: preparation and separation of complexes **39** and **40**

Research in the direction of more easily prepared catalyst led to the evolution of the *ortho* substituted *N* aryl complexes **41-46**, whose synthesis can be scaled up without particular issues.¹⁶ Catalyst screening for the RCM of sterically demanding benchmark substrate revealed **41** and **44** as the most successful catalysts; **44** resulted quite active also in challenging cross metathesis of hindered substrates.²² Complex **41** and **44** are today commercially available as an additional type of II generation Grubbs and Grubbs Hoveyda complexes: **41** (927429-60-5 about 400 euro per gram); **44** (927429-61-6 about 500 euro per gram)

²² Stewart, I. C.; Douglas, C. J.; Grubbs, R. H. *Org. Lett.* **2008**, *10*, 441.

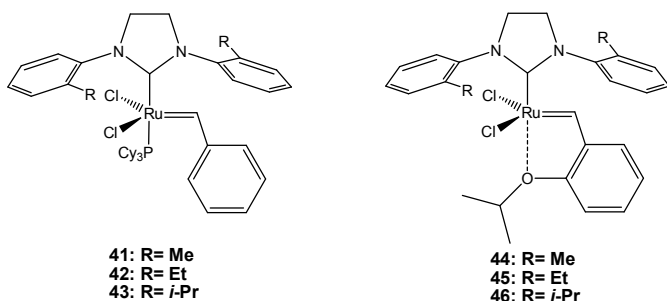


Figure 2. 14 ruthenium catalysts with increasing efficiency in the RCM of hindered di-olefins

A comparative study which pointed out the crucial parameters that have to be balanced to have good turnover and high stability in Ruthenium complexes was conducted by Grubbs in 2007.²³

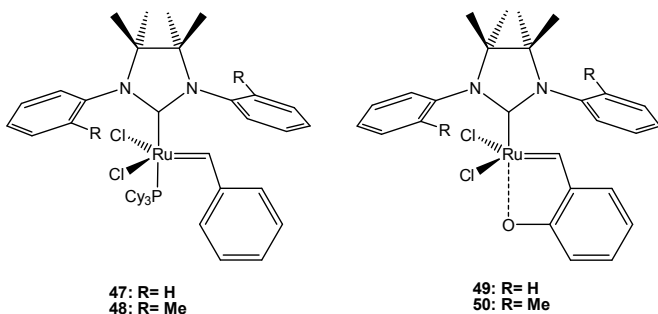


Figure 2. 15: NHC backbone methyl substituted ruthenium based catalysts

The screening study on the catalytic behavior of complex **47-50** in CM, RCM and ROMP reactions as well as the analysis of their decomposition pathways, suggested that the reduction of the bulkiness of the *N*-substituents results in a better catalytic activity while NHC backbone substitution increased catalyst lifetime.

To more deeply investigate the effect of NHC backbone modifications, the research group I am part of, focused on the preparation of phosphine and phosphine-free ruthenium complexes bearing *syn* and *anti* methyl substituents on the NHC backbone and different *N*-substituents (*o*-tolyl or *o*-isopropylphenyl groups).²⁴

²³ Chung, C. K.; R. H. Grubbs *Organic Letters* **2008**, *10*, 2693

²⁴ C. Costabile, A. Mariconda, L. Cavallo, P. Longo, V. Bertolasi, F. Ragone and F. Grisi *Chemistry a European Journal*, **2011**, *31*, 8618.

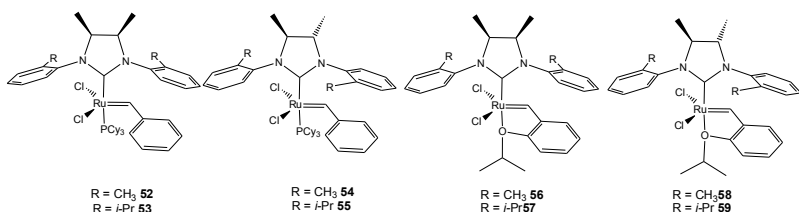


Figure 2. 16: *syn* and *anti* backbone symmetrical II generation Grubbs and Grubbs Hoveyda complexes

These complexes are highly efficient catalysts for RCM reactions; in particular, the *syn* complexes with *o*-isopropyl *N*-substituents are among the most efficient catalysts in the formation of tetrasubstituted olefins.²⁰ The presence of *syn* substituent is beneficial both for phosphine and phosphine-free catalysts. This finding makes the NHC backbone symmetry a new key element that needs to be taken into account in designing ruthenium catalysts for olefin metathesis.

A logical interpretation of the experimental data can be given by invoking steric factors. Very likely, the different reactivity in RCM observed can be justified by considering that the relative disposal of methyl groups on the backbone influences the conformation of the *N*-aryl rings of the NHC, defining a differently encumbered active space at the metal. More in detail, as reported by Grubbs and co-workers (Figure 2. 14 and Figure 2. 15),¹⁸ the high reactivity observed for catalyst **52**, **53**, **56**, **57** can be due to accessibility of conformations in which the *N*-aryl rings are rotated away from approaching and coordinated olefins, as a consequence of a preferential *syn* orientation displayed by *N*-tolyl rings. In particular, the *syn* orientation of the *N*-tolyl rings would be even more favored due to *syn* orientation of backbone methyl substituents.

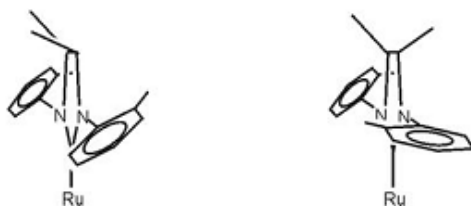


Figure 2. 17: Side Views of **52 and **54** complexes**

In my research group, DFT studies on the entire RCM catalytic cycle of hindered olefins were performed to rationalize the different behaviors of catalysts with *syn*- and *anti*-methyl groups on the NHC backbone.²⁰ According to these calculations, the activity difference between catalysts **52** and **54** is determined by the different energy barrier of the first cross metathesis of one of the substrate double bonds. The corresponding two transition states (**1[‡]** and **2[‡]** of Chart 2. 1) are characterized by differently shaped reactive pockets which result in very different interactions around the methylenedioxy moiety and the above *o*-tolyl ring.

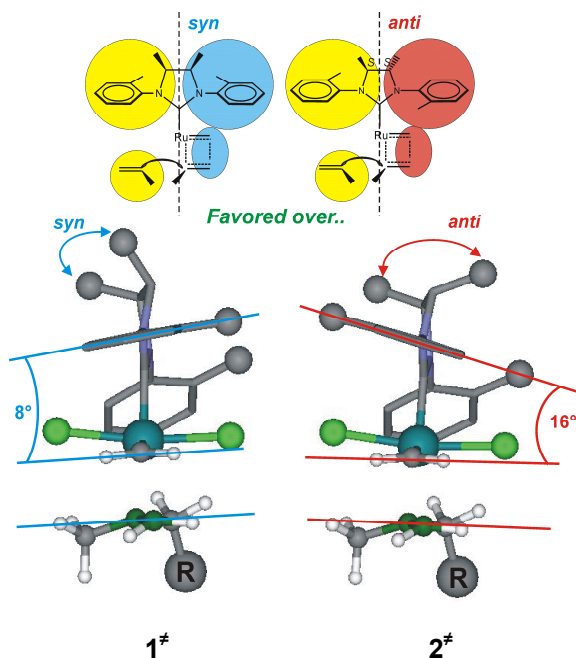


Chart 2. 1: Front and side view of the transition state **1[‡]** and **2[‡]** respectively for the *syn* catalyst **52** and the *anti* catalyst **54**. Distances are given in Å

In the *anti* transition state **2[‡]** these two groups are rotated with respect to one another by roughly 16°, which results in the C_{ortho} on the unsubstituted side of the *o*-tolyl ring and the nearby H_{methylene} at 3.0 Å only, (see Chart 2. 1). Conversely, in the *syn* transition state **1[‡]** the interaction between these two groups is more relaxed because the angle between the two planes is minor, 8° only, which results in the C_{ortho} on the unsubstituted side of the *o*-tolyl ring and

the nearby H_{methylidene} at 3.2 Å (Chart 2. 1). In other words, the geometry of the reacting atoms can better follow the flat shape casted by the *syn* catalyst, rather than the zig-zag shape of the *anti* catalyst.

Asymmetrically 1, 3-disubstituted imidazol and imidazolin 2-ylidene ligands

Unsymmetrical NHC frameworks, derived from the presence of two different *N*-side groups, were initially used in order to increase the electron-donating ability and to control the steric bulk of the NHCs. Indeed, variations of the electronic and steric parameters of NHC ligands directly influence the catalytic activity and the stereoselectivity of the resulting complexes. Despite this kind of complexes usually required more challenging synthetic routes to be prepared, many efforts in this direction were recently done. Indeed a key aspect which attracted the interest toward these asymmetric pre-catalysts was the finding that the utilization of unsymmetrical NHCs controls the selectivity in diastereoselective RCM reactions and the *E/Z* selectivity in CM reactions.

The first report on ruthenium complexes coordinated with unsymmetrical NHCs came from Fürstner's group in 2001.²⁵ Specifically, **60-62** were targeted as complexes able to metathesize their own heterocyclic carbene ligands, affording the corresponding chelates, with the goal of regenerating themselves after the quantitative consumption of the substrate. These complexes are efficient in the RCM of the encumbered *N,N*-dimethylallyl-*N*-tosylamine. The catalytic activity of **60-62** shows an interestingly systematic dependence on the tether length between the alkene group and the ruthenium center. This effect was postulated to depend on the different capabilities of **60-62** to form the corresponding chelate complexes in situ.

²⁵ Fürstner, A.; Ackermann, L.; Gabor, B.; Goddard, R.; Lehmann, C. W.; Mynott, R.; Stelzer, F.; Thiel, O. R. *Chem.Eur. J.* **2001**, *7*, 3236.

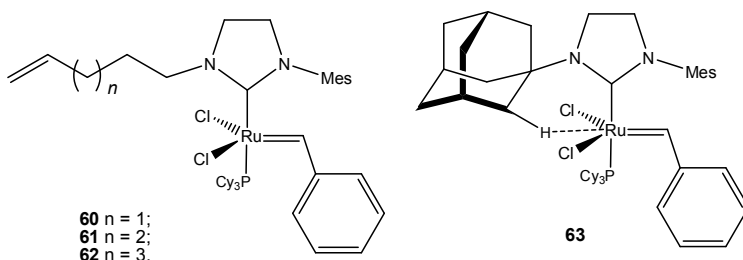


Figure 2. 18: unsymmetrical NHC ligand ruthenium based complexes.

In 2003 Mol et al²⁶. introduced a sterically encumbered mixed adamantyl/mesityl based NHC ligand. Since the *N* substituents must be introduced in different steps the overall synthesis resulted quite long, leading to the air stable green complex **63** in moderate yield. X Ray structure of this complex showed a possible weak interaction between the adamantyl hydrogen and the core metal centre. The excessive steric crowding imparted by the bulk 1-adamantyl group has been considered responsible for the negligible metathesis activity of complex **63**, which failed both the simple self metathesis of 1-octene and the RCM of the less hindered malonate derivative [DEDAM (**a**)]. This lack of activity persisted also increasing the temperature up to 100°C.

After anticipating that unsymmetrical ligands could alter the steric environment of key metathesis intermediates providing (stereo)selectivity in the metathetical process, Blechert *et al.*²⁷ postulated that replacing one mesityl moiety with a more electron donating alkyl group could lead to enhanced σ -donor properties of the NHC. So they carried out the synthesis of new ruthenium complexes bearing unsymmetrical saturated NHC ligands in order to gain new SAR (structure-activity relationship) data.²⁸

²⁶ Dinger, M. B.; Nieczypor, P.; Mol, J. *Organometallics* **2003**, 22, 5291

²⁷ Huwe, C. M.; Velder, J.; Blechert, S. *Angew. Chem.* **1996**, 35, 2376.

²⁸ Vehlouw, K.; Maechling, S.; Blechert, S. *Organometallics* **2006**, 25, 25.

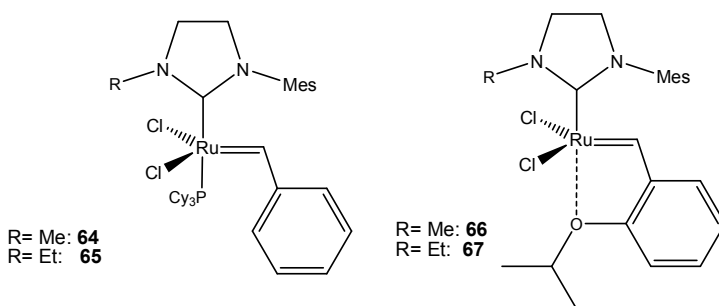
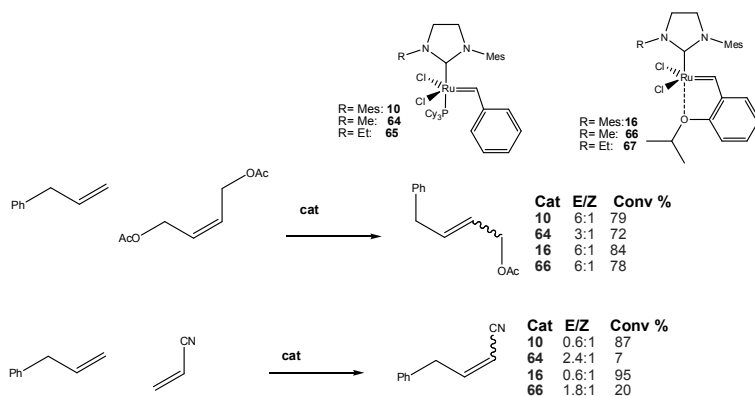


Figure 2. 19: *N*-alkyl, *N*-aryl substituted II generation Grubbs and Grubbs Hoveyda complexes 64-67

The novel metathesis initiators displayed activities similar to those of their symmetrical counterparts (**10** and **16**) in the RCM reaction of *N*-tosyl diallylamine.

Very interesting results were obtained testing the catalytic activity of the just mentioned complexes in some benchmark reactions. As a matter of fact while in the ring closing metathesis of *N*-tosyl diallylamine these new complexes displayed very similar activity to that of their commercially available analogues, in cross metathesis reaction differences in both yield and *E/Z* selectivity were obtained (as clear in Scheme 2. 3). It can be noticed that, in general, asymmetrical substitution at nitrogen atoms results in lower yields (from moderate to poor) and different *E/Z* ratios.



Scheme 2. 3 Comparative cross metathesis reactions.

Blechert *et al.*²⁹ also reported on a ruthenium-based catalyst bearing unsymmetrical NHC containing *N*-phenyl-*N'*-mesityl flaps, but unfortunately this complex undergoes fast decomposition. With the aim to further improve the application profile of Grubbs second-generation catalysts,³⁰ Ledoux *et al.* decided to synthesize Ru complexes with dihydroimidazolium NHC ligands bearing (in addition to a mesityl "flap") an aliphatic group with greater steric bulk than Me and Et reported by Blechert (**64-67** Figure 2. 19).

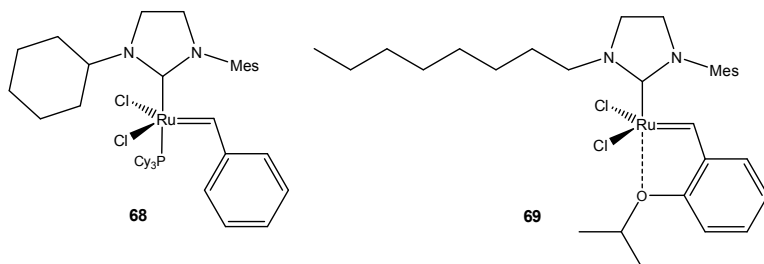


Figure 2. 20: NHC-Ru catalysts 68-69.

Complex **64** was synthesized and used as benchmark in a comparative study. The X-ray crystallographic analysis of **68** demonstrated that the mesityl group is coplanar with the phenyl ring of the benzylidene, showing that a π - π interactions between the mesityl arm and the benzylidene moiety constitutes an important structural element. Catalyst activities were explored in some standard metathesis reactions. A significant dependence of catalyst reactivity on the bulkiness of the NHC entities was observed. The most crowded NHCs correspond to the lowest RCM activity, while activity increases considerably for complexes bearing less bulky NHCs. The most active catalyst system was found to be complex **64** (Blechert catalyst), bearing an NHC ligand with the smallest alkyl moiety. This complex was found to display comparable activity with respect to **10**. It is therefore undeniable that the steric bulk of the *N*-side group is of great importance. These results clearly demonstrates that modification of the NHC ligand can induce substantial changes in the reactivity pattern of the corresponding

²⁹ Vehlow, K.; Gessler, S.; Blechert, S. *Angew. Chem.* **2007**, *46*, 8082.

³⁰ N. Ledoux, R. H. Linden, A.; Allaert, B.; Vander Mierde, H.; Verpoort, F. *Adv. Synth. Catal.* **2007**, *349*, 1692

catalysts and that systematic variation of the *N*-substituents may eventually allow for a fine-tuning of the catalytic properties.

Collins and Co-workers provided another family of ruthenium based systems bearing chiral monodentate NHC ligands.^{31,32} These complexes possess C_1 -symmetric *N*-heterocyclic carbene ligands adorned with one *N*-alkyl group and one *N*-aryl group. Complexes **70-73** showed high reactivity and high enantiomeric excess values in representative ARCM reactions, without the use of halide additives. It was also proposed that the barriers to the rotation of the NHC ligands in **70-73** play a significant role in determining the reactivity of the corresponding catalysts.

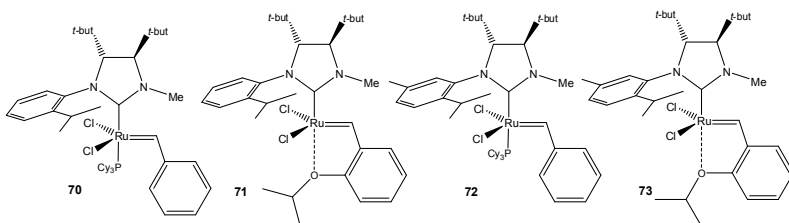


Figure 2. 21: Ruthenium complex 70-73 bearing chiral monodentate NHC ligands.

The balance between good turnover, high stability, ease of synthesis and handling as well as the possibility of re-use are ambitious goals to pursue. Theoretical and experimental studies together provide a fundamental starting point to try to reach the upper mentioned goals.

³¹ Fournier, P. A.; Collins, S. K. *Organometallics* **2007**, *26*, 2945

³² (a) Fournier, P. A.; Savoie, J.; Stenne, B.; Be'dard, M.; Grandbois, A.; Collins, S. K. *Chem.sEur. J.* **2008**, *14*, 8690. (b) Grandbois, A.; Collins, S. K. *Chem.sEur. J.* **2008**, *14*, 9323.

Chapter 3

Synthesis of new ruthenium based catalysts with a Syn Substituted N-heterocyclic Carbene Backbone

Abstract

A series of novel ruthenium olefin metathesis catalysts bearing N-heterocyclic carbene (NHC) ligands with varying degrees of backbone and N-aryl substitution have been synthesized and fully characterized. Many efforts were addressed in solution and solid state structure elucidation in order to explain the stability and the different catalytic behavior of these species. For catalyst activity evaluation see chapter 4 and 5.

Introduction

The research group in which I developed this PhD project has recently proved the pivotal role played by ligand symmetry in the design of highly active catalysts for the ring closing metathesis of hindered di-olefins. Both second generation Grubbs and Grubbs Hoveyda type complexes bearing a *meso* NHC ligand display better reactivity than their analogues with a C₂ symmetric NHC.

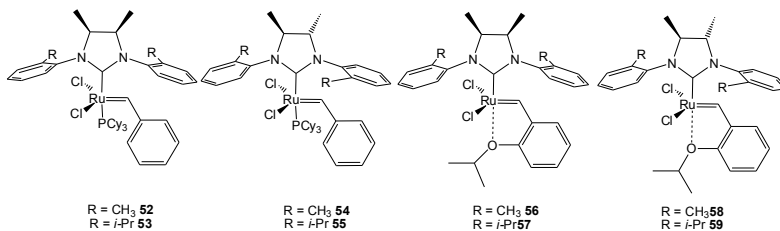


Figure 3. 1: *syn* and *anti* backbone symmetrical II generation Grubbs and Grubbs Hoveyda complexes

In particular, the *syn* complexes with *o*-tolyl N-substituents (**52** and **56**) are among the most efficient catalysts in the formation of tetrasubstituted olefins. The beneficial effect of the *syn* backbone is clearly noticeable in both phosphine and phosphine-free catalysts, highlighting that the observed reactivity is independent of the

initiation mechanism. This finding makes the NHC backbone symmetry a new key element that needs to be taken into account in designing ruthenium catalysts for olefin metathesis^{1,2}. The origin of this enhanced reactivity has been ascribed to the *syn* disposal of methyl groups on the backbone that induces a preferential *syn* orientation of the *N*-tolyl rings, thus providing a more accessible active space at the metal. Grubbs and co-workers already suggested *syn* orientation as the preferred one for catalysts **10** and **16**;³ nevertheless, no direct evidence has been reported up to now to confirm this hypothesis.

In an attempt to force *N*-aryl rings in adopting this beneficial conformation, thus enhancing catalyst efficiency, we address our synthetic efforts in order to produce monophosphine and phosphine-free NHC Ru catalysts with more encumbered *syn* backbone substituents, replacing methyl with phenyl groups

Our aim is to find the best compromise between electronic and steric effect of substituents on the backbone and at the *ortho* position of the *N*-aryl groups; this in order to reach top performances toward RCM, as well as to furnish a deeper understanding on the ligand symmetry relevance.

We also wanted to focus on other interesting aspects like the environmental sustainability⁴ and the industrial applicability of the technology.⁵

The first goal could be pursued by:

- synthesizing new complexes with a really good functional group tolerance in order to have the real possibility to lower the environmental impact of employed solvent (in addition to lowering its amount); or even better to completely avoiding solvents (neat conditions).

¹ Grisi, F.; Mariconda, A.; Costabile, C.; Bertolasi, V.; Longo, P. *Organometallics* **2009**, *28*, 4988

² Costabile, C.; Mariconda, A.; L. Cavallo, P. Longo, V. Bertolasi, F. Ragone and F. Grisi *Chemistry a European Journal*, **2011**, *31*, 8618

³ Stewart, I. C.; Benitez, D.; O'Leary, D. J.; Tkatchouk, E.; Day, M. W.; Goddard III, W. A.; Grubbs, R. H.; *J. Am. Chem. Soc.* **2009**, *131*, 1931.

⁴ Environmental sustainability is one of the three pillars of sustainability. More generally sustainable development, has been defined from the Brundtland Commission of the United Nations on March 20, 1987: "sustainable development is development that meets the needs of the present without compromising the ability of future generations to meet their own needs."

⁵ Nicola, T.; Brenner, M.; Donsbach, K. Kreye, P.; *Organic Process Research and Development* **2005**, *9*, 513.

- reducing the metal quantity necessary for the catalysis, which means less purification steps (time, money and pollution saving) and avoiding problems related to loss of metal (toxicity).

Another challenge we tried to pursue was the obtainment of an air and moisture stable complex (both in solution and solid state), whose reactivity could be controlled by temperature tuning and which offers the possibility to be reused (by linking on solid supports).⁶ These properties are, indeed, desirable in the scale up.

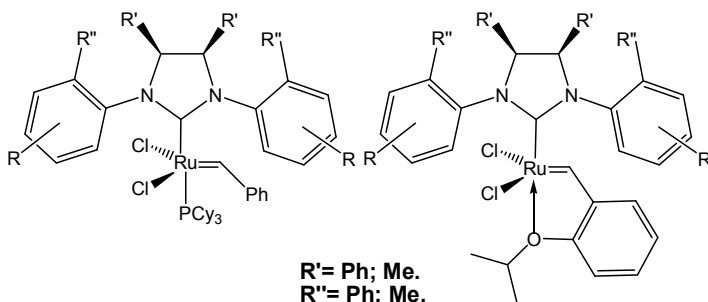


Figure 3. 2: new designed complexes.

Another of our goals is to achieve an easy synthesis for this class of highly efficient RCM catalysts, according to the new trend of environmental and economic sustainability (atom economy). These conditions are even more desirable, as previously mentioned, to perform the scale up of the reaction.

Modification of NHC backbone

Introduction

In order to realize all the just reported items, we decided to start changing the backbone substituents from methyl to phenyl groups. In this case, for the preparation of *syn* NHC-backbone substituted

⁶ (a) Yang, H.; Ma, Z.; Wang, Y.; Li Fang Y.; *Chem. Commun.*, **2010**, 46, 8659; (b) Keitz, B. K.; Grubbs R. H.; *Organometallics* **2010**, 29, 403; (c) Allen D. P.; Van Wingerden, M.M; Grubbs, R.H.; *Organic Letters*, **2009**, 6, 1261.

ligand, we used as starting material the commercially available “*meso*-1,2-diphenylethylenediamine”, a cheap and stable chemical at standard conditions.

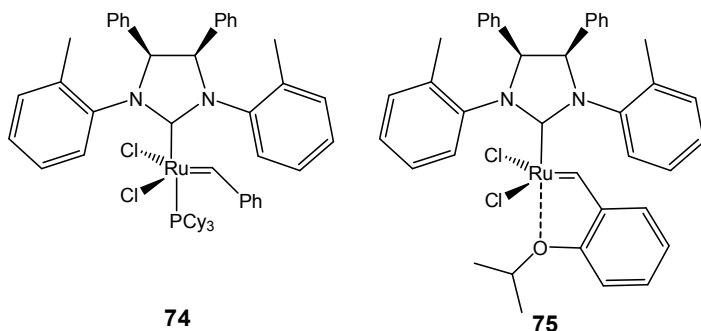
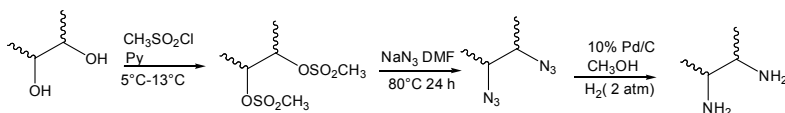


Figure 3. 3: newly synthesized phosphine and phosphine free complexes **74**, **75**

In this way, if the corresponding ruthenium complex (**74** and **75**) displays a catalytic behaviour at least similar (or even better) to that of the catalyst analogues derived from the *meso*-1,2-dimethylethylenediamine, we can skip three steps in the entire synthetic process (needed to prepare the starting diamine).⁷



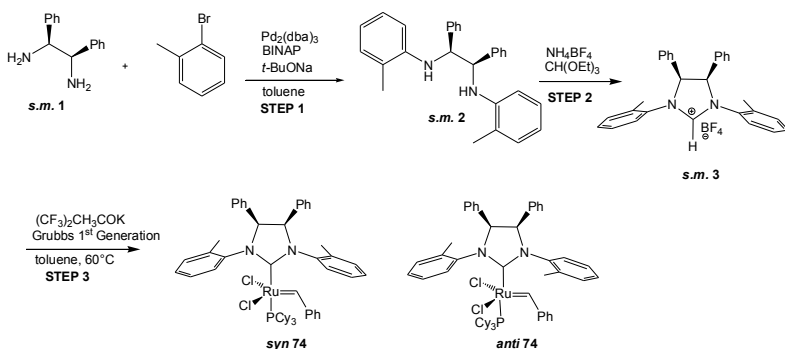
Scheme 3. 1: *meso*-1,2-dimethylethylenediamine synthesis.

Synthetic approach to complexes **74** and **75**

The synthesis of our first target (NHC-phosphine based Ru complex **74**, Scheme 3.2) was easily accomplished in three steps. The coupling of commercially available *meso*-1,2-diphenylethylenediamine (**s.m.1**) to *o*-tolyl groups by Pd-catalyzed reaction gave diamine **s.m.2**, which was subsequently converted to

⁷ Chooi, S. Y. M.; Leung, P.; Ng, S.; Quek, G. H.; Sim, K. Y. *Tetrahedron Asymmetry*, **1991**, *2*, 981.

imidazolidinium salt **s.m.3** by condensation with triethyl orthoformate. The corresponding free carbene was generated in situ by treatment of this salt with $(\text{CF}_3)_2\text{CH}_2\text{COK}$; $\text{RuCl}_2(=\text{CHPh})(\text{PCy}_3)_2$ (Grubbs' I) was then added and the solution was heated in toluene at 60°C .⁸ Surprisingly, chromatographic workup of the crude reaction mixture led to the isolation of two isomeric compounds. The major isomer, whose NMR showed an high symmetric conformational arrangement for the NHC ligand (second eluted compound, 42% yield), was named *syn* **74**; the minor isomer named *anti* **74**, (16% yield) was assumed to be the other reasonable conformation, in which the two methyl groups of the *N*-tolyl substituents on the NHC ligand are disposed in an *anti* relationship.



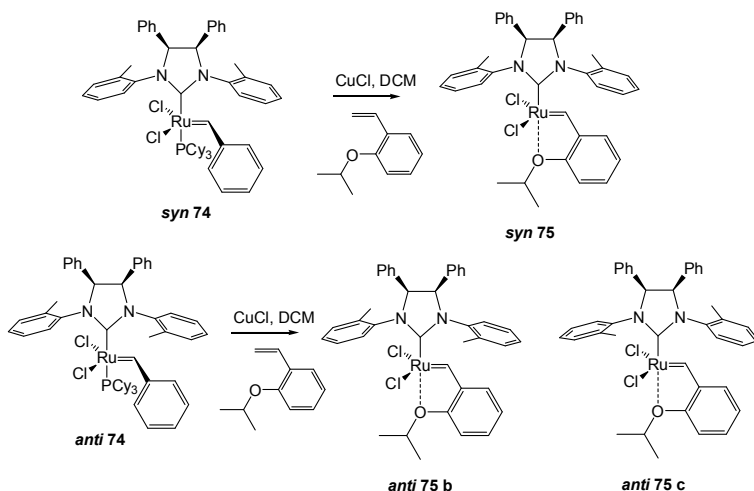
Scheme 3. 2: first explored synthetic strategy to *syn* **74 and *anti* **74**.**

To the best of our knowledge, this finding represents the first example of conformational control induced by substituents on the NHC backbone that allows for a separation of rotational isomers. Intrigued by these evidence we decided to further investigate on these isomeric structures. In particular, since many crystallization attempts failed we performed solution state structure studies (see Figure 3.6 to Figure 3.12). The obtained NMR data were not sufficient to corroborate irrefutably our structural hypothesis. So to gain further information, we decided to transform the two isomers of **74** into the corresponding II generation Grubbs Hoveyda complexes **75** exploiting an exchange ligand procedure reported first by

⁸ Funk, J. T. W.; Berlin, M.; Grubbs, R. H.; *J. Am. Chem. Soc.* **2006**, *128*, 1840.

Hoveyda and co-workers⁹. Indeed, by reducing the number of possible conformers of **74** through the introduction of the chelating 2-isopropoxybenzylidene ligand (Hoveyda ligand), we could deduce important structural information to prove our structural identification of isomers of **74**.

Syn 75 was quantitatively obtained exchanging the phosphine fragment of *syn 74* by reacting with 2-isopropoxystyrene in presence of CuCl. The same reaction was conducted on *anti 74* affording a mixture of two isomers of the corresponding Grubbs Hoveyda complex: *anti 75 b* and *anti 75 c* (84% of overall yield). *Anti 75 b* and *anti 75 c* were not separable by column chromatography. Characterization via ¹H and ¹³C NMR spectroscopy confirmed the presence of only two isomers in variable ratio (1:1.7 in CD₂Cl₂; 1:2.8 in C₆D₆), corresponding to the different arrangement of the *anti* oriented *N*-tolyl groups of the NHC with respect to the isopropoxybenzylidene ligand (*anti 75 b* and *anti 75 c*).



Scheme 3. 3: ligand exchange procedure toward ether based complex 75.

Actually the application of this synthetic strategy resulted as a winning solution to gain indirect information on **74** isomeric structures. In fact crystals of *syn 75* obtained by vapor diffusion of pentane into a saturated benzene solution at room temperature,

⁹ Garber, S. B.; Kingsbury, J. S.; Gray, B. L.; Hoveyda, A. H. *J. Am. Chem. Soc.* **2000**, *122*, 8168.

showed a diffraction pattern which confirms that the two *ortho* methyl groups at the nitrogen atoms are in a mutual *syn* arrangement and on the opposite side of the two encumbered backbone phenyl groups with respect to the NHC plane, as presumed for complex *syn* **74**.

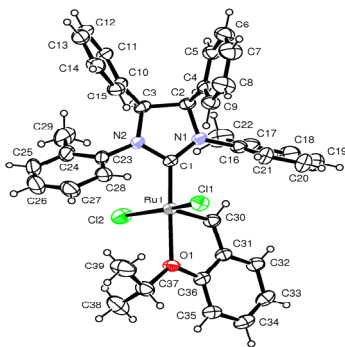
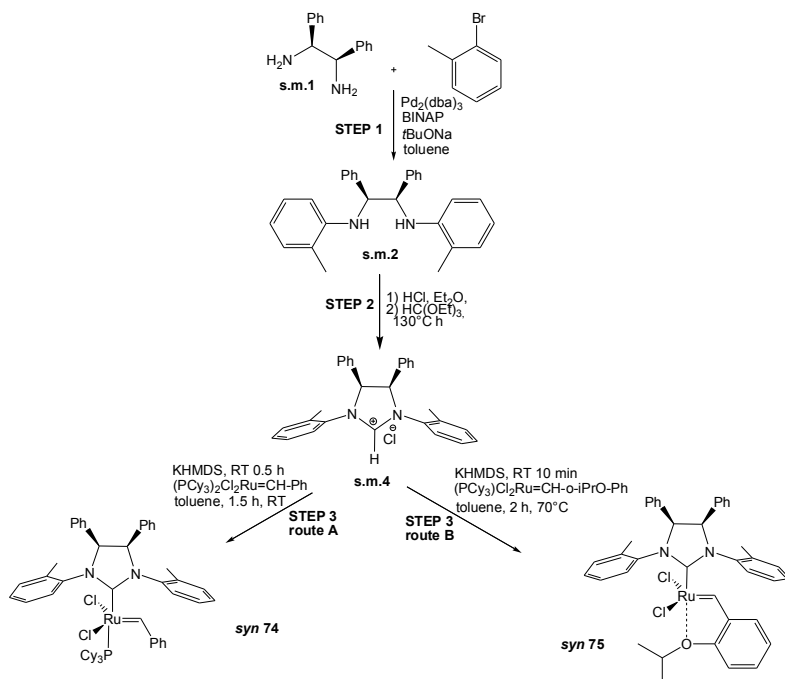


Figure 3. 4: ORTEP view of complex *syn* **75**.

Despite numerous attempts, crystals of *anti* **75** suitable for X ray analysis were not obtained (probably because of conformational disorder of this complex). Many efforts were also addressed to elucidate the structure in solution for this mixture of atropisomers through 2D NMR (NOESY and ROESY) and variable temperature experiments.

In an attempt to improve the yields of the synthesis of **74** and **75**, we decide to explore another synthetic route which involves the deprotonation of the imidazolium chloride (*s.m.* **4**) with KHMDS and the successive reaction with first generation Grubbs or Grubbs Hoveyda complex to gain respectively compounds **74** and **75** (Scheme 3. 4). Although overall yield is only little increased (60% for *syn* **74** and 55% for *syn* **75**), by following this synthetic route we did not observe the formation of the less abundant isomer (*anti* **74**) which should be strictly related to the previously illustrated experimental conditions. *Anti* **74**, as described in the next chapter, is less active in catalysis than its *syn* analogue (*syn* **74**); so the latter synthetic route which avoids its formation favouring increased amount of the most catalytic active isomer is much more fruitful. Moreover, the purification step to obtain pure *syn* **74** consists of

only methanol washing of the reaction mixture, instead of purification by column chromatography.



Scheme 3. 4: synthetic route to *syn* 74 and 75 via chloride salt intermediate *s.m.* 4

NMR studies of the conformational isomers of 74 and 75

Solution state studies represent a valid method to gain structural information. It furnishes dynamic information of molecules behavior in solution that can result quite different with respect to crystalline arrangement; so it results a complementary method over than an alternative.

Variable temperature (VT) NMR experiments were conducted in the range of $-60^\circ\text{C} < T < 25^\circ\text{C}$ for *syn* and *anti* 74 and from -60°C to 100°C for *syn* and *anti* 75. These analyses showed that both complexes 74 and 75 present atropisomers. In order to rationalize the dynamic behavior in solution, considering the possible rotations

(τ_1 , τ_2 , ϕ , θ in Chart 3. 1) within **74** and **75**, a different number of isomers of **74** and **75** is in principle possible in frozen conditions.

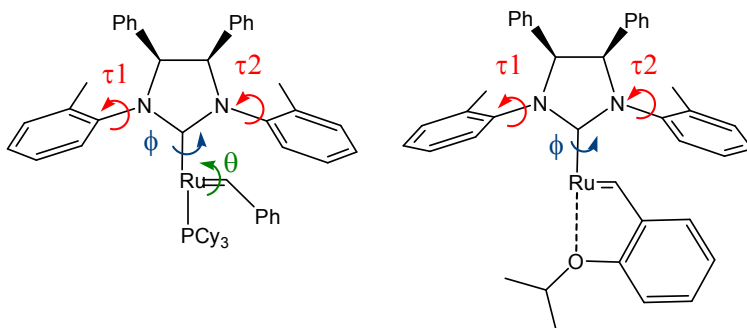


Chart 3. 1: dynamic processes in Grubbs and Grubbs-Hoveyda second generation complexes

We made the reasonable assumption that for complex **74** and **75** bearing two bulky phenyl on the backbone, τ rotations are inhibited for steric constriction. So we could expect the presence of isomers derived from both ϕ and θ rotations for phosphine based complexes and from only ϕ rotation for Hoveyda type ones.

Conformational studies on phosphine based complexes **74**

Variable Temperature ^1H and ^{31}P NMR experiments

Complex *syn* **74**

The room-temperature ^1H NMR spectrum of *syn* **74** shows evidence of an exchange process that produces a broad resonance for the carbenic protons as well as for the backbone protons.

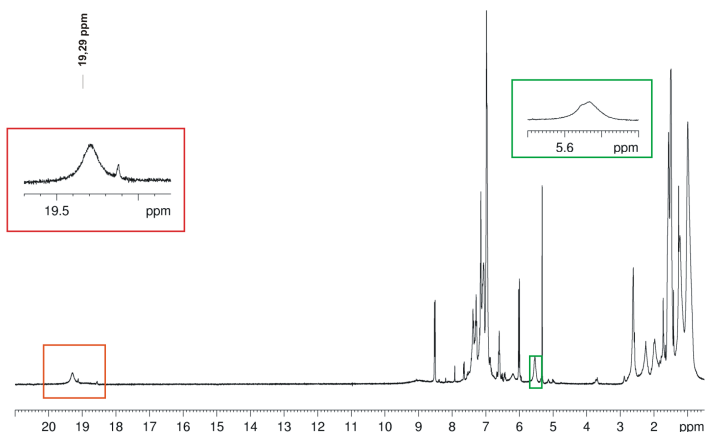


Figure 3. 5: ^1H -NMR for *syn* 74 dissolved in CD_2Cl_2 at 25°C

Most of the other signals result broadened and overlapped, further indicating the presence of more than one isomer in solution. Also ^{31}P -NMR (recorded in CD_2Cl_2 as well) presented a single broad signal at RT.

Upon cooling, both the ^1H and ^{31}P spectra (in CD_2Cl_2) sharpen, revealing the presence of two rotational isomers. Resonances corresponding to a major and minor form (average ratio about 9:1) can be identified (Figure 3.7, bottom) in both nuclei spectra.

As previously reported for analogous complexes,^{1,2,10} the favored NHC conformation is that with *syn*-related *N*-aryl groups and *syn* backbone phenyl substituents pointing on the opposite sides of the catalyst. As a consequence, in frozen conditions only two isomers are in principle possible, resulting from the rotation around the benzylidene C-Ru bond or the rotation about the Ru-NHC bond.

¹⁰ Berlin, J. M.; Campbell, K.; Ritter, T.; Funk, W.; Chlenov, A.; Grubbs, R. H. *Org. Lett.* **2007**, *9*, 1339

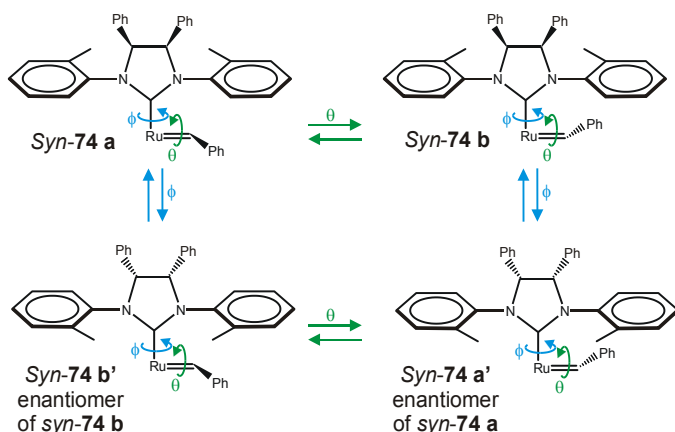


Figure 3. 6: possible rotational isomers for *syn 74*

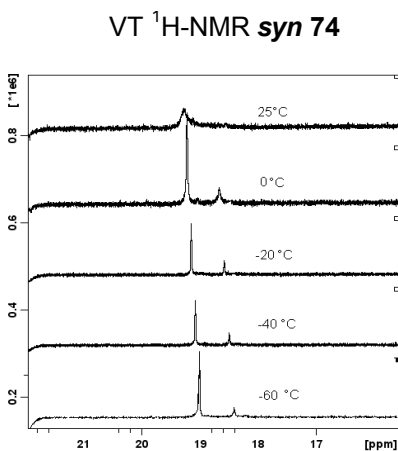


Figure 3. 7: VT $^1\text{H-NMR}$ of *syn 74*, in CD_2Cl_2 (carbenic region)

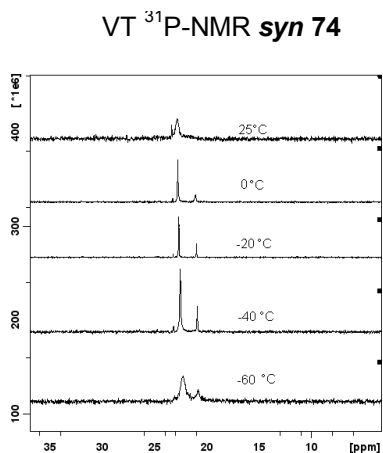


Figure 3. 8: VT $^{31}\text{P-NMR}$ of *syn 74* in CD_2Cl_2

Complex *anti 74*

At the first sight the $^1\text{H-NMR}$ of complex *anti 74* (Figure 3.9) indicates a different symmetry for the NHC ligand. In particular the protons on the backbone appear as two sharp singlets each integrating for one proton (δ around 5 ppm); while in *syn 74* they are NMR equivalent, resulting in a single broad signal (integrating for two protons). Another significant difference which catches

immediately the attention, is the sharpness of the alkylidene proton at 19.08 ppm (while in *syn* **75** the corresponding signal is a broad resonance at 19.29 ppm; see Figure 3.5).

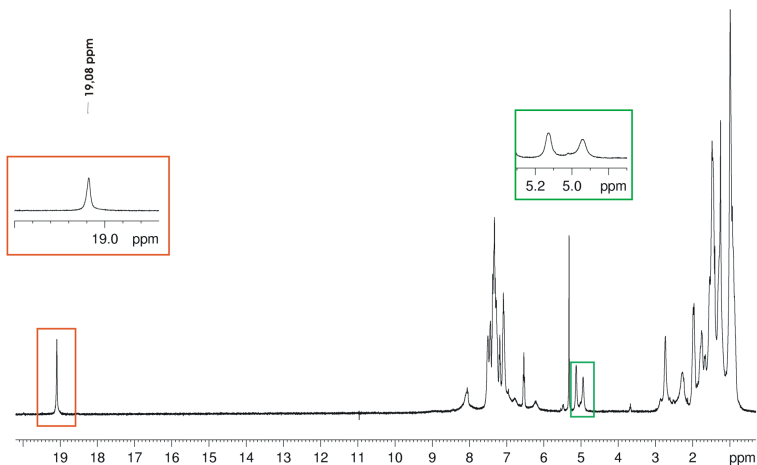


Figure 3. 9: $^1\text{H-NMR}$ for *anti* **74** dissolved in CD_2Cl_2 at 25°C

^1H and ^{31}P NMR experiments at variable temperature (in deuterated dichloromethane) for *anti* **74** highlights the presence of four isomers in solution at low temperature. These four rotational isomers can be justified by considering an *anti* orientation of *N*-tolyl groups and all the possible isomers obtained by rotating around the benzylidene C-Ru and/or Ru-NHC bond (Figure 3. 10 bottom).

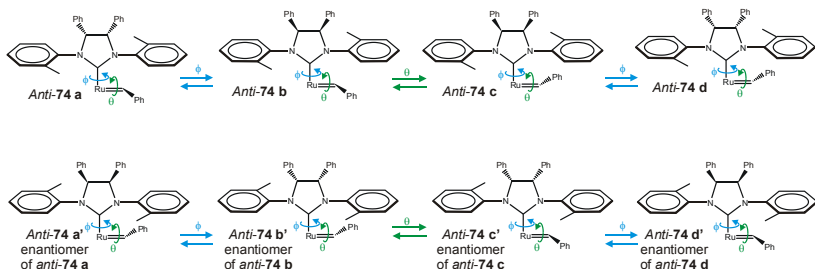
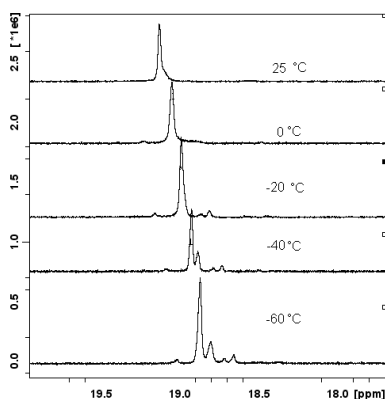
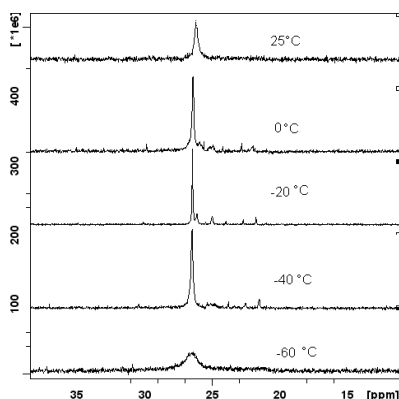


Figure 3. 10: possible rotational isomers for *anti* **74**

VT ^1H -NMR *anti* **74**Figure 3. 11: VT ^1H -NMR of *anti* **74**, in CD_2Cl_2 (carbenic region)VT ^{31}P -NMR *anti* **74**Figure 3. 12: VT ^{31}P -NMR of *anti* **74** in CD_2Cl_2

Conformational studies on Hoveyda derivative **75**

Variable Temperature ^1H and ^{31}P NMR experiments

Complex *syn* **75**

Variable temperature ^1H -NMR has been conducted varying the temperature from -60°C to 100°C . The low temperature experiments ($-60 < T < 25$) $^\circ\text{C}$ have been performed in CD_2Cl_2 while the high temperature analysis has been carried out in $\text{C}_2\text{D}_2\text{Cl}_4$. Collected spectra strongly suggest that this complex adopts a unique conformation. Indeed the NMR signal pattern does not undergo any significant changes both by lowering and increasing temperature. Carbenic region, in particular, shows always one resonance confirming the presence of a single isomer for this complex. This is in agreement with the experimental evidence that the transformation of *syn* **74** (2 isomers) into *syn* **75** via ligand exchange procedure leads to only one isomer. Since *syn* **75** contains a bidentate alkylidene ligand, the only possible rotation within this complex is around ϕ , which gives the enantiomer of *syn* **75** (not NMR distinguishable). The mutual orientation of phenyl and methyl substituents has been also confirmed by the crystallographic analysis conducted on this sample.

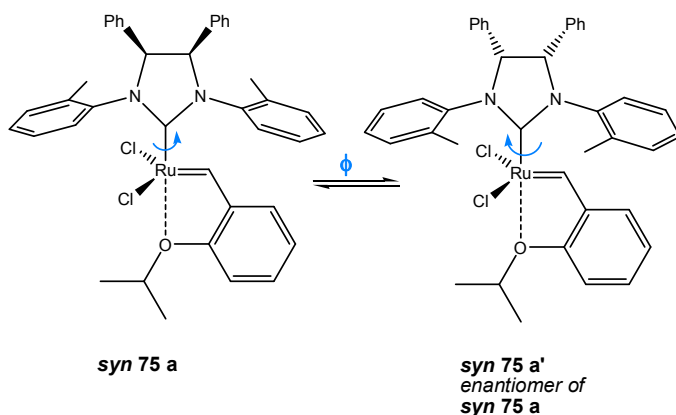


Figure 3. 13: rotational isomers for complex *syn 75*

It is worth to note that *syn 75* is extremely robust since its NMR spectrum remains unchanged at RT for several days also after both increasing and lowering the temperature in a range of 160°C (-60°C < T < 100°C).

The ¹H-NMR acquired at 100°C (see Figure 3.14) shows that the whole symmetry of the complex has changed. This is clearly visible by the vanishing of resonance at 8.8 ppm while signals related to the backbone protons overlap as the ones of the four methyl groups. This signal pattern could be related to the fast rotation of the NHC unit or to the lack of coordination among the oxygen of the isopropoxybenzylidene moiety and the metal, very likely because the high temperature renders labile this interaction allowing for nearly free rotation around the Ru-alkylidene bond.

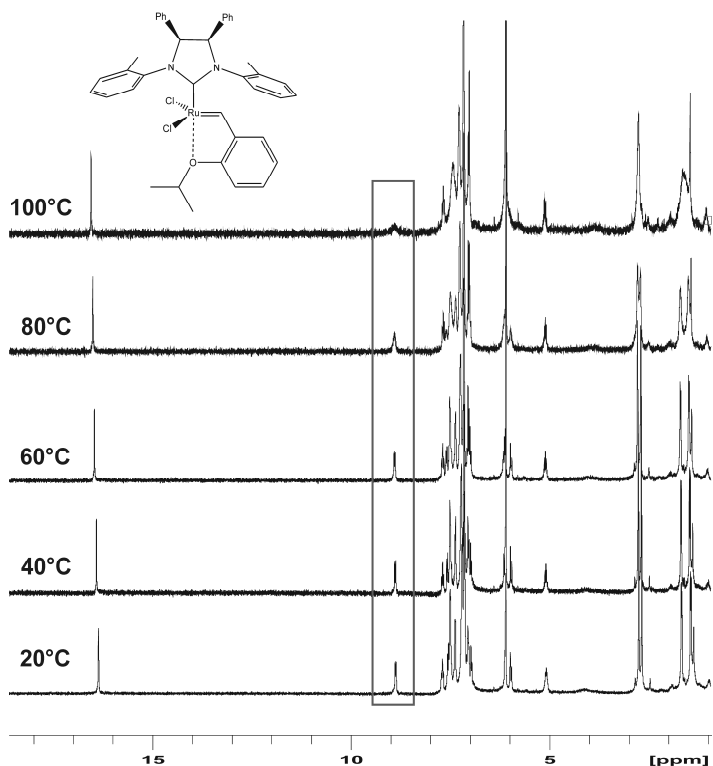


Figure 3. 14: HT $^1\text{H-NMR}$ analysis for complex *syn 75*. $\text{C}_2\text{D}_2\text{Cl}_4$

It is worth to note that standard conditions for the employment of Hoveyda type complexes in catalysis consider a reaction temperature of 60°C ; in fact it is generally accepted that the initiation step proceeds via an interchange mechanism, possibly with associative character for the substitution of the coordinated ether with the olefinic substrate. The weakening of the interaction oxygen-metal plausibly observed at 100°C could corroborate the proposed initiation reaction mechanism for this class of catalysts, underlining that the dissociation of the ether moiety of the chelating ligand requires very harsh conditions. The high thermal stability of Hoveyda complexes is strictly related to their structural peculiarity which renders this system more rigid.

Complex anti 75

Anti 75 exists in solution as a mixture of two isomers not separable by column chromatography, which ratio varies depending on analysis parameters (temperatures and deuterated solvents for instance).

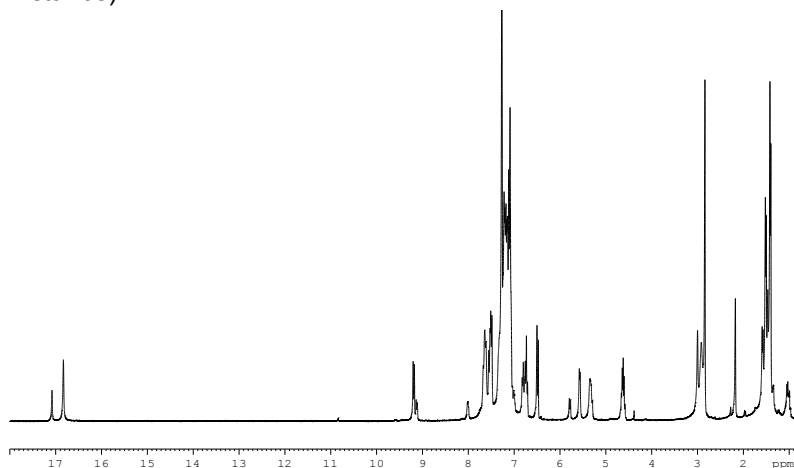


Figure 3. 15: $^1\text{H-NMR}$ (400 MHz, C_6D_6) of *anti-75*

Variable temperatures ^1H NMR experiments have been conducted ranging from -60 to $+70^\circ\text{C}$. The low temperatures experiments ($-60 < T < 25$) $^\circ\text{C}$ have been performed in CD_2Cl_2 while the high temperature ones have been carried out in $\text{C}_2\text{D}_2\text{Cl}_4$. The analysis of the signal patterns confirms the presence of two isomers with a temperature and solvent dependent ratio.

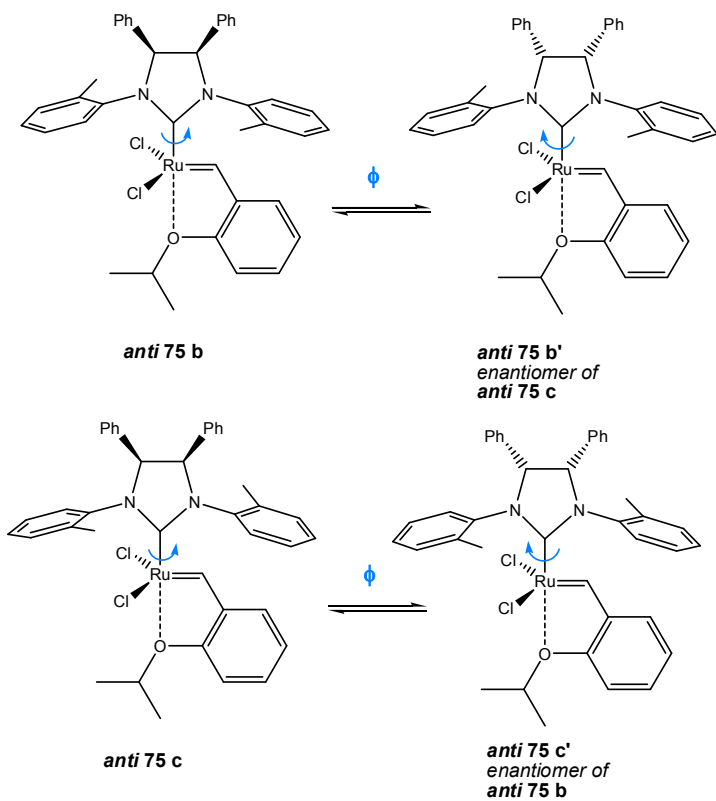


Figure 3. 16: rotational isomers for complex *anti* 75

Computational studies

According to Density Functional Theory (DFT) studies on the complex stability performed by Doct. Chiara Costabile, four minimum energy structures were located for complex **75**. Geometries and energies of the four possible isomers of complex **75** are shown in Figure 3. 17.

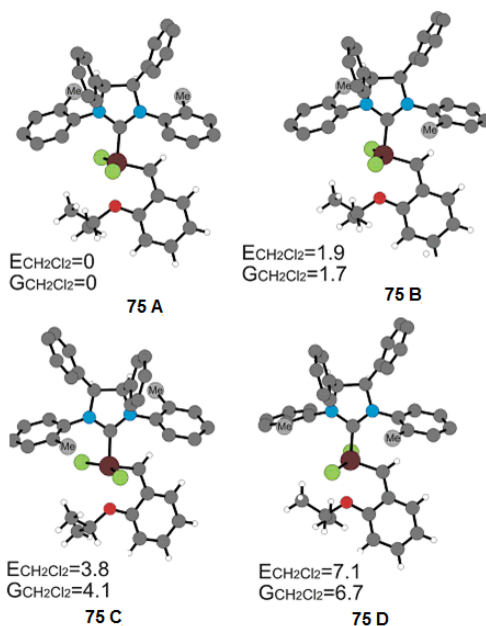


Figure 3. 17 relative energies for complexes **75**

Internal and free energies in CH_2Cl_2 reported in Figure 3. 17 indicate that the lowest energy structure **75A** corresponds to the most abundant *syn* **75** isomer, characterized by X-ray diffraction as well. Moreover, **75B** (*anti* **75b**) was found to be more stable than **75C** (*anti* **75c**), possibly indicating **75B** as the major *anti* form. The high energy of **75D** would explain the presence of only three isomers experimentally observed. Reaction thermodynamics for the isomerization process from the minor isomer to the major isomer of *anti* **75** were derived from VT ^1H NMR analysis ($\Delta H^\circ = -1.5 \text{ kcal mol}^{-1}$ and $\Delta S^\circ = -4.0 \text{ kcal mol}^{-1} \text{ K}^{-1}$) (see experimental procedures). The comparison of calculated and experimental energy differences

strongly indicates **75B** as the major *anti* isomer. Indeed, calculated ΔE between **75B** and **75C** is 1.9 kcal/mol (Figure 3.17) in good agreement with experimental ΔH of 1.5 kcal/mol.

2D NMR studies

Interesting information regarding the exchange process between the two isomers has been derived from 2D NOESY/EXSY experiments.

In fact at room temperature a chemical exchange between the major (*anti* **75 b**) and the minor isomer (*anti* **75 c**) that can occur through rotation of the NHC ligand has been observed.

Exchange cross-peaks observed in the EXSY spectrum of *anti*-**75** allowed us to evaluate as 1.35 s^{-1} the rate constant for the *anti* **75 b** \rightarrow *anti* **75 c** direct travel, corresponding to a free energy of activation of $17.3 \text{ kcal mol}^{-1}$, while a rate constant of 3.85 s^{-1} was evaluated for the inverse run *anti* **75 c** \rightarrow *anti* **75 b** ($\Delta G^\ddagger = 16.6 \text{ kcal mol}^{-1}$).

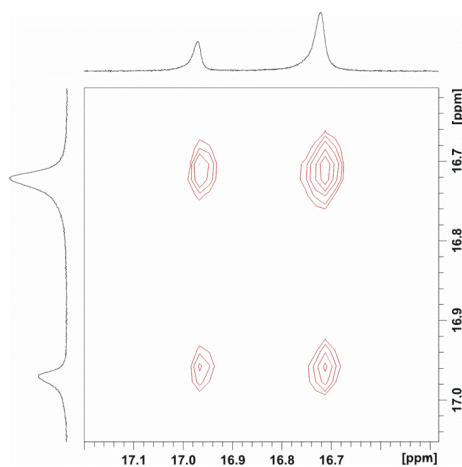


Figure 3. 18: Carbenic region of 400MHz ^1H 2D NOESY/EXSY in C_6D_6 at RT.

It is important to underline that complex *syn* **75** is extremely stable toward oxygen and water in the solid state. It is also very robust in solution where the retention of the benzylidene signal, monitored by ^1H NMR spectroscopy, is observed for very long periods (one week in CD_2Cl_2 and more than one month in C_6D_6). *Anti* **75** displayed a little lower stability than its NHC higher symmetry counterpart. In particular its related ^1H -NMR spectrum remains intact when complex is dissolved in benzene for two weeks while in dichloromethane it results stable for about three days.

Modification of NHC backbone and *N*-aryl substituents

Introduction

The systematic evaluation of the modification of substituents on the NHC ligand to determine their effect on the efficiency of the corresponding catalysts has led us to replace *o*-tolyl with *o*-phenyl groups in 1,3 positions, keeping the two *syn* phenyl groups on the backbone positions (4, 5).

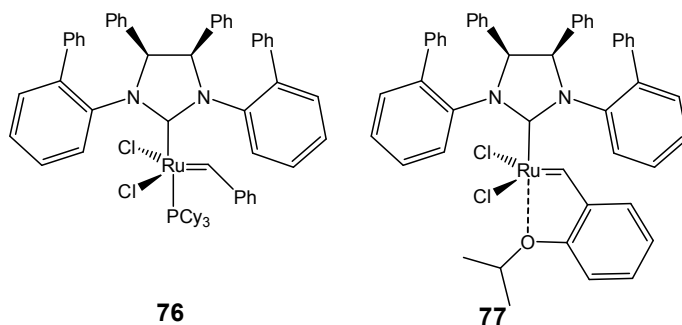


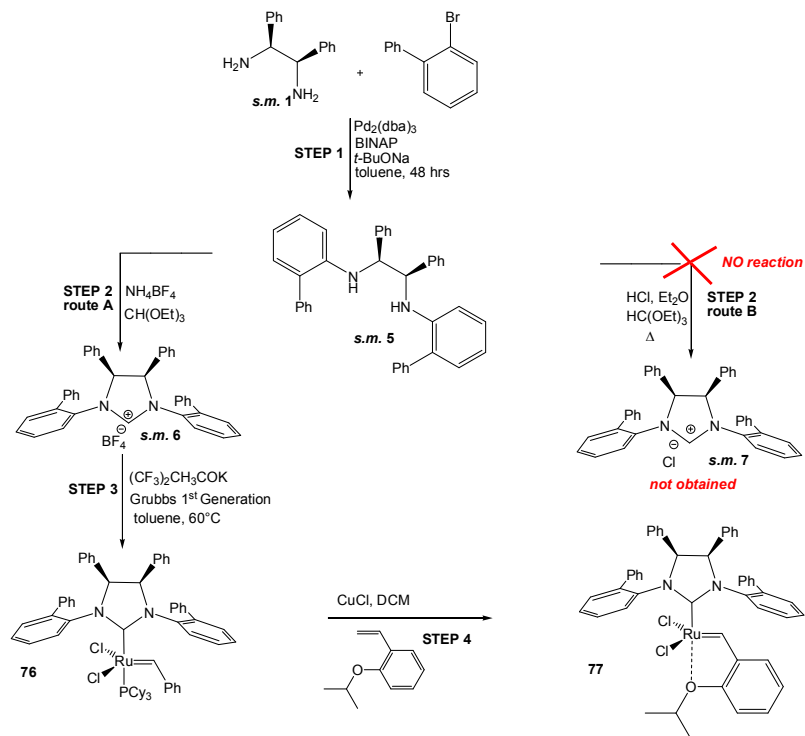
Figure 3. 19: newly synthesized phosphine and phosphine free complexes **76**, **77**

Synthetic strategy toward complexes **76** and **77**

The synthetic pathway to obtain this class of more encumbered complexes is quite similar to the one previously shown for complexes **74** and **75** (Scheme 3. 2 and Scheme 3. 3). For what concern the arylation step and the salification to the corresponding tetrafluoroborate salt we just needed to refine and optimize some of the reaction conditions seen before. (In particular since the desired adducts of this scheme resulted more encumbered, reaction conditions needed to be more harsh).

The synthesis **76** (Scheme 3.5) consists in three steps. The coupling of commercially available *meso*-1,2-diphenylethylenediamine (**s.m.1**) to *o*-bromobiphenyl was accomplished by Pd-catalyzed reaction which provides quantitatively diamine (**s.m.5**); this intermediate was subsequently converted to imidazolidinium salt **s.m.6** by condensation with triethyl orthoformate. This salt was treated with (CF₃)₂CH₃COK and

$\text{RuCl}_2(=\text{CHPh})(\text{PCy}_3)_2$ (Grubbs' I) to afford the desired complex **76** in a good yield of 66%.¹¹



Scheme 3. 5: synthetic strategies toward **76 and **77****

It is worth to note that we could never perform a direct synthesis of the II generation Grubbs Hoveyda derivatives **77** from the chloride salt **s.m.7** since its formation was not observed.

Complex **77** was quantitatively obtained employing the phosphine exchange procedure from corresponding II generation complex **76** (previously described to form **75** from **74**, see Scheme 3. 3)

Solution Structure studies

To gather precious information about solution state structure of this class of complexes, we performed variable temperature NMR analysis.

¹¹ Funk, J. T. W.; Berlin, M.; Grubbs, R. H.; *J. Am. Chem. Soc.* **2006**, *128*, 1840.

Complex 76

The variable temperature analysis for this complex has been carried out in deuterated dichloromethane ranging the temperature from -60 to $+30$ for both ^1H and ^{31}P nuclei. Again we analyzed the most diagnostic regions of the NMR spectra to gain information about the real number of isomers in solution. At RT carbenic proton results as a broad peak which splits in two singlets lowering the temperature. This effect is already observable slightly cooling from 25 to 10°C . At temperatures as low as -60°C the two isomers exist in a major to minor ratio of $2.3:1$. By increasing the temperature the mixture results enriched in the less stable isomer, (reaching a 1.6 to 1 ratio at 10°C . Carbene peaks overlaps at 20°C and also all the other NMR signals of the complex appear broadened at room temperature.

This experimental evidence is in agreement with a *syn* isomeric structure of **76**, that is characterized by the two *ortho* phenyls both located from the opposite side of the two backbone substituents with respect to the NHC plane and where rotations can occur around ϕ or θ (see Figure 3. 20)

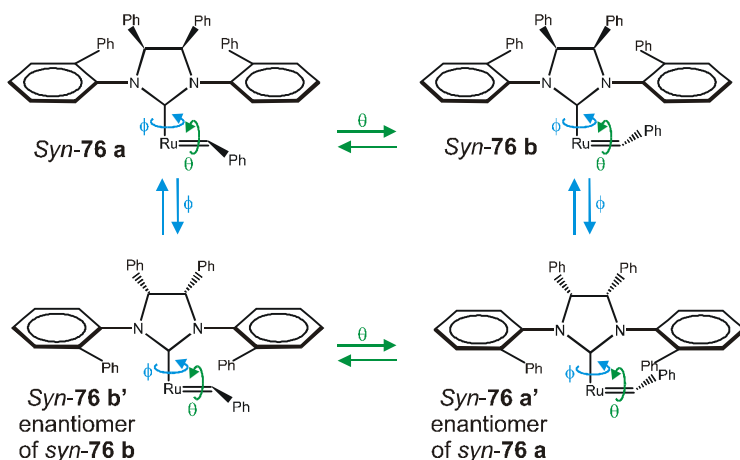


Figure 3. 20: allowed rotations for complex **76**

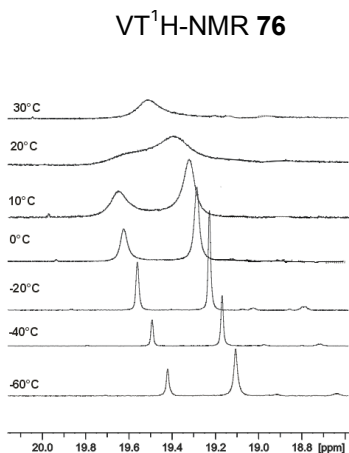


Figure 3. 21: variable temperature ¹H-NMR for **76**, CD₂Cl₂ carbenic region.

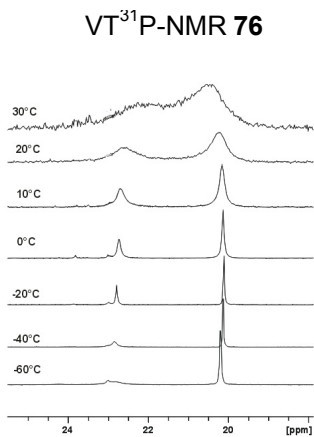


Figure 3. 22: variable temperature ³¹P-NMR for **76**, CD₂Cl₂.

Complex **77**

Variable temperature analysis has been conducted also on the Hoveyda derivative **77** revealing the presence of a single isomer coherent with a *syn* arrangement of the *N*-aryl groups on the opposite side of the phenyl substituents on the NHC backbone. On the other hand, this was quite predictable since complex was obtained from *syn* **76** by substituting the phosphine ligand.

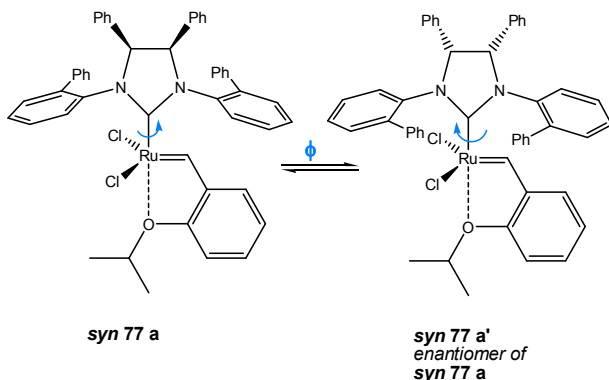


Figure 3. 23: active rotation for complex **77**

Modification of NHC backbone and *N*-aryl substituents

Introduction

A further modification of the NHC ligand has been achieved by exchanging the phenyl groups on the backbone with the methyls while keeping the *ortho* *N*-aryl substitution with a phenyl group. In this paragraph is reported the synthesis of the corresponding II generation phosphine and ether based complexes.

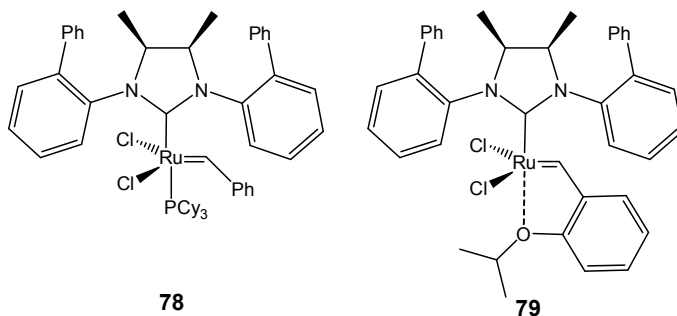
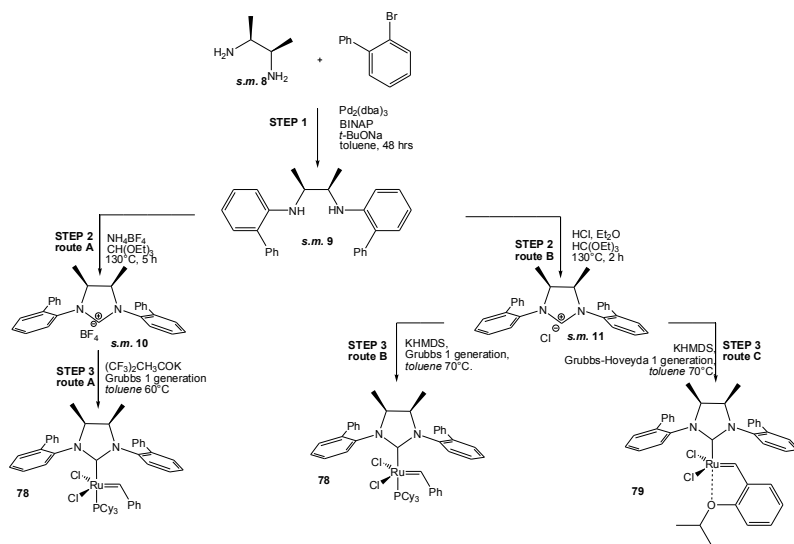


Figure 3. 24: newly synthesized phosphine and phosphine free complexes **78**, **79**

Synthetic strategy toward complexes **78** and **79**

Synthesis of phosphine and ether based second generation complexes **78** and **79** were accomplished following the procedures previously illustrated for **74** and **75**. It is worth to note that the starting diamine now is not commercially available so the whole synthetic process was longer and less easy handling since it involves a diazide as an intermediate (see Scheme 3. 1).



Scheme 3. 6: synthetic pathway to 78 and 79

Synthesis of complexes **78** and **79** is described in Scheme 3. 6. Starting diamines **s.m. 8** was prepared according to a published procedure⁷ (see Scheme 3. 1) and subsequently coupled to *o*-bromo biphenyl by Pd-catalyzed coupling to give diamines **s.m. 9**. Both dihydroimidazolium salts **s.m. 10** and **s.m. 11** were obtained by salification of the precursor, followed by condensation with triethyl orthoformate. The corresponding free carbene was generated in situ by treatment of those precursors with potassium hexamethyldisilazide (KHMDs) at room temperature and then reacted with alternatively first generation Grubbs or Grubbs Hoveyda complexes to afford the desired complexes respectively **78** (33% yield) and **79** (72% yield) as air- and moisture-stable solids after flash chromatography. **78** and **79** were fully characterized by ^1H , ^{13}C , and ^{31}P NMR. We explore another synthetic route in order to improve yield for complex **78**, that can also be obtained by using as starting material of **STEP 3** the tetrafluoroborate salt **s.m. 10** which is converted in the corresponding free carbene by reacting with $(\text{CF}_3)_2\text{CH}_3\text{COK}$ and finally coupled with Grubbs₃ first generation complex. Final yield is very similar to the one obtained exploiting the first commented synthetic route.

Solution Structure studies

Complex 78

The variable temperature NMR analysis of this complex has been carried out in dichloromethane varying the temperature from -60 to $+30$ for both ^1H and ^{31}P nuclei. As clearly visible in the bottom figures, by lowering the temperature the presence of at least two isomers in solution emerged. Carbene proton (^1H -NMR) resonates as a broad peak at 25°C but it splits in two singlets at lower temperatures. This effect is already visible passing from 25 to 0°C . At -60°C the two isomers exist almost in equal ratio ($1.3 : 1 =$ major: minor). The isomeric composition resulted enriched in the less stable isomer increasing the temperature from -60°C to RT where coalescence of the signals occurs. It is worth to note that at this temperature all the signals of the NMR spectra appear broad. In Figure 3. 27 and Figure 3. 27 are reported the spectra recorded. Signals variations are in agreement with the possible rotations (around ϕ or θ) for a complex in which the *ortho* phenyls are *syn* related and located from the opposite side of the two backbone methyl substituents with respect to the NHC plane.

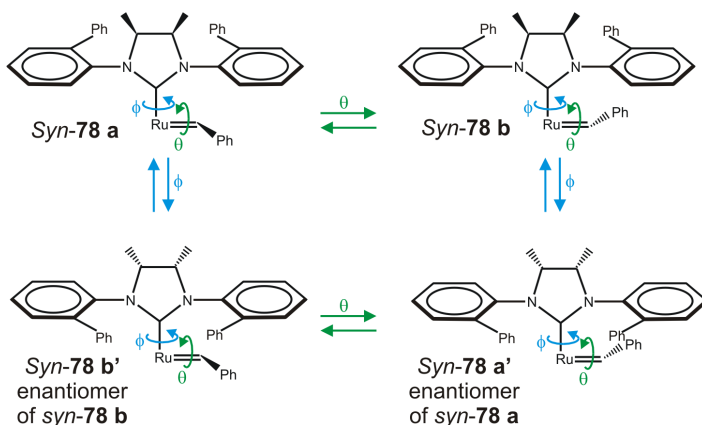


Figure 3. 25: allowed rotations for complex 78

VT ^1H -NMR 78

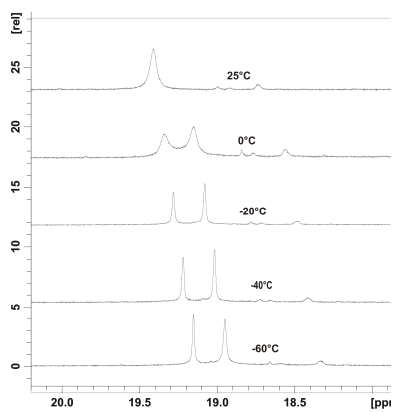


Figure 3. 26: variable temperature ^1H NMR for 78

VT ^{31}P -NMR 78

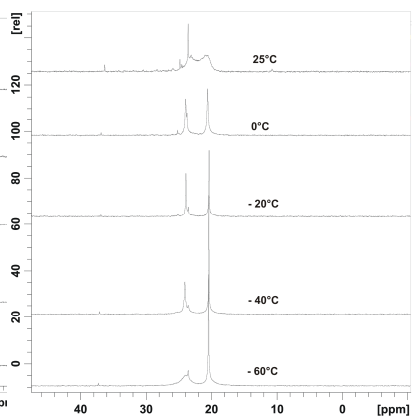


Figure 3. 27: variable temperature ^{31}P NMR for 78

It is worth to note that this complex results quite unstable both in solid and solution state. For this reason an accurate ^{13}C -NMR characterization was not performed; indeed **78** decomposes in benzene solution over a weekend and it is quite unstable also as solid: even if stored in a glove box at -20°C compound **78** decomposes in about one months.

Complex **79**

Variable temperature NMR analysis conducted upon cooling from 30 to -60°C on Hoveyda derivative **79** confirms the presence of a single isomer in solution which can be justified considering a mutual *syn* orientation of the *ortho* phenyl groups which are both tilted away with respect to the NHC plane. By rotating around Ru-NHC bond complex **79** generates its enantiomer which is, of course, not NMR distinguishable.

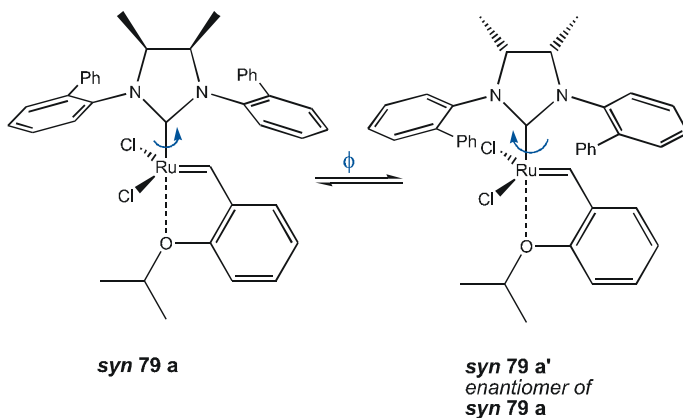


Figure 3. 28: active rotation for complex **79**

Conclusion

Eight new complexes have been synthesized and fully characterized. The employment of a suitable substituted NHC (with two phenyl groups in mutual *syn* stereochemical relationship) enables, for the first time, the facile synthesis of separated, stable conformers of *N*-tolyl Ru complexes.

Together with previously reported catalysts **52**,¹ **56**,¹ complexes **74-79** form a library on which we focused in order to highlight differences on intriguing aspects like stability and SAR arising from different steric and electronic properties of the NHC ligand.

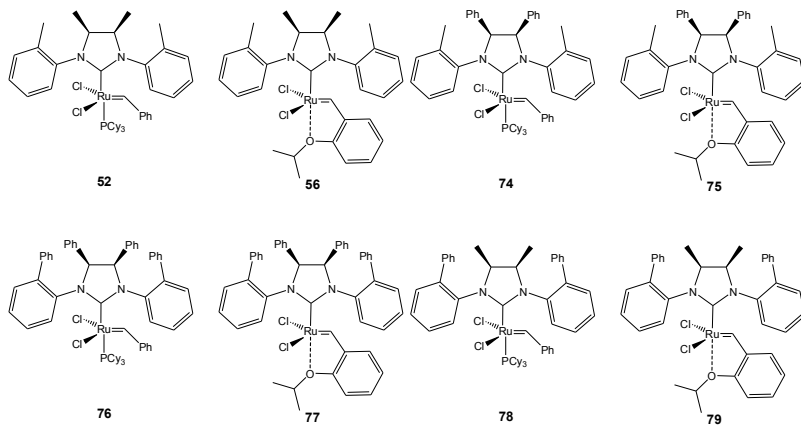


Figure 3. 29: catalyst developed library

Experimental Procedure

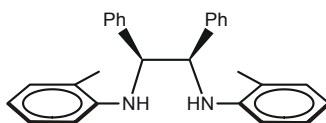
General information.

All reactions involving metal complexes were performed under nitrogen atmosphere using standard Schlenk or glovebox techniques. All of the reagents were purchased from Sigma-Aldrich Company and were of reagent grade quality. These products were used without any further purification. Solvents were dried and distilled before use. Deuterated solvents were degassed under an N₂ flow and stored over activated 4 Å molecular sieves. Flash column chromatography of organic compounds was performed using silica gel 60 (230-400 mesh), and flash column chromatography of ruthenium compounds was performed using silica gel 60 (230-400 mesh) from TSI Scientific (Cambridge, MA). Analytical thin-layer chromatography (TLC) was performed using silica gel 60 F254 precoated plates (0.25 mm thickness) with a

fluorescent indicator. Visualization of TLC plates was performed by UV light and KMnO_4 or I_2 stains.

NMR spectra were recorded on a Bruker Avance 250 spectrometer (250 MHz for ^1H ; 62.5 MHz for ^{13}C), a Bruker AM 300 spectrometer (300 MHz for ^1H ; 75 MHz for ^{13}C), or a Bruker AVANCE 400 spectrometer (400 MHz for ^1H ; 100 MHz for ^{13}C ; 161.97 MHz for ^{31}P). The ^1H and ^{13}C NMR chemical shifts are referenced to Me_4Si ($\delta = 0$ ppm) using the residual portion impurities of the deuterated solvents as internal standard. ^{31}P NMR spectra were referenced using H_3PO_4 ($\delta = 0$ ppm) as an external standard. Spectra are reported as follows: chemical shift (ppm), multiplicity, integration and coupling constant (Hz). Multiplicities are abbreviated as follows: singlet (s), doublet (d), triplet (t), quartet (q), multiplet (m), and broad (br). Elemental analyses were done on a PERKIN-Elmer 240-C analyzer. ESI-MS were performed on a Waters Quattro Micro triple quadrupole mass spectrometer.

Synthesis



S.m.2

Synthesis of *s.m.2*

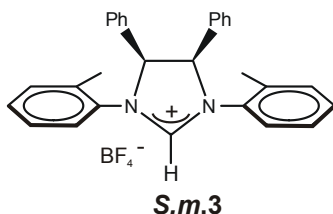
Under nitrogen atmosphere, tris(dibenzylideneacetone)dipalladium(0) ($\text{Pd}_2(\text{dba})_3$) (0.236 mmol, 216 mg), 2,2'-bis(diphenylphosphino)-1,1'-binaphthyl (BINAP) (0.565 mmol, 351 mg), sodium *tert*-butoxide (NaOtBu) (14.1 mmol, 1.36 g) and toluene (15.8 mL) were introduced in a flask equipped with a reflux condenser and stirred for 20 min. After this time, *meso*-1,2-diphenylethylenediamine **s.m.1** (4.71 mmol, 1g) and 2-bromotoluene (9.12 mmol, 1.2 mL) were added and the solution was then heated to 90°C for 16 hours. The reaction mixture was then cooled at room temperature, diluted with hexane and filtered

through a plug of silica gel. The product was eluted from silica gel with methylene chloride. The solvent was removed under vacuum to give **s.m.2** as a pale yellow solid (4.60 mmol, 1.80 g, 97.5%).

¹H NMR (250 MHz, CDCl₃): δ 7.23 (t, 6H), 7.05 (br s 1H), 7.02-6.97 (m, 5H), 6.91 (t 2H *J* = 7.77 Hz) 6.60 (t, 2H *J* = 7.24 Hz), 6.32 (d, 2H), 4.98 (d, 2H *J* = 6.06 Hz), 4.46 (br d, 2H, *J* = 7.33 Hz), 2.16 (s, 6H).

¹³C NMR (75 MHz, CDCl₃): δ 144.4, 138.6, 130.2, 128.5, 127.9, 127.6, 127.1, 122.7, 117.7, 111.7, 62.6, 17.8.

ESI⁺MS: *m/z* = 393.15 (MH⁺).



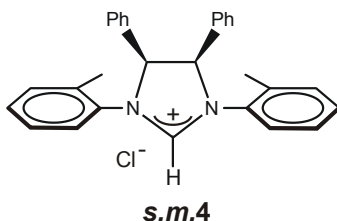
Synthesis of **s.m. 3**

Triethyl orthoformate (2.7 mL), diamine **s.m.2** (2.05 mmol, 800 mg) and ammonium tetrafluoroborate (2.46 mmol, 258 mg) were introduced in a 50 mL round-bottom flask equipped with a magnetic stirrer. The reaction mixture was heated at 120°C for 12 h. After cooling to room temperature, the product was precipitated and washed with Et₂O (3 x 10 mL). The solid obtained was dissolved in the minimum amount of CH₂Cl₂ and then filtered. The solution was concentrated and purified by silica gel chromatography (*n*-hexane/Et₂O = 1:1 to DCM /MeOH = 20:1). The fractions containing the desired product were collected and the volatiles were removed *in vacuo* to afford **s.m.3** as a yellow solid (1.45 mmol, 712 mg, 70.9% yield).

^1H NMR (250 MHz, CDCl_3): δ 8.46 (s, 1H), 7.55 (d, 2H), 7.19-7.18 (m, 6H), 7.0 (s, 10H), 6.7 (s, 2H), 2.6 (s, 6H).

^{13}C NMR (75 MHz, CDCl_3): δ 158.17, 133.39, 132.81, 132.31, 130.66, 129.68, 129.04, 128.68, 128.53, 127.86, 126.19, 71.26, 18.77.

ESI⁺MS: m/z = 403.1 [$\text{M} + (-\text{BF}_4^-)$].



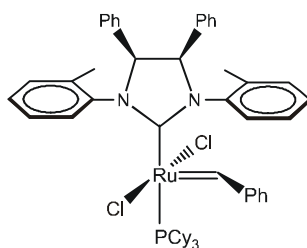
Synthesis of S.m.4

A diethyl ether solution of **s.m.2** was treated with a solution of hydrogen chloride (2.0 M in diethyl ether) to precipitate the diamine hydrochloride salt as an off-white powder. The product was collected by filtration and washed with diethyl ether. The diamine salt (1.94 mmol, 902 mg) and a large excess of triethyl orthoformate (3.3 mL) was placed in a 50 ml round bottom flask equipped with a magnetic stirrer. The flask was fitted with a condenser and heated to 135 °C in an oil bath for 2 hours. Upon cooling to room temperature, the solid product was washed several times with hexane and then with Et_2O to give the desired imidazolium chloride salt **s.m.4** as a pale yellow solid (1.52 mmol, 668 mg, 78.4% yield).

^1H -NMR (250 MHz, CD_3CN): δ 9.41 (br s, 1H); 7.52 (br s, 2H); 7.36–7.26 (br m, 6H); 7.14-7.10 (br m, 10H); 6.73 (br s, 2H); 2.6 (br s, 6H).

^{13}C NMR (62.5 MHz, CD_2Cl_2): δ 161.1, 133.9, 133.4, 132.4, 131.7, 130.0, 129.7, 128.6, 128.6, 127.9, 127.5, 72.3, 20.0

ESI⁺MS: m/z = 403.1 [M+(-Cl⁻)]



Syn-74

Synthesis of syn-74

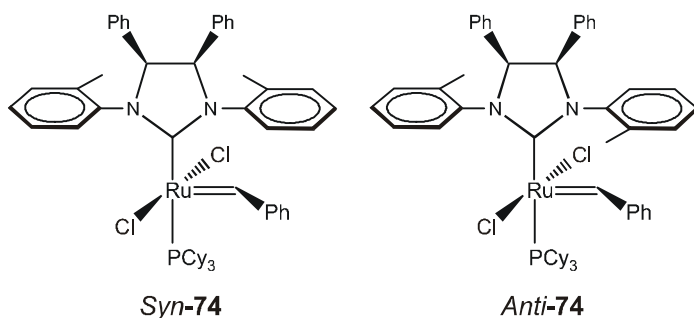
In a glovebox, a 10 mL Schlenk tube was charged with imidazolium salt **s.m.4** (0.341 mmol, 150 mg); potassium hexamethyldisilazide (KHMDS) (0.341 mmol, 0.68 mL, 0.5M in toluene) and (PCy₃)₂Ru(=CHPh)Cl₂ (0.227 mmol, 186 mg) were dissolved in 2 mL of toluene. The reaction mixture was stirred at room temperature for 1h; then toluene was evaporated under vacuum and a small amount of MeOH was added under stirring. The precipitated was filtered off, washed with MeOH, and dried *in vacuo*. The desired complex **syn-74** was obtained as a brown powder (0.114 mmol, 107 mg, 50%).

¹H NMR (400 MHz, C₆D₆): δ 19.83 (br s, 1H); 9.07 (d, 1H); 7.22 (t, 1H); 6.96 (m, 6H); 6.87 (t, 2H); 6.80 (t, 3H), 6.75-6.64 (overlapped m, 6H); 6.41 (t, 2H); 5.98 (d, 2H); 5.45 (br d, 2H); 2.78 (s, 6H); 2.24-1.0 (33H).

¹³C NMR (100 MHz, C₆D₆): δ 299.4; 222.3 (br s); 151.1; 139.6; 138.6; 137.5; 136.1; 133.8; 133.1; 131.9; 130.3; 129.7; 129.5; 128.82; 125.9; 73.9; 73.2; 33.1; 33.0; 29.1; 28.0; 26.7; 20.8; 19.3.

³¹P NMR (161.97 MHz, C₆D₆): δ 22.8.

Anal. Calcd for C₅₄H₆₅Cl₂N₂PRu (944.33): C, 68.63, H, 6.93, N, 2.96. Found C, 69.15, H, 6.98, N, 2.99.



Synthesis of **74** (*syn* and *anti*)

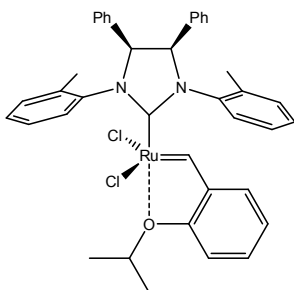
In a glove box, a solution of **s.m.3** (0.571 mmol, 280 mg), potassium hexafluoro-*tert*-butoxide $[(CF_3)_2CH_3COK]$ (0.571 mmol, 126 mg) in 8 mL of toluene was stirred at room temperature for five minutes. $(PCy_3)_2Ru(=CHPh)Cl_2$ (0.389 mmol, 320 mg) was then added, the reaction flask was removed from the glove box and heated at 60°C for 3 hours. The mixture was allowed to cool at room temperature and the crude product was purified by flash column chromatography on TSI silica gel (*n*-hexane/ Et_2O = 95:5 to 1:1). The purification step allowed us to isolate two isomers (*anti* **74** and *syn* **74**). The solvent was removed under vacuum to give *anti* **74** (first eluted compound) as a dark pink powder (0.062 mmol, 58 mg, 16%) and *syn* **74** as a brown powder (0.163 mmol, 154 mg, 42%).

anti 74: 1H NMR (400MHz, CD_2Cl_2): δ : 19.12 (s, 1H); 8.1 (br s 1 H); 8.05 (d, 1 H); 7.49 (br s, 3H); 7.43 (d, 3H); (7.39-7.25 m, 9H); 7.18 (t, 1H); 7.09 (t, 4H); 6.53 (t, 1H); 5.13 (br d, 1H, $J = 9.72$ Hz); 4.96 (s, 1H); 2.73 (br s, 3H); 2.33 (br s, 3H); 1.98 (br s, 3H); 1.54-0.92 (m, 30H).

^{13}C NMR (100 MHz, C_6D_6): δ 297.7; 221.4 (br d, $J(P,C) = 72.3$ Hz); 151.8; 140.34; 136.67; 131.5; 130.4; 127.0; 125.6; 78.0; 33.1; 32.9; 30.2; 29.3; 29.2; 28.11; 28.0; 26.7; 20.6; 19.45.

^{31}P NMR (161.97 MHz, CD_2Cl_2): δ 19.12

Anal. Calcd for $C_{54}H_{65}Cl_2N_2PRu$ (944.33): C, 68.63, H, 6.93, N, 2.96. Found C, 68.92, H, 6.98, N, 3.01.



syn-75

Synthesis of *syn-75*

Route A: In a glove box, to a suspension of **s.m.4** (0.752 mmol, 330 mg) in toluene was added KHMDS (0.827 mmol, 165 mg). The reaction mixture was stirred for 15 minutes at RT and then $(\text{PCy}_3)\text{Ru}(=\text{CH}-o\text{-O}/\text{PrC}_6\text{H}_4)\text{Cl}_2$ (0.399 mmol, 239 mg) was added. The flask was removed from the glove box and stirred at 70°C for 2.0 hours. The reaction mixture was cooled at room temperature, and purified by column chromatography on TSI silica gel (*n*-hexane/diethylether = 2:1 to 1:1). The solvent was removed in vacuo to give *syn-75* as a green powder (0.219 mmol, 158 mg, 55.0%).

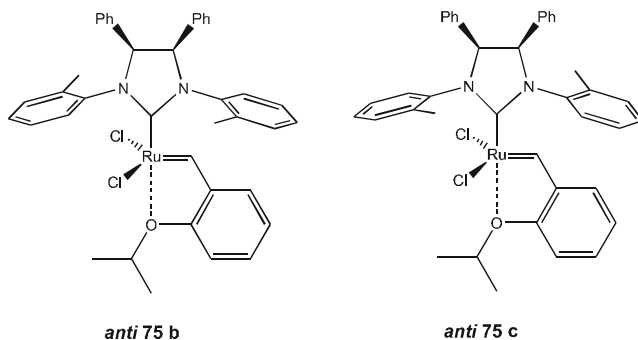
Route B: In a glove box, the ruthenium complex *syn-74* (0.042 mmol, 40 mg) and CuCl (0.044 mmol, 4.4 mg) were added to 2 mL of CH_2Cl_2 in a vial. A solution of 2-isopropoxystyrene (0.042 mmol, 7 mg) in CH_2Cl_2 (0.5 mL) was then added, the vial was removed from the glove box and stirred at 40°C for 1h. After cooling to room temperature, the solution was concentrated and filtered through a Pasteur pipette containing a plug of cotton to remove the insoluble copper-phosphine before loading on column chromatography (TSI silica gel). Elution with *n*-hexane/diethyl ether= 2:1 to 1:1 led to isolate, after removal of the solvent, the desired complex as a green powder (0.040 mmol, 29 mg, 95%).

^1H NMR (400 MHz, CD_2Cl_2): δ 16.22 (s, 1H); 8.78 (d, 1H, $J = 7.64$ Hz); 7.57 (t, 1 H); 7.54 (d, 1 H, $J = 7.90$ Hz) 7.42-7.35 (m, 2H); 7.27-7.24 (m, 2H); 7.17-7.14 (m, 4H) 7.09-7.02 (m, 6H); 7.00-6.90

(m, 2H); 6.86-6.84 (m, 1H); 6.03 (d, 2H, $J = 9.96$ Hz); 5.93 (d, 2H, $J = 9.96$ Hz); 5.02 (q, 1H, $J = 6.15$ Hz); 2.66 (s, 3H); 2.56 (s, 3H); 1.54 (d, 3H, $J = 6.15$ Hz); 1.33 (d, 3H, $J = 6.15$ Hz).

^{13}C NMR (75 MHz, C_6D_6): δ 294.4; 215.3; 153.3; 144.6; 141.3; 140.6; 138.0; 137.5; 133.8; 132.2; 131.2; 130.8; 129.5; 122.34; 113.3; 75.0; 74.3; 72.6; 22.4; 22.0; 20.6; 18.9.

Anal. Calcd for $\text{C}_{39}\text{H}_{38}\text{Cl}_2\text{N}_2\text{ORu}$ (722.14): C, 64.81, H, 5.30, N, 3.88. Found C, 64.80, H, 5.27, N, 3.85.



Synthesis of *anti*-75 (75 B and 75 C)

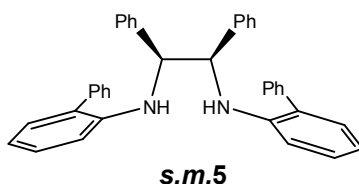
Using the procedure described for the preparation of *syn*-74 (route B), the ruthenium complex *anti*-74 (0.042 mmol, 40 mg), CuCl (0.044 mmol, 4.4 mg) and 2-isopropoxystyrene (0.042 mmol, 7 mg) were reacted in 2.5 mL of CH_2Cl_2 . After cooling to room temperature, the reaction mixture was concentrated and filtered through a Pasteur pipette containing a plug of cotton to remove the insoluble copper-phosphine before loading on column chromatography (TSI silica gel). Elution (*n*-hexane/diethylether = 1:1) afford *anti*-75 (0.035 mmol, 25 mg, 84%) as a green powder. This complex exists in solution as an isomeric mixture (1:1.9 in CD_2Cl_2 ; 1:2.8 in C_6D_6).

^1H -NMR (400 MHz, C_6D_6): δ 16.97 (s, minor isomer); 16.72 (s, major isomer); 9.08 (d, major); 9.02 (d, minor); 7.90 (br t, minor); 7.56-6.60 (overlapped m); 6.38 (d); 5.68 (d, $J = 7.48$ Hz, minor); 5.46 (d, $J = 5.34$ Hz, major); 5.24 (br s, major); 5.19 (d, $J = 7.48$ Hz,

minor,); 4.51 (q); 2.89 (s, minor); 2.81 (br s, major); 2.73 (s, major); 2.07 (s, minor); 1.47 (d, minor $J = 6.08$ Hz); 1.40 (d, major, $J = 5.99$ Hz); 1.30 (d, $J = 6.08$ Hz)

^{13}C NMR (100 MHz in C_6D_6): δ 295.72 (major); 293.99 (minor); 214.96 (minor); 214.29 (major); 153.14; 145.09; 142.61; 140.66; 140.05; 139.20; 139.01; 138.61; 134.75; 133.77; 132.03; 131.80; 131.24; 130.73; 129.73; 128.97; 128.83; 127.08; 126.88; 122.50; 122.29; 113.25; 82.32; 78.68; 76.73; 75.16; 31.97; 30.22; 23.05; 22.23; 22.18; 22.05; 21.83; 21.20; 20.95; 19.33; 18.98; 14.35.

Anal. Calcd for $\text{C}_{39}\text{H}_{38}\text{Cl}_2\text{N}_2\text{ORu}$ (722.14): C, 64.81, H, 5.30, N, 3.88. Found C, 64.85, H, 5.32, N, 3.89.



Synthesis of s.m. 5

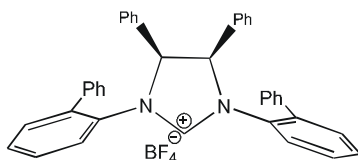
Under N_2 atmosphere, tris(dibenzylideneacetone)dipalladium(0) ($\text{Pd}_2(\text{dba})_3$) (0.236 mmol, 216 mg), 2,2'-bis(diphenylphosphino)-1,1'-binaphthyl (BINAP) (0.565 mmol, 352 mg), sodium *tert*-butoxide (NaOtBu) (14.1 mmol, 1.36 g) and toluene (16.0 mL) were introduced in a flask equipped with a reflux condenser and stirred for 20 min. After this time, *meso*-1,2-diphenylethylenediamine **s.m.1** (4.71 mmol, 1g) and 2-Bromobiphenyl (9.42 mmol, 1.6 mL) were added and the solution was heated to 105°C for 48 hours. The reaction mixture was then cooled at room temperature, diluted with hexane and filtered through a plug of silica gel. The product was eluted from silica gel with methylene chloride. The solvent was removed under vacuum to give **s.m.5** as a pale yellow solid (4.61 mmol, 1.80 g, 99.4%).

ESI⁺MS: $m/z = 516.98$ [M⁺].

^1H -NMR (400 MHz, CDCl_3): δ : 7.41-7.35, (overlapped multiplet, 5H); 7.23, (d, 2H); 7.22 (br s, 2H); 7.12 (t, 2H, $J = 7.30$ Hz); 7.04 (t,

6H, $J = 7.76$); 7.00-6.98 (overlapped multiplet, 2H); 6.68 (d, 2 H); 6.56-6.53 (overlapped multiplet, 5H); 6.30 (d, 2H); 4.78 (d, 2H), 4.66 (d, 2H).

$^{13}\text{C-NMR}$ (75 MHz, CD_2Cl_2) δ : 143.59; 139.56; 138.63; 130.25; 129.68; 129.38; 129.17; 128.72; 128.65; 128.47; 127.77; 127.64; 127.45; 117.65; 111.93; 62.34.



s.m.6

Synthesis of **s.m.6**

Triethyl orthoformate (2.4 mL, 13.95 mmol), diamine **s.m.5** (1.55 mmol, 800 mg) and ammonium tetrafluoroborate (1.91 mmol, 200 mg) were introduced in a 50 mL round-bottom flask equipped with a magnetic stirrer. The reaction mixture was heated at 120°C for 12 h. After cooling to room temperature, the product was precipitated and washed with diethylether (3 times x 10 mL). The solid obtained was dissolved in the minimum amount of methylene chloride and then filtered. The crude was first washed with *n*-hexane and then eluted with a mixture *n*-hexane/ethylacetate = 1:3. The fractions containing the desired product were collected and the volatiles were removed in vacuo to afford **s.m.6** as a yellow solid (0.77 mmol, 474 mg, 50% yield).

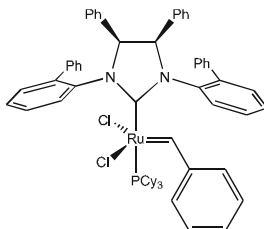
This reaction yield is quite low with respect to the usual values for this step. This is due to the incomplete cyclization of the starting material toward the bulky cyclic adduct which bears all phenyl substituents. The presence of the side product has been confirmed monitoring reaction proceed via NMR as well as by careful examination of all the eluted fraction from column chromatography.

ESI⁺MS: found $m/z = 526.82$ [$\text{M}^+(-\text{BF}_4^-)$].

$^1\text{H-NMR}$ (300 MHz in CD_2Cl_2) δ : 9.23 (s, 1H); 7.84 (d d, 2H); 7.67-7.62 (overlapped multiplet 6H); 7.45 (quintuplet, 4H); 7.35-

7.27(overlapped multiplet 6H); 7,05-6.90 (overlapped multiplets, 6H); 6.55 (d d, 4H); 4.8 (s, 2H).

^{13}C -NMR (75 MHz in CD_2Cl_2) δ : 158.72; 138.33; 137.48; 132.19; 132.04; 130.27; 129.85; 129.73; 129.57; 129.46; 129.25; 129.06; 129.03; 128.64; 127.64; 71.19



76

Synthesis of 76

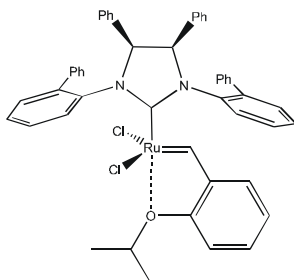
In a glove box, a solution of **s.m.6** (0.218 mmol, 134 mg), potassium hexafluoro-tert-butoxide $[(\text{CF}_3)_2\text{CH}_2\text{COK}]$ (0.218 mmol, 48 mg) in 6.5 mL of toluene was stirred at room temperature for five minutes. $(\text{PCy}_3)_2\text{Ru}(\text{=CHPh})\text{Cl}_2$ (0.148 mmol, 122.0 mg) was then added, the reaction flask was removed from the glove box and heated at 60°C for 1.25 hours in a oil bath. The mixture was then allowed to cool at room temperature and the crude product was purified by flash column chromatography on silica gel (*n*-hexane/diethylether = 95:5 to 3:1). The purification step allowed us to isolate **76** (104.5mg MW 1068.36, yield 66%) as a pastel green powder.

^1H -NMR (400MHz in CD_2Cl_2) δ : 19.50 br s, (1 H); 9.39 d, (2 H, $J = 7.62$); 8.31 br s, (2 H); 7.89 br s, (2 H); 7.65 br s, (2 H); 7.59 m, (3 H); 7.52 t, (3 H); 7.44 t, (3 H); 7.34 br m, (3 H); 7.01 br s, (2 H), 6.91 t, (2 H); 6.73 m, (3 H); 6.61 m, (3 H); 6.12 br s, (3 H); 4.68 br s, (1 H); 4.53 d, (1 H, $J = 10.08$); 1.75-0.87 overlapped multiplet, (33 H).

^{13}C NMR (100 MHz in C_6D_6) δ : 306.49; 300.50; br d, 219.00; 151.32; 140.85; 139.88; 138.23; 138.14; 134.01; 133.32; 133.00; 132.69; 131.31; 130.36; 130.29; 129.72; 129.55; 129.14; 128.97; 127.04; 72.17; 71.75; 33.52; 33.37; 32.36; 31.76; 31.64; 30.49;

30.24, 29.87; 29.24; 28.27; 28.10; 27.99; 27.87; 27.29; 27.18;
26.83.

^{31}P NMR (161.97 MHz CD_2Cl_2), δ : 22.70; 20.40



77

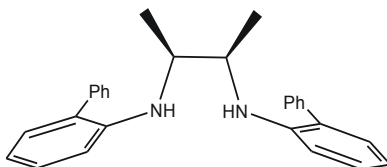
Synthesis of 77

Ruthenium complex **76** (0.146 mmol, 156.3 mg) and CuCl (0.146 mmol, 14.5 mg) were weighted into a 50mL round bottomed flask in a glovebox and dissolved in 5 mL of dry methylene chloride. A solution of 2-isopropoxystyrene (0.142 mmol, 24.7 mg) in methylene chloride (5.5 mL) was then added, the flask was removed from the glove box and stirred at 40°C for 1h. After cooling to room temperature, the solution was concentrated and filtered through a Pasteur pipette containing a plug of cotton to remove the insoluble copper-phosphine before loading on column chromatography (TSI silica gel). Elution with *n*-hexane to *n*-hexane/methylene chloride= 1:1 led to isolate, after removal of solvent, the desired complex as a green powder (0.142 mmol, 120 mg, 99.9%). Traces of grace and of an undefined side product were removed by extraction using a mixture of *n*-hexane/acetonitrile (the desired complex is soluble in the acetonitrile phase while apolar contaminants were transferred in *n*-hexane).

^1H -NMR (400MHz in CD_2Cl_2) δ : 17.06 (s, 1 H); 9.54; (d, 1 H); 7.83 (d, 2 H); 7.79 (br s, 2 H); 7.62 (m, 8 H); 7.41 (m, 7 H); 7.33 (d, 1 H); 7.17 (t, 1 H); 7.07 (d, 2 H); 7.01 (t, 1 H); 6.93 (t, 1 H); 6.85 (m, 2 H);

6.73 (t, 2 H); 6.26 (d, 2 H); 5.20 (m, 1 H, $J = 6.04$ Hz); 4.80 (d, 1 H, $J = 9.94$ Hz); 4.39 (d, 1 H, $J = 9.94$ Hz); 1.86 (d, 3 H, $J = 6.04$ Hz); 1.60 (3 d H, $J = 6.04$ Hz).

^{13}C NMR (100MHz in CD_2Cl_2) δ : 299.07; 213.33; 153.56; 144.25; 141.39; 140.20; 139.93; 139.82; 138.86; 137.60; 134.10; 132.85; 132.33; 131.59; 130.98 130.85; 129.95; 129.73; 129.21; 129.18; 129.05; 128.96; 128.71; 128.32; 128.12; 128.04; 127.97; 127.84; 127.26; 126.22; 122.97; 122.82; 113.70; 75.42; 72.11; 70.69; 23.05; 22.54.

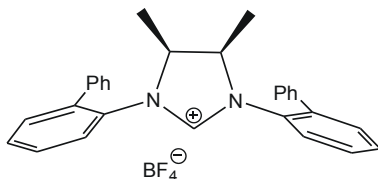


Synthesis of **s.m.9**

Starting material (**s.m.8**) was synthesized following literature procedure.⁷ Arylation was accomplished by Pd catalyzed Heck coupling. Under nitrogen atmosphere, tris(dibenzylideneacetone)dipalladium(0) ($\text{Pd}_2(\text{dba})_3$) (0.249 mmol, 228 mg), 2,2'-bis(diphenylphosphino)-1,1'-binaphthyl (BINAP) (0.60 mmol, 373 mg), sodium *tert*-butoxide (NaOtBu) (15.0 mmol, 1.44 g) and toluene (16.6 mL) were introduced in a flask equipped with a reflux condenser and stirred for 20 min. After this time, *meso*-1,2-dimethylethylenediamine **s.m.8** (4.99mmol, 440mg) and 2-Bromobiphenyle (9.98 mmol, 1.72 mL) were added and the solution was heated to 100°C for 20 hours. The reaction mixture was then cooled at room temperature, diluted with hexane and filtered through a plug of silica gel. The product was eluted from silica gel with methylene chloride. The solvent was removed under vacuum to give **s.m.9** as yellow solid (2.80 mmol, 1.1 g, 56%).

^1H -NMR (300MHz in CD_2Cl_2) δ : 7.53-7.09 (overlapped multiplets 12H); 7.03 (d d, 2H); 6.74 (d t, 2H); 6.68 (d, 2H); 3.91 (d, 2H); 3.75 (multiplet, 2 H); 0.97 (d, 6 H).

¹³C-NMR (75 MHz in CD₂Cl₂) δ: 144.61; 139.77; 133.40; 131.70; 130.63; 129.74; 129.59; 129.11; 128.95; 128.51; 128.34; 127.97; 127.86; 127.43; 117.09; 111.42; 51.82; 16.16.

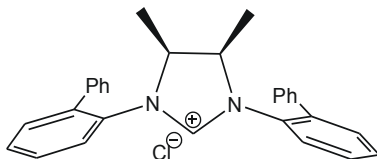


Synthesis of *s.m.10*

Triethyl orthoformate (1,7 mL, 10,16 mmol), diamine *s.m.9* (1,27 mmol, 500 mg) and ammonium tetrafluoroborate (1.54 mmol, 159 mg) were introduced in a 50 mL round-bottom flask equipped with a magnetic stirrer. The reaction mixture was heated at 130°C for 11 h. After this time the mixture was allowed to cool to room temperature; the product was precipitated and washed with diethylether (3 times x 10 mL). The solid obtained was dissolved in the minimum amount of methylene chloride and then filtered. The product was washed with *n*-hexane and the reaction mixture was purified via column chromatography (Dichloromethane/methanol = 20:1). The fractions containing the desired product were collected and the volatiles were removed in vacuo to afford *s.m.10* as a yellow solid (1.0 mmol, 490 mg, 79% yield).

¹H-NMR (300MHz in CD₂Cl₂) δ: 8.25 (s, 1H); 7.72-7.48 (overlapped multiplet 10H); 7.49-7.44 (overlapped multiplet, 2 H); 7.43-7.29 (overlapped multiplet, 6 H); 3.88 (br s 2 H); 0.96 (br d, 6H).

¹³C-NMR (75 MHz in CD₂Cl₂) δ: 156.12; 138.36; 137.81; 132.04; 131.48; 130.72; 129.79; 129.72; 129.03; 127.54; 61.94; 12.54.

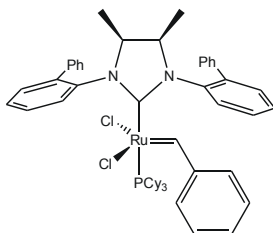


Synthesis of *s.m.11*

Diethyl ether (6ml) was added to starting material **9** (0.78 mmol, 309mg); the mixture resulted homogeneous so 3 ml of dichloromethane were added to promote **s.m.9** dissolution. A solution of hydrogen chloride (2.0 M in diethyl ether; 2.35mmol, 1,2 ml) was added drop wise to precipitate the diamine hydrochloride salt as an off-white powder. The product was collected by filtration and washed with diethyl ether. Dried diamine salt (1.94 mmol, 902 mg) and a large excess of triethyl orthoformate (3.3 mL) were placed in a 50 ml round bottom flask equipped with a magnetic stirrer. The flask was fitted with a condenser and heated to 135 °C in an oil bath for four hours. Upon cooling to room temperature, the solid product was washed several times with hexane and then with Et₂O to give the desired imidazolium chloride salt **s.m.11** as a faint yellow solid (0.389 mmol, 171 mg, 5% yield).

¹H-NMR (400MHz in CDCl₃) δ: 9.58 (br s 1 H); 8.44 (br s 2 H); 7.57 (br s 2 H); 7.54-7.44 (overlapped multiplets 8 H); 7.39-7.32 (d, 6 H); 3.80 (br s, 2 H); 0.99 (br s 6 H).

¹³C-NMR (100MHz in CDCl₃) δ: 157.01; 137.61; 137.59; 131.23; 130.99; 129.87; 129.42; 129.06; 128.85; 128.54; 128.29; 61.30; 12.35



Synthesis of 78

Route A

In a glove box, a solution of **s.m.10** (0.564 mmol, 277 mg) and potassium hexafluoro-tert-butoxide [(CF₃)₂CH₃COK] (0.564 mmol, 124 mg) in 6.0 mL of toluene was stirred at room temperature for five minutes. (PCy₃)₂Ru(=CHPh)Cl₂ (0.384 mmol, 315.0 mg) was added and the reaction flask was removed from the glove box and

heated at 60°C for three hours. The mixture was allowed to cool at room temperature and the crude product was purified by flash column chromatography on silica gel (*n*-hexane/diethylether = 95:5 to 7:3). The purification step allowed the isolation of **78** (117mmol, 110mg, yield 30%) as a light green powder.

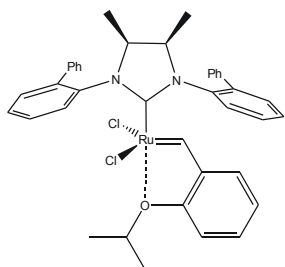
Route B

In a glove box, to a suspension of **s.m.10** (0.442 mmol, 194 mg) in toluene (4,1ml) was added KHMDS (0.455 mmol, 90,8 mg). The reaction mixture was stirred for 15 minutes at RT and then first generation Grubbs (PCy₃)Ru(=CH-*o*-O/PrC₆H₄)Cl₂ (0.380 mmol, 312 mg) was added. The flask was removed from the glove box and stirred at 70°C for one hour. The reaction mixture was cooled at room temperature, and purified by column chromatography on TSI silica gel (*n*-hexane/diethylether = 95:5 to 4:1). The solvent was removed in vacuo to give **78** as a bright green powder (0.126 mmol, 119 mg, 33.0%).

¹H-NMR (400MHz in C₆D₆) δ: 19.92 (s s, 1 H); 9.63 (d, 1 H); 8.51 (d, 2H); 8.30-7.79 (overlapped br signals, 3 H); 7.63-7.50 (overlapped multiplet, 3 H); 7.48-7.36 (overlapped multiplet, 3 H); 7.27 (t, 1 H); 7.24-7.17 (overlapped multiplet, 5 H); 7.03-6.76 (overlapped broad multiplet, 3 H); 6.75-6.52 (br s, 2 H); 3.39 (d, 2 H); 2.45-0.83 (overlapped signals, 33H); 0.46 (d, 3 H); 0.05 (d, 3 H).

³¹P NMR (161.97 MHz, C₆D₆) δ: 21.95 (sharp); 21.79 (broad).

³¹C-NMR We could not acquire this characterization since complex **78** decompose overnight even in benzene (which is usually choose as deuterated solvent for long experiments because it generally ensures stability also to labile phosphine based complexes).

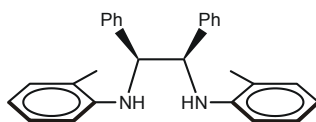


Synthesis of **79**

A suspension of **s.m.10** (0.389 mmol, 171 mg) in toluene (2,5 mL) was prepared and stirred for couple of minutes in glove box. KHMDS (0,428 mmol, 85,3 mg) was added and the solution was stirred for five minutes at RT. First generation Grubbs-Hoveyda complex (0,206 mmol, 123mg) was then added and the reaction was heated and stirred at 70°C for one hour. Crude was purified chromatographically on TSI silica gel (solvent polarity was varied from pentane: diethyl ether = 7:1 to 1:1 to afford **79** as deep green powder (148 mmol, 107 mg, 72% yield). **79** needed an extraction with a mixture of acetoitrile/n-hexane to eliminate grease trace and the side product due to the oligomerization of the Hoveyda ligand.

¹H-NMR (400 MHz CD₂Cl₂) δ: 17.11 (s, 1H); 9.28 (d, 1 H, *J* = 7.62 Hz); 7.82, (d, 2 H); 7.83-7.78 (m, 2 H); 7.68-7.64 (overlapped multiplet, 2 H); 7.61 (s, 1 H); 7.60 (m, 1 H); 7.57-7.49 (overlapped multiplet, 6 H); 7.32-7.24 (overlapped multiplet, 4 H); 7.01 (d, 1 H, *J* = 8.40 Hz); 6.93-6.87 (overlapped multiplet 2 H); 5.12 (quintuplet, 1 H, *J* = 6.14 Hz); 3.49 (quintuplet, 1 H, *J* = 6.76 Hz); 3.28 (quintuplet, 1 H, *J* = 6.52 Hz); 1.76 (d, 3 H, *J* = 6.09 Hz); 1.52 (d, 3 H, *J* = 6.09 Hz); 0.81 (d, 3 H, *J* = 6.52 Hz); 0.64 (d, 3 H, *J* = 6.76 Hz).

¹³C-NMR (100 MHz CD₂Cl₂) δ: 297.1; 209.4; 153.4; 144.4; 140.9; 140.3; 139.9; 139.8; 138.5; 138.1; 132.6; 132.1; 131.3; 130.6; 130.5; 129.7; 129.3; 129.1; 128.8; 128.5; 128.3; 128.1; 127.6; 127.2; 122.9; 122.5; 113.6; 75.2; 60.6; 60.4; 30.1; 22.9; 22.4; 13.9; 12.9.



S.m.2

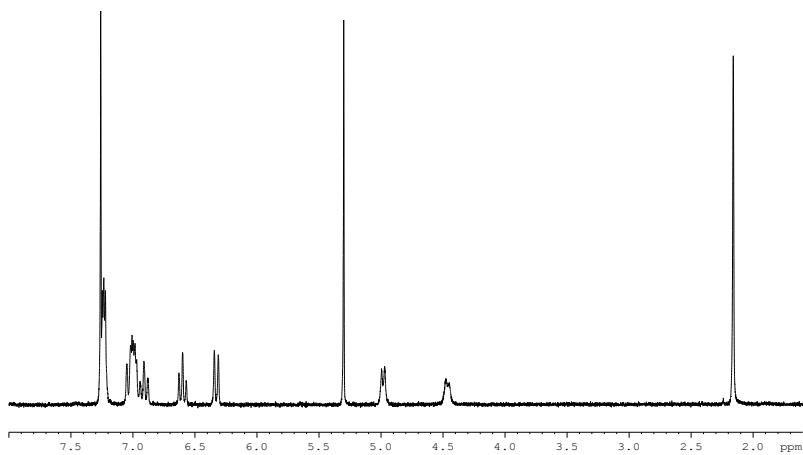


Figure 3. 30: ¹H NMR (250 MHz, CDCl₃) of *S.m.2*

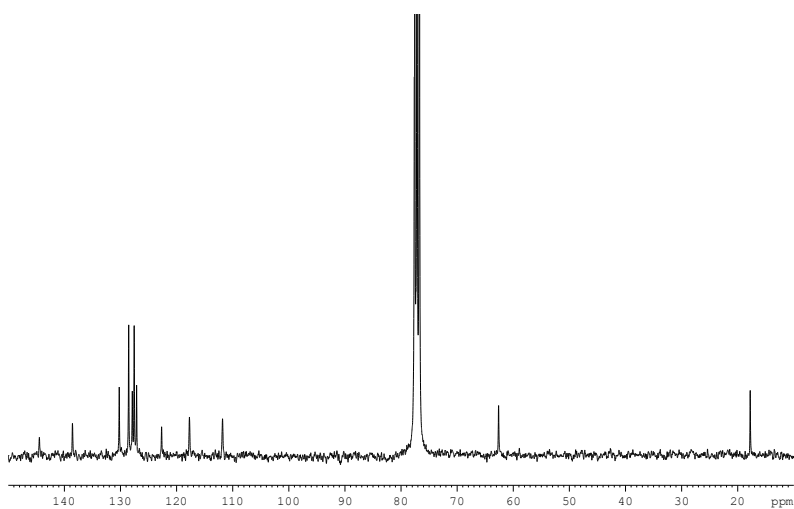


Figure 3. 31: ¹³C NMR (75 MHz, CDCl₃) of *S.m.2*

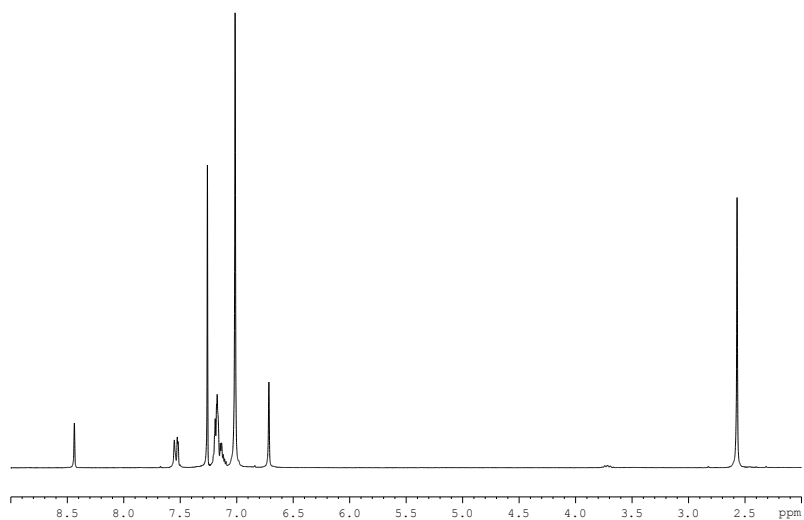
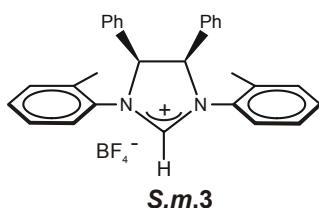


Figure 3. 32: ^1H NMR (250 MHz, CDCl_3) of **S.m.3**

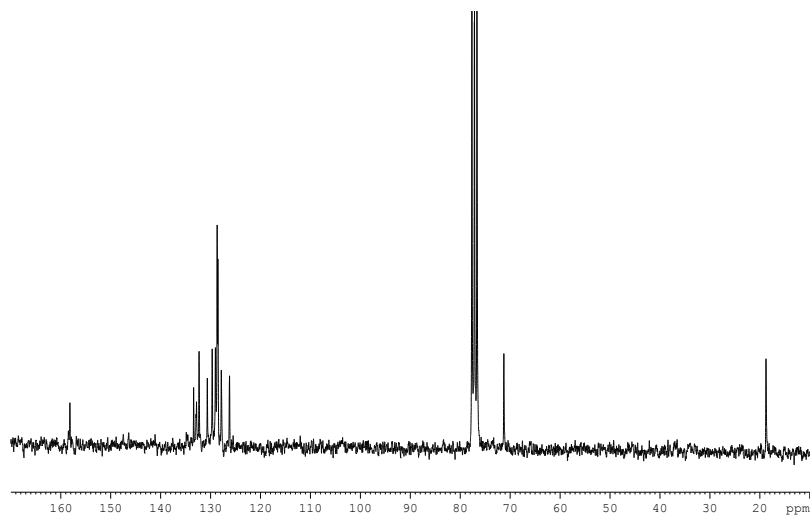


Figure 3. 33: ^{13}C NMR (75 MHz, CDCl_3) of **S.m.3**

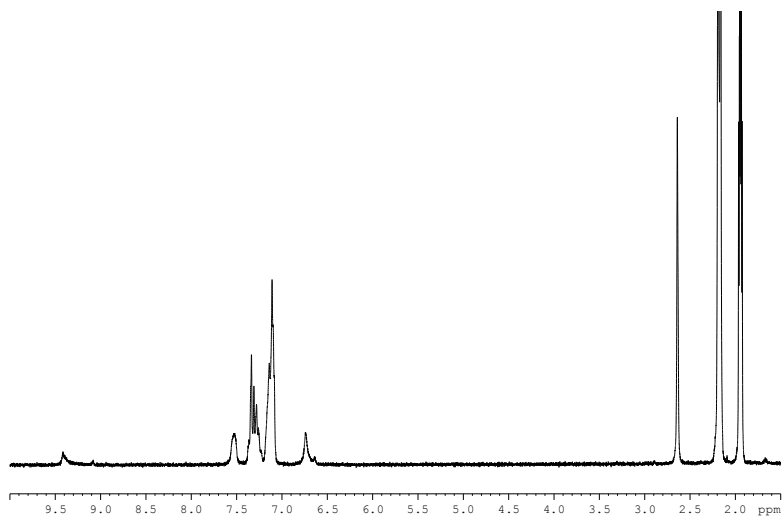
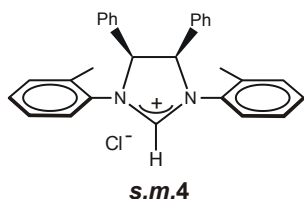


Figure 3. 34: $^1\text{H-NMR}$ (250 MHz, CD_3CN) of *S.m.4*

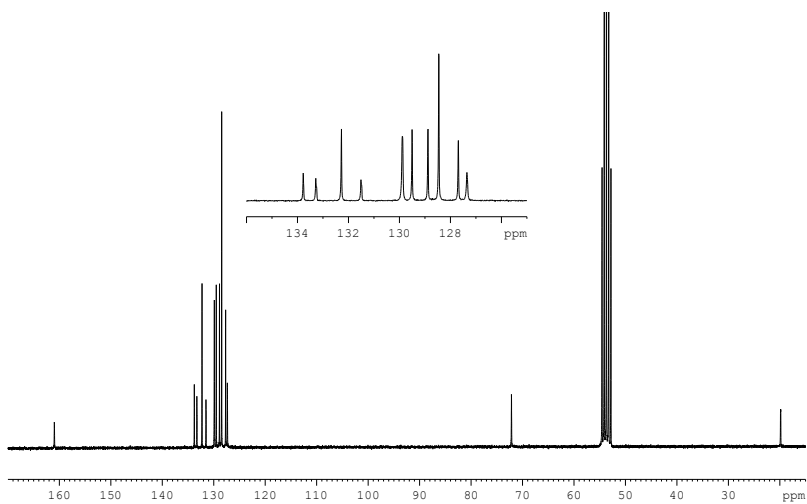


Figure 3. 35: $^{13}\text{C-NMR}$ (62.5 MHz, CD_2Cl_2) of *S.m.4*

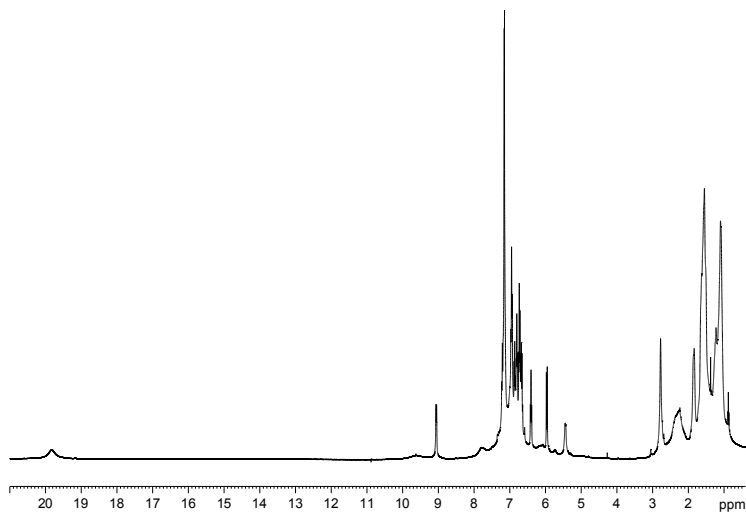
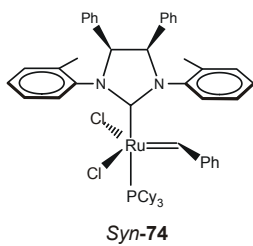


Figure 3. 36: ¹H NMR (400 MHz, C₆D₆) of *syn-74*

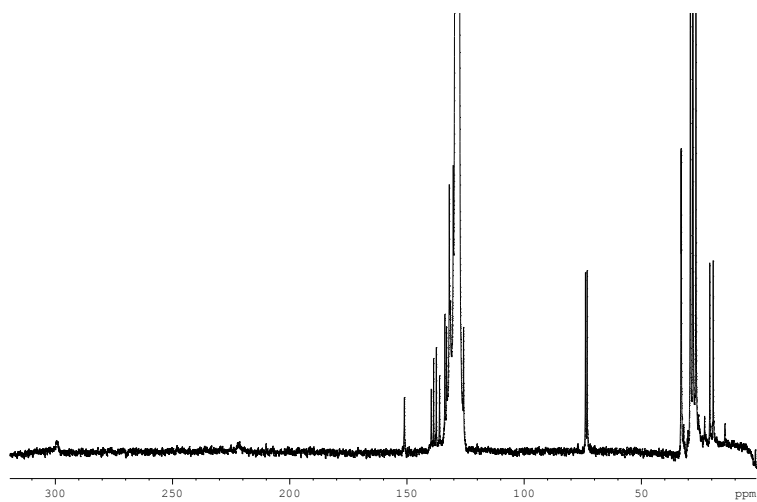


Figure 3. 37: ¹³C NMR (100 MHz, C₆D₆) of *syn-74*

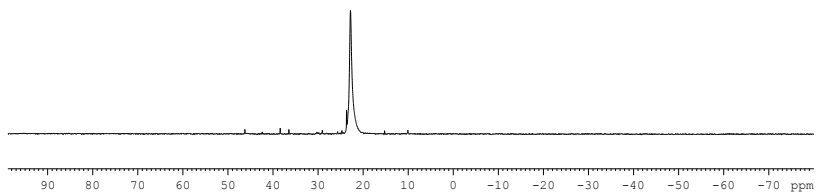


Figure 3. 38: ^{31}P NMR (161.97 MHz, C_6D_6) of *syn*-74

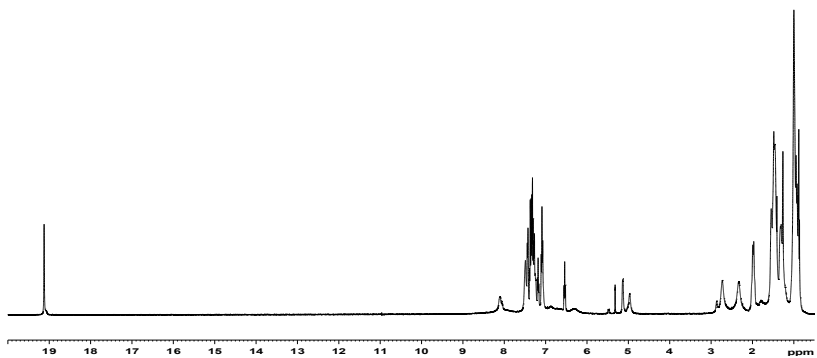
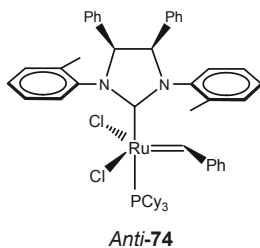


Figure 3. 39: ^1H NMR (400 MHz, CD_2Cl_2) of *anti*-74

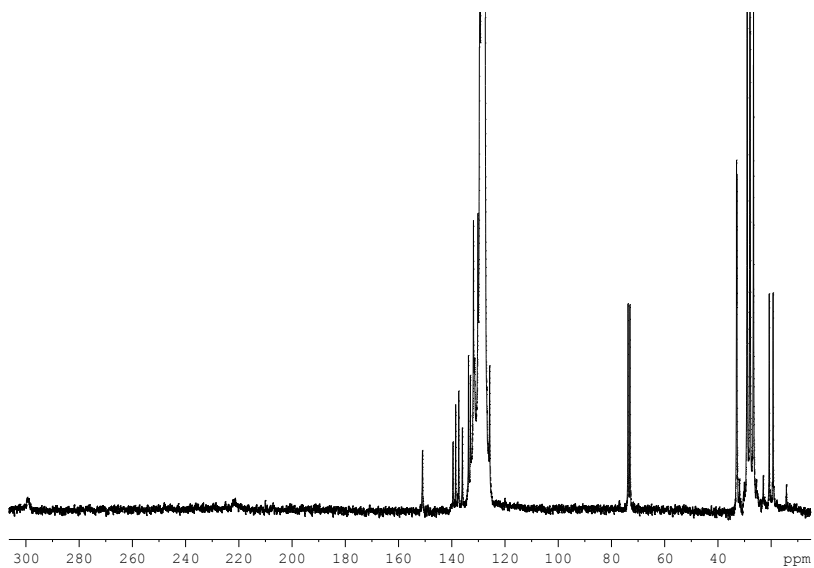


Figure 3. 40: ^{13}C NMR (100 MHz, C_6D_6) of *anti*-74

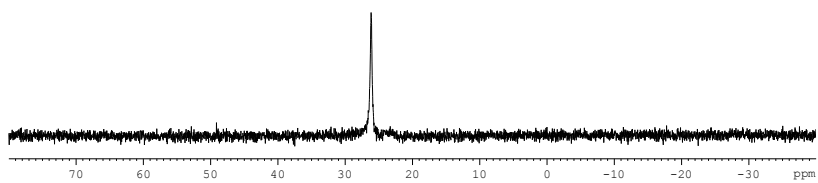
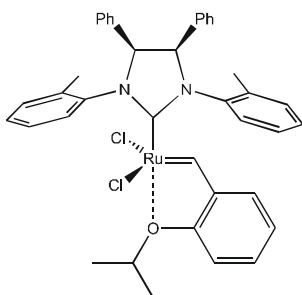


Figure 3. 41: ^{31}P NMR (161.97 MHz, CD_2Cl_2) of *anti*-74



syn-75

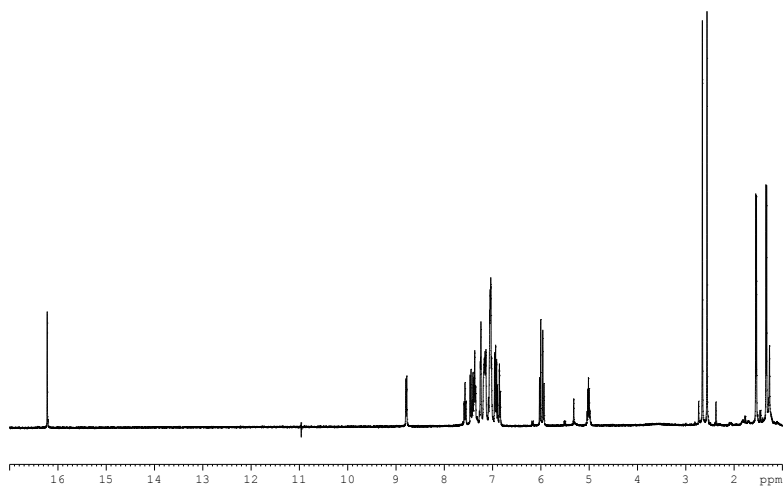


Figure 3. 42: ¹H NMR (400 MHz CD₂Cl₂) of *syn-75*

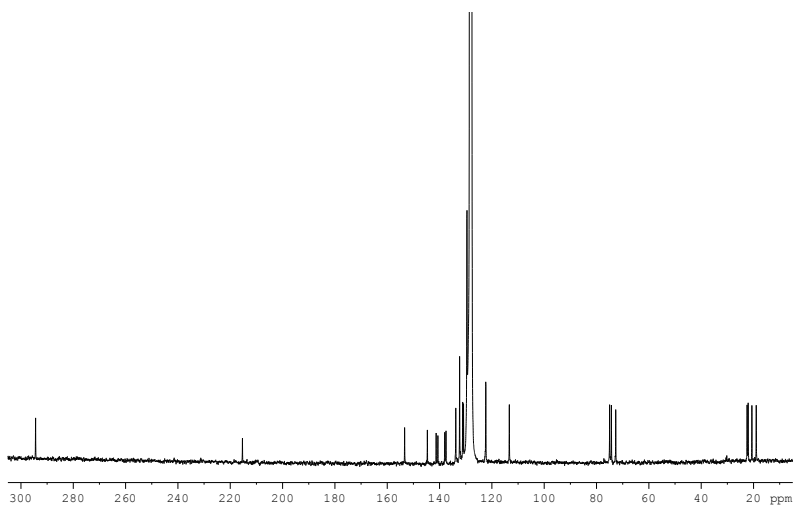


Figure 3. 43: ^{13}C NMR (75 MHz, C_6D_6) of *syn*-75

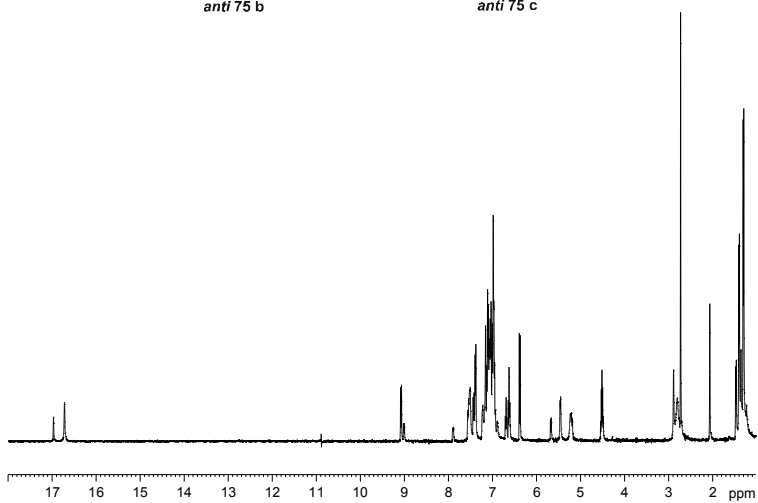
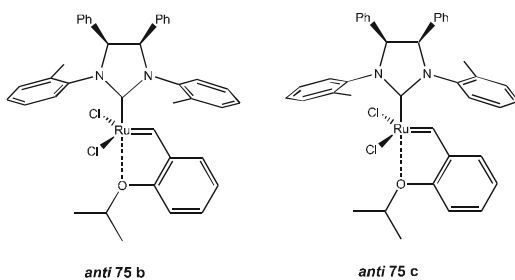


Figure 3. 44: ^1H -NMR (400 MHz, C_6D_6) of *anti*-75

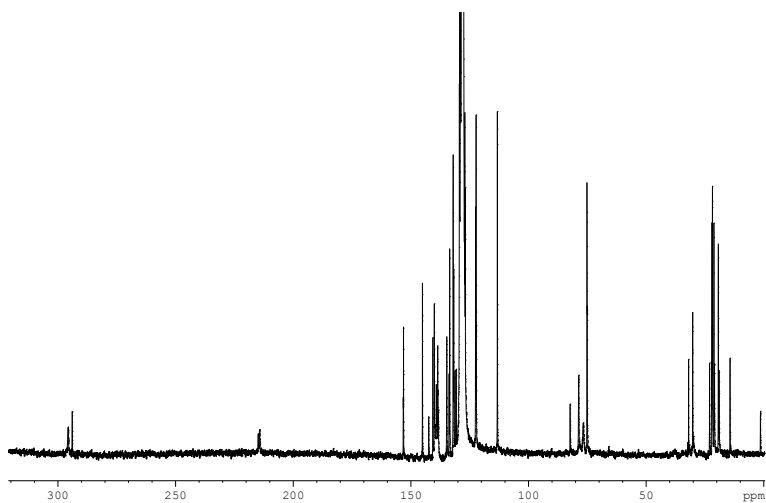


Figure 3. 45: ^{13}C NMR (100 MHz in C_6D_6) of *anti*-75

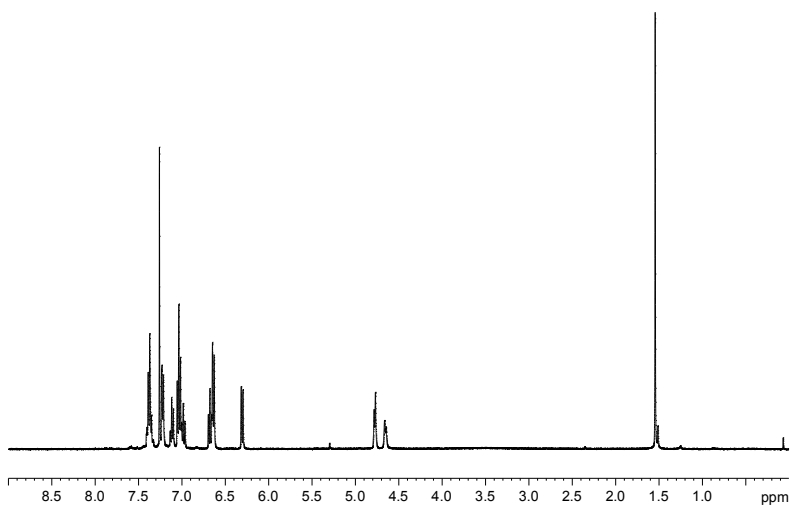
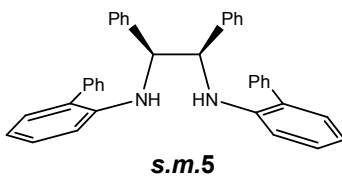


Figure 3. 46: ^1H -NMR of *s.m.5* in CDCl_3

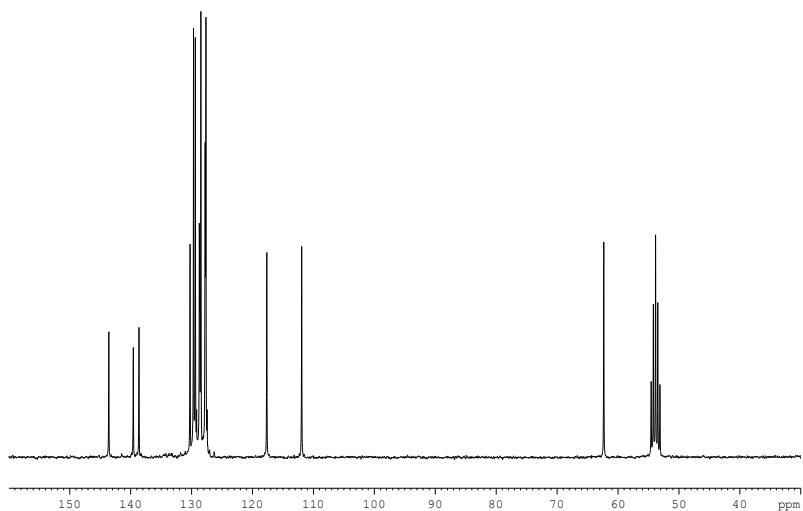
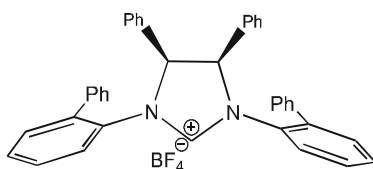


Figure 3. 47: ^{13}C -NMR of *s.m.5* in CD_2Cl_2



s.m.6

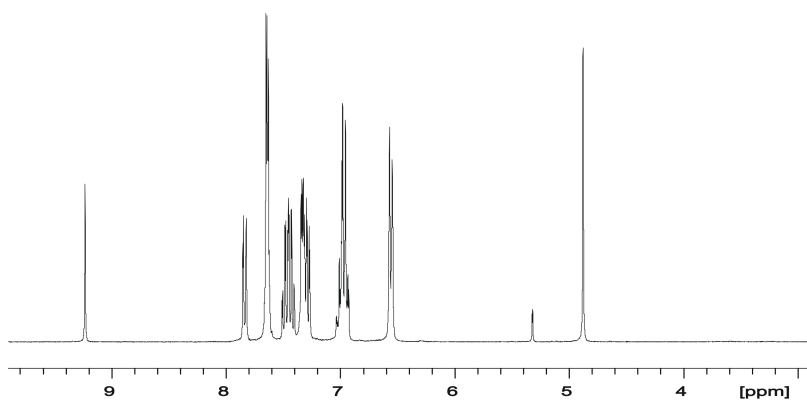


Figure 3. 48: ^1H -NMR in CD_2Cl_2 300 MHz

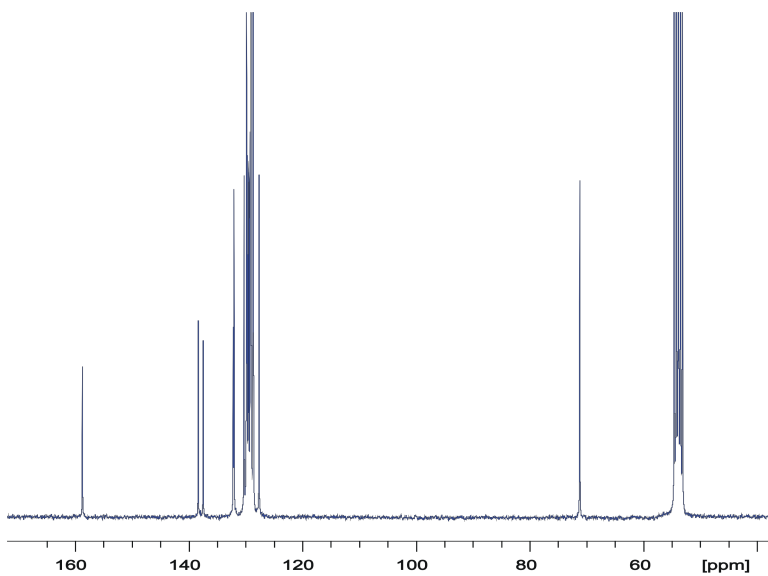


Figure 3. 49: ^{13}C -NMR in CD_2Cl_2 75 MHz

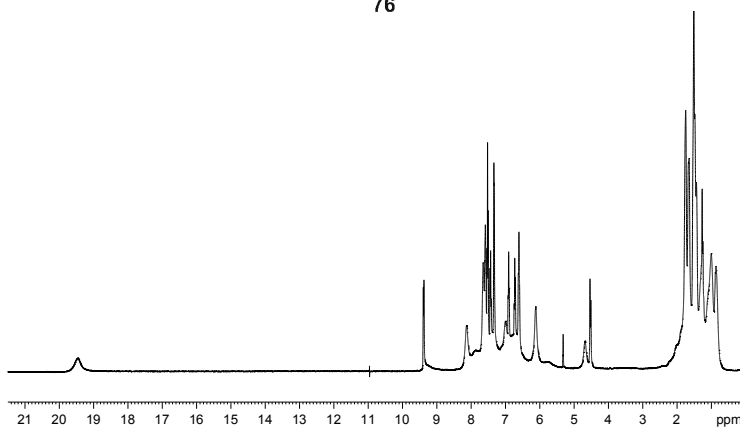
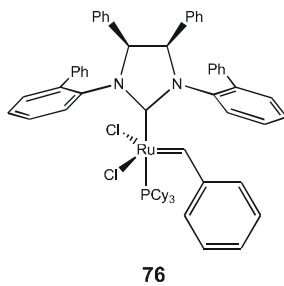


Figure 3. 50: ^1H -NMR of **76** in CD_2Cl_2

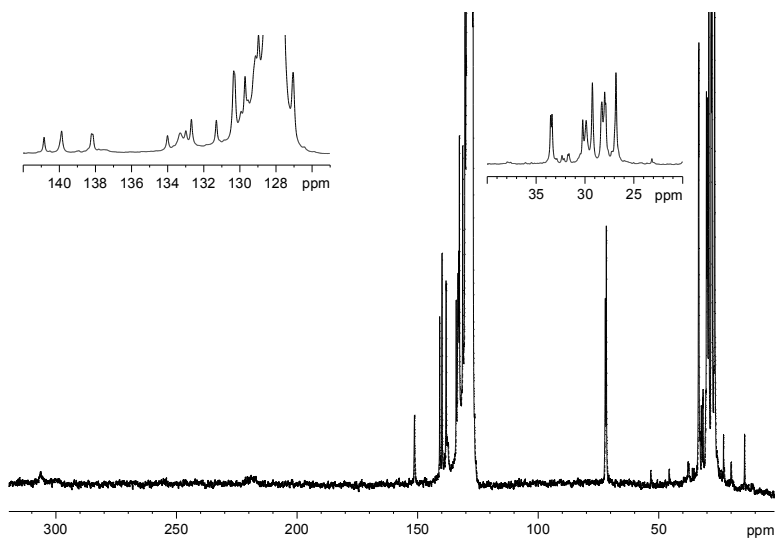


Figure 3. 51: ^{13}C -NMR of 76 in C_6D_6

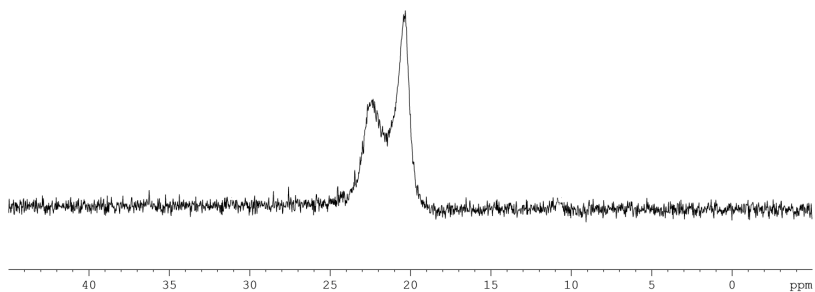
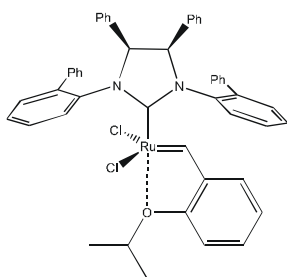


Figure 3. 52: ^{31}P -NMR of 76 in CD_2Cl_2



77

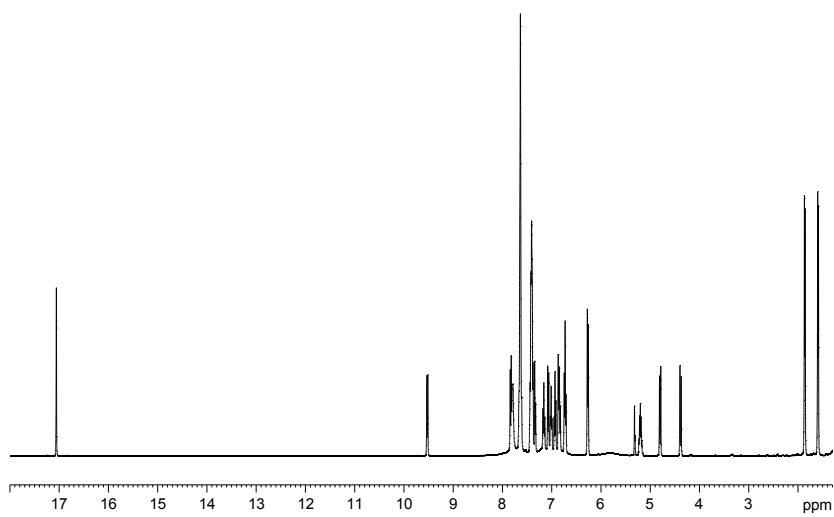


Figure 3. 53: ¹H-NMR of 77 in CD₂Cl₂

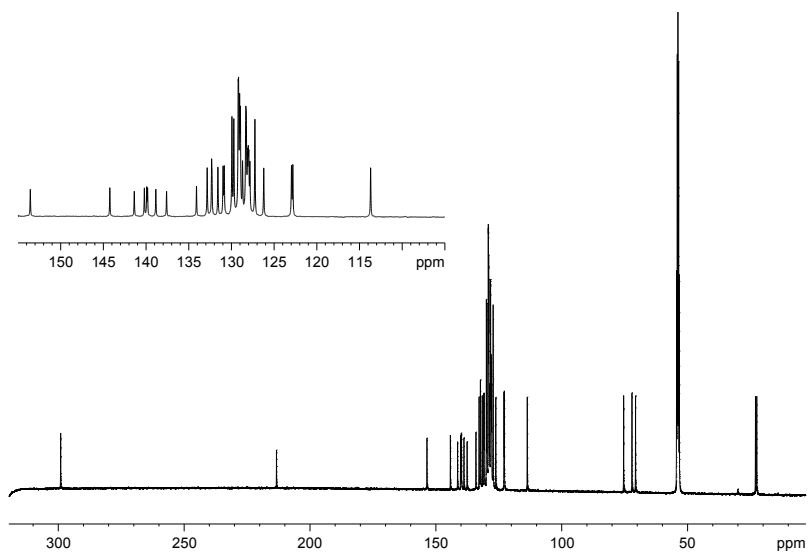
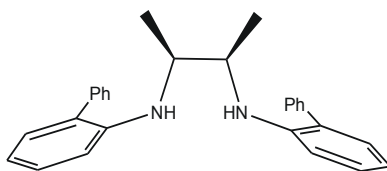


Figure 3. 54: ^{13}C -NMR of 77 in CD_2Cl_2



s.m.9

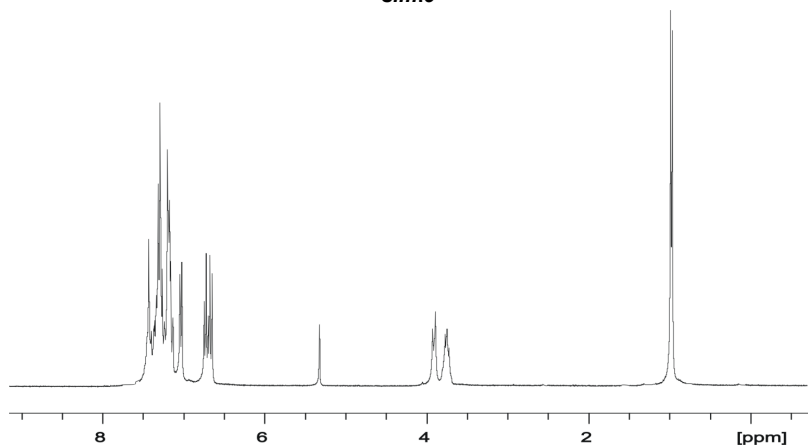


Figure 3. 55: ^1H -NMR of *s.m.9* in CDCl_3

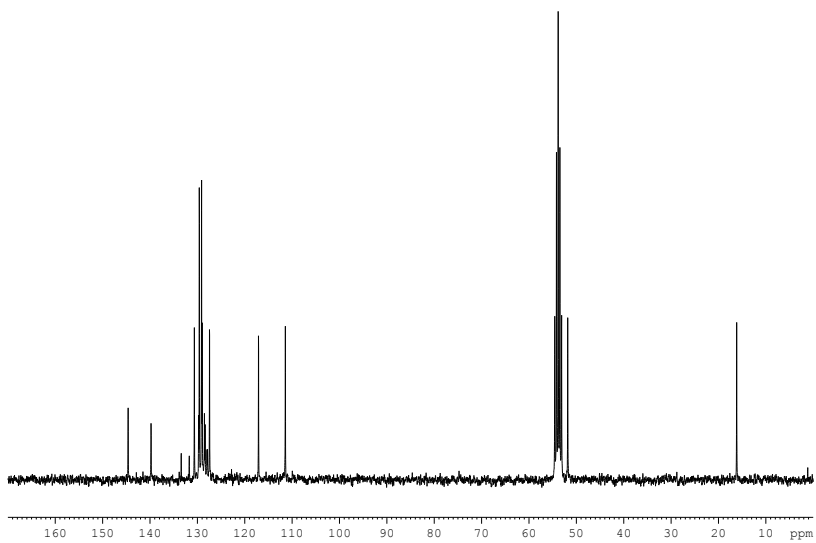


Figure 3. 56: ^{13}C -NMR of *s.m.9* in CD_2Cl_2

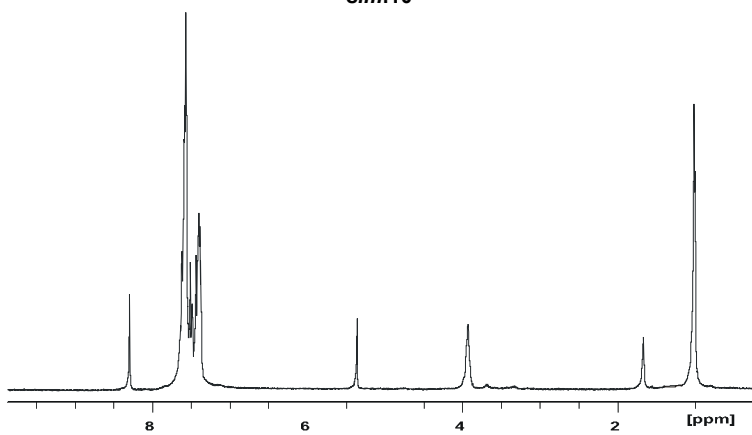
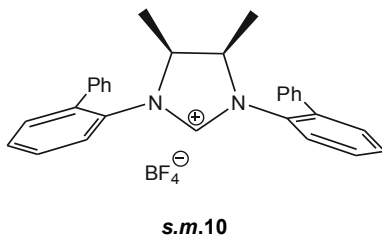


Figure 3. 57: ^1H -NMR of *s.m.10* in CD_2Cl_2

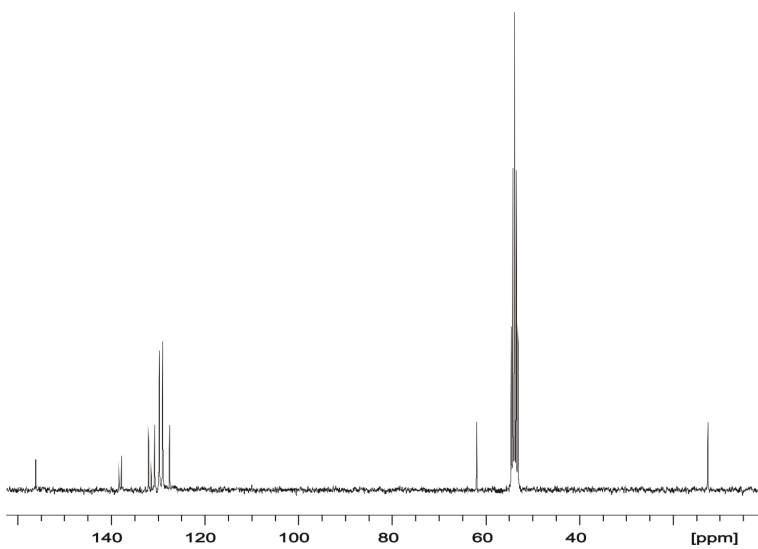
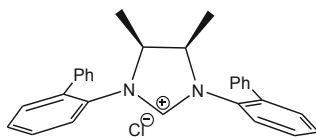


Figure 3. 58: ^{13}C -NMR of *s.m.10* in CD_2Cl_2



s.m. 11

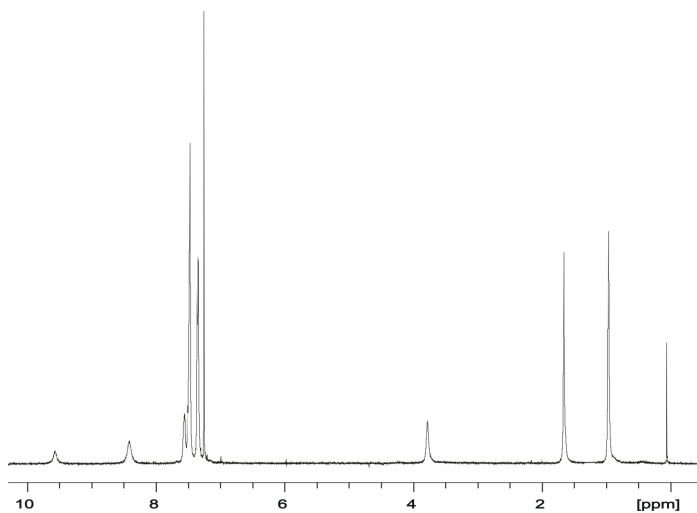


Figure 3. 59: ^1H -NMR of *s.m.11*

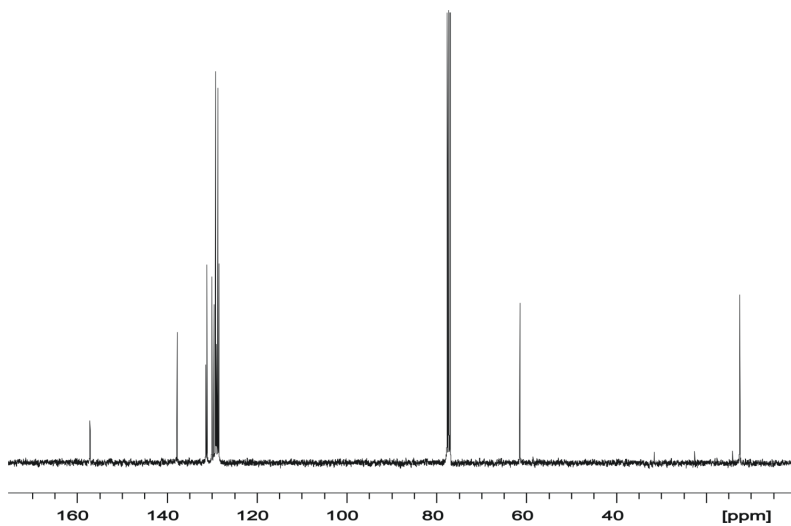
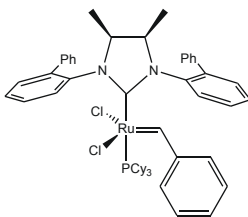


Figure 3. 60: ^{13}C -NMR of *s.m.11* in CDCl_3



78

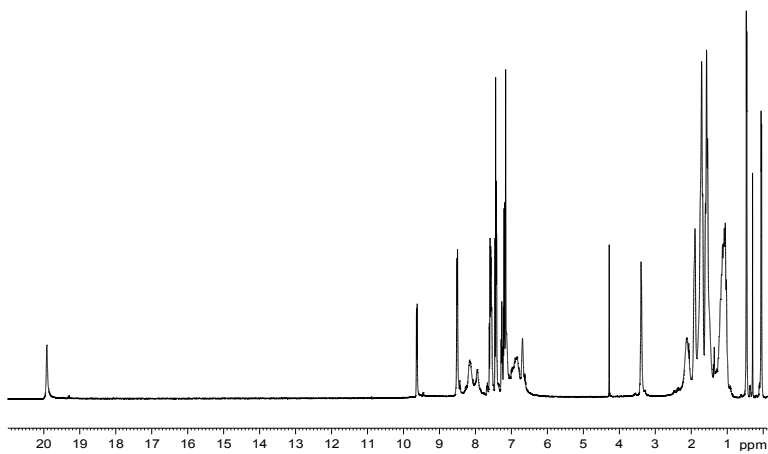


Figure 3. 61: ^1H -NMR of 78 in C_6D_6

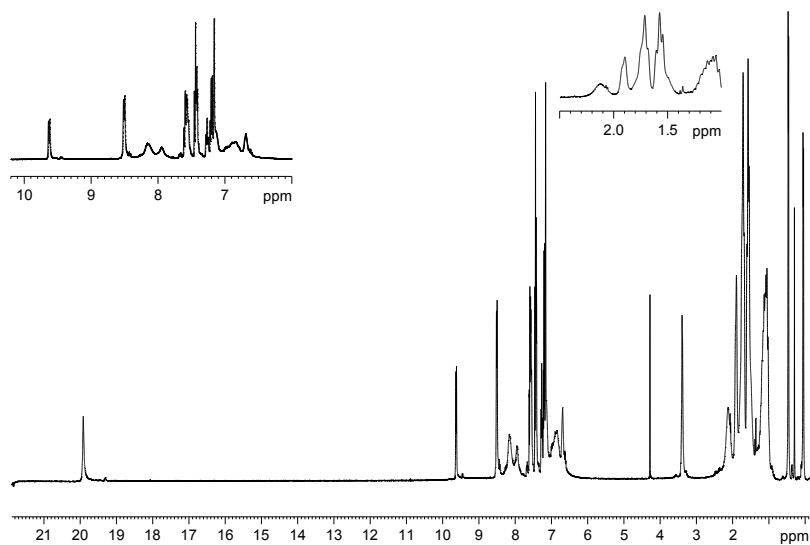


Figure 3. 62: $^1\text{H-NMR}$ of 78 in C_6D_6

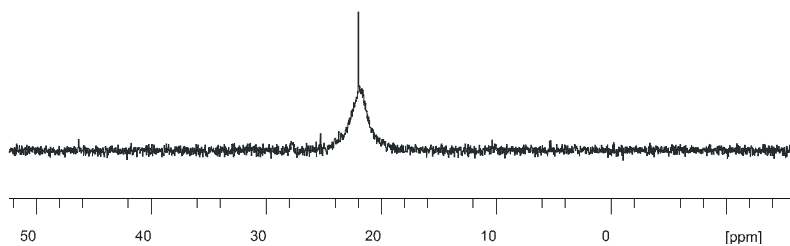
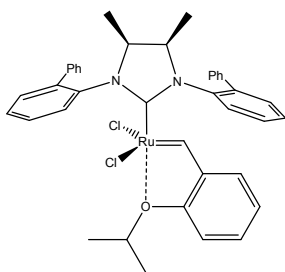


Figure 3. 63: $^{31}\text{P-NMR}$ of 78 in C_6D_6



79

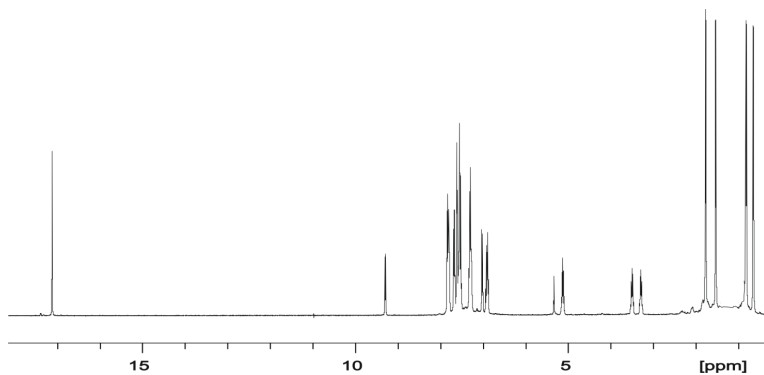


Figure 3. 64: ^1H NMR of 79 in CD_2Cl_2

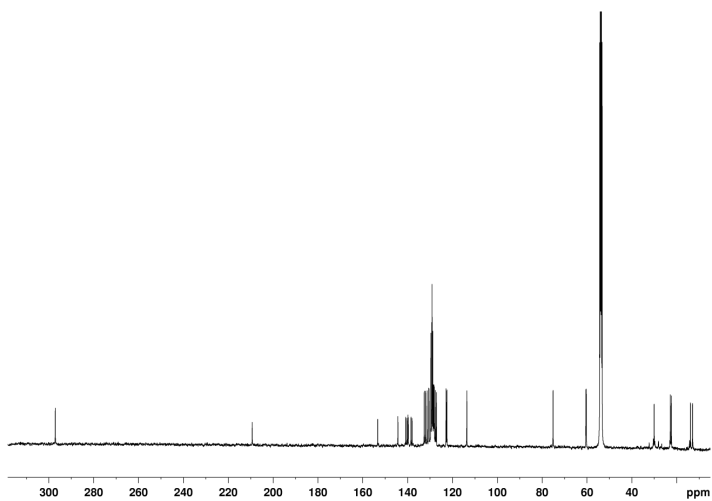


Figure 3. 65: ^{13}C NMR of 79 in CD_2Cl_2

Determination of the thermodynamic parameters for the equilibrium between the major and minor forms of anti-75 (75B-75C).

The equilibrium constant for the equilibrium process minor form

————→ major form of **anti-75** was evaluated at different temperatures according to the following equation:

$$K_{eq} = [\text{major}] / [\text{minor}] = I_{(\text{major})} / I_{(\text{minor})}$$

where the concentration of the major and minor forms were evaluated from the intensities of the carbenic proton resonances of the two forms, $I_{(\text{major})}$ and $I_{(\text{minor})}$ respectively. The equilibrium constants K_{eq} at each temperature are given in Table-1.

T (K)	1/T	K_{eq}	$\ln K_{eq}$
273	0.00366	2.1	0.742
263	0.00380	2.3	0.833
253	0.00395	2.6	0.956
243	0.00412	2.9	1.06
233	0.00429	3.4	1.22

Table 3. 1: Equilibrium constants K_{eq} for anti-75 at different temperatures.

The standard enthalpy (ΔH°) and the standard entropy (ΔS°) were extrapolated from the inverse temperature plot of $\ln(K_{eq})$:

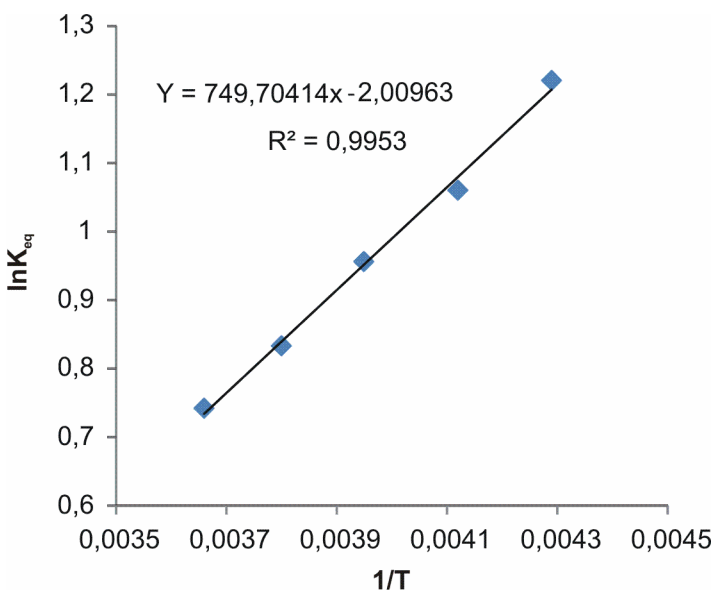


Figure 3. 66: $\ln K_{eq}$ vs $1/T$ plot

$$\ln(K_{eq}) = - \Delta H^\circ / RT + \Delta S^\circ / R$$

$$\Delta H^\circ = - R \cdot \Delta H^\circ / R = - 1,987(749,70414 \pm 29,73124) = - 1489,662 \pm 59,076 \text{ cal mol}^{-1} = - 1,489 \pm 0.059 \text{ Kcal mol}^{-1}$$

$$\Delta S^\circ = R \cdot \Delta S^\circ / R = 1.986(-2,00963 \pm 0,11804) = -3,991 \pm 0,234 \text{ cal mol}^{-1}$$

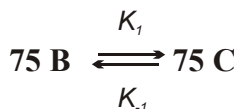
Units of measurements are in SI.

2D EXSY determination of exchange rate constant between 8B and 8C isomers

The 2D EXSY spectra were recorded at 298K in C_6D_6 at different mixing times (300-700 ms). The rate constants (k) were calculated employing the equations reported below,¹² in which τ_w is the mixing time, I_{BC} and I_{CB} are the cross-peak intensities, I_{BB} and I_{CC} are the diagonal peak intensities, $X_{75 B}$ and $X_{75 C}$ are the molar fractions of

¹² Pons, M.; Millet, O. *Prog. Nucl. Magn. Reson. Spectrosc.* **2001**, *38*, 267-281.

75 B (*anti* **75 b**) and **75 C** (*anti* **75 c**) isomers, which were obtained by integration in the ^1H NMR spectrum of *anti*-**75** (see previous paragraph).

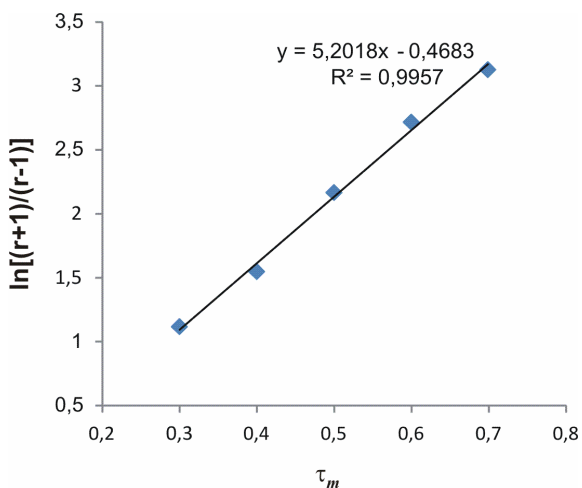


$$k = k_1 + k_{-1}$$

$$k_1 \times X_{75 \text{ B}} = k_{-1} \times X_{75 \text{ C}}$$

$$k = 1/\tau_m \times \ln [(r+1)/(r-1)]; \quad r = 4 X_{75 \text{ B}} X_{75 \text{ C}} [(I_{\text{BB}} + I_{\text{CC}}) / (I_{\text{BC}} + I_{\text{CB}})] - (X_{75 \text{ B}} - X_{75 \text{ C}})^2$$

A plot of $\ln [(r+1)/(r-1)]$ versus τ_m yields a straight line with slope $k = 5.20 \text{ s}^{-1}$:



Plot 3. 1: (modified Eyring plot) plot of $\ln [(r+1)/(r-1)]$ versus τ_m employed for K calculation

Thus, $k_1 = 1.35 \text{ s}^{-1}$ and $k_{-1} = 3.75 \text{ s}^{-1}$. Using the equation $\Delta G^\ddagger = -RT \ln kh/TK_B$ we obtain $(\Delta G^\ddagger)_1 = 17.3 \text{ Kcalmol}^{-1}$ and $(\Delta G^\ddagger)_{-1} = 16.6 \text{ Kcalmol}^{-1}$.

Units of measurements are in SI.

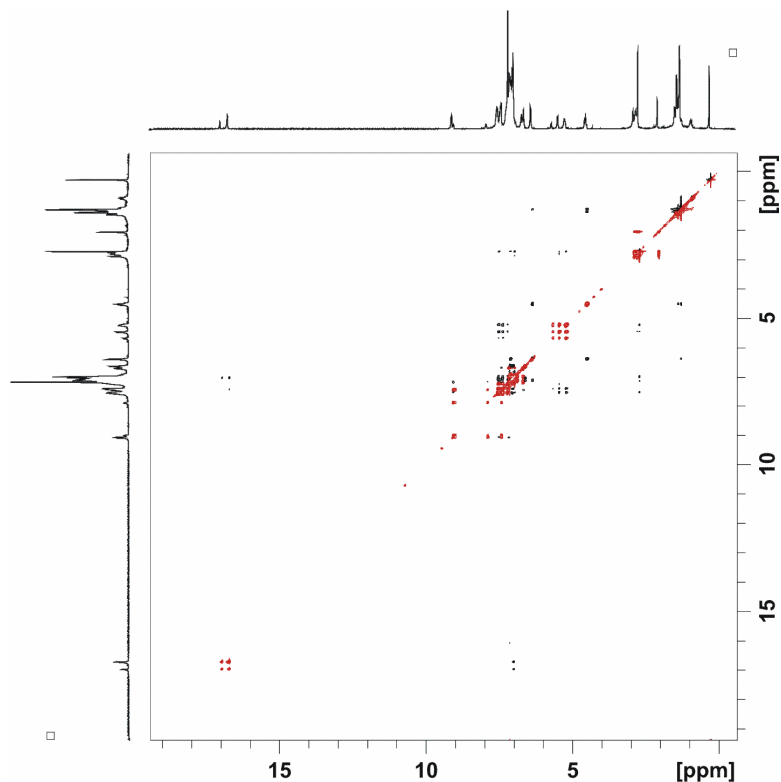


Figure 3. 67: NOESY/EXSY (600 ms mixing time) spectrum of anti **75** in C_6D_6 at $25^\circ C$

Crystal structure details

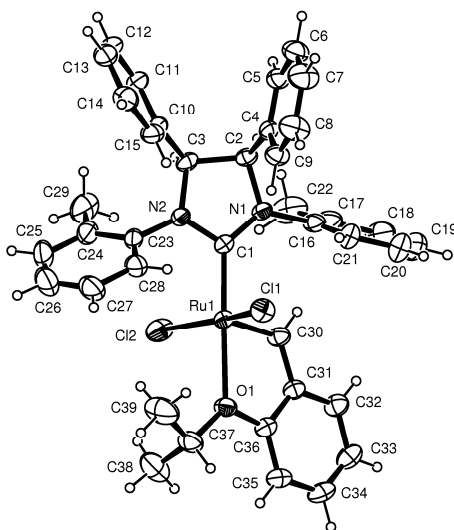
Experimental section: the crystal data of compound *syn-75* (**75 A**) were collected using a Nonius Kappa CCD diffractometer with graphite monochromated Mo- $K\alpha$ radiation and corrected for Lorentz, polarization and absorption effects (SORTAV¹³); solution by direct methods (SIR97¹⁴); refinement on F^2 using full-matrix least-squares with all non-hydrogen atoms anisotropically and hydrogens included on calculated positions, riding on their carrier atoms. $C_{39}H_{38}Cl_2N_2ORu, C_6H_6$, $M = 800.79$, Orthorhombic, $Pbca$

¹³ R.H. Blessing, *Acta Crystallogr. Sect A*, **1995**, *51*, 33-38;

¹⁴ A. Altomare, M. C. Burla, M. Camalli, G.L. Cascarano, C. Giacovazzo, A. Guagliardi, A.G. Moliterni, G. Polidori, R. Spagna, SIR97, *J. Appl. Crystallogr.* **1999**, *32*, 115-119;

(N.61), $a = 15.8915(1) \text{ \AA}$, $b = 15.7464(1) \text{ \AA}$, $c = 32.9881(4) \text{ \AA}$, $V = 8254.7(1) \text{ \AA}^3$, $Z = 8$, $D_c = 1.289 \text{ g cm}^{-3}$, $\mu = (\text{Mo-K}\alpha) = 0.544 \text{ mm}^{-1}$, $T = 295 \text{ K}$, 8967 independent reflections, $\theta \leq 27.00^\circ$, 6550 observed reflections [$I \geq 2\sigma(I)$], $R_1 = 0.0398$ (observed reflections), $wR_2 = 0.1094$ (all reflections), $\text{GOF} = 1.040$, 452 parameters. The crystal contains a molecule of benzene solvent *per* molecule of Ru complex. All calculations were performed using SHELXL-97¹⁵ and PARST¹⁶ implemented in WINGX¹⁷ system of programs. The crystal data and selected bond distances and angles are given below.

CCDC deposition number 893407.



Crystal data

Bond precision: C-C = 0.0066 A Wavelength=0.71073

Cell: a=15.8915(1) b=15.7464(1) c=32.9881(4)

alpha=90 beta=90 gamma=90

¹⁵ G. M. Sheldrick, SHELX-97, *Program for Crystal Structure Refinement*, University of Gottingen, Germany, 1997;

¹⁶ M. Nardelli, *J. Appl. Crystallogr.*, **1995**, 28, 659-659;

¹⁷ L.J. Farrugia, *J. Appl. Crystallogr.*, **1999**, 32, 837-838;

Temperature: 295 K

Calculated	Reported	
Volume	8254.74(12)	8254.74(12)
Space group	P b c a	P b c a
Hall group	-P 2ac 2ab	?
Moiety formula	C ₃₉ H ₃₈ Cl ₂ N ₂ ORu, C ₆ H ₆	C ₃₉ H ₃₈ Cl ₂ N ₂ ORu, C ₆ H ₆
Sum formula	C ₄₅ H ₄₄ Cl ₂ N ₂ ORu	C ₄₅ H ₄₄ Cl ₂ N ₂ ORu
Mr	800.79	800.79
Dx, g cm ⁻³	1.289	1.289
Z	8	8
Mu (mm ⁻¹)	0.544	0.544
F000	312.0	3312.0
F000'	3305.26	
h,k,lmax	20,20,42	20,20,42
Nref	9009	8967
Tmin,Tmax	0.866,0.947	0.886,0.949
Tmin'	0.845	

Correction method= EMPIRICAL

Data completeness= 0.995 Theta(max)= 27.000

R(reflections)= 0.0398(6550) wR2(reflections)= 0.1094(8967)

S = 1.040 Npar= 452

Distances (Å)

1	Ru1	Cl1	2.3481(7)	23	C7	H7	0.931(4)
2	Ru1	Cl2	2.3325(8)	24	C7	C8	1.379(5)
3	Ru1	C1	1.961(2)	25	C8	H8	0.929(3)
4	Ru1	C30	1.825(3)	26	C8	C9	1.381(5)
5	Ru1	O1	2.300(2)	27	C9	H9	0.930(3)
6	C1	N1	1.343(3)	28	C10	C11	1.399(4)
7	C1	N	1.355(3)	29	C10	C15	1.370(4)
8	N1	C2	1.477(3)	30	C11	H11	0.929(3)
9	N1	C1	1.448(3)	31	C11	C12	1.384(5)
10	C2	H2	0.981(2)	32	C12	H12	0.930(3)
11	C2	C3	1.553(4)	33	C12	C13	1.355(5)
12	C2	C4	1.507(3)	34	C13	H13	0.930(4)
13	C3	H3	0.980(2)	35	C13	C14	1.372(6)
14	C3	N2	1.483(3)	36	C14	H14	0.931(3)
15	C3	C10	1.499(4)	37	C14	C15	1.395(4)
16	N2	C23	1.445(3)	38	C15	H15	0.930(3)
17	C4	C5	1.382(4)	39	C16	C17	1.368(4)
18	C4	C9	1.386(3)	40	C16	C21	1.390(4)
19	C5	H5	0.930(3)	41	C17	C18	1.434(5)
20	C5	C6	1.392(4)	42	C17	C22	1.488(5)
21	C6	H6	0.929(3)	43	C18	H18	0.931(4)
22	C6	C7	1.360(5)	44	C18	C19	1.353(8)

45	C19	H19	0.931(5)	67	C30 H30	0.930(3)
46	C19	C20	1.347(8)	68	C30 C31	1.434(4)
47	C20	H20	0.930(5)	69	C31 C32	1.397(4)
48	C20	C21	1.385(6)	70	C31 C36	1.399(4)
49	C21	H21	0.931(3)	71	C32 H32	0.930(3)
50	C22	H22A	0.959(5)	72	C32 C33	1.389(4)
51	C22	H22B	0.961(4)	73	C33 H33	0.930(3)
52	C22	H22C	0.960(4)	74	C33 C34	1.359(4)
53	C23	C24	1.388(5)	75	C34 H34	0.931(3)
54	C23	C28	1.388(4)	76	C34 C35	1.389(4)
55	C24	C25	1.420(5)	77	C35 H35	0.930(3)
56	C24	C29	1.482(7)	78	C35 C36	1.379(4)
57	C25	H25	0.930(5)	79	C36 O1	1.378(3)
58	C25	C26	1.38(1)	80	O1 C37	1.458(4)
59	C26	H26	0.929(5)	81	C37 H37	0.980(3)
60	C26	C27	1.337(8)	82	C37 C38	1.526(5)
61	C27	H27	0.930(5)	83	C37 C39	1.489(5)
62	C27	C28	1.395(6)	84	C38 H38A	0.959(5)
63	C28	H28	0.930(3)	85	C38 H38B	0.961(4)
64	C29	H29A	0.960(5)	86	C38 H38C	0.960(5)
65	C29	H29B	0.961(5)	87	C39 H39A	0.960(5)
66	C29	H29C	0.960(5)	88	C39 H39B	0.961(5)

89	C39	H39C	0.961(5)
90	C1A	H1A	0.93(1)
91	C1A	C2A	1.39(2)
92	C1A	C6A	1.39(2)
93	C2A	H2A	0.93(1)
94	C2A	C3A	1.39(2)
95	C3A	H3A	0.931(6)
96	C3A	C4A	1.39(2)
97	C4A	H4A	0.93(1)
98	C4A	C5A	1.39(2)
99	C5A	H5A	0.930(9)
100	C5A	C6A	1.39(2)
101	C6A	H6A	0.930(6)

Angles (degrees)				23 C2 C3 H3	108.0(2)	
1	Cl1	Ru1	Cl2	159.67(3)	24 C2 C3 N2	101.1(2)
2	Cl1	Ru1	C1	89.64(7)	25 C2 C3 C10	116.7(2)
3	Cl1	Ru1	C30	101.14(8)	26 H3 C3 N2	108.0(2)
4	Cl1	Ru1	O1	89.55(5)	27 H3 C3 C10	107.9(2)
5	Cl2	Ru1	C1	92.93(7)	28 N2 C3 C10	114.7(2)
6	Cl2	Ru1	C30	98.18(9)	29 C1 N2 C3	112.9(2)
7	Cl2	Ru1	O1	88.23(5)	30 C1 N2 C23	122.9(2)
8	C1	Ru1	C30	100.8(1)	31 C3 N2 C23	124.2(2)
9	C1	Ru1	O1	178.59(8)	32 C2 C4 C5	118.5(2)
10	C30	Ru1	O1	78.26(9)	33 C2 C4 C9	122.4(2)
11	Ru1	C1	N1	131.9(2)	34 C5 C4 C9	119.0(2)
12	Ru1	C1	N2	120.7(2)	35 C4 C5 H5	119.7(3)
13	N1	C1	N2	107.3(2)	36 C4 C5 C6	120.6(3)
14	C1	N1	C2	113.7(2)	37 H5 C5 C6	119.7(3)
15	C1	N1	C16	127.2(2)	38 C5 C6 H6	120.0(3)
16	C2	N1	C16	119.1(2)	39 C5 C6 C7	119.9(3)
17	N1	C2	H2	108.7(2)	40 H6 C6 C7	120.1(3)
18	N1	C2	C3	101.2(2)	41 C6 C7 H7	119.8(3)
19	N1	C2	C4	114.0(2)	42 C6 C7 C8	120.1(3)
20	H2	C2	C3	108.8(2)	43 H7 C7 C8	120.1(4)
21	H2	C2	C4	108.8(2)	44 C7 C8 H8	119.7(4)
22	C3	C2	C4	115.0(2)	45 C7 C8 C9	120.5(3)

46	H8	C8	C9	119.8(3)	69	N1	C16	C21	119.1(2)
47	C4	C9	C8	120.0(3)	70	C17	C16	C21	121.4(3)
48	C4	C9	H9	120.0(3)	71	C16	C17	C18	116.9(3)
49	C8	C9	H9	120.0(3)	72	C16	C17	C22	121.2(3)
50	C3	C10	C11	118.3(2)	73	C18	C17	C22	121.8(3)
51	C3	C10	C15	123.2(2)	74	C17	C18	H18	119.7(4)
52	C11	C10	C15	118.5(2)	75	C17	C18	C19	120.6(4)
53	C10	C11	H11	120.0(3)	76	H18	C18	C19	119.7(5)
54	C10	C11	C12	120.1(3)	77	C18	C19	H19	119.2(5)
55	H11	C11	C12	119.9(3)	78	C18	C19	C20	121.6(5)
56	C11	C12	H12	119.5(3)	79	H19	C19	C20	119.2(5)
57	C11	C12	C13	120.7(3)	80	C19	C20	H20	120.1(5)
58	H12	C12	C13	119.7(3)	81	C19	C20	C21	119.7(4)
59	C12	C13	H13	120.0(4)	82	H20	C20	C21	120.3(5)
60	C12	C13	C14	120.0(3)	83	C16	C21	C20	119.8(3)
61	H13	C13	C14	120.0(4)	84	C16	C21	H21	120.1(3)
62	C13	C14	H14	119.9(3)	85	C20	C21	H21	120.1(4)
63	C13	C14	C15	120.0(3)	86	C17	C22	H22A	109.4(3)
64	H14	C14	C15	120.0(3)	87	C17	C22	H22B	109.4(3)
65	C10	C15	C14	120.6(3)	88	C17	C22	H22C	109.4(3)
66	C10	C15	H15	119.6(3)	89	H22A	C22	H22B	109.5(4)
67	C14	C15	H15	119.7(3)	90	H22A	C22	H22C	109.6(4)
68	N1	C16	C17	119.5(2)	91	H22B	C22	H22C	109.4(4)

92	N2	C23	C24	121.0(3)	115	H29B	C29	H29C	109.4(5)
93	N2	C23	C28	117.8(3)	116	Ru1	C30	H30	119.9(2)
94	C24	C23	C28	121.2(3)	117	Ru1	C30	C31	120.3(2)
95	C23	C24	C25	116.3(4)	118	H30	C30	C31	119.8(3)
96	C23	C24	C29	122.5(3)	119	C30	C31	C32	122.7(2)
97	C25	C24	C29	121.0(4)	120	C30	C31	C36	118.9(2)
98	C24	C25	H25	119.2(5)	121	C32	C31	C36	118.4(2)
99	C24	C25	C26	121.3(5)	122	C31	C32	H32	120.0(3)
100	H25	C25	C26	119.4(5)	123	C31	C32	C33	120.2(3)
101	C25	C26	H26	119.3(6)	124	H32	C32	C33	119.8(3)
102	C25	C26	C27	121.4(5)	125	C32	C33	H33	119.9(3)
103	H26	C26	C27	119.3(6)	126	C32	C33	C34	120.1(3)
104	C26	C27	H27	120.4(5)	127	H33	C33	C34	120.0(3)
105	C26	C27	C28	119.2(4)	128	C33	C34	H34	119.3(3)
106	H27	C27	C28	120.4(4)	129	C33	C34	C35	121.3(3)
107	C23	C28	C27	120.5(3)	130	H34	C34	C35	119.4(3)
108	C23	C28	H28	119.8(3)	131	C34	C35	H35	120.6(3)
109	C27	C28	H28	119.7(3)	132	C34	C35	C36	118.9(3)
110	C24	C29	H29A	109.5(4)	133	H35	C35	C36	120.5(3)
111	C24	C29	H29B	109.5(4)	134	C31	C36	C35	121.1(2)
112	C24	C29	H29C	109.5(4)	135	C31	C36	O1	113.0(2)
113	H29A	C29	H29B	109.5(5)	136	C35	C36	O1	125.9(2)
114	H29A	C29	H29C	109.5(5)	137	Ru1	O1	C36	109.6(1)

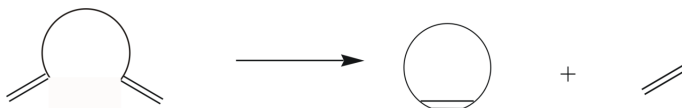
138	Ru1 O1 C37	131.3(2)	161	C1A C2A H2A	120(1)
139	C36 O1 C37	119.0(2)	162	C1A C2A C3A	120(1)
140	O1 C37 H37	109.5(3)	163	H2A C2A C3A	120(1)
141	O1 C37 C38	109.8(3)	164	C2A C3A H3A	120(1)
142	O1 C37 C39	106.5(3)	165	C2A C3A C4A	120.0(9)
143	H37 C37 C38	109.5(3)	166	H3A C3A C4A	120.0(9)
144	H37 C37 C39	109.5(3)	167	C3A C4A H4A	119.9(9)
145	C38 C37 C39	111.9(3)	168	C3A C4A C5A	120.0(9)
146	C37 C38 H38A	109.5(4)	169	H4A C4A C5A	120(1)
147	C37 C38 H38B	109.4(4)	170	C4A C5A H5A	120(1)
148	C37 C38 H38C	109.4(4)	171	C4A C5A C6A	120.0(9)
149	H38A C38 H38B	109.4(4)	172	H5A C5A C6A	120(1)
150	H38A C38 H38C	109.5(4)	173	C1A C6A C5A	120.1(9)
151	H38B C38 H38C	109.5(4)	174	C1A C6A H6A	120(1)
152	C37 C39 H39A	109.4(4)	175	C5A C6A H6A	120(1)
153	C37 C39 H39B	109.4(4)			
154	C37 C39 H39C	109.5(4)			
155	H39A C39 H39B	109.5(4)			
156	H39A C39 H39C	109.5(4)			
157	H39B C39 H39C	109.5(4)			
158	H1A C1A C2A	120(1)			
159	H1A C1A C6A	120(1)			
160	C2A C1A C6A	120(1)			

Chapter 4

Screening of new Ru-Based catalysts in ring closing metathesis

Abstract

Ring closing metathesis (RCM) represents a powerful tool in organic synthesis which has been successfully applied both in academic and in industry environments. This process requires no additional reagents beyond the diene starting material and the metal catalyst and it produces simple and volatile side products like ethylene. Apart from the easy by-product removal another interesting aspect which renders this reaction very attractive and practical is related to its atom economy (usually the formation of an unsaturated ring requires much more atom waste in term of side product carbon number).



Scheme 4. 1: schematic representation for a ring closing metathesis reaction

Modern Ruthenium based systems (e.g. **10**, **16**) tolerate many functional groups common in bio-molecules including amides, alcohols, and carboxylic acids. Under some circumstances, metathesis occurs even in the presence of amines and sulfur-containing moieties.¹ The considerable efficiency reached by the new ruthenium based catalytic systems has expanded enormously ring closing metathesis applicability.

Introduction

My research group has recently synthesized some of the most active Ru based catalysts toward the RCM of challenging di-olefins known up now (**52**, **56**). The understanding of crucial SAR parameters has spurred our interest in the synthesis of even more efficient catalytic systems for this class of metathesis reactions.

¹ Binder, J. B.; Raines, R., T.; *Current Opinion in Chemical Biology* **2008**, *12*, 767.

The catalytic behaviors of the newly synthesized complexes (**74**, **75**, **76**, **77**, **78**, **79**) have been extensively studied in the RCM of a ten member substrate library.

In particular we assessed the utility of catalysts (**74-79**) by employing standard RCM tests, i.e. the RCM of diethylmalonate and *N*-tosyl amine derivatives with increasing steric hindrance to form five-membered cyclo-olefins. Complexes with the best efficiency toward the most challenging above mentioned standard substrates, have been also tested in promoting the ring closure of:

- the commercially available terpene alcohol linalool (**g**, in racemic form);
- the enyne standard substrate **h**;
- the 16-membered diene esters **i** and **l**.

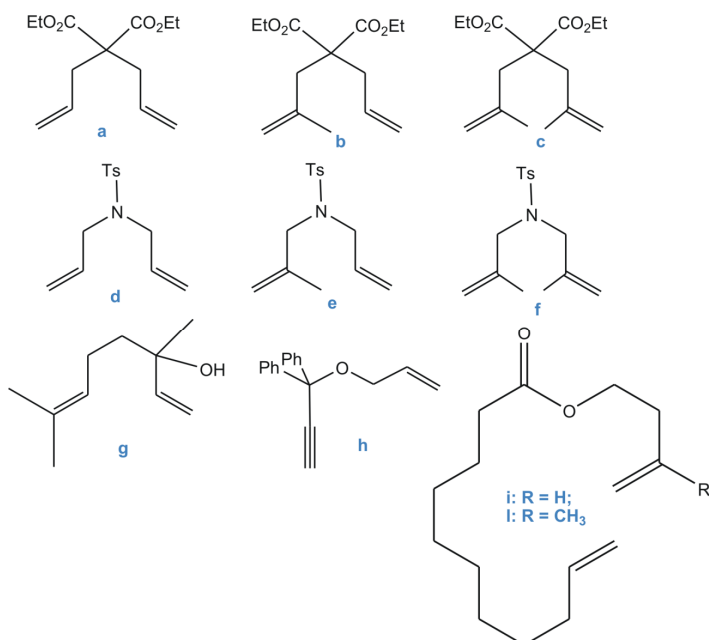


Figure 4. 1: Selected Ring-Closure Substrates.

The course of the reaction was monitored over the time via ¹H-NMR spectroscopy for substrates **a-h**; while macro-cyclization reaction was followed by gas-chromatography.

Results and discussion

RCM standard tests on malonate derivatives

RCM of Diethyldiallyl malonate (a)

The catalytic behavior of new complexes **74-79** was first investigated in the RCM of diethyldiallyl malonate. We were particularly interested in seeing performance differences between atropisomers of the same complex (*syn* and *anti* **74** and **75**) to obtain valuable information on the role that the arrangement of aryl rings plays in influencing catalyst efficiency.

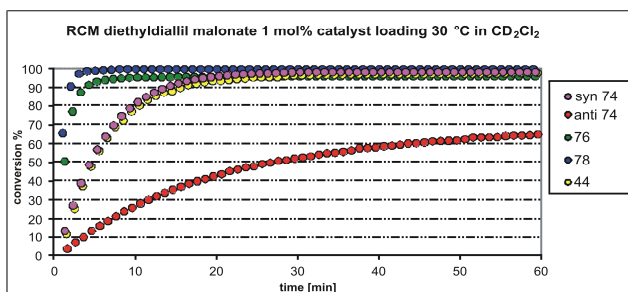


Figure 4. 2: RCM diethyldiallyl malonate at 1 mol% catalyst loading of phosphine derivatives

By observing the reactivity profiles reported in Figure 4. 2 a marked activity difference between *syn* **74** and *anti* **74** catches our attention. *Anti* **74** results definitely the worst catalyst for this cyclization reaction reaching 66% of conversion in one hour (80% conversion within one day), whereas its conformer *syn* **74** displays considerable higher reactivity affording the desired product quantitatively in 30 minutes (the kinetic profile traces that of the commercially available catalyst **41**). As for the other tested catalysts, complex **78** reaches 90% conversion in two minutes completing the metathesis reaction in five. **76** displays a fast initiation as well, but cannot overcome the 96 percentage conversion to the disubstituted cycloalkene. A key role in increasing initiation rates of **76** and **78** could be imputable to the increased steric bulk of the *N*-aryl groups of the NHC ligand; indeed the slopes of the curves recorded for their congeners **52** and *syn* **74**

(which present less bulky *N*-tolyl substituents) are much less pronounced.

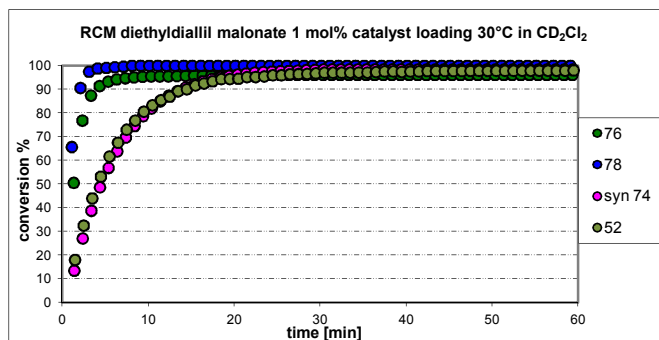


Figure 4. 3: slope curves comparison among differently *N*-ortho aryl substituted phosphine based complexes.

Encouraged by the very good performance of complexes **76** and **78** bearing the *o*-biphenyl groups at the nitrogen atoms of the NHC, we performed the same ring closure lowering the catalyst loading to 0.1 mol %. The different catalytic behavior related to the catalyst structure peculiarity appears thus emphasized.

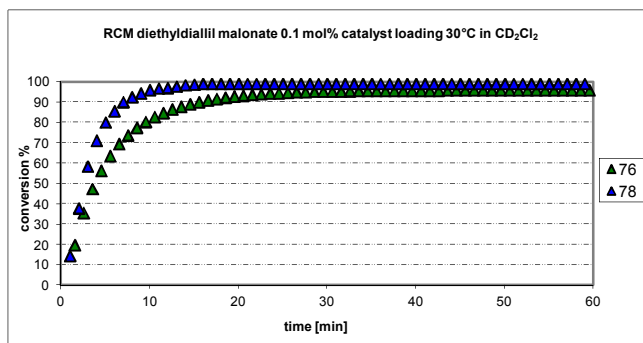
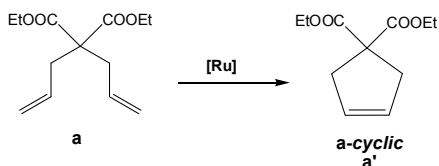


Figure 4. 4: RCM diethylidiallil malonate at 0.1 mol% catalyst loading of selected phosphine derivatives

Catalytic activity of Hoveyda type derivatives was then explored. RCM reactions promoted by this class of complexes are commonly carried out at 60°C in benzene. All the newly synthesized complexes perform quantitatively DEDAM cyclization in very short time with a loading of 1 mol %; the reported results are summarized in Table 4. 1



run	complex	time [min]	conversion %	time [min]	conversion%
1	<i>syn</i> 75	1	75	2	100
2	<i>anti</i> 75	1	29	7	100
3	77	1	63	2	100
4	79	1	77	2	100

Table 4. 1: RCM of diethylidiallyl malonate, at 1 mol% catalyst loading, C₆D₆ 60°C.

In order to emphasize catalytic behavior differences and even more to pursue our goal of reducing the amount of employed metal, we performed RCM reactions at 0,1 mol% of catalyst loading. In these conditions **77** and **79** require less than 10 minutes to furnish quantitatively the cyclic adduct **a'** while *syn* **75** takes half an hour. *Anti* **75**, instead, is able to convert 97% of the starting material in 60 minutes, completing the cyclization process in about two more hours.

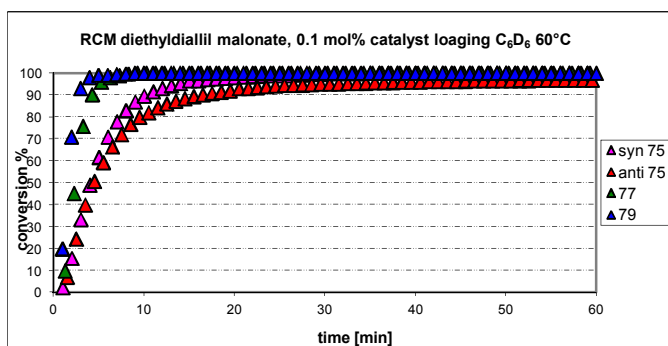


Figure 4. 5: RCM of the diethylidiallyl malonate at 0,1 mol% catalyst loading, 60°C, benzene for Hoveyda derivatives

RCM of Diethylallylmethyl malonate (b)

By increasing starting material steric bulk a partial inversion in reactivity trend is registered. In the RCM of the diethylallylmethyl malonate, complexes **76** and **78** continue to display faster initiation

rates but in this case complex *syn* **74** overcomes complex **76** performance providing 95% yield of the cyclic adduct (**b-cyclic**) in about 30 minutes. **78** keeps its high efficiency while *anti* **74** confirms itself as the worst catalyst for this process, reaching 70% conversion in 24 hours.

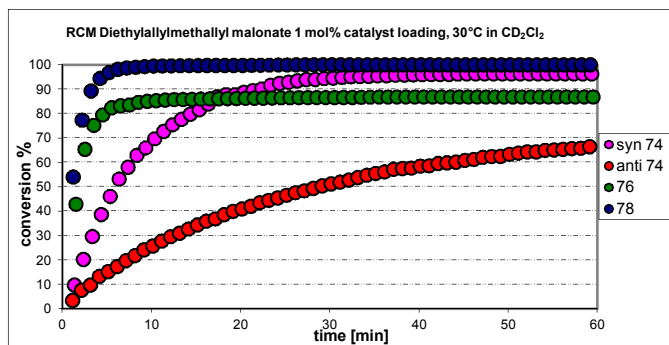
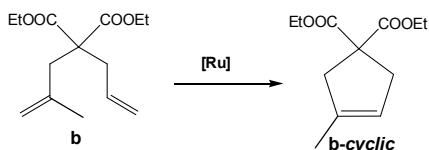


Figure 4. 6: RCM diethylallylmethylallyl malonate at 1 mol% catalyst loading of phosphine derivatives

Intrigued by the loss of catalyst **76** efficiency, we performed the ring-closing metathesis of **b** lowering the catalyst loading to gain further data that could help us in formulating an hypothesis to explain this phenomenon. For comparison, the conversion of **b** to **b-cyclic** modulated by **78** is also reported.

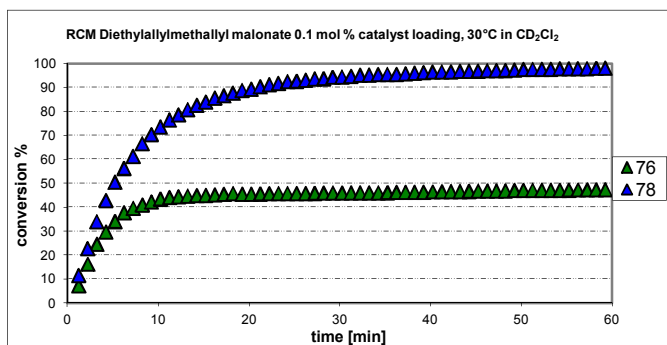


Figure 4. 7: RCM diethylallylmethyl malonate at 0.1 mol% catalyst loading of selected phosphine derivatives

By lowering catalyst loading (and monitoring the reaction overnight) it appears clear that complex **76** has turnover times of 15 minutes. This is strongly indicative that in this reaction conditions (dichloromethane, 30°C) catalyst decomposition pathways prevail on di-olefin transformation after fifteen minutes from the beginning of the reaction. This can be reasonably interpreted by considering that decomposition pathways (accelerated by the presence of free tricyclohexylphosphine and/or ethylene) have the chance to begin since olefin approach becomes slower.

The RCM of di-olefin **b** has been successfully performed by Grubbs Hoveyda's derivatives. *Anti* **75** displays the same reactivity trend observed in the RCM of **a**, and the employment of a more encumbered starting material like **b** allows for underlining this catalyst behavior. Results concerning runs at 1% of catalyst loading are summarized in table 4. 2.

run	complex	time [min]	conversion %	time [min]	conversion%
1	<i>syn</i> 75	2	82	7	100
2	<i>anti</i> 75	2	32	60	95
3	77	2	58	9	100
3	79	2	93	4	100

Table 4. 2: RCM of diethylallylmethyl malonate, at 1 mol % catalyst loading, C₆D₆ 60°C.

The conversion vs time plots for these derivatives at 0,1% of catalyst loading is reported below (Figure 4. 8). The combined effects of lower catalyst loading and increased steric olefin

hindrance contribute to magnify behavior differences that have been just hinted up to now.

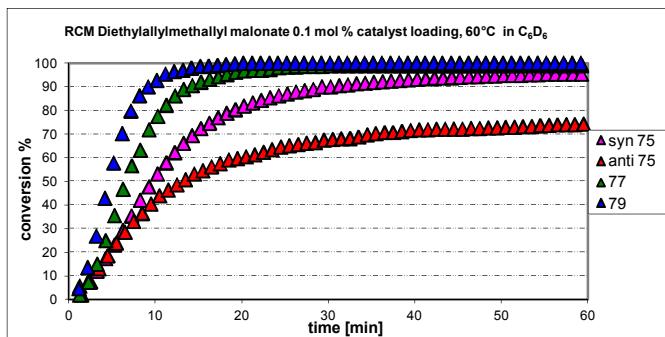


Figure 4. 8: RCM of the diethylallylmethyllyl malonate at 0,1 mol % catalyst loading of the Hoveyda derivatives

It is worth to note that while all the correctly oriented *N*-aryl complexes need about 30 minutes to cyclize **b** with a very good yield (from 90% to 100%), *anti* **75** does not overcome 77% conversion even after a week. It is clear that in this condition, a decomposition of the catalytic active species occurs: some degradation processes relative to C-H activation probably become faster than olefin reaction. Very likely the mutual *anti* *N*-aryl disposal hampers the coordination of the more encumbered diethylallylmethyllyl malonate to the metal center, favoring undesired side reactions.

RCM of Diethyldimethyllyl malonate (c)

The ring closing metathesis of the sterically more demanding diethyldimethyllyl malonate (**c**) represents one of the most challenging benchmark reaction to test catalyst efficiency, allowing us appreciate even small differences in the catalytic behaviour of complexes (**74-79**).

In Figure 4. 9 the comparison among complexes with increasing NHC steric hindrance and with different NHC ligand symmetry is reported

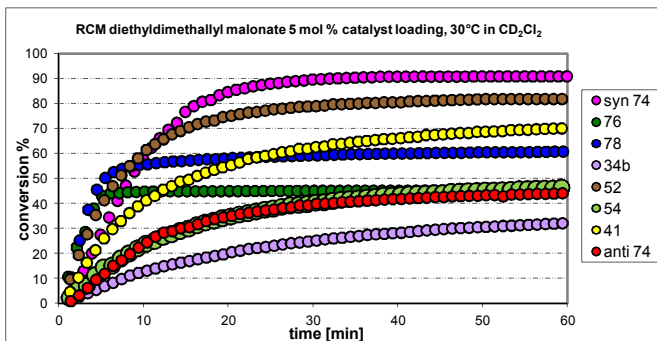
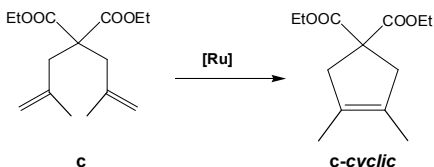


Figure 4. 9: RCM diethyl dimethylallyl malonate 5 mol % catalyst loading of phosphine derivatives

The kinetic plots of the RCM of **c** are shown in three separate figures (Figure 4. 10-Figure 4. 14), where comparison of the catalytic performance of catalysts (**34b**, **41**, **52**, **54**, **74-79**) with different substituents on the NHC ligand or different NHC symmetry are clearly highlighted.

The first comment regards comparison of the catalyst activities of the new phosphine based complexes **74**, **76**, **78** and the commercially available catalyst **41** with *o*-tolyl groups in the 1,3 positions of the NHC.

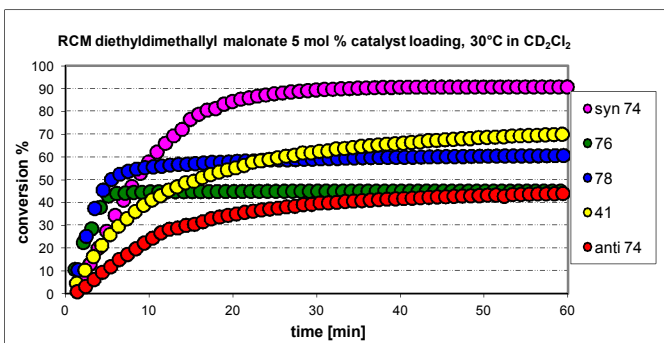


Figure 4. 10: Complexes comparison in the RCM of diethyl dimethylallyl malonate at 5 mol % catalyst loading.

Despite both **76** and **78** show the highest initial reaction rate their efficiency is affected by decomposition of the catalytically active species; their conversions are in fact quite low with respect to that of *syn* **74**, which reveals as the most active phosphine ruthenium based system known up to now.

Both complexes bearing at the *ortho* *N*-aryl position two encumbered phenyl groups (**76** and **78**) display poor efficiency as a consequence of catalyst decomposition. The more starting material steric bulk increases, the more decomposition issue is appreciable.

The importance of correctly oriented *N*-tolyl substituents is again highlighted and magnified; indeed, *N*-aryl orientation is the only structural discrimination between complex **74** isomers (*syn* or *anti*). This slight structural difference is responsible of yield halving.

The comparison among *syn* **74**, **52** and **41** (Figure 4. 11) furnishes further evidences of the pivotal role played by *syn* NHC backbone substitution to correctly orient *N*-aryl groups, thus assuming a conformation suitable to ensure high catalytic activity.

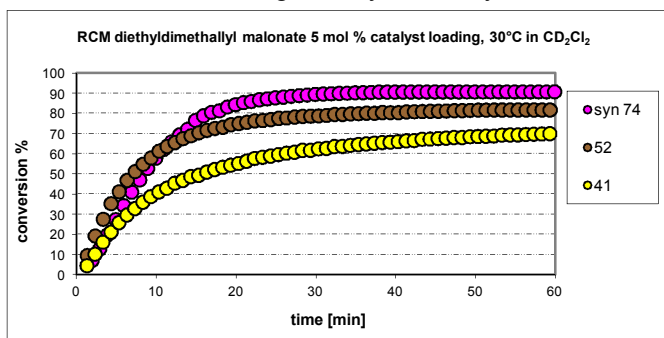


Figure 4. 11: RCM of diethyldimethylallyl malonate modulated by *syn* backbone substituted complexes

Syn **74** which is characterized by a locked *anti* orientation among backbone and *N*-aryl substituents provides a cosier coordination site for the incoming olefin. The presence of a unique appropriate symmetry metal pocket renders *syn* **74** the fastest catalyst to afford **c'**.

52 which presents two smaller methyl substituents at backbone level, is not characterized by frozen *N*-aryl conformation: rotation around C-N bond are thereafter possible providing a small percentage of *anti* oriented *N*-aryl groups. So complex **52** contains a small amount of the NHC-lower symmetry ligand which is

characterized by a more gauche active site. The overall catalysis is therefore slowed because of the presence of this second species in solution. The worst catalyst among the three reported in this plot is the commercially available **41** which presents an unsubstituted backbone. *N*-aryl rotation are therefore unrestricted; this means that the percentage of C_2 symmetric NHC-Ru raises to the detriment of the *meso*- NHC. This isomerisation process results in a drop of the utter yield.

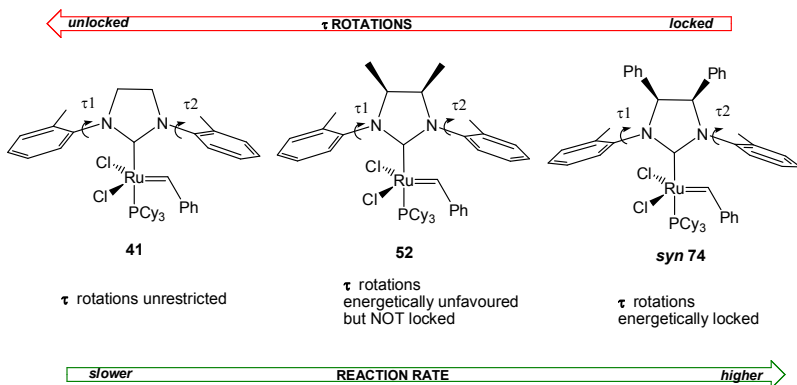


Figure 4. 12: C-N rotations for complexes **41**, **52**, *syn* **74**

The crucial role of *N*-tolyl group orientation on catalyst activity was furthermore confirmed by DFT calculations performed by Doct Chiara Costabile. In particular, the behavior of *syn* and *anti* **74** was compared by modelling the determining energy transition state structures of the RCM catalytic cycle of **c** for all possible *N*-tolyl orientations (see Appendix A). Lowest energy structure TS-A presents *syn* *N*-tolyl groups in an *anti* relationship with respect to the backbone phenyl groups. In fact, this *N*-group orientation minimizes the internal NHC repulsions as well as the repulsions of Ru ligands with the incoming substrate **c** and accounts for the higher activity of *syn* **74** (Figure 4. 13).

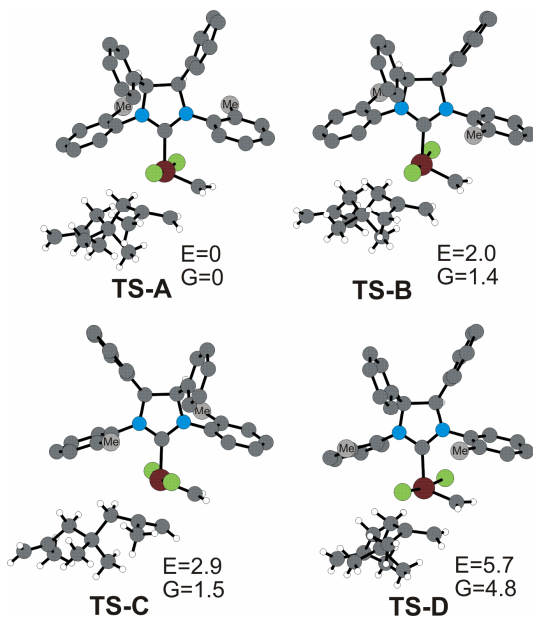


Figure 4. 13: Determining energy transition state structures of the RCM catalytic cycle of **c** for all possible *N*-tolyl orientations of **74**. Internal and free energies, calculated in CH_2Cl_2 , are in kcal/mol.

The comparison reported in Figure 4. 14 completes our study highlighting that the complex bearing a C_2 -symmetric NHC ligand (**34b**) is the worst catalyst for this transformation.

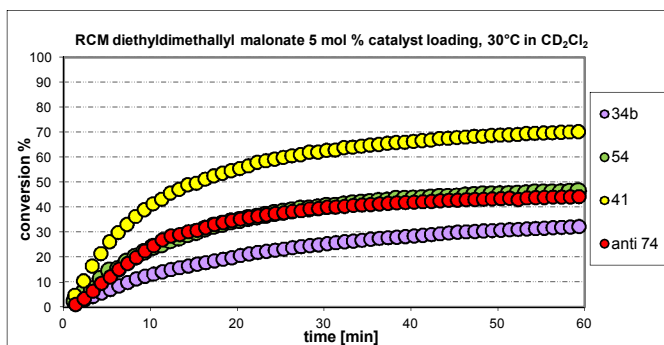


Figure 4. 14: RCM diethylidimethylallyl malonate at 5 mol % of catalyst loading for selected derivatives.

The trend observed up to now is fully respected: the more the percentage of complex bearing the anti oriented *ortho* tolyl NHC-Ru

raises, the more the corresponding catalytic activity lowers. In fact **34b** characterized almost exclusive by *anti* methyl mutual orientation results the less efficient catalyst for this RCM.

The very challenging RCM of **c** was also carried out with oxygen-chelated catalysts *syn* and *anti* **75**, **77**, **79**, and compared to that performed with their less hindered congeners **56**, **58** and to that with the commercial derivative **44**. As depicted in Figure 4. 15, all the reported complexes efficiently complete the ring closing furnishing the desired cyclized product with conversions ranging from moderate (47% for **77**) to excellent (up to 99% for *syn* **75**) within 30 min. The differences in overall activity are much less pronounced than for phosphine-based analogous (because of mechanistic difference between phosphine and ether based complexes, and also due to the kinetic effect of the raised temperature).

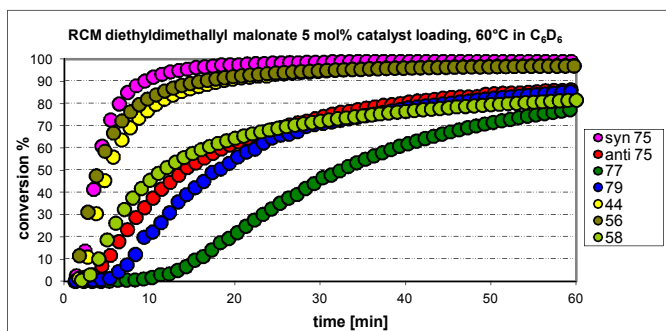


Figure 4. 15: RCM diethylidimethylallyl malonate at 5 mol % of catalyst loading for oxygen chelating systems

From this test *syn* **75** emerges as the best performing system; its less encumbered precursor **56** displays a slightly lower activity (comparable to the one of the commercially available derivative **44**), that can be related to the presence of a small percentage of *anti* oriented *ortho* tolyl groups. Hoveyda catalysts ranking traces the one of their phosphine congeners: *syn* **75** results the best catalyst because it exposes a wider empty catalytic pocket since *N*-aryl flipping results forbidden.

Notably, **77** and **79** complexes with bulkier *N*-aryl substituents on the NHC ligand show distinct differences in the initial reaction rates with respect to the less sterically encumbered *syn*-**75** and **56**

complexes. This behavior seems to support an interchange mechanism, possibly with associative character, for the first step of the initiation reaction.² Indeed, encumbered substrates would hardly be able to approach more sterically hindered complexes.

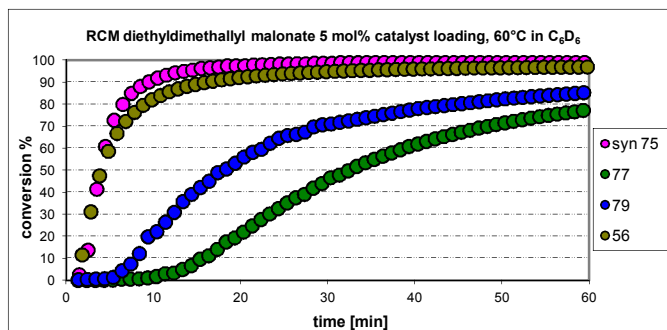


Figure 4. 16: RCM of diethyldimethylallyl malonate at 5 mol % of catalyst loading for selected ether based complexes

It is worth to note that both **77** and **79** are able to complete the ring closing in about 22 hours (they both take about 3 hours to reach a satisfying conversion of 95%). This means that their active related species are still present after this time (this is not true for their phosphine based analogous).

The difference of reactivity between *syn* and *anti* **75** (Figure 4. 17) remains significant even if less marked with respect to their phosphine analogous: *anti* **75**, infact, complete the cyclization in about twenty hours. *Anti* **75** displays a short initiation period and affords the tetrasubstituted alkene in 96 % of conversion after three hours, while *syn* **75** starts the ring closure very quickly and needs just fifteen minutes to afford the same conversion (96%).

² T. Vorfalt, K.-J Wannowius, H. Plenio, *Angew. Chem.* **2010**, *122*, 5665.

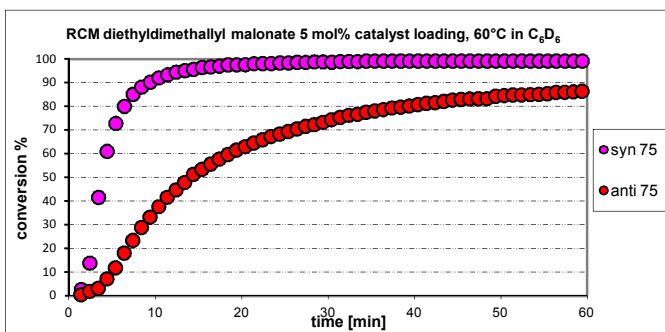


Figure 4. 17: *syn* and *anti* 75 comparison in the RCM of the diethyldimethylallyl malonate, 60°C in C₆D₆

By lowering of ten times catalyst loading, *syn* 75 maintains high performance furnishing quantitatively the cyclic adduct in a bit more than three hours.

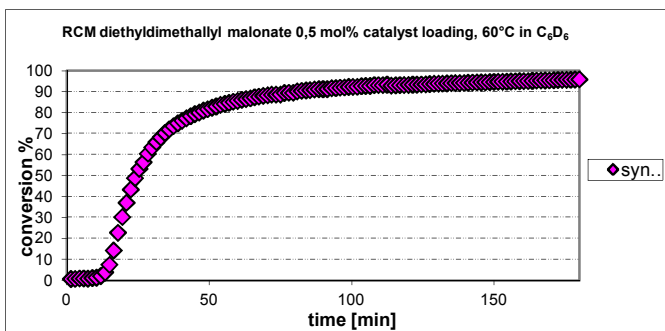


Figure 4. 18: RCM of diethyldimethylallyl malonate 0,5 mol % catalyst loading of *syn* 75

RCM standard tests on *N*-tosyl ammine derivatives

RCM of *N*-tosyldiallylamine (**d**)

Ru-catalyzed RCM reactions of *N*-Tosyl di-olefins are usually faster than the RCM of the corresponding malonate derivatives³ (probably for electronic factors). This trend is observed also for the RCM reactions promoted by the newly synthesized complexes **74**, **76**, **78**. Again, with this class of substrates differences in catalytic performance are more pronounced as olefin steric hindrance increases.

All the newly synthesized complexes show high efficiency in the ring closing metathesis of **d**, furnishing the corresponding cyclic adduct with yield from good to quantitative in a very short time.

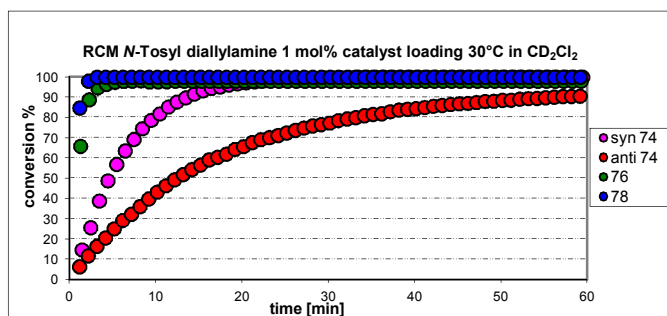
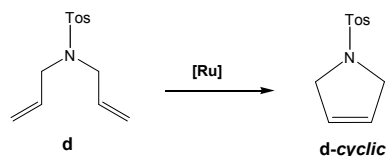


Figure 4. 19: RCM of *N*-tosyldiallyl amine modulated by the newly phosphine based synthesized complexes.

The difference in initiation rate previously observed in the RCM of the less encumbered malonate derivative **a** is maintained in the ring closing of the amine derivative **d**.

To catch differences in **76** and **78** catalytic behaviors (which are not detectable at this loading) we carried out two runs lowering catalyst loading to 0.1 mol%.

³ See for example : Fürstner, A.; Ackermann, L.; Gabor, B.; Goddard, R.; Lehmann, C. W.; Mynott, R.; Stelzer, F.; and Thiel O.R.; *Chem. Eur. J.* **2001**, *7*, 3236

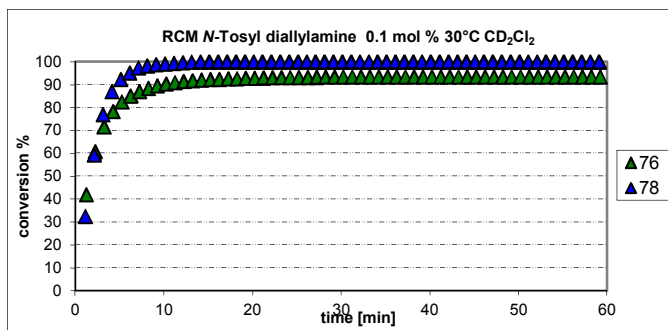


Figure 4. 20: RCM *N*-Tosyl diallyl amine, 0.1 mol % catalyst loading of selected phosphine derivatives

Complex **76** decomposition is observed also in this case, corroborating hypothesis that decomposition is modulated by several factors like the presence of free tricyclohexylphosphine that can corrupts the active species and the nature of the substituents of the NHC ligand that can promote C-H activation processes.

The RCM efficiency of Hoveyda's derivatives was tested on the upper mentioned standard di-olefin at 60 °C in deuterated benzene at 1, 0,1 and 0,05 mol % of catalyst loading. The runs performed at low catalyst loading allow us to underline slight differences among the selected complexes.

run	complex	time [min]	conversion %	time [min]	conversion %
1	<i>syn</i> 75	1	64	2	100
2	<i>anti</i> 75	1	56	7	100
3	77	1	85	2	100
3	79	1	95	2	100

Table 4. 3: RCM of *N*-tosyldiallyl amine, 1 mol % catalyst loading, C₆D₆ 60°C.

Even at 0,1 % of loading kinetic profiles of catalysts **75**, **77**, **79** are very similar (Figure 4. 21)

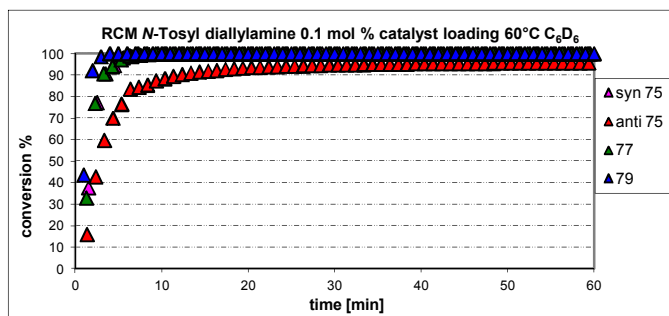


Figure 4. 21: RCM of *N*-tosyldiallyl amine, 0,1 mol % catalyst loading, C₆D₆ 60°C

To better appreciate catalyst behavior differences, the conversion vs time values for the first minutes of the RCM are tabulated.

<i>syn 75</i>		<i>anti 75</i>		77		79	
T[min]	Conv%	T[min]	Conv%	T[min]	Conv%	T[min]	Conv%
1,0	41,9	1,3	15,9	1,2	32,9	0,9	43,6
2,0	83,2	2,3	42,7	2,2	76,8	1,9	92,0
3,0	94,1	3,3	59,7	3,2	90,6	2,9	98,5
4,0	96,1	4,3	70,0	4,2	94,0	3,9	100
5,0	99,7	5,3	76,5	5,2	97,0	4,9	100
6,0	100	6,3	83,6	6,2	99,0	5,9	100
7,0	100	7,3	84,4	7,2	100	6,9	100

Table 4. 4: RCM of *N*-tosyldiallyl amine, 0,1 mol % catalyst loading, C₆D₆ 60°C.

As underlined in Table 4. 4, **79** is the first complex that allows to reach quantitative conversion of **d** in four minutes; *syn 75* and **77** requires respectively 5 and 6 minutes to match this value, while *anti 75* takes about 30 minutes to yield 95% of cyclic adduct.

To further demonstrate the efficiency of our newly synthesized catalysts (in particular of **syn 75** which has emerged as the best performing system in the challenging ring closing metathesis of the hindered diethyl dimethylmalonate **c**), we performed the RCM of

N-tosyldiallyl amine at 0,05 mol % of catalyst loading. Also in this condition metathesis results are really very good since **syn 75** is able to afford 99% conversion in 7 minutes.

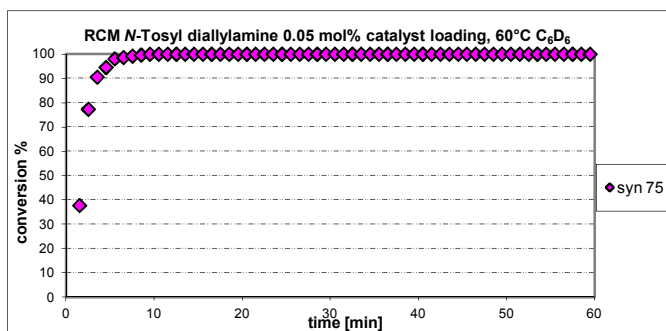


Figure 4. 22: RCM of *N*-tosyldiallyl amine, 0,05 mol % catalyst loading, C₆D₆ 60°C

RCM of *N*-tosyl allylmethylamine (**e**)

Catalytic activity of phosphine based complexes was explored in the RCM of the more sterically demanding di-olefin **e**. As for the RCM of its malonate di-olefin counterpart **b**, **76** and **78** demonstrate faster initiation rates providing the desired product in yields from high to quantitative in five minutes (90 and 100% respectively). *Syn 74* matches complex **78** performances in about half an hour, while its *anti* analogous does not overcome 85% conversion even after one day. Also for *N*-tosyl amine derivatives, passing from the olefin substrates (**a** and **d**) which furnish disubstituted cyclic adducts to those (**b** and **e**) which provide trisubstituted cycloolefins, a reactivity trend inversion is observed. *Syn 74*, in fact, outperforms complex **76** (100% vs 95% conversion, respectively).

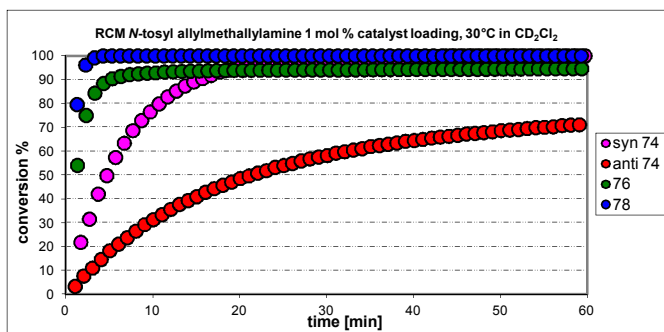


Figure 4. 23: *N*-Tosyl allylmethylamine, 1 mol % catalyst loading of selected phosphine derivatives

The same standard tests has been performed with Hoveyda derivatives at 1, 0,1 and 0,05% of catalyst loading. In the first case, differences of reactivity are not appreciable from the corresponding kinetic plots, so we summarize conversion values vs time in Table 4. 5

<i>syn 75</i>		<i>anti 75</i>		77		79	
T[<i>min</i>]	Conv%	T[<i>min</i>]	Conv%	T[<i>min</i>]	Conv%	T[<i>min</i>]	conv%
1,1	40,2	1,2	21,82	1,3	59,3	0,9	77,4
2,1	86,2	2,2	59,92	2,3	95,5	1,9	100
3,1	100	3,2	83,52	3,3	100	2,9	100
4,1	100	4,2	92,72	4,3	100	3,9	100
5,1	100	5,2	95,92	5,3	100	4,9	100
6,1	100	6,2	97,8	6,3	100	5,9	100
7,1	100	7,2	99,0	7,3	100	6,9	100
8,1	100	8,2	100	8,3	100	7,9	100

Table 4. 5: RCM of *N*-Tosyl allylmethylamine, 60°C in C₆D₆, 0,1 mol % catalyst loading of Grubbs Hoveyda derivatives

The plots related to the RCM at 0.1 mol % of catalyst loading are reported in Figure 4. 24. All the derivatives provide a quantitative transformation of the starting material, with *anti 75* emerging again

as the worst catalyst toward the RCM taking 30 minutes to reach 97% conversion (complete conversion has been observed after two hours).

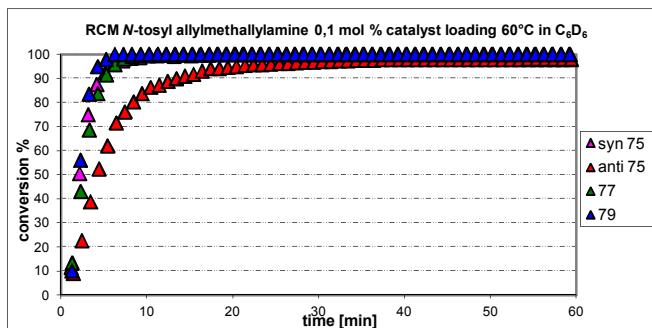


Figure 4. 24: *N*-Tosyl allylmethylamine, 60°C in C₆D₆, 0,1 mol % catalyst loading of Grubbs Hoveyda derivatives

Syn 75 continues to display very good performances even when its loading is lowered to 0,05 mol%. *e-cyclic* is indeed quantitatively obtained in less than twenty minutes.

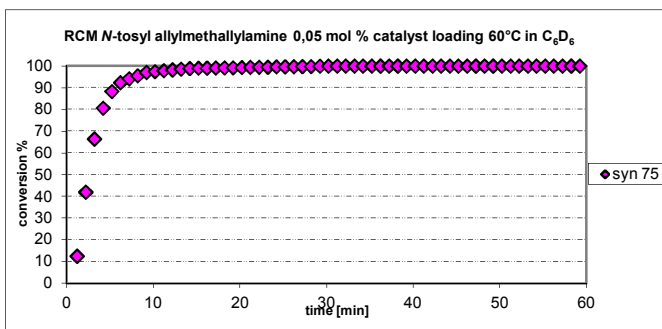


Figure 4. 25: RCM of *N*-Tosyl allylmethylamine, 60°C in C₆D₆, 0,05 mol % of catalyst loading

RCM of N-tosyl dimethylamine (f)

By increasing the steric bulk of *N*-tosyl amine derivatives, differences in catalyst performance are maximized for both phosphine and ether based systems.

Although **76** and **78** kept higher initiation rate with the more steric demanding di-olefin, decomposition issue affects their afforded yields (like for the malonate counterparts **c**) which result remarkably

lower than the one provided from the more stable *syn* **74**. The latest complex in fact fully converts the starting material into the desired adduct while **78** and **76** do not overcome the 80% and 60% of conversion respectively. The 60% of conversion is also afforded by *anti* **74** even if it takes almost five times as much needed by **76**.

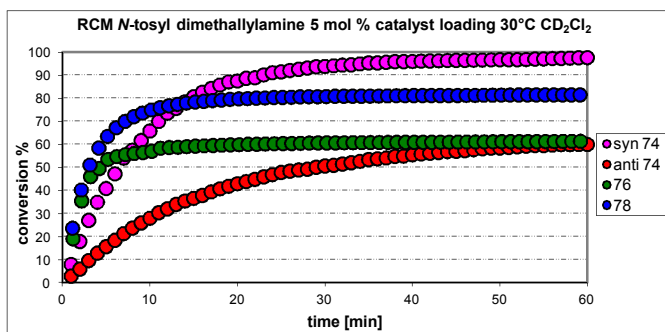
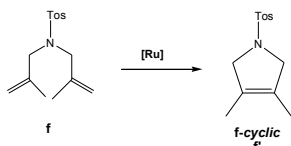


Figure 4. 26: RCM of *N*-tosyldimethylallylamine, CD₂Cl₂ 30°C, at 5 mol% of catalyst loading for phosphine derivatives.

Hoveyda derivatives were also tested in this benchmark reaction. Differences of reactivity between the two isomers of complex **75** are again underlined by increasing di-olefin hindrance. In Figure 4. 27 we can observe a difference of conversion of almost 40% between the two reported isomers; while **77** and **79** display a very similar efficiency with respect to *syn* **75**.

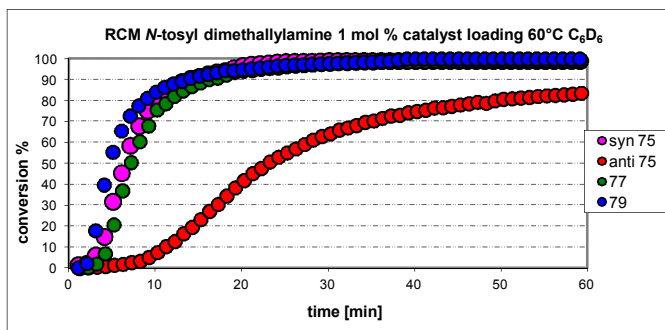


Figure 4. 27: RCM of *N*-tosyldimethylallylamine at 1 mol% catalyst loading for ether based derivatives, C₆D₆, 60°C.

Encouraged by this nice results we lowered the catalyst loading up to 0.1 mol % for **75** isomers. *Syn* isomer provides cyclic adduct **f'** in 95% yield within 40 minutes, while the mixture of NHC Ru anti isomers takes one hour to convert 30% of the starting di-olefin **f**.

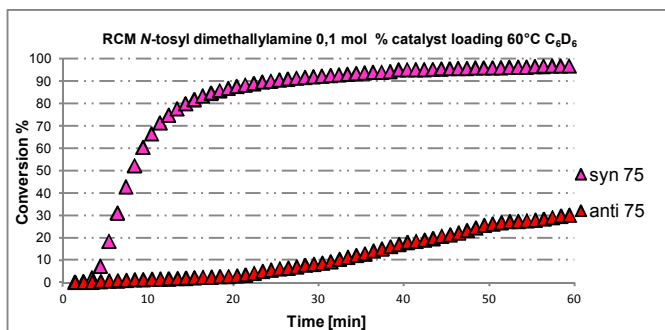
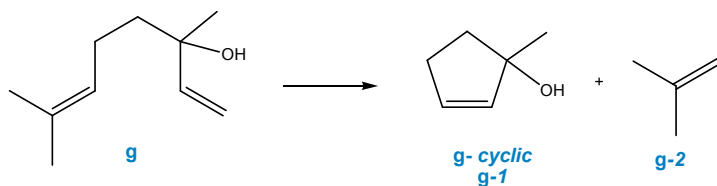


Figure 4. 28: RCM of *N*-tosyldimethylallylamine 0,1 mol % catalyst loading for selected Hoveyda derivatives, C₆D₆, 60°C.

Analyzing all the information obtained up to now, we identified *syn* **74** and **75** as the best catalysts on which focus further catalytic investigations. Indeed they offer the best compromise among good efficiency, easy handling and economic synthesis. Since we are intrigued by catalytic activity differences shown by *syn* and *anti* atropisomers, we decide to compare their behaviors in the ring closing of other interesting di-olefins.

RCM of \pm Linalool (g**)**

Our catalysts have been also tested in the cyclization of linalool **g** to the five membered ring **g-cyclic** or **g-1** (1-methylcyclopent-2-en-1-ol). This adduct represents a particularly intriguing feedstock because of its molecular structure which includes an alcohol moiety, a chiral centre and a double bond; therefore a facile route to obtain a such interesting synthon sounds very attractive.



Scheme 4. 2: RCM of linalool

Although the RCM of linalool proceeds through a sterically hindered transition state the reaction is facilitated by the coordination of the allylic alcohol to the metal center.⁴

In Figure 4. 29 is reported the comparison of *syn* and *anti* oriented isomers for complex **74** with the commercially available *N*-tolyl derivative **41**.

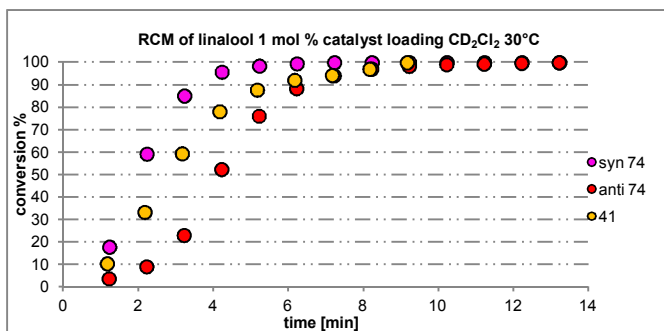


Figure 4. 29: RCM of linalool. 1 mol % catalyst loading, 30°C CD₂Cl₂

Slight differences of reactivity are detectable at this catalyst loading. In particular *syn* **74** turns out as the most efficient system to perform this reaction (successfully completing the metathesis transformation in five minutes), while *anti* **74** requires twice the time to furnish the same cyclic adduct. As intuitively expected, the activity of the commercially available catalyst **41**, which presents a floating *N*-tolyl orientation, is between the activity of the two **74** isomers in both the reported catalyst loadings (1 and 0,1%).

By lowering catalyst loading of ten times both the **74** isomers, as well as the commercial available catalyst **41**, are not able to complete the metathesis reaction even after a week.

⁴ Hoye T. L.; Zhao H. *Organic Letters* **1999**, 1, 1123

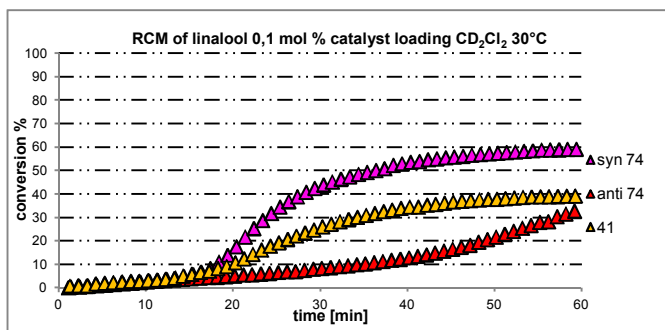


Figure 4. 30: RCM of linalool. 0,1 mol % catalyst loading, 30°C CD₂Cl₂

We also studied the behaviour of Hoveyda Grubbs derivatives in the ring closing metathesis of \pm linalool at different catalyst loadings, keeping the previously used reaction conditions for this class of catalysts. At 1 mol% of loading, **syn** and **anti 75** isomers show a reactivity which results comparable to that of the commercially available Hoveyda Grubbs catalyst **44**; all the three systems afford the cyclic adduct quantitatively in six minutes (see Table 4. 6).

Syn 75		Anti 75		44	
T [min]	Conv%	T [min]	Conv %	T [min]	Conv %
1,1	45,1	1,22	55,2	1,0	59,4
2,1	90,5	2,22	95,5	2,0	94,2
3,1	95,3	3,22	98,8	3,0	97,1
4,1	97,8	4,22	99,5	4,0	98,7
5,1	98,9	5,22	100	5,0	99,1
6,1	99,9	6,22	100	6,0	99,5
7,1	100	7,22	100	7,0	100

Table 4. 6: RCM of linalool modulated Hoveyda type complexes; 1 mol % of catalyst loading C_6D_6 60°C

By lowering of ten times the catalyst amount, differences in catalytic behaviour resulted amplified. A gap of 11% conversion as maximum value is detectable at the thirtieth minute of the kinetic measurements for the RCM performed with *syn 75* and *anti 75* (Figure 4. 31).

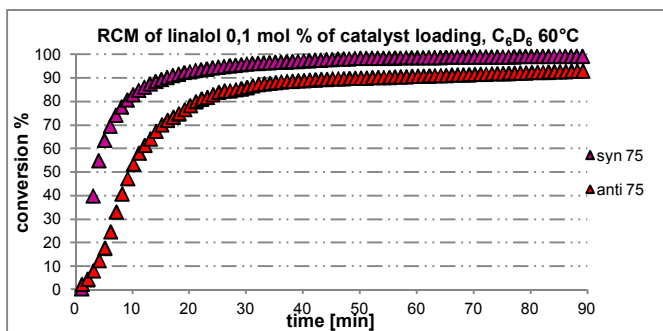
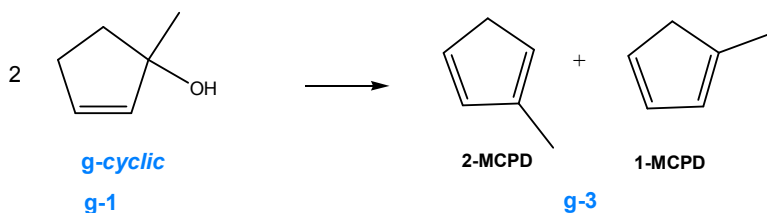


Figure 4. 31: RCM of linalool. 0,1 mol % catalyst loading of ether based derivatives 60°C C_6D_6

Also for *anti 75* at 0,1 mol % of loading we observed an incomplete conversion to the cyclic adduct since it does not overcome a 96 % conversion even after several days.

By monitoring all these reactions over the time, we observed an extremely interesting evolution of the cyclic adduct in valuable side

products. In fact the cyclic product 1-methylcyclopent-2-en-1-ol undergoes a spontaneous dehydration-isomerization process which affords a mixture of 2-methylcyclopentadiene and 1-methylcyclopentadiene (Scheme 4. 3).



Scheme 4. 3: dehydration-isomerization adducts

This transformation occurs in the presence of both the phosphine and ether based complexes in their own standard conditions (which are respectively CD_2Cl_2 30°C and C_6D_6 , 60°C).

The first time we observed this interesting evolution we were monitoring the incomplete RCM carried out at 0,1 mol % of catalyst loading for phosphine derivatives (reported in Figure 4. 30). We actually observed (leaving the mixture reacts for two days at 30°C) that all the cyclized adduct **g-1** underwent the dehydration-isomerization process while the un-reacted starting linalool (**g**) was still intact in solution.

Intrigued by this evolution, we performed further studies to fully understand this phenomenon that takes place at different timings depending on the type and the loading of catalyst employed.

To better interpret NMR spectra, complicated by signal overlaps derived from the incomplete cyclization of the starting linalool, we choose to perform these RCM at 1 mol % of catalyst loading, since in these experimental conditions all the catalysts full convert the starting material in the corresponding cyclic adduct.

For what concern phosphine based systems (**74** isomers and their commercial available analogous **41**) we performed RCM reactions for two hours obtaining the following information:

- the conversion of the cyclised alcohol to methyl cyclopentadiene derivatives starts about five minutes after cyclization is completed;

- the first formed adduct is 2-methyl cyclopentadiene, which is then slowly isomerized to 1-methyl cyclopentadiene (the isomerization takes about two days to reach a constant isomeric ratio);
- in both the transformations modulated by the newly synthesized isomers of **74** the final mixture contains 2-methyl cyclopentadiene (2-MCPD, 57%) and 1-methyl cyclopentadiene (1-MCPD, 43%) as unique species; thus, all the cyclized adduct is transformed into these valuable side products;
- also the commercial **41** fully converts **g-cyclic** in a mixture of 2-MCPD and 1-MCPD with an isomeric ratio 65:35, respectively.

In all reported cases the final mixture composition does not change by the time even after two weeks (peaks related to the Diels Alder adduct between MCPD derivatives are barely detectable).

Very likely dehydration is catalyzed by the presence of catalytic amount of HCl; the production of this inorganic acid is probably due to the reaction of the catalyst with the alcohol to exchange alkoxide ligand with the chloride or to the development of traces of HCl (C-H activation side product). This process would release a small amount of HCl which could then led to the dehydration process.⁵ In Figure 4. 32 is reported the evolution of linalool into methylcyclopentadiene derivatives and moreover a plausible dehydration reaction mechanism.

⁵ Meylemans, H. A.; Quintana, R. L.; Goldsmith, B. R.; Harvey B. G. *ChemSusChem* **2011**, *4*, 465

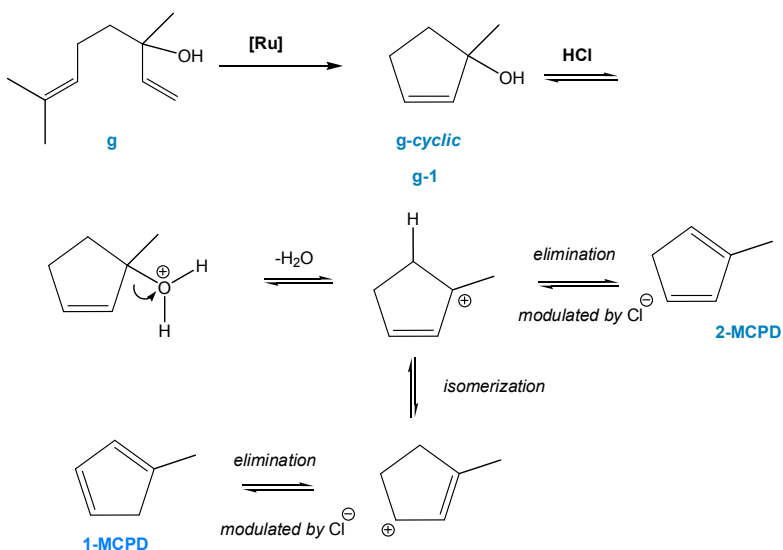
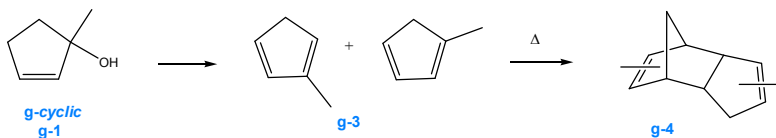


Figure 4. 32: dehydration-isomerization process

The dehydration process in the presence of Hoveyda type complexes (**44**, *syn* **75** and *anti* **75**) requires considerably longer time (we observed the formation of methyl cyclo-pentadiene derivatives after one day). This is in perfect agreement with a superior stability of the Hoveyda catalysts with respect to the Grubbs' ones. They are indeed less prone to decomposition; therefore until the catalyst is intact in the reaction mixture, no product evolution is observed. It is worth to note that by employing the Hoveyda derivatives at 60°C in benzene 1-MCPD and 2-MCPD do not represent the only components of the reaction mixture, in fact the presence of Diels Alder adducts between the methylcyclopentadiene derivatives [dimethyl-tricyclo deca-3,8-diene], together with the residual cyclized **g-1**, is detected.



Scheme 4. 4: evolution of **g-1** in presence of Hoveyda derivatives, in benzene at 60°C.

Product compositions over the time are tabled below.

Time [days]	Conversion %					
	Syn 75			Commercial 44		
	g-1	g-3	g-4	g-1	g-3	g-4
1	43,1	47,3	9,6	42,0	51,0	7,0
2	25,1	42,9	32,0	13,9	69,0	17,1
3	23,7	42,9	33,4	8,7	68,7	22,6
7	19,8	42,4	37,8	4,4	65,8	29,85
10	17,0	36,2	46,8	4,3	62,0	33,7

Table 4. 7: evolution of g-1 in presence of 1 mol % of Hoveyda derivatives, in C_6D_6 at 60°C: percentage composition of reaction crude.

The occurring of [4+2] cyclo-additions in this case is reasonable, since the reaction temperature (60°C) is high enough to enable the dimerization of the methylcyclopentadiene isomers. On the contrary, a milder temperature of 30°C, employed for the RCM of linalool modulated by the phosphine based systems, is not sufficient to afford the same result.

To confirm the role played by catalyst decomposition in the dehydration process, we performed the ring closing metathesis of linalool at 1 mol % of loading by the Hoveyda derivative **syn 75** in CD_2Cl_2 .

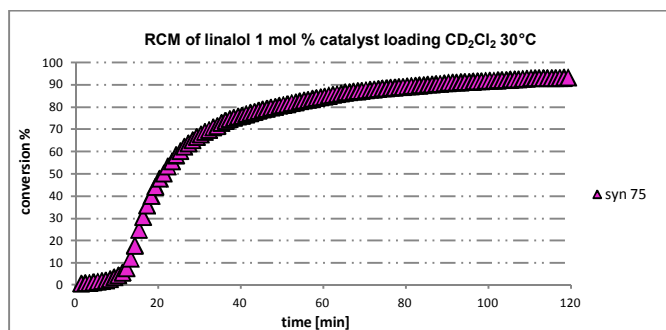


Figure 4. 33: RCM of linalool at 1 mol% of **syn 75**, CD_2Cl_2 30°C

To comment briefly Figure 4. 33 I would like to underline how much reaction conditions influence catalyst activity. Indeed the same catalyst affords **g-1** quantitatively in seven minutes if employed at 1 mol percentage of loading in benzene at 60°C. By using a dichloromethane solution at 30°C the reaction takes 4,5 hours to be quantitative.

Even leaving the reaction mixture at 30°C for a week, we did not observe the dehydration of the cyclic adduct. This evidence is quite relevant since it corroborates that the catalytic amount of HCl, necessary for the dehydration-isomerization process, is originated from catalyst decomposition and not from the reaction of the catalyst with the alcohol or from possible residual solvent HCl impurities (chlorinated solvents like CHCl_3 or CH_2Cl_2 could contain HCl traces).

Interestingly, adding a trace amount of tricyclohexylphosphine to the above reaction batch and allowing the mixture to react over weekend we observed the formation of the methyl ciclopentadiene derivatives along with a small quantity of the Diels Alder dimers).

Entry	Time [days]*	Product percentage compositions		
		g-1	g-3 (2MCPD/1MCPD)	g-4
1	3	80	15 (3:1)	5,0
2	4	77,1	16,5 (2,14: 1)	6,4
3	5**	75,9	18,5 (1,95: 1)	7,1
4	6	67,2	24,5 (1,83:1)	8,3

Values in (brackets) are relative to 2MCPD:1MCPD ratio

*in this table days are counted starting from the day in which tricyclohexylphosphine was added. Reaction was indeed monitored for seven days

** further addition of tricyclohexylphosphine.

Table 4. 8: RCM of linalool modulated by *syn* 75 at 1 mol % of loading in CD₂Cl₂

As we can see in Table 4. 8, the adding of tricyclohexylphosphine allows the dehydration isomerisation process to start.

NMR-scale conversion of linalool to **g-cyclic** under diluted conditions have been previously reported in the literature; catalysts used for this transformation comprise first and second generation Grubbs and Hoveyda-Grubbs type systems.^{3,6,7,8} Despite this investigation spontaneous and quantitative dehydration-isomerization phenomena have never been observed.

In 2011 Harvey and Co-workers,⁴ which recent interest have been addressed into the production of high density fuels from terpenes, reported a solvent free conversion of linalool to methyl cyclopentadiene derivatives. Albeit this study foregoes our observation of this interesting phenomenon, there are important differences among the final results.

They observed the spontaneous dehydration in presence of ruthenium complexes just in one case when testing the effect of raised temperature in the RCM modulated by first generation Grubbs and Hoveyda Grubbs systems. Then to investigate the extent to which a Lewis acid would dehydrate **g-1** the alcohol was made to react with different Lewis acids.

⁶ Braddock, D. C.; Matsuno, A.; *Tetrahedron Lett* **2002**, 43, 3305.

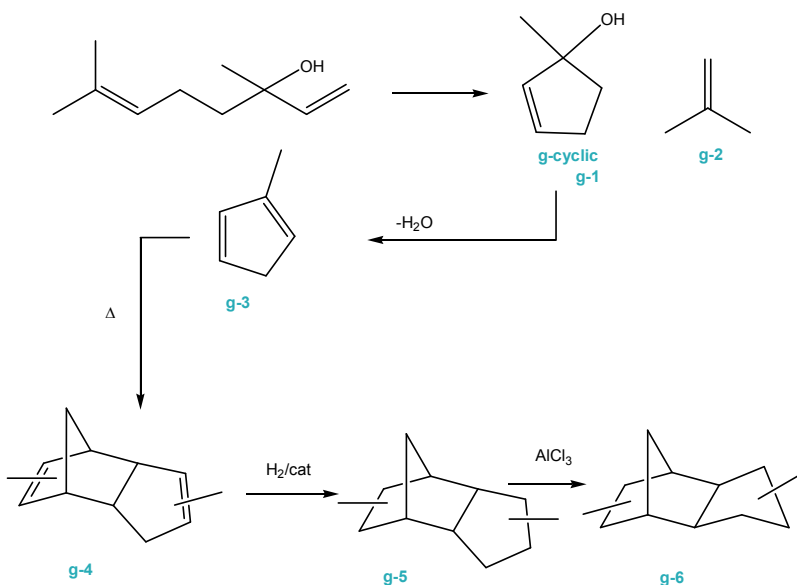
⁷ Conrad, J.C.; Parnas, H. H.; Snelgrove, J. L.; Fogg, D. E. J. Am. Chem. Soc. **2005**, 127, 11882.

⁸ Vielle-Petite L.; Claiver, H.; Linden, A.; Blumentritt, S.; Nolan, S. P.; Dorta, *Organometallics*, **2010**, 29, 775

In both case they obtain a very complex mixture of starting linalool, cyclopentenol ethers, MCPD and their dimers.

Our crude mixture instead results much cleaner since we get only a mixture of 2-MCPD-1-MCPD.

In conclusion, we can confirm that the RCM of linalool represents a facile route to products of significant interest as they can be converted to renewable fuel and polymers. Isobutylene is a valuable side-product that can be selectively trimerized to produce jet fuel,⁹ dimerized or alkylated to C4 raffinate to produce high-octane gasoline¹⁰ or polymerized to polyisobutylene.¹¹ Meanwhile **g-cyclic** is a promising precursor for the synthesis of cyclopentadiene dimers (Scheme 4. 5).



Scheme 4. 5: catalytic conversion of linalool to well refined renewable fuels.

⁹ Alcàntara, R.; Alcàntara, E.; Canoira, L.; Franco, M.J.; Herrera, M.; Navarro, A. *React. Funct. Polym.* **2000**, *45*, 19.

¹⁰(a) Haskell, D.M.; Floyd, F.; US Patent No 4301315 1981; (b) Evas, T.I., Karas, L.J.; Rameswaran, R. US Patent No 5877372, **1999**.

¹¹ Vasilenko, I.V.; Frolov, A. N.; Kostjuk, S. V. *Macromolecules* **2010**, *43*, 5503.

Dimer **g-4** can be hydrogenated and isomerized to produce high density missile fuel **g-6** (RJ-4).¹²

For what strictly concern the reactivity of newly synthesized complexes in the ring closing metathesis of the racemic alcohol **g** at 1 and 0,1% of catalyst loading, we can summarize that the differences of reactivity between the two atropisomers of each class are respected even if less pronounced than those previously observed. Probably the nature of the substrate that can coordinate through the hydroxyl group plays a key role in levelling catalytic activity differences.

¹² (a) Burdette, G. W.; Schneider, A. I. US patent number 4398978, **1983**. (b) Chickos, J.S.; Wentz, A. E.; Hillesheim-Cox, D.; Ind. Eng. Chem. Res. **2003**, *42*, 2874

RCM of 4-(allyloxy)-4,4-diphenylbut-1-yne (**h**)

The ring closing metathesis of this molecule, which present many functional groups, represents an example of ring-closing enyne metathesis (RCEYM). The cyclization of this substrate leads to a valuable adduct which presents many sites for further functionalizations.

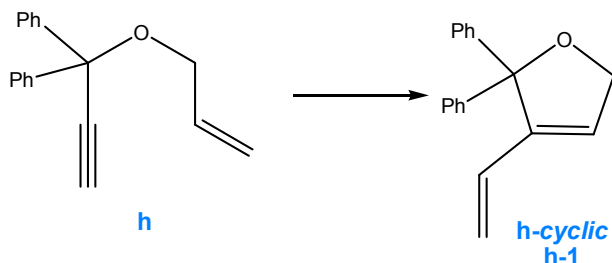


Figure 4. 34: Enyne metathesis of **h**

We explored the activity of both the atropisomers of complexes **74** and **75** toward the ring closing of this enyne (both at 1 and 0.1 mol% of catalyst loading).

Syn and *anti* **74** displayed excellent activity in this reaction affording, in standard conditions (dichloromethane, 30°C, 1 mol % of catalyst loading), **h-cyclic** in respectively two and four minutes. Results of these runs are reported in Table 4. 9 to better elucidate behavior differences not detectable by plotting conversion vs time curves. Their corresponding Hoveyda analogues **75** are extremely active toward this reaction as well. The activity of Hoveyda catalysts at 1 mol % of loading is so pronounced that differences are hardly appreciable.

NHC-Phosphine Ru systems				NHC-o-isopropoxyphenylmethylidene Ru systems			
<i>syn 74</i>		<i>anti 74</i>		<i>syn 75</i>		<i>anti 75</i>	
T[<i>min</i>]	conv%	T[<i>min</i>]	conv%	T[<i>min</i>]	conv%	T[<i>min</i>]	conv%
1,1	97,66	1,05	55,22	0,85	78,97	0,83	78,16
2,1	100	2,05	95,21	1,85	100	1,83	100
3,1	100	3,05	99,17	2,85	100	2,83	100
4,1	100	4,05	100	3,85	100	3,83	100
5,1	100	5,05	100	4,85	100	4,83	100

Table 4. 9: RCM of **h** at 1 mol % catalyst loading. Standard conditions for phosphine based systems :CD₂Cl₂, 30°C; for ether based catalysts: C₆D₆, 60°C.

Intramolecular enyne metathesis results thermodynamically favorite because its adduct bears a conjugated double bond; even more initiation time, usually due to slow olefin approach, is minimized because of a plausible substrate-oxygen coordination to the ruthenium centre.

Also lowering phosphine based catalyst loading of ten times, conversion to the cyclic adduct **h** remains quantitative, with *syn 74* confirming a faster initiation with respect to its lower symmetry NHC analogous (*anti 74*).

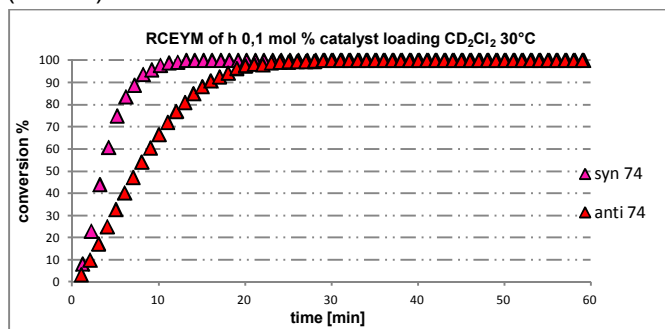


Figure 4. 35: RCM of **h** modulated by 0,1 mol % of phosphine based systems at 30°C in CD₂Cl₂

By testing Hoveyda lower and higher NHC-symmetry isomers at 0,1 mol % of loading, we could catch a slight difference of catalytic

behaviour which is more relevant in the first minutes of the reaction (a magnification of conversion vs time plot is reported in Figure 4. 36 to highlight it); both complexes reach complete conversion to the cyclic adduct **h-1** in five minutes.

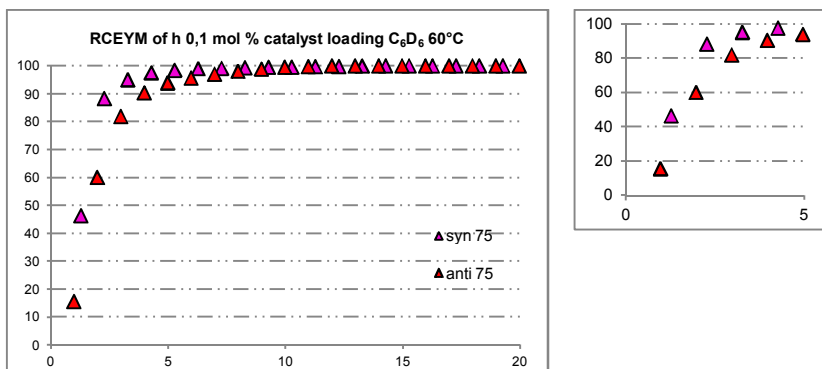


Figure 4. 36: RCM of h modulated by Hoveyda isomeric derivatives at 0,1 mol % in benzene at 60°C

RCM toward macrocycles with different steric hindrance (i and I)

A ring architecture of twelve or more atoms is frequent in a great number of natural and synthetic macro lactones, lactams, ethers, and ketones; these macrocycles often exhibit important biological properties, such as antitumor, antibiotic, and antifungal activities. Some of these compounds are also used in cosmetic industries (as perfumery ingredients for instance).¹³ The total synthesis of large cycles can result quite laborious; but novel approaches often involve a ring closing metathesis step which greatly simplify the synthetic route to the target. Recent evolution and developments highlight the notion that RCM is amongst the most straightforward entries into large ring systems and competes to all current strategies.¹⁴

The main issue concerning this reaction is the lack of selectivity and of its predictability toward the formation of *E/Z* double bonds, together with the formation of oligomers of the starting material instead than the desired cycle. The latter issue is usually overcome by strongly diluting the reaction mixture.

In the ring closing reaction for the formation of lactones **i** and **I** at increased steric hindrance, we selected and employed the most active among the newly phosphine and ether based synthesized complexes. From the precedent catalyst screening in the RCM for the synthesis of five membered rings, complexes bearing phenyl backbone substituents and *o*-tolyl groups in 1 and 3 positions of the NHC, emerged as the most efficient systems (since they combine good activity at high stability). So we tested isomers *syn* **74** and **75** in the ring closing of these challenging substrates.

¹³ Nicolaou, K. C.; Bulger, P. G.; Sarlah, D.; *Angew. Chem.* **2005**, *117*, 4564; *Angew. Chem. Int. Ed.* **2005**, *44*, 4490

¹⁴ Review and articles on macrocycle syntheses: (a) Roxburgh, C. J. *Tetrahedron* **1995**, *51*, 9767. (b) Fürstner, A.; and Langemann, K.; *J. Org. Chem.* **1996**, *61*, 3942. (c) Lee, W. C.; and Grubbs, R. H. *J. Org. Chem.* **2001**, *66*, 7155. (d) Parenty, A. Moreau, X. and Campagne J.-M. *Chem. rev.* **2006**, *106*, 911.

Macrocyclization of but-3-enyl undec-10-enoate (*i*)

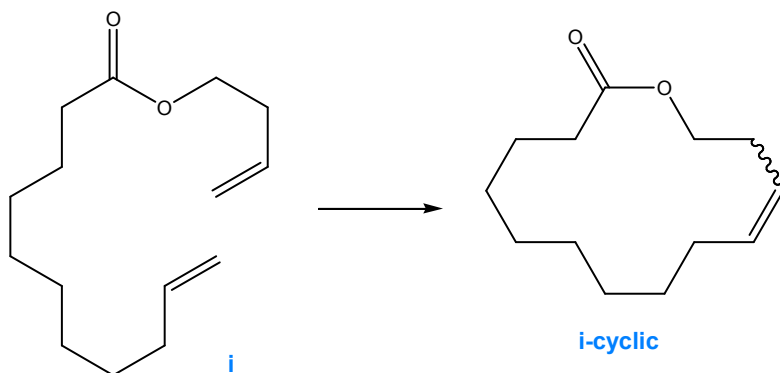


Figure 4. 37: schematic ring closing metathesis toward the 14-membered lactone *i*.

Both selected complexes *syn* **74** and **75** display high catalytic activity leading to the cyclic adduct of *i* with yields of respectively 95,6% and 98,8% in 30 minutes. Both catalysts which give quantitative cyclization of *i*, displaying bad selectivity toward the *Z* alkene. Indeed NMR and GC-analysis for purified product shows very high *E/Z* ratio. More in detail, *syn* **74** furnishes the desired product with *E/Z* ratio is 9:1; while *syn* **75** provides *i-cyclic* with *E/Z* ratio of 15.6/1. This experimental evidence can be explained considering that the stereochemical outcome of the RCM reaction to produce macrocycles is not easy to predict and control, and, in principle, the *E/Z* selectivity of the olefin product reflects the thermodynamic stabilities of both geometrical isomers.

Macrocyclization of 3-methylbut-3-enyl undec-10-enoate (I)

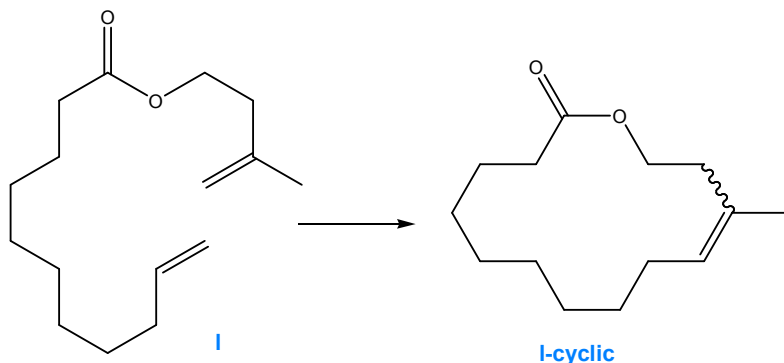


Figure 4. 38: schematic ring closing metathesis toward the macrocycle of I

Passing from a macrocycle containing a di-substituted double bond to a tri-substituted final product as target, the challenge of this process raises considerably. This appears clear looking at the kinetic evolution of this cyclization reported below.

	Syn 74	Syn 75
time [h]	conversion%	conversion%
0,5	57,8	10,1
1,0	62,3	12,9
1,5	67,9	21,4
2,0	68,1	16,3
2,5	68,3	22,9
24	75 (82/18)	47 (75/25)

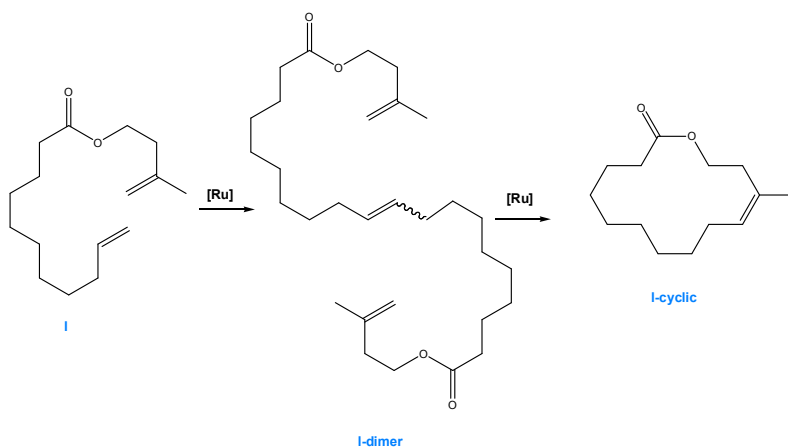
Table 4. 10: RCM of ester I performed at 5 mol % of catalyst loading in refluxing dichloromethane (40°C). Final values for E/Z ratio are reported in (brackets).

The results shown in Table 4. 10 highlight that *syn 74* is a better catalyst for this macrocyclization with respect to its Hoveyda analogous *syn 75*. It is worth to note that for the ring closing metathesis of small dienes previously described (see RCM of diethylmalonate and *N*-tosyl amine derivatives in the first part of this

chapter), Hoveyda derivatives have always displayed superior catalytic activities. The different catalytic behavior observed in the macro-RCM can be interpreted by considering that phosphine and ether based complexes are characterized by different initiation mechanism. In particular Hoveyda complexes display a barely latent behaviour since they need higher temperature (60°C) to gain enough energy to overcome more quickly the interchange-associative step (which is the first of the metathesis cycle). The reaction conditions generally employed for the macrocyclization are much more similar to those usually employed for phosphine based systems (in the RCM toward five membered rings, DCM, 30°C), than those routinely employed for Hoveyda catalysts (benzene, 60°C). The *E/Z* ratio slightly changes during the course of the reaction to approach the thermodynamic value, as a consequence of secondary metathesis reactions that can cause isomerization.

Column chromatography work up of the crude mixtures of both the cyclizations (performed by **syn 74** and **75**) led us to isolate a dimer of ester **I** lactone which has recently been identified by Fürstner et al¹⁵ as the intermediate for the macrocyclization reaction. In particular the reaction proceeds first via dimerization, then on prolonged heating **I**-dimer almost disappear while **I**-cyclic becomes the major product. This actually occurs also in our case since by monitoring the reaction via GC we saw **I**-dimer peak decreases over the time while **I**-cyclic related signal increases.

¹⁵ Fürstner, A.; Thiel, O. L.; Ackermann, L.; *Org.Lett.* **2001**, 3, 449.



Scheme 4. 6: macrocyclization intermediates of I. experimental condition: refluxing dichloromethane, 5 mol % of catalyst loading

Conclusion

The catalytic behaviour of the newly synthesized II generation complexes have been extensively studied in the ring closing metathesis toward five membered cycloalkenes.

The replacement of methyl groups by more encumbered phenyl on the NHC backbone of Ru complexes improves catalyst efficiency, confirming the relevance of the presence of NHC backbone substituents with a *syn* stereochemical relationship to obtain highly active RCM catalysts; overall in the RCM of hindered diolefins. As a matter of fact *syn* **74** and **75** have emerged as the most active ruthenium based catalysts for hindered di-olefins known up to now.¹⁶ Moreover, catalysts **74** and **75** are more easily prepared with respect to their congeners **52** and **56**, and this aspect makes them very attractive for commercial applications.

In addition, the employment of suitable substituted NHC backbone enables, for the first time, the facile synthesis of separated, stable conformers of *N*-tolyl Ru complexes (**74** and **75**) Notably, the different performances of isolated *syn* and *anti* isomers of **74** and **75** provide the first unequivocal proof for the significance of correctly disposed *N*-aryl groups to successfully accomplish RCM reactions.

¹⁶ Perfetto A., Costabile, C.; Longo, P.; Bertolasi, V.; Grisi, F.; *Chem. Eur. J.* **2013**, *19*,10492.

74 and **75**, selected as the best performing systems belonging to the different classes (II gen. Grubbs and Grubbs Hoveyda), have been screened in the macrocyclization reaction as well as in the ring closure toward interestingly functionalized synthons. It is worth to note that in some cases we reach excellent yields in short time with a catalyst loading of 0.05mol%, matching the industrial scale up requirements for metal catalysis quantities.

A peculiar catalytic behaviour of our complexes has been noted and deepen in the ring closing metathesis of the commercially available terpene (**g**); these findings represent further evidence that support the possibility to convert a renewable feedstock in high density fuels surrogates.⁵

Syn **74** and **75** display very good activity in furnishing the macrocyclic adduct **i** and **I**, ranking themselves among the most efficient catalysts in this particularly challenging reaction.

Experimental Procedures

The ring closing metathesis of dienes **a-h** has been performed on small scale and the conversion of the starting materials to products over time was determined by integrating diagnostic signals in the starting material and in the product in the ¹H-NMR spectrum.

The formation of unsaturated lactones (**i** and **I**) was monitored by GC analysis over a period of 24 h. Crude mixture of cyclic adduct for **i** and **I** have been purified by column chromatography in order to confirm both conversion and E/Z product ratio obtained from GC. All reactions were performed at least in duplicate to confirm reproducibility. All the starting materials (apart from the ones commercially available) have been synthesized following reported procedures¹⁷

Representative Procedure for the ring closing of dienes **a-h**: an NMR tube with a screw-cap septum top was charged with 0.80 mL of a CD₂Cl₂ or C₆D₆ solution of catalyst (molarity of the solution was

¹⁷ For the synthesis of di-olefins **a-g** see supporting information of Gatti, M.; Vieille Petit, L.; Xinjun Luan, Mariz, R.; Drinkel, E.; Linden, A.; and Dorta, R. *J. Am. Chem. Soc.*, **2009**, *131* (27), 9498. For the synthesis of **h** see Fürstner, K. Langemann, *J. Org. Chem.* **1996**, *61*, 3942. For the synthesis of **i** see: Fürstner, A.; Thiel, O. R.; and Ackermann, L. *Org. Lett.*, **2001**, *3* (3), 449

varied according to the desired one for the RCM tests: from 5 to 0.05 mol%). After equilibrating at the appropriate temperature the sample in the NMR probe, 0.080 mmol of diene was injected into the tube. The reaction was monitored as a function of time, and the conversion to the cyclic adduct was determined by integrating diagnostic signals for the starting material and the product.

Representative Procedure for the Synthesis of Macrocyclic Compounds **i** and **I**: 100-mL three-necked round-bottomed flask was fitted with a condenser and two additional funnels. Solutions of the ruthenium carbene (6.0 μmol) and the diene (120 μmol **i** or **I**), each in CH_2Cl_2 (10 mL), were independently added dropwise to refluxing CH_2Cl_2 (10 mL) over a period of 15 min under a nitrogen atmosphere. Aliquots were removed periodically for GC analysis, and GC retention times and integration were confirmed with samples of authentic material. After 24 h, the solvent was removed in vacuo, and the residue was purified by flash chromatography to afford analytically pure compounds. ^1H and ^{13}C -NMR were perfectly coherent to the one previously reported for compounds **i**-cyclic^{14b} and **I**-cyclic.¹⁵

Evolution by the time of reaction crude for the RCM of linalool modulated by *syn* **74** is reported in Figure 4. 39-Figure 4. 41.

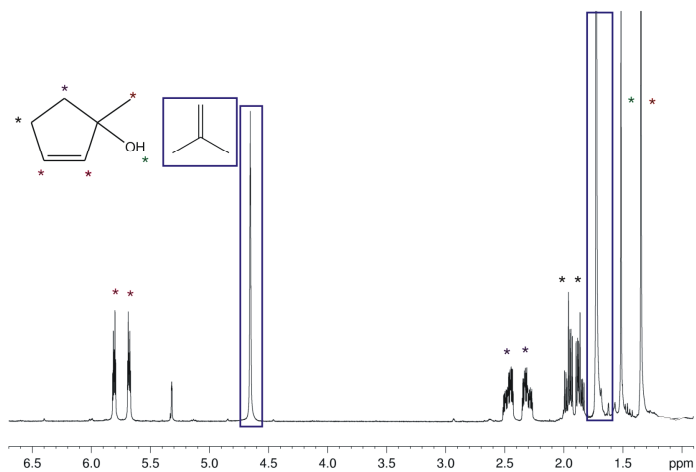


Figure 4. 39: $^1\text{H-NMR}$ of g-1 in CD_2Cl_2 . Reaction crude of the RCM of g modulated by *syn* 74 (1 mol%); reaction time about 10 min

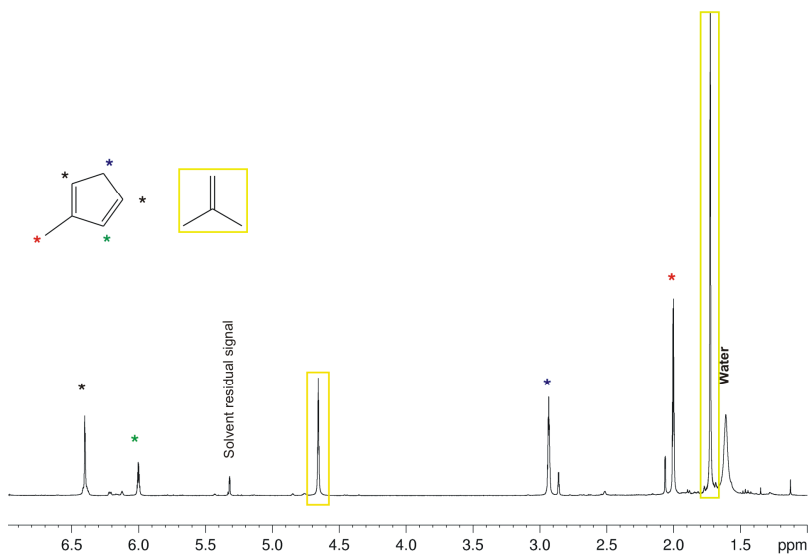


Figure 4. 40: $^1\text{H-NMR}$ of 2-MCPD in CD_2Cl_2 . Crude reaction related to the RCM of g modulated by *syn* 74 (1 mol%); reaction time about 100 min

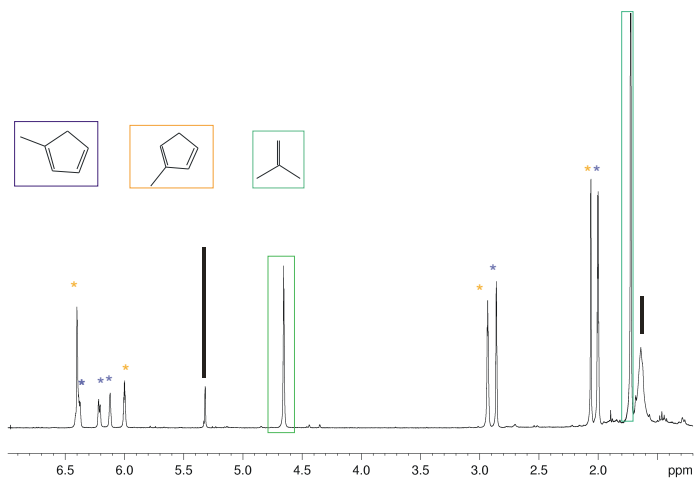


Figure 4. 41: $^1\text{H-NMR}$ of for the 2-MCPD/1-MCPD mixture in CD_2Cl_2 . Crude reaction related to the RCM of **g** modulated by *syn* **74** (1mol%); reaction time about 24 hours

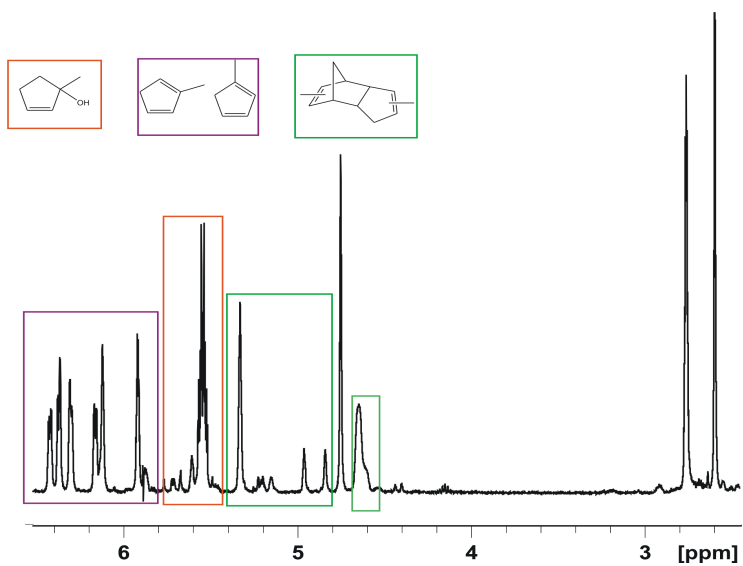


Figure 4. 42: $^1\text{H-NMR}$ of the crude of the RCM of **g** modulated by *syn* **75** (1mol%) in C_6D_6 ; reaction time about 10 days

Chapter 5

Screening of selected new Ru-Based catalysts in ring opening metathesis polymerization and cross metathesis

Abstract

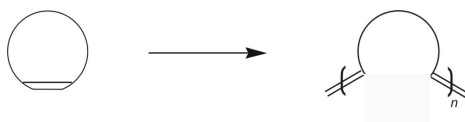
After full investigation of the newly synthesized complexes (see chapter 3 and chapter 4) in ring closing metathesis reactions, we choose to broaden catalytic exploration on **74** and **75** systems which offer the best compromise among high activity; excellent stability, easy and cost effective synthesis. In particular we tested catalytic activity of complexes *syn* and *anti* **74** and **75** at different loadings toward the Ring Opening Metathesis Polymerization; while for what concern activity toward Cross Metathesis, we conducted a comparative study between the upper mentioned phosphine based systems (**74** isomers) bearing lower and higher NHC symmetry. We were again particularly interested in catching catalytic behavior differences among atropisomeric complexes, over than exploring their activity toward these new classes of reactions.

Ring opening metathesis polymerization

Introduction

Ring opening metathesis polymerization is a powerful methodology for the preparation of a wide range of synthetic polymers characterized by different architectures. An interesting aspect of this class of reactions is the possibility to control polymer microstructures comprising double bond arrangements (*cis/trans*), relative monomer configurations (e.g. head to tail, tail to tail and so on) and various tacticities. It is pleonastic to remember that microstructural control is essential to modulate polymer properties.¹

¹ Keitz, B. K., Fedrov, A.; Grubbs, R.H.; *J. Am. Chem. Soc.* **2012**, *134*, 2040.



Scheme 5. 1: Schematic ROMP reaction

Ring-opening metathesis polymerization has been successfully applied in the synthesis of commercial available polymers; a great variety of materials obtained from ROMP is now on the market: Vestenamer[®] (derived from the ROMP of cyclooctene), Norsorex[®] (ROMP of norbornene), and numerous other products from the ROMP of dicyclopentadiene (Telene[®], Metton[®], Prometa[®], Pentam[®]).²

ROMP reactions, like most olefin metathesis processes, are generally reversible and the equilibrium position (monomer \leftrightarrow polymer) can be controlled by considering process thermodynamics. As most of the ring opening polymerization process, ROMP driving force relieves in ring strain release balanced by entropic penalties. The most common monomers used in this reaction are cyclic olefins which possess a considerable degree of strain (>5 kcal/mol) such as cyclooctene and norbornadiene. If ring strain is low, cyclic olefins have very little enthalpic driving force to be polymerized via ROMP.³

Usually to perform the polymerization via ring opening metathesis of sterically hindered or electronically deactivated olefins, it was necessary the use of a tungsten or molybdenum based catalysts like **80** and **81**, whose high efficiency compensates the low monomer reactivity.

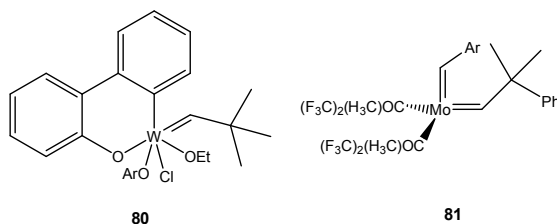


Figure 5. 1: tungsten and molybdenum based systems

² [a] Mol, J. C.; *Journal of Molecular Catalysis A: Chemical*, **2004**, *213*, 39; [b] Trimmer, M.S.; Grubs R. H.; *Handbook of Metathesis*, **2003**, *3*, 407.

³ Bielawski, C. W.; Grubbs, R. H.; *Progress in Polymer Science*, **2007**, *32*, 1.

These complexes display high initiation rate and they can produce “living” polymerization with excellent control of polydispersivity and chain tacticity, but their low functional group tolerance limits the monomers available. Ruthenium metathesis catalysts tend to have worst overall performances, but their major stability and inertness toward oxygen, moisture and many functional groups, make them “user friendly” and enable their use for the polymerization of functionalized monomers and various additives. These evidences have spurred great interest on ruthenium based systems, and in the past few years, intense investigation on catalyst design have led to Ru-based complexes which displayed dramatically enhancement of metathesis activity while maintaining good stability. These complexes are currently in use for challenging ROMP processes.⁴

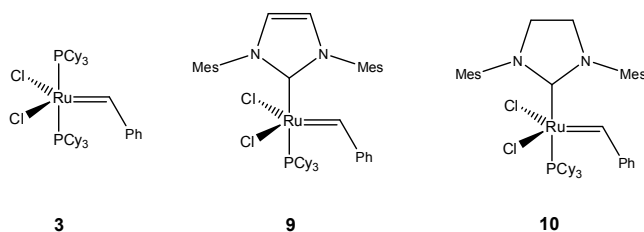


Figure 5. 2: phosphine based ruthenium catalysts

For what concern the micro-structural control of the final polymer, main issues are due to secondary metathesis reactions; in particular the eventual isomerization process of the *Z* kinetic product to the thermodynamically favored *E*. This double bond geometry isomerization usually takes place in the late stage of the process, resulting in a frequent and significant complication which renders the development of *cis*-selective catalytic transformation a difficult task.⁵

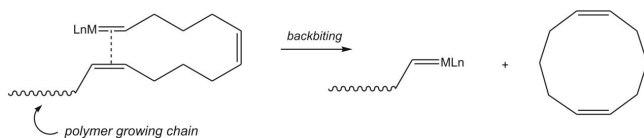
There are moreover other secondary metathesis reactions (that can be controlled by an appropriate catalyst choice and by modulating reaction conditions) that also affect the product distribution. In particular re-coordination of a double bond of the growing polymer chain to the metal center can lead to cyclic oligomers through a ring-closing metathesis reaction (“backbiting”, **pathway A**, Scheme

⁴ Bielawski, C. W.; Grubbs, R. H.; *Angew. Chem.* **2000**, *112*, 3025.

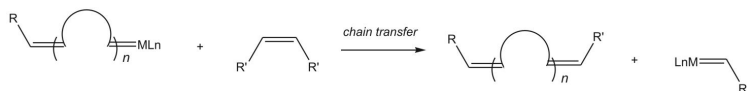
⁵ Khan, R. K. M.; Torker, S.; Hoveyda, A. H.; *J. Am. Chem. Soc.* **2013**, *135*(28), 10258.

5. 2). Chain transfer (cross metathesis, **pathway B**, Scheme 5. 2) between a growing polymer unit and an adjacent polyalkenamer also leads to broadened molecular weights.³

pathway A



pathway B



Scheme 5. 2: secondary metathesis reactions contributing in affecting product distribution.

Chain transfer can anyway be used to improve processability of the resulting polymer: addition of an acyclic olefin (chain-transfer agent) can limit chain molecular weights and introduce terminal functional groups (also leading to telecheric polymers).^{2,3,6}

Results and discussion

The catalytic behavior of both atropisomers of complexes **74** and **75** (*syn* and *anti*) has been studied in the ring opening metathesis polymerization of two monomers with increasing steric hindrance: **m** and **n** (it is worth to note that usually an increased starting material encumbrance implies a major challenge):

- 1,5-cyclooctadiene (COD);
- 1,5-dimethyl-1,5-cyclooctadiene (DMCOD).

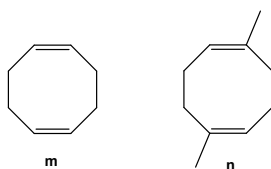


Figure 5. 3: selected Ring-Opening Metathesis Polymerization substrates

⁶Slugovc, C.; Macromol Rapid Communication, **2004**, 25, 1283.

The evaluation of the catalytic activity of complexes **74** and **75** toward this new type of metathesis reaction has also been aimed at understanding possible behavior differences between *syn* and *anti* conformers of **74** and **75**, as already observed in the RCM reactions.

ROMP of 1,5-cyclooctadiene (m, COD)

In the ring-opening metathesis polymerization (ROMP) of cyclooctadiene (**m**), monitored by ^1H NMR, *syn* **74**⁷ disclosed higher activity than its lower NHC symmetry isomer (*anti* **74**).

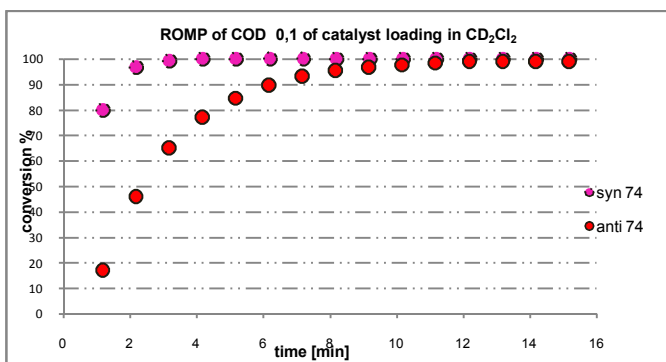
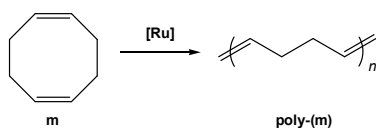


Figure 5. 4: COD ROMP modulate by phosphine based isomeric derivatives of **74. 0,1mol % of loading CD₂Cl₂, 30°C**

Related values of experimental cis/trans ratio are reported in Table 5.1

⁷Ritter, T.; Hejl, A.; Wenzel, A. G.; Funk, T. W.; Grubbs, R. H.; *Organometallics*, **2006**, *25*, 5740.

run	catalyst	time [min]	yield % ^a	cis/trans ^b
1	<i>Syn</i> 74	3	>99	0,92
2	<i>Anti</i> 74	12	>99	1,27
3	41	5	>99	1,0

Experimental conditions: CD₂Cl₂, 30 °C, catalyst 0.1 mol %, m= 0.5 M. ^a Determined by NMR. ^b Ratio based on ¹H-NMR data analysis.

Table 5. 1: COD ROMP modulate by phosphine based isomeric derivatives of **74 and the commercial **41**.**

¹H-NMR (and when performed, ¹³C NMR) spectroscopic analysis allowed the determination of the *Z* fraction of the newly formed double bond in the polymer chains. It is worth to point out that generally Grubbs second generation catalysts give rise to a polyalkenamer with a predominately *E* olefin content, as a consequence of an equilibrium-controlled polymerization in which secondary chain transfer occurs.⁴ On the other hand, first-generation catalyst **3** leads to a higher *Z* olefin content, but it is also dramatically less active.

The data reported in Table 5.1 highlight that *syn* **74** is the best performing system in term of conversion rate; while its isomer *anti* affords the desired polymer, albeit more slowly, with an higher *Z/E* ratio. The activity and the cis/trans ratio of the commercial available complex **41** are between those of the two isomers of **74**.

Indeed by monitoring the polymerization proceeding via ¹H-NMR we can observe that the *Z/E* ratio begins significantly to change when the conversion of **m** to the corresponding polymer is higher than 75%, indicating that secondary metathesis on existing polymer chains is strongly competitive with the polymer growing, and it prevails when the concentration of monomer becomes too low. After complete polymerization of **m**, it can be observed that the catalysts still work to isomerizes the double bonds of the polymer chains from *Z* to *E*.⁴

By lowering of ten times catalyst loading, catalytic behavior differences between the two conformers of **74** are maximized.

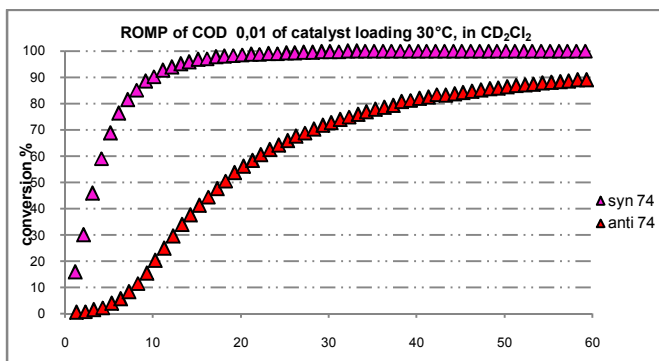


Figure 5. 5: COD ROMP modulate by phosphine based isomeric derivatives of 74. 0,01 mol % of loading CD_2Cl_2 , 30°C

First of all we can observe that *syn* **74** successfully completes the polymerization process in twenty minutes while *anti* **74** does not overcome the 90% conversion in one hour. Cis/trans ratios result extremely different (see bottom reported in Table 5.2) but these values are consistent with such a profound difference of reactivity. Cis/trans ratio remains quite close to the statistical value ($75/25=3$) for *run* 4, reasonably because there is still enough starting material in solution which competes with the double bond unit of the polymer for the catalyst active site. This competition slower the isomerization process.

Run	Catalyst	Time [min]	Yield ^a %	Cis/Trans ^b
3	<i>Syn</i> 74	20	>99	1,4
4	<i>Anti</i> 74	60	90	2,3

Experimental condition: CD_2Cl_2 , 30 °C, catalyst 0.01 mol %, $m=0.5$ M. ^a Determined by NMR. ^b Ratio based on data from 1H and ^{13}C NMR of isolated products.

Table 5. 2: COD ROMP modulate by phosphine based isomeric derivatives of 74. 0,01 mol % of loading CD_2Cl_2 , 30°C;

It is worth to note that a slightly structural difference due to the *ortho* substituents mutual arrangement seems to play an important role since it affects both the reaction rate and the cis/trans ratio of the final polymer.

Catalytic activity of Hoveyda type derivatives was also explored toward this new type of metathesis. Reaction conditions selected

for this class of complexes contemplate a 60°C temperature and the use of benzene as solvent. Both **75** isomers at 0,1 mol % of loading perform cyclooctadiene (**m**) ring opening metathesis polymerization in very short time (two minutes); the results are reported in Table 5.3 to allow a better catalyst behavior comparison.

run	complex	conversion% ^a	yield% ^b	cis/trans ^c
5	<i>syn</i> 75	98,1	100	0,41
6	<i>anti</i> 75	99,0	100	0,25

Experimental conditions: C₆D₆, 60 °C, catalyst 0.1 mol %, m= 0,5 M. ^a ¹H-NMR conversion at 1 minute; ^b time= 2min^c. Ratios are based on ¹H-NMR data.

Table 5. 3: ROMP of COD modulated by Hoveyda derivatives (*syn* and *anti* **75). 0,1mol % of loading, C₆D₆, 60°C**

The poor *Z/E* ratios can be motivated by the high activity for both **75** isomers: in fact very likely to an high polymerization activity corresponds an high isomerization rate. Even lowering catalyst loading of ten times, behavior differences between the two isomers of **75** remain minimal: they both convert quantitatively all the starting material in about five minutes. *Z/E* reported ratios result quite low and differences are not particularly significant, so at this catalyst loading, it is impossible to discriminate among the performances of these two catalytic systems.

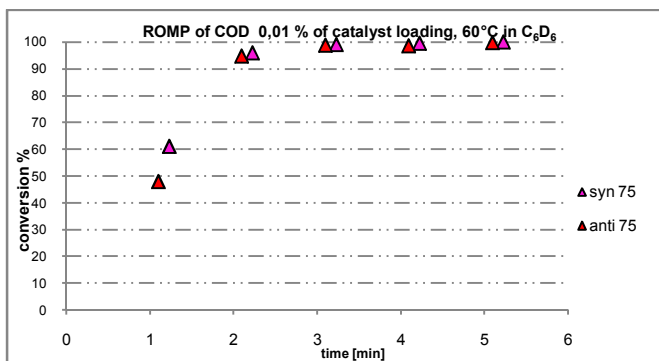


Figure 5. 6: ROMP of COD modulated by Hoveyda derivatives *syn* and *anti* 75; 0,01% of loading, 60°C in C₆D₆

Run	Complex	Conversion ^a %	Yield% ^b	Cis/trans ^c
7	<i>syn</i> 75	60,9	100	0,59
8	<i>anti</i> 75	47,7	100	0,39

Experimental conditions: C₆D₆, 60 °C, catalyst 0.01 mol %, m= 0,5 M. ^a ¹H-NMR conversion at 1 minute; ^b time= 2min. ^c Ratio are based on data from ¹H-NMR of the crude.

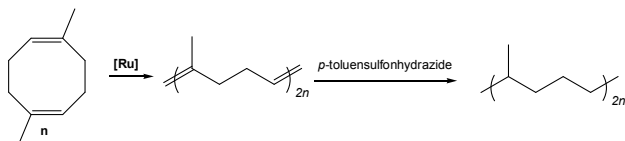
Table 5. 4: ROMP of COD modulated by Hoveyda derivatives *syn* and *anti* 75; 0,01% of loading, 60°C in C₆D₆

All of the reported complexes displayed very high activity in this ROMP reaction also at low catalyst loading. By monitoring reaction via ¹H-NMR and analyzing accurately the first minutes of the polymerization, it emerges that no one of the reported systems is *cis* selective (the *Z/E* values for the obtained polymers after one minute are close to a statistical distribution of the geometric isomers). Despite the lack of *cis*-selectivity very interesting results have been obtained since we were able to gain the desired polymer with high *cis* content. The best results have been gained employing the phosphine derivatives **74** (see Table 5.2). *Anti* **74** in particular at 0,01 mol percentage of loading affords in about one hour polybutadiene in high yield with 2,3 as *Z/E* ratio, while its commercial available analogous **41** in the same condition affords the desired polymer with a considerably smaller *Z/E* ratio (0,77). *Syn* **74**

completes the polymerization in less than thirty minutes, furnishing poly(**m**) with a good Z/E ratio of 1,4.

Romp of 1,5-dimethyl-1,5-cyclooctadiene (**n**, DMCOD)

The ring opening metathesis of the sterically hindered 1,5-dimethyl-1,5-cyclooctadiene has been first reported by Grubbs et al⁸ in 2000. The ROMP of this challenging monomer carried out in the presence of **10**, affords poly(isoprene) in 90% of yield in 24 hours. Subsequent hydrogenation led to the quantitative formation of an ethylene-propylene copolymer, which previously needed six steps to be obtained exploiting a metathetical route.⁹



Scheme 5. 3: synthesis of ethylene-propylene copolymer from ROMP of DMCOD.

We decided to begin this investigation using the Grubbs Hoveyda derivatives which displayed very high activity toward the ROMP of the less encumbered COD (**m**). The first runs were performed following the experimental procedure already exploited for the ROMP of COD (ROUTE A, experimental part). Both catalytic systems at 0,1 mol % of loading were not able to afford the desired poly-isoprene even after 4 days. It is reasonable to assume that solution was too diluted to favor the polymerization process. Therefore, we decided to change procedure and to explore two recent protocols reported by Grubbs' group to afford the desired poly-isoprene. The first one⁴ (ROUTE B, experimental part) considers the neat reaction between the catalyst and the liquid monomer, while the second¹⁰ (ROUTE C, experimental part) employs a toluene reacting solution. To avoid precious complex waste, we decided to perform first a preliminary study using *syn* **75** as catalyst. This choose was done considering the easier synthesis

⁸ Bielawski, C. W.; Grubbs, R. H.; *Angew. Chem.* **2000**, *39*, 2903.

⁹ Z. Wu; R. H. Grubbs; *Macromolecules* **1995**, *28*, 3502.

¹⁰ R. M. Thomas, R. H. Grubbs, *Macromolecules* **2010**, *43*, 3705.

of *syn* **75** with respect to its lower symmetry analogous. In both the explored experimental conditions we obtained a poor conversion that does not overcome the 20 % even after two days.

ROUTE B

Time [hours]	Conversion% ^a
1	18
2	20
24	20
48	20

Neat reaction conducted at 55 °C, catalyst/monomer=1/1000 ^a
Conversion determined by ¹H-NMR.

Table 5. 6: ROMP of DMCOD (Route B)

Reaction conditions still need to be optimized in order to obtain this valuable polymer in more satisfying yields. Moreover it will be interesting also the screening of phosphine based derivatives activity (**74** isomers) in this challenging process. Furthermore it is important to remember that when catalytically activity for a selected system highlights poor efficiency toward a type of reaction, an accurate analysis of the obtained data remains important to gain new information of crucial SAR parameters. As chemists which deal with metathesis well know, the design of a catalyst which displays very good activity toward the entire class of metathesis processes is really challenging: so a carefully collecting of all information (also in case of activity lack) can play a fundamental role in understanding crucial aspects of catalyst reactivity.

ROUTE C

Time [hours]	Conversion% ^a
24	17,4%

Reaction conducted at 50 °C, 24 h in toluene; DMCOD sol [0,2] M.
^a Conversion determined by ¹H-NMR.

Table 5. 5: ROMP of DMCOD (Route C)

Cross metathesis

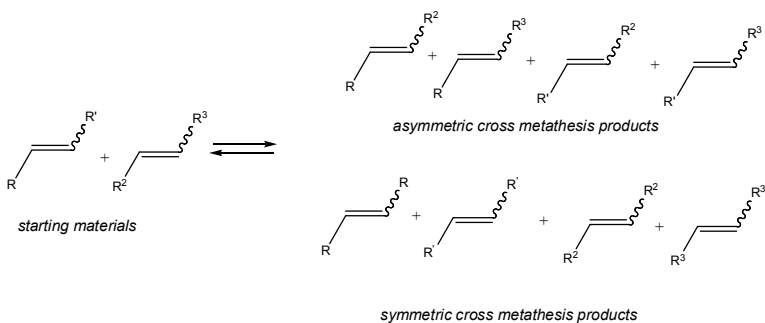
Introduction

In the past century, olefin cross metathesis has played a key role in the industrial olefin synthesis. Its main application concerns the petrochemical industry and of particular interest are the SHOP and the OCT processes. The first one “*Shell Higher Olefin Process*” allows the production of linear α olefins by combining ethylene oligomerization and olefin metathesis; while the “*Olefin Conversion Technology*” enables the synthesis of propene by the cross metathesis of ethylene with 2-butene.^{2a}

In recent years, olefin cross metathesis (CM) has emerged as a powerful and convenient synthetic technique also in organic chemistry, since it represents a facile route to gain functionalized olefins, starting from simple precursors. Its main issues are related to the lack of chemo and stereo selectivity in the product formation. Cross metathesis is more challenging than the previously discussed processes RCM and ROMP, because it lacks of entropic driving force (such as for RCM) and/or of ring-strain release (such as for ROMP). Moreover, as previously mentioned, statistically CM reactions often lead to relatively low yields of the desired cross-product, as well as poor *E/Z* cross-product selectivity.¹¹

Considering for instance the generic cross metathesis reaction reported below, we can in principle obtain a very complex crude mixture. Infact even neglecting the stereochemical issue, for a not selective metathesis the reaction mixture will be composed by four different symmetric products (derived from homocoupling reactions), four different cross metathesis adducts, and the two alkene starting materials. The number of possible species doubles considering the stereochemical aspect of the reaction.

¹¹ For a general model on the selectivity of CM reactions, see: A. K. Chatterjee, T. Choi, D. P. Sanders, R. H. Grubbs, *J. Am. Chem. Soc.*, **2003**, *125*, 11360.



Scheme 5. 4: not selective cross metathesis reaction.

An additional event that complicates the crucial aspect of stereoselection in a cross metathesis process is due to the thermodynamic nature of metathesis. Indeed at higher conversions a lower in *Z/E* ratio is typically observed due to the secondary metathesis of *Z*-olefin to the thermodynamically favorable *E*-one.

Some of these issues have been overcome by the development of new catalytic systems, but inability to predict cross metathesis selectivity remains a relevant issue for the practical application of cross metathesis.

In 2003 Grubbs' group has provided an empirical model to predict product selectivity in CM. In particular a general classification for olefin reactivity in CM by categorizing them in four different classes was proposed. Olefin assignment to a specific category depends on its intrinsic properties (electronic and steric) and on the catalyst used to carry out the metathesis.

Chemo and regio selectivity can be achieved by an appropriate choice of both olefin and catalytic system.¹²

Results and discussion

Catalytic activity of both isomers of complex **74** was explored in the representative cross-metathesis reaction of *allyl* benzene (**o**) and *cis*-1,4-diacetoxy-2-butene (**p**)

¹² Chatterjee, A. K.; Choi, T. L.; Sanders, D. P. and Grubbs, R. H. *J. Am. Chem. Soc.* **2003**, *125*, 11360.

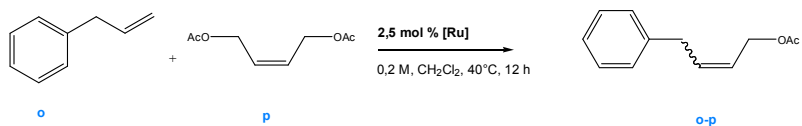


Figure 5. 7: standard cross metathesis reaction between allyl benzene (o**) and *cis*-1,4-diacetoxy-2-butene (**p**).**

Both the catalysts showed high conversions to the desired product **o-p**. *Syn* and *anti* **74** are quite selective in affording the heterocoupled adduct **o-p**. In fact in both the runs, conversions are quantitative and yields range from high to very high. In both the reported case, the side product obtained consists in a mixture of E and Z geometrical isomers of 1,4-diphenylbut-2-ene (derived from allylbenzene homocoupling); so both **74** isomers lead to a quite selective transformation (since the only side product is the one related to allylbenzene homocoupling) For what concern stereoselectivity the two isomeric derivatives afford similar results with respect to the commercially available **41** bearing two *N*-tolyl substituents at the NHC ligand (**41**). (*Z/E* = 1/8)

Run	Catalyst	Conversion %	Yield %	<i>Z/E</i>
9	<i>Syn</i> 74	100	91	1/7,6
10	<i>Anti</i> 74	100	81	1/8,2

Experimental conditions: 2,5 mol% of catalyst loading, CH₂Cl₂, 40°C, 12 h.

Table 5. 7: standard cross metathesis reaction between allyl benzene (o**) and *cis*-1,4-diacetoxy-2-butene (**p**) modulated by the newly synthesized phosphine based complexes *syn* and *anti* **74**.**

For cross metathesis modulated by commercially available ruthenium phosphine based systems ⁷(see Table 5.8), the *N*-mesityl substituted **10** emerges as the catalyst which better combines a good yield with a discrete *Z* selectivity. It is worth to point out that the phenyl backbone substitution produces a more efficient catalyst. In fact, by comparing *syn* **74** and **41** activities we can underline an improvement of 30 % in term of yield and also a slight increase in stereoselectivity.

Catalyst	Yield	Z/E
3	80%	1/7
10	79	1/6
41	60%	1/8

Experimental conditions: 2,5 mol% of catalyst loading, CH₂Cl₂, 40°C, 12 h.

Table 5. 8: standard cross metathesis reaction between allyl benzene (**o**) and *cis*-1,4-diacetoxy-2-butene (**p**) modulated by the commercially available phosphine based complexes.

Both atropisomers of complex **74** afford the desired **o-p** hetero-coupled product with yield varying from good to high. *Cis/trans* ratios are in line with those expected for a second generation catalyst. The comparison of these results with the one reported for the commercial available **41** which represents complex **74** structural analogous highlights *syn* **74** as the best performing system since it provides higher yield and higher *cis*-content.

Experimental procedures

Representative Procedure for the ring opening metathesis polymerization of cyclooctadiene **m** and of 1,5-dimethyl-1,5-cyclooctadiene **n** (ROUTE A): an NMR tube with a screw-cap septum top was charged with 0.80 mL of a CD₂Cl₂ or C₆D₆ solution of catalyst (molarity of the solution was varied according to the desired one for the ROMP tests to afford a catalyst loading of 0,1 or 0,01 mol%). After equilibrating at the appropriate temperature the sample in the NMR probe, 0.40 mmol of diene **m** or **n** was injected into the tube. The reaction was monitored as a function of time (via ¹H-NMR), and the conversion to the cyclic adduct was determined by integrating diagnostic signals for the starting material and the product.

Representative Procedure for the ring opening metathesis polymerization of 1,5-dimethyl-1,5-cyclooctadiene **n** (ROUTE B):

Under nitrogen atmosphere, 1,9 mg of *syn* **75** (0,0026 mmol) were weighted into a vial equipped with a magnetic stirrer. 0,40 ml of DMCOD (2,5 mmol) were syringed into the flask which was sealed and placed into an oil bath at 55°C. Reaction was monitored by the time via ¹H-NMR (aliquots of the crude reaction mixture were taken and diluted in deuterated benzene). Reaction was finally quenched by adding ethylvinyl ether after two days.

Representative Procedure for the ring opening metathesis polymerization of 1,5-dimethyl-1,5-cyclooctadiene **n** (ROUTE C):

In a glove box a solution of catalyst *syn* **75** (1,15mg; 0,0016 mmol) in toluene (4 ml) was prepared in a vial equipped with a magnetic stirrer. DMCOD (109 mg, 0,125 ml) was syringed and the reaction mixture was allowed to react for 24 hours at 50°C. Reaction was then stopped adding ethyl vinyl ether and conversion was determined analyzing ¹H-NMR crude reaction mixture.

Representative Procedure for the cross metathesis of allyl benzene (**o**) and *cis*-1,4-diacetoxy-2-butene (**p**):

An oven-dried 4-ml vial (equipped with a magnetic stirrer) was introduced in a dry box. 6,14 mg of catalyst (0,0065 mmol) were

weighted and dissolved in 1.25 ml of dry dichloromethane. Allyl benzene (0,25 mmol) and *cis*-1,4-diacetoxy-2-butene (0,50 mmol) were sequentially added and reaction flask was placed into an oil bath at 40°C; the reaction mixture was allowed to react for 12 hours. After this time, ethyl vinyl ether was added and the crude product was purified via column chromatography. The product was eluted from silica gel using *n*-hexane: ethylacetate= 9:1. The solvent was removed under vacuum to afford **o-p** crossmeathesis product as a transparent pale yellow oil. Its related ¹H-NMR and ¹³C-NMR signals correspond perfectly with the published ones.¹²

Chapter 6

Electrochemical behavior of II Generation Grubbs and Grubbs Hoveyda type complexes

Abstract

The electrochemical behavior of newly synthesized NHC ruthenium complexes was studied and compared to that of classical Grubbs and Hoveyda Grubbs II generation catalysts using cyclic voltammetry. This study was extended also to previously reported Ru catalysts bearing different NHC backbone and/or *N*-aryl substituents. The measured redox potentials allowed us to perform a detailed analysis of the influence of the various substituents on the NHC-Ru bond. It was found that not only the electronic properties of the NHC ligand influence the redox potentials but also their conformations.

Introduction

The understanding of structural relation parameters is crucial for improving catalyst system design. In metal based catalysis the rationalization of the electronic and steric properties of ligands represents a key point for the upper mentioned item.¹ Subtle variations of steric bulk and electron density at the active site may have drastic effects on the catalytic efficiency.² Consequently, the

¹ Homogeneous Catalysis, P. W. N. M. vanLeeuwen, Kluwer Academic Publ., Dordrecht 2004.

² (a) DeVasher, R. B.; Spruell, J. M.; Dixon, D. A.; Broker, G. A.; Griffin, S. T.; Rogers, V.; Shaughnessy, K. H.; *Organometallics* **2005**, *24*, 962. (b) Shaughnessy, K. H.; Kim, P.; Hartwig, J. F.; *J. Am. Chem. Soc.* **1999**, *121*, 2123. (c) Occhipinti, G.; Bjørsvik, H.-R.; Jensen, V. R.; *J. Am. Chem. Soc.* **2006**, *128*, 6952. (d) Fürstner, A.; Ackermann, L.; Gabor, B.; Goddard, R.; Lehmann, C. W.; Mynott, R.; Stelzer, F.; Thiel, O. R.; *Chem. Eur. J.* **2001**, *7*, 3236. (e) Altenhoff, G.; Goddard, R.; Lehmann, C. W.; Glorius, F.; *J. Am. Chem. Soc.* **2004**, *126*, 15195.

quantification of the steric and electronic ligand properties³ such as through Tolman approach,⁴ is essential.

Recently the use of *N*-heterocycle carbenes in transition metal promoted catalysis has exponentially grown with applications ranging from cross coupling reactions to hydrosilylation and olefin metathesis. For the latter transformation this class of ligands has convincingly demonstrated its superiority over the classic phosphorus based ones, owing to their special donor properties.⁵ Consequently it is highly desirable to better understand the precise nature of the NHC-Ru bond with the final aim of tuning the catalytic properties of transition metals complexes.

A number of experimental and theoretical studies have been carried out by different researchers. Nolan⁶ and Hermann⁷ have recently investigated on the donor properties of a large number of NHCs by synthesizing their respective nickel and rhodium carbonyl compounds. In particular the electron-donating ability was evaluated recording IR spectra and analyzing the CO stretching frequencies.

From these and other studies, the overall electron-donating ability of NHC ligands can be determined experimentally, but the identification of the individual contributions that generate the electrochemical response (type of substituents, their positions and stereochemical arrangements) results difficult. Anyway, the idea that NHC ligands were predominantly σ -donors⁶⁻⁸ was refined since their ability to act as π -donors in electron-deficient metal complexes have also emerged.⁹

³ (a) Fernandez, A. L.; Wilson, M. R.; Prock, A.; Giering, W. P. *Organometallics* **2001**, *20*, 3429. (b) Perrin, L.; Clot, E.; Eisenstein, O.; Loch, J.; Crabtree, R. H.; *Inorg. Chem.* **2001**, *40*, 5806. (c) Guzei, I. A.; Wendt, M. *Dalton Trans.* **2006**, 3991.

⁴ Tolman, C. A.; *Chem. Rev.* **1977**, *77*, 313.

⁵ Subner, M.; Plenio, H.; *Chem. Comm.* **2005**, 5419

⁶ Dorta, R.; Stevens, E. D.; Scott, N. M.; Costabile, C.; L. Cavallo, L.; Hoff, D. H.; Nolan, S. P. *J. Am. Chem. Soc.* **2005**, *127*, 2485 .

⁷ Herrmann, W. A.; Schütz, J.; Frey, G. D.; Herdtweck, E. *Organometallics* **2006**, *25*, 2437.

⁸ (a) Green, J. C.; Herbert, B. J. *Dalton Trans.* **2005**, 1214. (b) Magill, A. M.; Cavell, K. J.; Yates, B. F. *J. Am. Chem. Soc.* **2004**, *126*, 8717 (c) S. Saravanakumar, S.; Oprea, A. I.; Kindermann, M.; Jones, P. G.; Heinicke, J. *Chem. Eur. J.* **2006**, *12*, 3143 (d) Hahn, F.E.; Jahnke, M.C.; Pape, T. *Organometallics* **2007**, *26*, 150 .

⁹ Scott, N. M.; Dorta, R.; Stevens, E.; Correa, A.; Cavallo, L.; Nolan, S.P. *J. Am. Chem. Soc.* **2005**, *127*, 3516

Moreover, NHCs can act also as π -acid ligands;¹⁰ by accepting back-donation from filled d orbitals of electron rich metals. Bielawski reported on Rh complexes containing a cyclooctadiene ligand in trans position to differently substituted NHCs. Their electronic properties has been investigated analyzing coordinated COD chemical shift oscillation. It was found that chemical shift increases with ewg substituent strength¹¹ and this result highlights the π -accepting character of the NHC ligand.

A great contribution in finding direct method to characterize electrochemically NHC-Ruthenium species was provided by Plenio & co-workers. In particular he measured Ru(II)/Ru(III) redox potentials by cyclic voltammetry to gain information on the electronic situation at the metal center.

His initial screening was performed in 2005 to underline donor differences between:

- phosphine and NHC units;
- saturated and unsaturated NHC in both II generation type complexes;
- redox potentials associated to complexes which bears the same NHC on respectively Ru-tricyclohexylphosphine or Ru-*o*-isopropoxy moiety to demonstrate the role of the trans ligand to the NHC.

He also reported a systematic study^{5,12} on the influence exerted by different groups in *para* positions at the *N*-aryl rings by measuring redox potentials of ruthenium complexes.

Selected data are here reported to provide an overview on the above mentioned results.

¹⁰ (a) Hu, X. Castro-Rodriguez, I.; Olsen, K.; Meyer, K. *Organometallics* **2004**, *23*, 755. (b) Sanderson, M. D.; Kamplain, J.W.; Bielawski, C. W.; *J. Am. Chem. Soc.* **2007**, *129*, 16 514. (c) Nemcsok, D.; Wichmann, K; Frenking, G.; *Organometallics* **2004**, *23*, 3640 (d) Mercks, L.; Labat, G.; Neels, A.; Ehlers, A.; Albrecht, M. *Organometallics* **2006**, *25*, 5648. (e) Jacobsen, H.; Correa, A.; Costabile, C.; Cavallo, L. *J. Organomet. Chem.* **2006**, *691*, 4350.

(f) Fürstner, A.; Ackermann, L.; Gabor, B.; Goddard, R.; Lehmann, C. W.; Mynott, R.; Stelzer, F.; Thiel, O. R.; *Chem. Eur. J.* **2001**, *7*, 3236.

¹¹ Khramov, D. M.; Lynch, V. M.; Bielawski, C. W. *Organometallic* **2007**, *26*, 6042.

¹² Leuthaußer, S.; Schmidts, V.; Thiele, C. M.; Plenio, H. *Chem. Eur. J.* **2008**, *14*, 5465

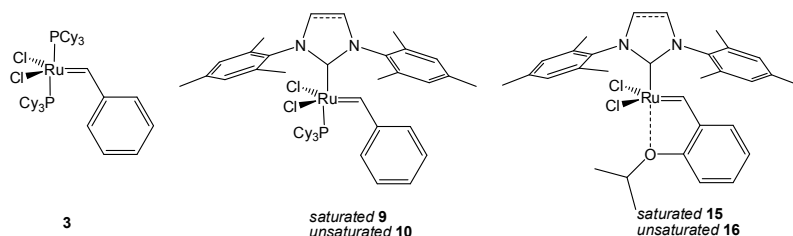


Figure 6. 1: selected Ru based commercial catalysts

Compound	$\Delta E_{1/2}$ [V]	$(E_a - E_c)$ [mv]
3	0,585	87
9	0,455	82
10	0,447	77
15	0,765	75
16	0,850	91

Experimental conditions: CH₂Cl₂/NBu₄PF₆ 0,1 M; internal reference octamethylferrocene

Table 6. 1: Redox potentials for selected commercial catalysts

NHC ligands are significantly more electron-donating than phosphines: a cathodic shift of the redox potential (ca 130 mV) has been indeed detected by substituting a phosphine ligand (in complex **3**) with an NHC (**9-10**); while the redox potentials recorded for **9** and **10** (with unsaturated and saturated NHC, respectively) are almost identical. These close $\Delta E_{1/2}$ values are indicative of similar donor properties of these two ligands despite complex properties in catalysis are very different. This is strongly indicative that for phosphine based complexes (**9**, **10**) differences in catalyst activity do not originate from dissimilar electron density at the metal centre, while slightly different steric requirements of saturated and unsaturated NHC ligands may be responsible^{13,14}

The change of the second phosphine ligand with an ether oxygen donor in Grubbs Hoveyda type catalysts results in a drastic anodic shift of the redox potential (+400 mV). Moreover, significant differences in electrochemical behavior passing from the

¹³ Occhipinti, G.; Bjorsvik, H.-R.; Jensen, V. R.; *J. Am. Chem. Soc.* **2006**, *128*, 6952.

¹⁴ Clavier, H.; Nolan, S. P.; *Chem. Eur. J.* **2007**, *13*, 8029.

unsaturated to the saturated backbone complex (see $\Delta E_{1/2}$ for complexes **10** and **16** Table 6.1) are detected. Here Ru(II)/(III) redox potentials of derivatives with saturated NHC are significantly more anodic than their unsaturated counterparts (85 mV, in the reported example). For this class of complexes together with a different electrochemical response also differences in catalytic activity result significant since saturated system usually displayed better reactivity than their unsaturated counterparts.¹⁵

A profound influence of the *para* *N*-aryl substituents has been detected by replacing the methyl units alternatively with electron-donating or attracting groups leading to both symmetrical or asymmetrical NHC.

Explanation will be provided on the substitution effect in *para* position at *N*-aryl level for saturated systems (see Table 6.2).

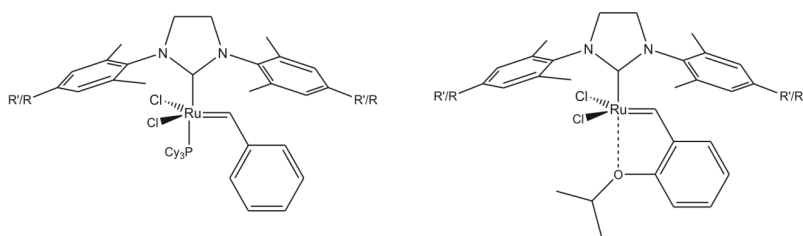


Figure 6. 2: *para* substituted Ru-NHC based catalysts.

R, R'	Phosphine based complexes $\Delta E_{1/2}$ [V]	Ether based complexes $\Delta E_{1/2}$ [V]
Br, Br	0,537	0,935
Br, H	0,503	0,905
H, H	0,469	0,870
Me, Me	0,455	0,850
OR, OR	0,454	0,836

Experimental conditions: CH_2Cl_2/NBu_4PF_6 0,1 M; internal reference octamethylferrocene

Table 6. 2: redox potentials for differently substituted NHC II generation Grubbs and Grubbs Hoveyda derivatives

¹⁵ Merino, E.; Poli, E.; Diaz, U.; Brunel, D. Dalton Trans., **2012**, 41, 10913.

In both phosphine and ether based complexes the substitution in *para* with an electron-withdrawing group led to measure a more anodic potential, while complex redox potentials decrease with increasing the electron-donating ability of the *para*-substituent. This is actually in agreement with the intuitive idea that the more electron density around the metal increases the more its tendency to reduction decreases; or, alternatively, an electron rich complex is more prone to Ru(II)->Ru(III) oxidation. This is because an electron rich ligand better stabilizes a cationic core metal than an electron poor one.

As visible in table 6.2, Hoveyda derivatives present a considerable higher potential than their phosphine analogous, underlining the importance of the trans group to the NHC that can donate or attract electrons through the d-orbital of the metal center.

Anyway it was unexpected that a *para* group on the aryl substituents at the nitrogen atoms could so deeply influence the electrochemical response of the species: indeed seven bonds separate the R groups from the redox active Ruthenium center, and even more because the electronic communication through π -orbitals is unlikely, as the aromatic ring of the *N*-substituent is orthogonal to the NHC ring (as deduced from the solid structure studies).¹⁶ This represents an evidence for π - π interaction between the aromatic ring of the NHC and the Ru benzylidene unit.

Fürstner & co-workers were the first to propose a possible π -stacking interaction after considering the short distances (around 300 pm) between the benzylidene unit and the *N*-aryl group of the NHC in several solid state structures of Grubbs II generation complexes. Further evidence for this kind of interaction comes from the observation that in unsymmetrical mixed alkyl-aryl complexes the co-facial orientation of the *N*-aryl group and the ruthenium benzylidene unit is the preferred one.¹⁷

¹⁶ Janiak, C.; *J Chem. Soc. Dalton Trans.* **2000**, 3885

¹⁷ Ledoux, N.; Allaert, B.; Pattyn, S.; Mierde, H. V.; Vercaemst, C.; Verpoort, F.; *Chem. Eur. J.* **2006**, *12*, 4654.

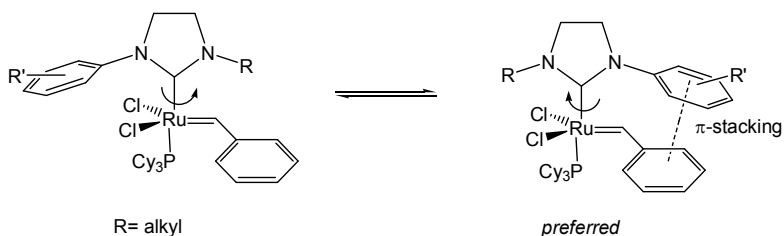


Figure 6. 3: co-facial orientation among *N*-aryl and the ruthenium benzylidene units for alkyl-aryl complexes.

Moreover recently Grubbs et al. reported unsymmetrical mixed aryl complex displaying a preferential orientation of the more electron rich aryl above the Ru=CHR group.¹⁸

However while for Grubbs II generation complex Ru=CH unit is in the same plane affording a face-to-face orientation of the respective π -orbitals, in the Grubbs Hoveyda complexes instead, the same C-H unit is pointing towards the center of the six-membered *N*-aryl ring, resulting in a even more intimate contact between the two units.

The use of unsymmetrical substituted NHC ligands (bearing different 4,4'-substituents on the aryl rings) in Grubbs II complexes results in two atropisomers, which are obtainable by rotating around the Ru-C(NHC) bond.

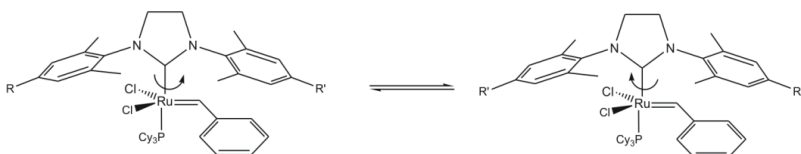


Figure 6. 4: atropo-isomers in asymmetrically 4-substituted Grubbs II complexes.

As we can see in Figure 6. 4 they are distinguishable by different orientation of 4-R and 4- R' substituents with respect to the benzylidene unit. These atropisomers are characterized by different redox potentials. In particular Plenio showed that the relative orientation of the 4-R groups of the NHC ligand relative to the Ru=CHPh unit is primary responsible for the Ru redox potentials.

¹⁸ Vougioukalakis, G. C.; Grubbs, R. H.; *Organometallics* **2007**, *26*, 2469.

This observation is not compatible with an exclusive through-bond electron transfer of the electron density from the 4-substituents to Ru, but matches well with considerable trans-annular interactions of the aryl flap and the Ru=CHR unit.

In an attempt to relate the just commented electrochemical properties to catalytic activity Plenio's group undertook a comparative study on II generation Grubbs and Grubbs Hoveyda complexes. The benchmark reaction selected for the Grubbs Hoveyda type complexes was the ring closing of the diallyltosylamine (**d**, see chapter 4), while for phosphine based derivatives diethyldiallyl malonate (**a**) and the diallyltosylamine (**d**) were used to test the ring closing efficiency.

In the ring-closing metathesis of diethyldiallyl malonate (see also chapter 4 for further detail on this reaction), the activity of the respective II generation derivatives within the two series of complexes with saturated and unsaturated *N*-heterocyclic carbene ligands is ranked according to the electron richness of the respective Ru centers (in perfect agreement with Grubbs rule)^{19,20} 4-NEt₂ > 4-H » 4-Cl. This order of reactivity was also found in the ring-closing metathesis of diallyltosylamine (Figure 6. 5).

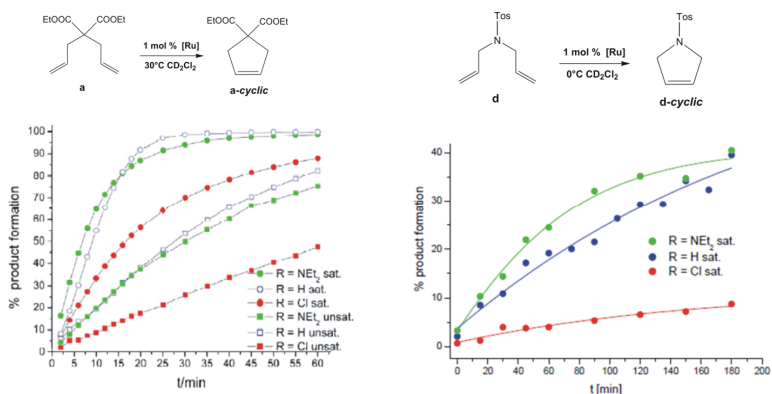


Figure 6. 5: Ring closing metathesis of differently substituted NHC-PCy₃ complexes.

¹⁹ Phosphines, which are larger and more electron donating, and likewise halogens, which are smaller and more electron withdrawing, lead to more active catalysts.

²⁰ Dias, E. L.; Nguyen, S. T.; Grubbs, R. H. *J. Am. Chem. Soc.* **1997**, *119*, 3887.

R=R'	Saturated $\Delta E_{1/2}$ [V]	Unsaturated $\Delta E_{1/2}$ [V]
NEt₂	0.196	0.271
H	0.469	0.470
Cl	0.529	0.535

Experimental conditions: CH₂Cl₂/NBu₄PF₆ 0,1 M; internal reference octamethylferrocene

Table 6. 3: redox potentials for screened catalysts in the RCM of DEDAM and diallyl tosilamine

In both metathesis reactions the reactivity differences between 4-NEt₂ and 4-H substituted complexes are small compared with what could have been expected from the large differences in the redox potentials.

This was astonishing considering the strong donation of the 4-R = NEt₂ group. However, it is appropriate to remember that π -stacking interactions can only be operative while the Ru=CHR substructure exists, which is not always the case during the catalytic cycle.

This indicated that the redox potentials cannot be used as a unique parameter to predict catalytic activity.

By analyzing Hoveyda derivative redox potentials and their corresponding catalytic activity curves, a different trend was observed. In particular the comparison among the selected catalytic systems was conducted in the RCM of diallyltosylamine (**d**) in dichloromethane at 30°C, with a 1 mol % of catalyst loading. Again, a profound influence of the nature of R was exerted on the catalytic activity of those complexes. In this case it seems that catalyst activity raises with the electron withdrawing character of the substituents. Nevertheless this dependence does not appear linear since the mono and di 4-Br derivatives display almost the same activity (mono bromide complex seems even faster in promoting the RCM).

So a direct correlation between the redox potential and the catalytic activity of the Hoveyda derivatives is not detectable up to now (reported data to the best of our knowledge are still very few).

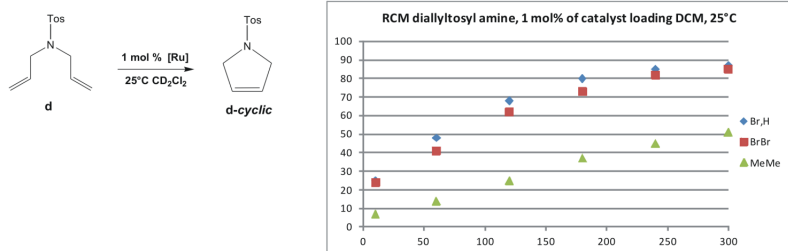


Figure 6. 6: ring closing metathesis of *N*-tosyldiallyl amine (**d**) modulated by selected differently substituted NHC-Hoveyda derivatives.

R, R'	Ether based complexes $\Delta E_{1/2}$ (mV)
Br, Br	0,953
Br, H	0,905
H, H	0,870
Me, Me	0,850

Experimental conditions: CH₂Cl₂/NBu₄PF₆ 0,1 M; internal reference octamethylferrocene

Table 6. 4: redox potentials for screened catalysts in the RCM of diallytosylamine (**d**)

In this brief introduction the most significant electrochemical studies on second generation Grubbs and Grubbs Hoveyda derivatives are reported. It is worth to note that direct methods to characterize electronic properties of catalysts are still few and voltammetric studies represents a pioneering approach to this issue.

Results and discussion

The redox potentials of ruthenium complexes were measured by cyclic voltammetry (Table 6.5-Table6.10). In the first part of this paragraph, comments are divided considering catalysts belonging to a specific class; then a direct comparison among Grubbs and Hoveyda-Grubbs type derivatives (bearing the same NHC) is reported. Our aim in creating this parallelism is to highlight any similarity in electrochemical behavior trend among two different types of complexes bearing the same NHC.

Results for Grubbs second generation type complexes

The II generation Grubbs type complexes we studied by cyclic voltammetry are reported below (Figure 6. 7).

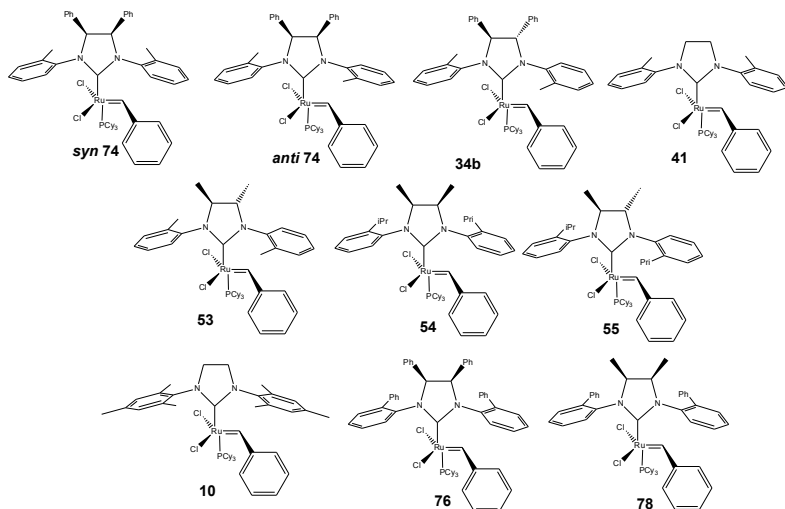


Figure 6. 7: phosphine based complexes studied by cyclic voltammetry

Run	Name	ΔE^a , vs FcMe ₈ . [V]
1	Syn 74	0,559
2	Anti 74	0,676
3	34b	0,586
4	41	0,575
5	53	0,542
6	54	0,250
7	55	0,510
8	10	0,490
9	76	0,688
10	78	0,567

^a ΔE values are related to octamethylferrocene as internal standard.

Experimental conditions: CH₂Cl₂, N₂ atmosphere, NBu₄PF₆ as supporting electrolyte.

Table 6. 5: redox potentials for screened phosphine based complexes.

For the sake of clarity comments will be provide by re-organizing results in four different tables in which complexes are associated depending on substituent differences and/or ligand symmetry. In Table 6.6 we reported redox potentials of phosphine based complexes bearing a 4,5-diphenyl-1,3-di-*o*-tolylimidazolidine carbene ligand. The experimental ΔE values strongly indicate that significant variations are due to the mutual orientation of *N*-tolyl groups: by passing from *syn* **74** to *anti* **74** an anodic shift of 117 mV is recorded (see Table 6.6). This occurrence is particular important since it underlines that electronic environment at Ru center is not only influenced by the intrinsic electronic nature (electron withdrawing or donating groups) of the substituents on the NHC, but also by small structural differences that just concern their conformation.

The same observation can be made by comparing ΔE values between *anti* **74** and **34b** (table 6.6). Redox potentials measured for *anti* **74** is 90 mV more anodic than that of **34b**; in this case mutual *N*-aryl orientation is *anti*, while backbone configuration is *syn* or *anti*, respectively. Again we observed a marked influence of substituent orientation in complex electrochemical behaviour.

When both *N*-aryl and backbone substituents switch from a *syn* to an *anti* arrangement, ΔE differences result negligible: indeed redox potentials registered for *syn* **74** and **34b** result very close (0,559 and 0,586 respectively). We could have expected a more pronounced difference by changing so deeply ligand symmetry. Plausibly this odd arises from the different overall electronic interaction among substituent units and this is the reason why factorization of different contributes results impossible. It is important to remember that through-bond electron transfer (σ) of the electron density seems to influence the electrochemical response less than π -stacking. This means that we cannot simply add contributes arising from a specific NHC substituent but we have to take into account that the nature of this Ru-NHC interaction is better interpreted as a through space via donation from the C_{ipso} atom of the *N*-substituent.²¹

²¹Credendino R.; Falivene, L.; Cavallo, L. *J. Am. Chem Soc.* **2012**, *134*, 8127.

Name	ΔE^a , vs Fc. [V]
Syn 74	0,559
Anti 74	0,676
34b	0,586

^a ΔE values are related to octamethylferrocene as internal standard.
 Experimental conditions: CH_2Cl_2 , N_2 atmosphere, NBu_4PF_6 as supporting electrolyte.

Table 6. 6: redox potentials for phosphine based complexes bearing 4,5-diphenyl-1,3-di-*o*-tolylimidazolidine carbene ligand

Complexes **53** and **55**²² which differs just for R-aryl substituent bulkiness (respectively **53**: R= Me; **55**: R= *i*-Pr) display comparable voltammetric response; reasonably this is due to the very similar electronic properties of these two complexes.

Name	ΔE^a , vs FcMe ₈ . [V]
53	0,542
55	0,510

^a ΔE values are related to octamethylferrocene as internal standard.
 Experimental condition: CH_2Cl_2 , N_2 atmosphere, NBu_4PF_6 as supporting electrolyte.

Table 6. 7: redox potentials for selected phosphine based complex.

The ΔE values for complexes **54** and **55** which differs for ligand symmetry (*meso* and C_2 respectively) are reported in Table 6.8. In this case (differently from what seen before, Table 6.6 an important anodic shift is observed passing from the complex which bears a *meso* NHC to the one with a C_2 symmetric NHC. It is worth to point out anyway, that rotation around C-N bond is not strictly forbidden in these complexes, so a direct comparison of ΔE differences between the **syn 74-34b** and **54-55** pairs is not perfectly pertinent.

Name	ΔE^a , vs FcMe ₈ , V
54	0,250
55	0,510

^a ΔE values are related to octamethylferrocene as internal standard.
 Experimental condition: CH_2Cl_2 , N_2 atmosphere, NBu_4PF_6 as supporting electrolyte.

Table 6. 8: redox potentials for selected phosphine based complexes bearing *meso* or C_2 ligand: 1,3-bis(2-isopropylphenyl)-4,5-dimethylimidazolidine.

²² Costabile, C.; Mariconda, A.; L. Cavallo, P. Longo, V. Bertolasi, F. Ragone and F. Grisi *Chemistry a European Journal*, **2011**, 31, 8618

For what concern the redox potentials related to our newly synthesized complexes characterized by NHC *meso* symmetric ligand (*syn* **74**, **76**, **78**), we can observe that by changing the *ortho* tolyl with *ortho* phenyl groups, while backbone positions are occupied by *syn* phenyl substituents, the redox potential shifts to a more anodic value. This means that complex **76** is less prone to the oxidation. This evidence fits with the intuitive idea that complex propensity to the oxidation raises proportionally to the electron density around the metal. In term of electronic nature of substituents this is reasonable since phenyl groups, over than being electro-donating, can delocalize electrons due to their aromaticity, while methyl groups display just an electron-donating character: so the ruthenium core of complex *syn* **74** should be more electron rich than the one of **76**.

Syn **74** and **78** redox potentials are quite close. This evidence can be explained considering that they are constitutional isomers, characterized by the same ligand symmetry (*meso*); therefore it is reasonable to assume that the electronic environment at ruthenium core is very similar.

Name	ΔE^a , vs FcMe ₆ , [V]
<i>Syn</i> 74	0,559
76	0,688
78	0,567

^a ΔE values are related to octamethylferrocene as internal standard.

Experimental conditions: CH₂Cl₂, N₂ atmosphere, NBu₄PF₆ as supporting electrolyte

Table 6. 9: redox potentials for our newly synthesized phosphine based complexes.

Results for Grubbs Hoveyda second generation type complexes

Redox potentials for Hoveyda type derivatives were recorded by performing cyclic voltammetry experiments (ΔE values are all expressed considering octamethylferrocene as external standard). All of them resulted more anodic than the ones related to the phosphine based analogs. As before, all results are first reported together; then, for an easier understanding and to better appreciate differences, they are re-organized in different tables in which again complexes are associate depending on substituent differences or ligand symmetry.

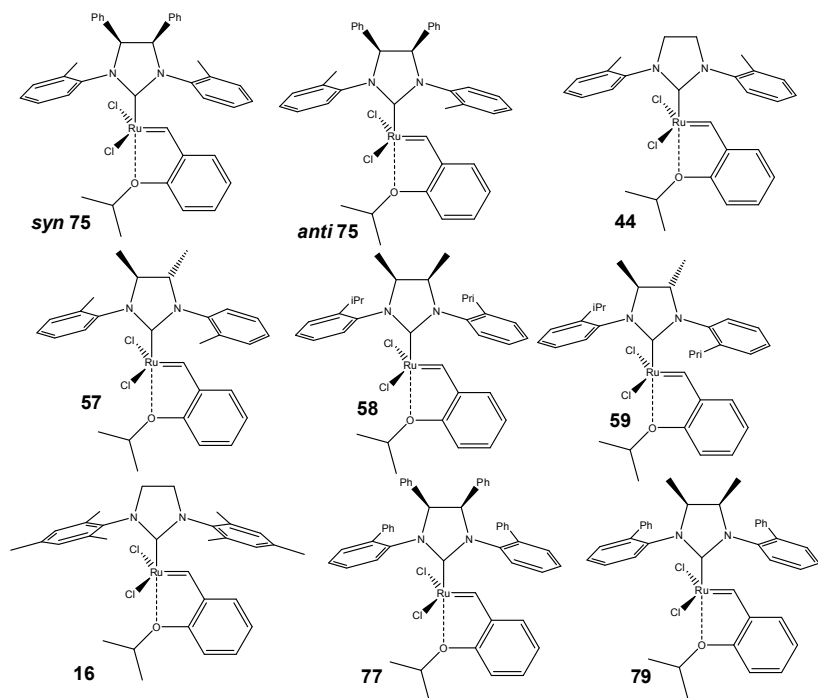


Figure 6. 8: Hoveyda type complexes studied via voltammetry

Run	Name	ΔE^a , vs FcMe ₈ , [V]
11	Syn 75	0,624
12	Anti 75	0,730
13	44	0,614
14	57	0,586
16	58	0,587
17	59	0,514
18	16	0,574
19	77	0,817
20	79	0,629

^a ΔE values are related to octamethylferrocene as external standard.

Experimental conditions: CH₂Cl₂, N₂ atmosphere, NBu₄PF₆ as supporting electrolyte.

Table 6. 10: ether based complexes redox potentials.

As clearly visible in Table 6. 11 the mutual orientation among *N*-tolyl substituents is more relevant than the presence of the two phenyl groups in influencing redox potential values, since passing from *syn* **75** to its *anti* isomer an important anodic shift (106 mV) is registered. Redox potentials for *syn* **75** and its commercially available counterpart (lacking substituents on the NHC backbone) **44** result close. This evidence is important since it highlights the crucial role played by substituent orientation in influencing electron density at the metal centre. It is worth to point out anyway that while *syn* **75** is characterized by a quite rigid geometry, within **44** rotations around C-N bond are unrestricted so complex performances are influenced by the presence of different isomers in solution.

Name	ΔE^a , vs FcMe ₈ , [V]
Syn 75	0,624
Anti 75	0,730
44	0,614

^a ΔE values are related to octamethylferrocene as external standard.

Experimental conditions: CH₂Cl₂, N₂ atmosphere, NBu₄PF₆ as supporting electrolyte.

Table 6. 11: redox potentials for selected ether based complexes

The redox potentials associated to the two ether based complexes which bear a *meso* or C₂ symmetric NHC (substituted at backbone level by two methyl groups and at the *N*-aryl by two ortho *i*-propyl

groups) differ of 73 mV, in contrast with the results gained for the phosphine based analogs (see Table 6.8). This evidence points out the importance of the trans ligand to the NHC. In fact passing from a phosphine to an *o*-isopropoxy chelating moiety voltammetric response is reversed (over than being numerically different).

Name	ΔE^a , vs FcMe ₈ , [V]
58	0,587
59	0,514

^a ΔE values are related to octamethylferrocene as external standard.

Experimental conditions: CH₂Cl₂, N₂ atmosphere, NBu₄PF₆ as supporting electrolyte.

Table 6. 12: redox potentials for selected Hoveyda type complexes bearing meso or C₂ ligand: 1,3-bis(2-isopropylphenyl)-4,5-dimethylimidazolidine

The substitution of the *ortho* tolyl with an *ortho* phenyl group, while keeping a *syn* phenyl substituted backbone, shifts the redox potential to a more anodic value; this means that for complex **77** the overall electronic situation at the ruthenium core is considerably more poor than the one of complex *syn* **75**. So between these two complexes *syn* **75** is the most prone to oxidation and this behavior is perfectly comparable to the one reported in Table 6.9. Moreover, *syn* **75** and **79** redox potentials are quite close, following the same trend before observed for *syn* **74**, **76**, **78** (Table 6.9). This similarity is justifiable by considering that NHC ligands of both **79** and *syn* **75** display a *meso* arrangement over than being constitutional isomers.

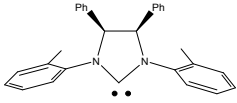
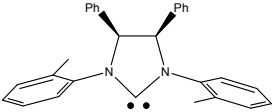
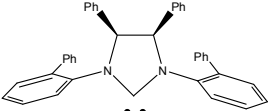
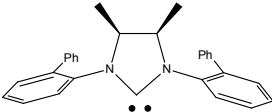
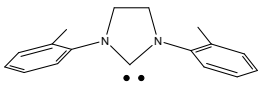
Name	ΔE^a , vs FcMe ₈ , [V]
<i>Syn</i> 75	0,624
77	0,817
79	0,629

^a ΔE values are related to octamethylferrocene as external standard.

Experimental conditions: CH₂Cl₂, N₂ atmosphere, NBu₄PF₆ as supporting electrolyte.

Table 6. 13: redox potentials recorded for our newly synthesized ether based complexes

With the final purpose of highlighting similarities in electrochemical trend between the two different II generation types complexes bearing the same NHC, we report their redox potentials in Table 6.14.

NHC ligand	ΔE^a [V] for Grubbs II gen type complexes	ΔE^a [V] Hoveyda-Grubbs II gen type complexes
	0,559	0,624
	0,676	0,730
	0,688	0,817
	0,567	0,629
	0,574	0,614

^a ΔE values are related to octamethylferrocene as external standard. Experimental conditions: CH_2Cl_2 , N_2 atmosphere, NBu_4PF_6 as supporting electrolyte

Table 6. 14: electrochemical comparison among II generation type complexes bearing the same NHC.

It is worth to note that we observed a direct correlation between the recorded redox potentials and the catalytic behaviour for isomers *syn* and *anti* of both phosphine and Hoveyda derivatives (**74** and **75**). In both cases in fact the complexes characterized by lower ΔE result the most active in catalysis. This trend has been previously observed by Plenio's group (Table 6. 3-Table 6. 4) but the complexes they have studied and compared present substituents (in *para* position at *N*-aryl, see Figure 6. 5-Figure 6. 6) with different electronic properties, while in our case significant differences in both electrochemical and catalytic behaviours arise from mutual arrangement of NHC substituents. This further evidence underlines

again the importance of the ligand conformation in influencing complex properties (see Figure 6. 9-Figure 6. 10).

A complete rationalization results anyway still far since the NHC electron donation capacity is not always governed by the same factors which influence the catalytic behaviour.

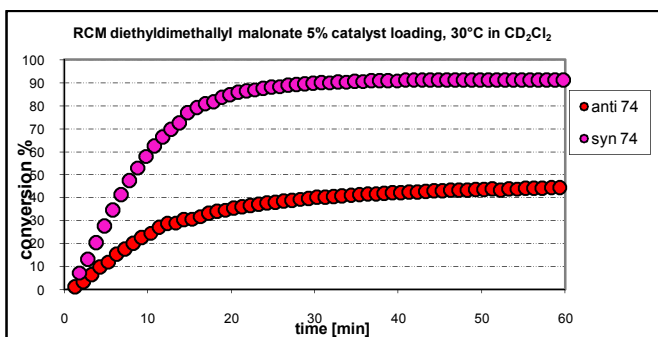
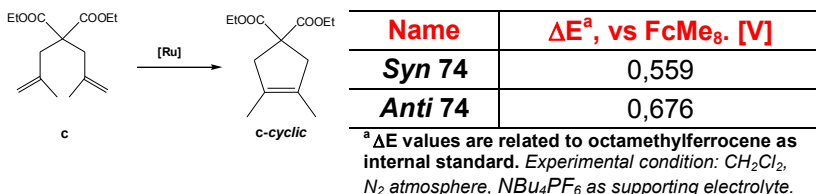


Figure 6. 9: tiling among catalyst activity and voltammetric response for isomeric phosphine complexes

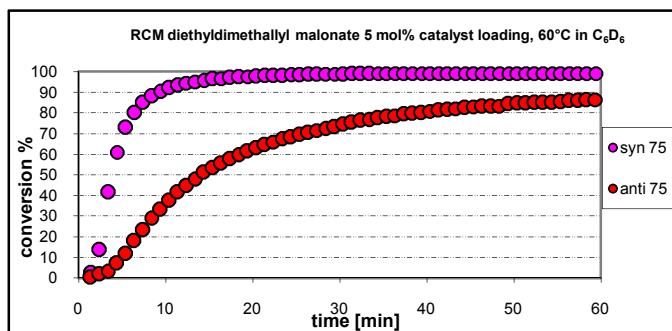
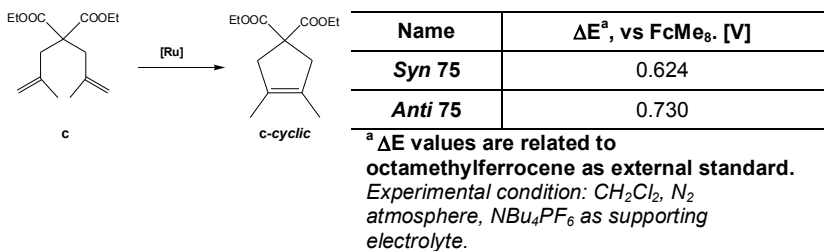


Figure 6. 10: tiling among catalyst activity and voltammetric response for isomeric Hoveyda complexes

In summary, this electrochemical study has been conducted to provide new information on electronic properties of ruthenium based systems whose high activity and stability have spurred great interest in catalysis. We are still far from a fully understanding of the experimental data and of their correlation with complex efficiency in catalysis, but this pioneering analysis could constitute, together with more established analytic techniques, a new methodology to identify structural modification of the NHC ligand relevant to improve ruthenium complex catalytic properties.

Experimental Procedures

These experiments have been conducted in collaboration with Doct. Tonino Caruso.

The standard electrochemical instrumentation consisted of an AUTOLAB PG STAT 302N potentiostat galvanostat. A three-electrode configuration was employed. The working electrode was a Pt disk (diameter 2 mm) sealed in a PEEK bar with a Pt bar as counter electrode. The pseudo reference electrode was Pt bar. Potentials were calibrated alternatively internally or externally against the octamethylmethylferrocene redox couple.

All cyclic voltammograms were recorded in dry CH_2Cl_2 under a nitrogen atmosphere; NBu_4PF_6 ($c=0.1$ [mol/L]) was used as supporting electrolyte. Scan rate 100mV/S.

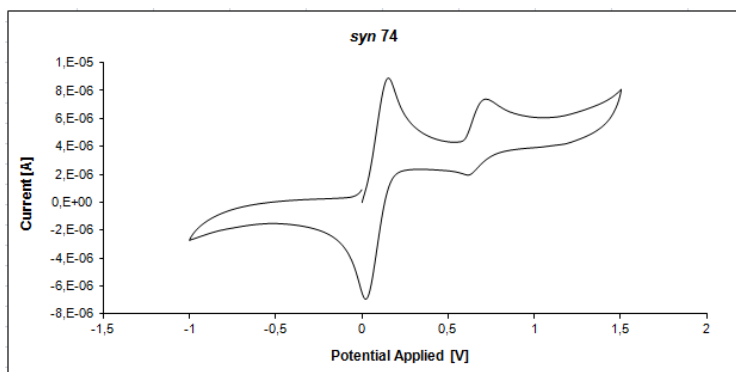


Figure 6. 11: voltammogram of *syn 74*; octamethylferrocene as internal standard. Experimental conditions: CH_2Cl_2 , N_2 atmosphere, NBu_4PF_6 as supporting electrolyte.

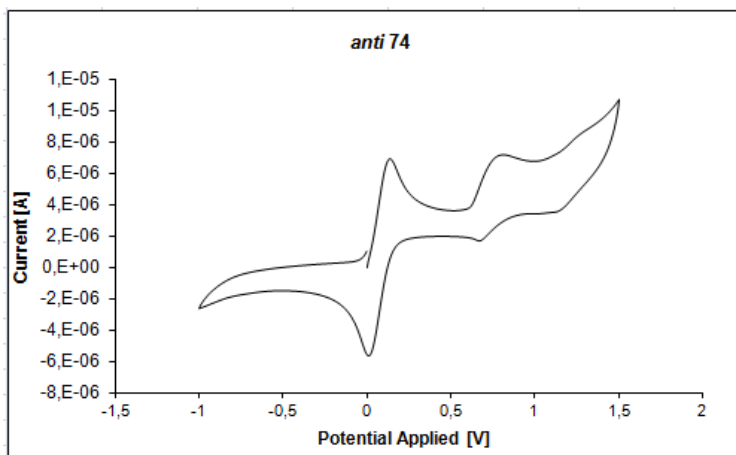


Figure 6. 12: voltammogram of anti 74; octamethylferrocene as internal standard. Experimental conditions: CH_2Cl_2 , N_2 atmosphere, NBu_4PF_6 as supporting electrolyte.

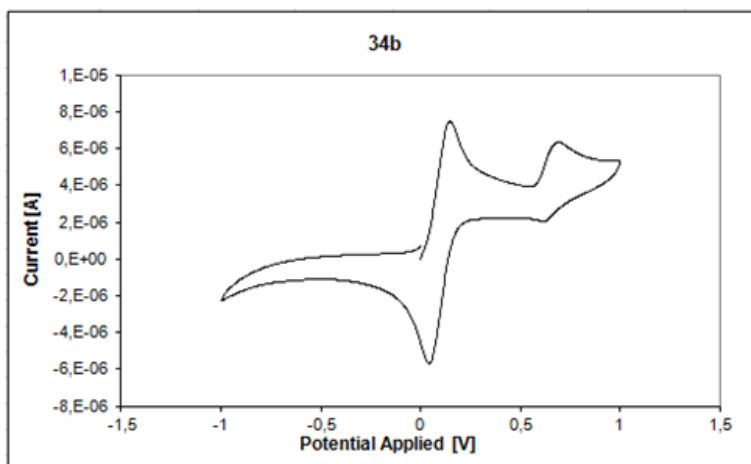


Figure 6. 13: voltammogram of 34 b; octamethylferrocene as internal standard. Experimental conditions: CH_2Cl_2 , N_2 atmosphere, NBu_4PF_6 as supporting electrolyte.

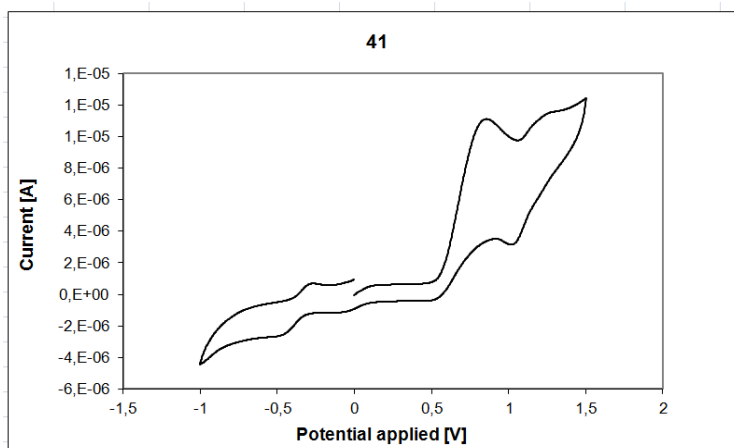


Figure 6. 14: voltammogram of 41; octamethylferrocene as external standard. Experimental conditions: CH_2Cl_2 , N_2 atmosphere, NBu_4PF_6 as supporting electrolyte.

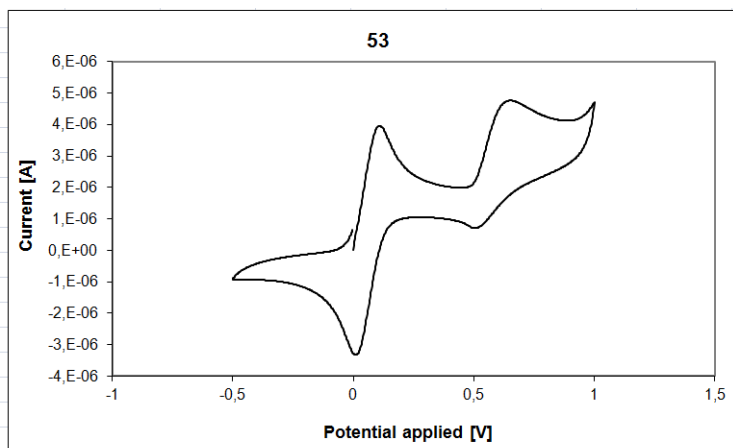


Figure 6. 15: voltammogram of 53; octamethylferrocene as internal standard. Experimental conditions: CH_2Cl_2 , N_2 atmosphere, NBu_4PF_6 as supporting electrolyte.

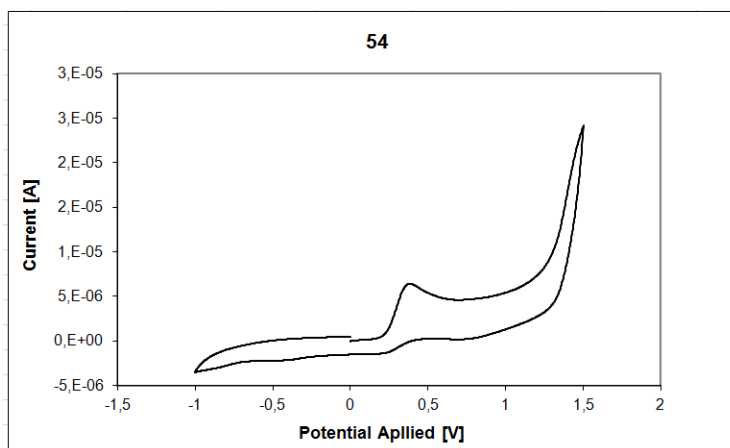


Figure 6. 16: voltammogram of 54; octamethylferrocene as external standard.
 Experimental conditions: CH_2Cl_2 , N_2 atmosphere, NBu_4PF_6 as supporting electrolyte.

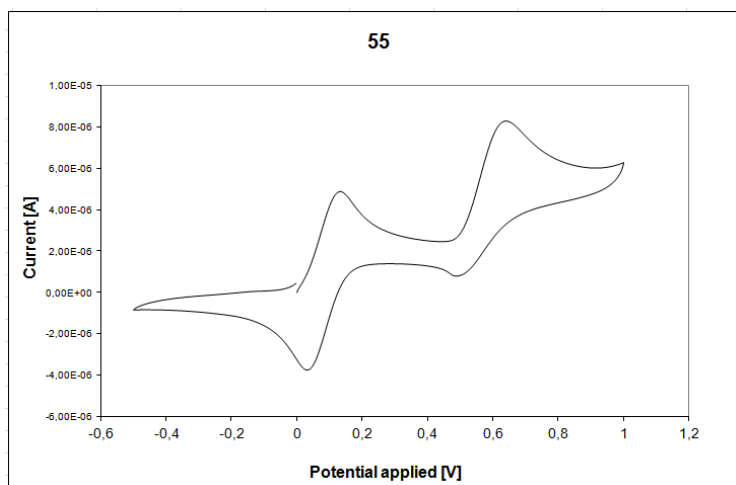


Figure 6. 17: voltammogram of 55; octamethylferrocene as internal standard.
 Experimental conditions: CH_2Cl_2 , N_2 atmosphere, NBu_4PF_6 as supporting electrolyte.

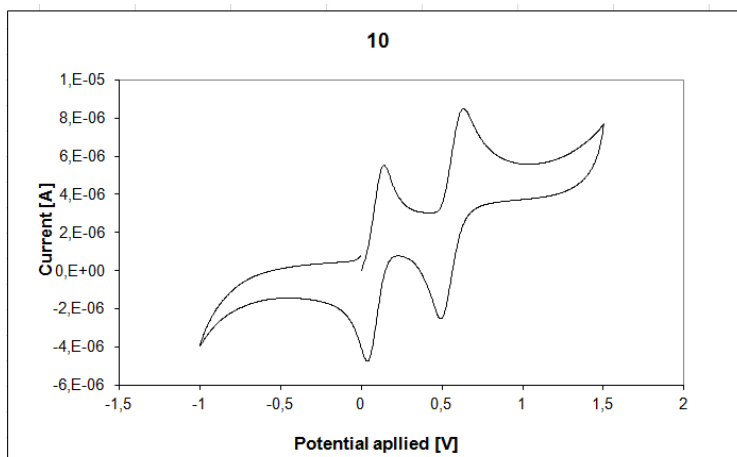


Figure 6. 18: voltammogram of **10**; octamethylferrocene as internal standard. Experimental conditions: CH_2Cl_2 , N_2 atmosphere, NBu_4PF_6 as supporting electrolyte.

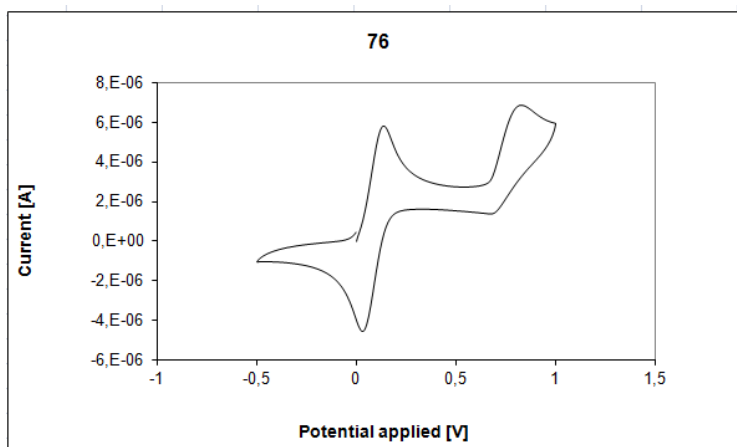


Figure 6. 19: voltammogram of **76**; octamethylferrocene as internal standard. Experimental conditions: CH_2Cl_2 , N_2 atmosphere, NBu_4PF_6 as supporting electrolyte.

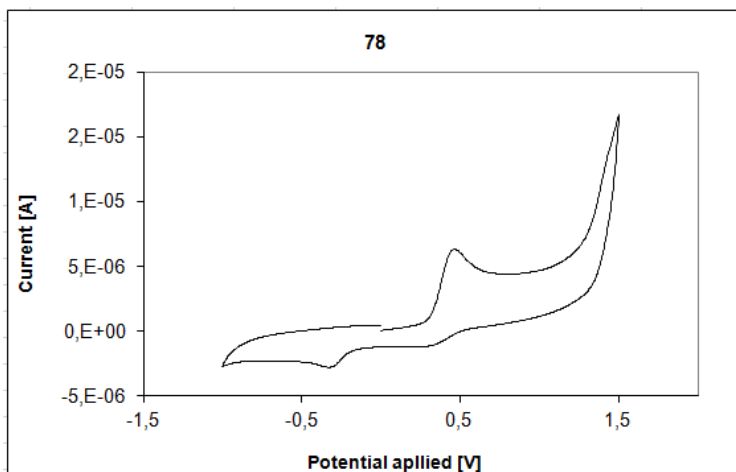


Figure 6. 20: voltammogram of 76; octamethylferrocene as external standard. Experimental conditions: CH_2Cl_2 , N_2 atmosphere, NBu_4PF_6 as supporting electrolyte.

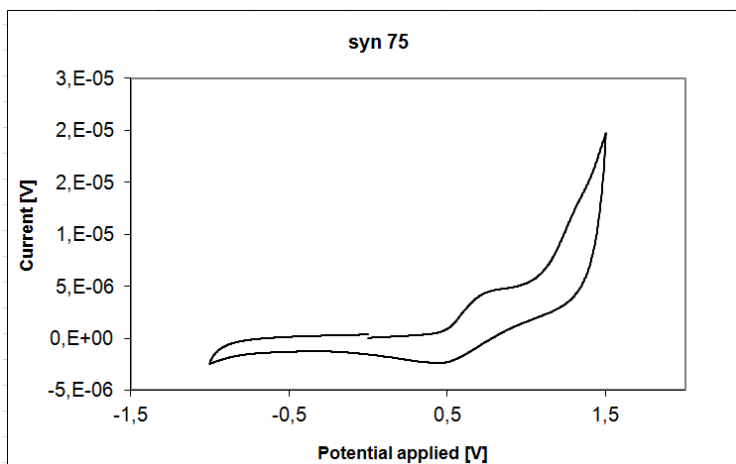


Figure 6. 21: voltammogram of syn 75; octamethylferrocene as external standard. Experimental conditions: CH_2Cl_2 , N_2 atmosphere, NBu_4PF_6 as supporting electrolyte.

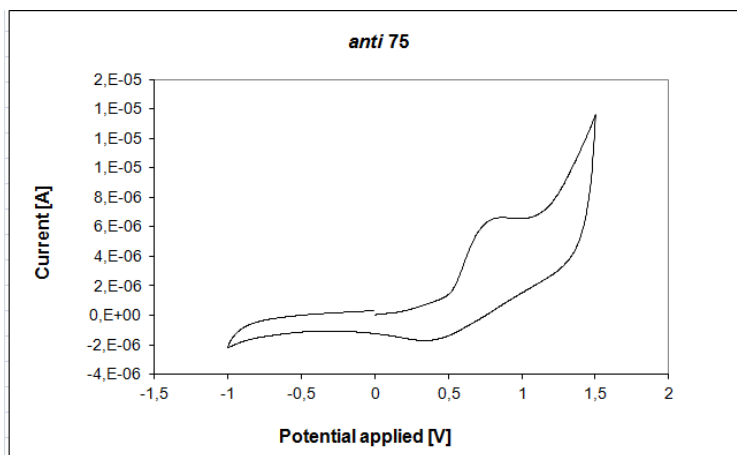


Figure 6. 22: voltammogram of *anti* 75; octamethylferrocene as external standard. Experimental conditions: CH_2Cl_2 , N_2 atmosphere, NBu_4PF_6 as supporting electrolyte.

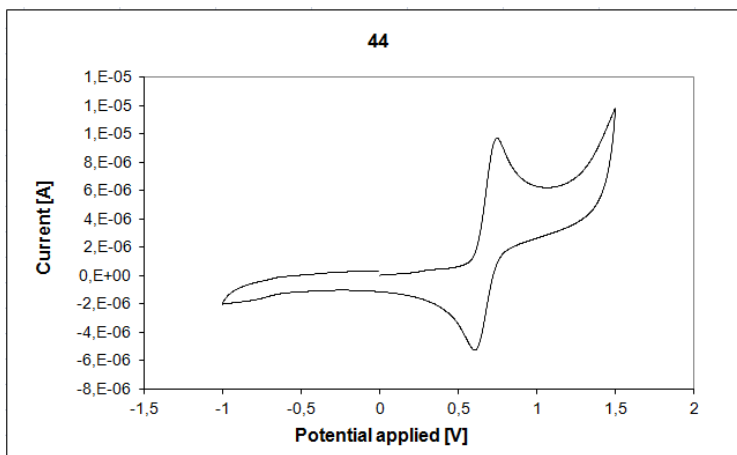


Figure 6. 23: voltammogram of 41; octamethylferrocene as external standard. Experimental conditions: CH_2Cl_2 , N_2 atmosphere, NBu_4PF_6 as supporting electrolyte.

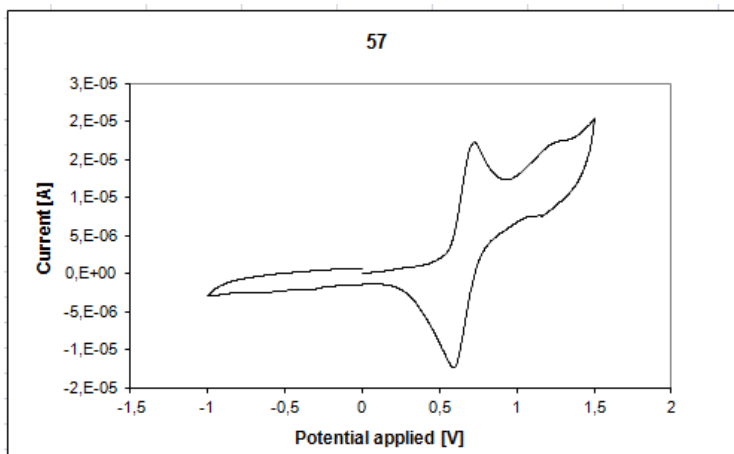


Figure 6. 24: voltammogram of 57; octamethylferrocene as external standard.
Experimental conditions: CH₂Cl₂, N₂ atmosphere, NBu₄PF₆ as supporting electrolyte.

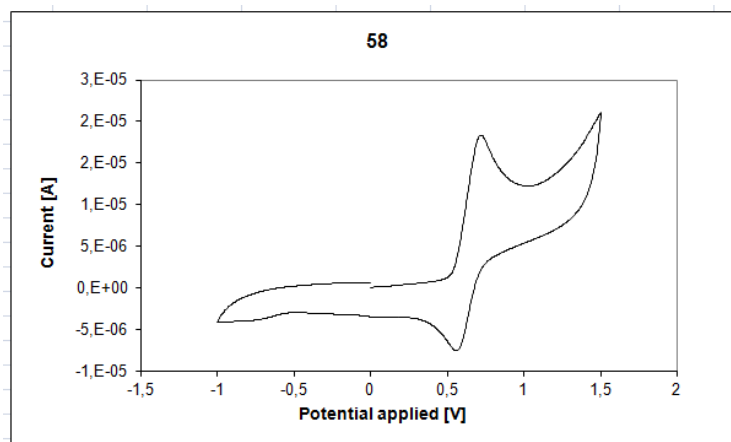


Figure 6. 25: voltammogram of 58; octamethylferrocene as external standard.
Experimental conditions: CH₂Cl₂, N₂ atmosphere, NBu₄PF₆ as supporting electrolyte.

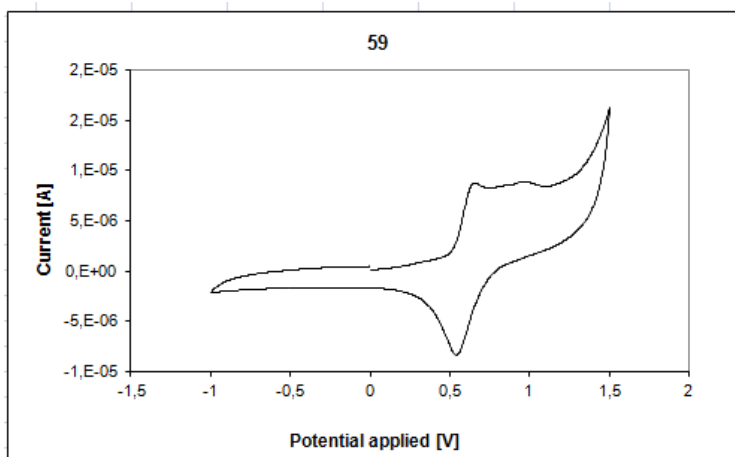


Figure 6. 26: voltammogram of **59**; octamethylferrocene as external standard. Experimental conditions: CH_2Cl_2 , N_2 atmosphere, NBu_4PF_6 as supporting electrolyte.

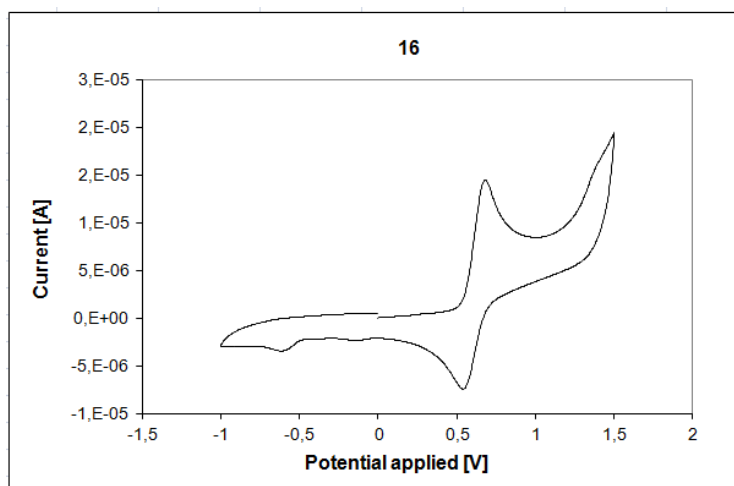


Figure 6. 27: voltammogram of **16**; octamethylferrocene as external standard. Experimental conditions: CH_2Cl_2 , N_2 atmosphere, NBu_4PF_6 as supporting electrolyte.

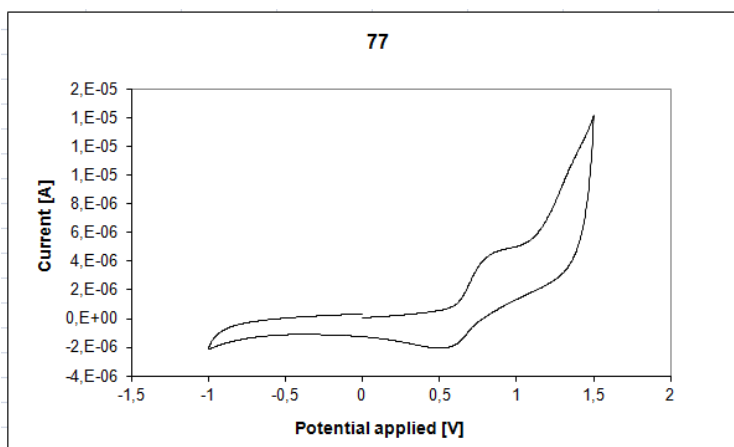


Figure 6. 28: voltammogram of 77; octamethylferrocene as external standard.
Experimental conditions: CH_2Cl_2 , N_2 atmosphere, NBu_4PF_6 as supporting electrolyte.

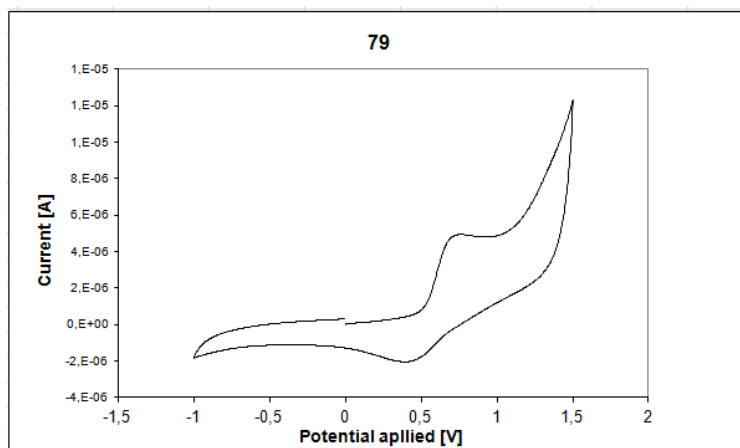


Figure 6. 29: voltammogram of 79; octamethylferrocene as external standard.
Experimental conditions: CH_2Cl_2 , N_2 atmosphere, NBu_4PF_6 as supporting electrolyte.

Conclusion

The employment of suitable substituted NHC backbone enables, for the first time, the facile synthesis of separated, stable conformers of *N*-tolyl Ru complexes (**74** and **75**). Compounds *syn* **74** and *syn* **75** are among the most efficient catalysts in the RCM of hindered olefins, requiring catalyst loadings as low as 0.05–0.5 mol%. Notably, the different performances of isolated *syn* and *anti* isomers of both **74** and **75** provide the first unequivocal proof for the significance of correctly disposed *N*-aryl groups to successfully accomplish RCM reactions. The secret of their efficiency lies in the space that the NHC-ligand leaves around the metal to accommodate encumbered olefins.

The substitution at the *ortho* *N*-aryl position with more encumbered phenyl groups bestows on complexes **76** and **78** a higher initiation rate but affects their stability. Confirming how important is stability in the overall catalyst efficiency.

The study of the ring closing metathesis of linalool **g** resulted particularly interesting since it represents a facile route to renewable high density fuel precursor.

Finally from the voltammetric studies it has emerged that not only the electronic properties of the NHC ligand influence the redox potentials but also their conformations.

Ringraziamenti

Questo lavoro è il risultato finale di un percorso formativo a cui hanno contribuito più persone.

Prima di tutto vorrei esprimere la mia gratitudine alle persone che mi hanno insegnato a fare ricerca accademica:

il professore Longo per il suo ottimismo contagioso e la costruttiva libertà concessami nello sviluppo del progetto di ricerca.

Sono grata alla dottoressa Grisi che ha contribuito enormemente alla mia formazione, dall'insegnarmi come far diventare l'esano blu fino a presentare i miei risultati in modo rigoroso. Grazie della tua infinita pazienza e dell'esempio che come chimico/donna/madre mi hai dato!

Ringrazio entrambi per non avermi sterilmente suggerito le risposte quando avevo difficoltà nell'interpretazione dei dati sperimentali. Vi ringrazio per avermi spronata a "ragionarci assieme" anche quando per voi i risultati erano chiari già da un semplice $^1\text{H-NMR}$!

Grazie ai miei controrelatori tutti per avermi offerto nuovi punti di vista e spunti di riflessione e per avermi aiutata a dare alla tesi "il tocco finale".

Sono stata molto fortunata a lavorare con colleghi simpatici ed in gamba!! Grazie di cuore a tutti per la vostra amicizia (un grazie doppio ad Annaluisa, Esther ed Antonio). Grazie Simona L. e Serena per essere state il mio IT help-desk. Grazie a tutti i membri del lab 2!

Durante questi tre anni ho goduto della presenza di molti studenti con cui ho condiviso pause pranzo, caffè e gossip innocenti! Oltre allo scambio di competenze, porto dentro di me il buono che ognuno mi ha regalato. Tra di loro un grazie speciale alla "mia Vero" che in poco più di un anno è diventata come una sorella; grazie anche alla cara Simona D. per la sua pazienza, simpatia e per la sua amicizia. Grazie Elisa, Anita, Antonio e Rosita.

Grazie a tutti i colleghi dottorandi: a voi compagni e contendenti del 400 MHz. Il laboratorio NMR è stato il crocevia in cui ci siamo scambiati competenze e supporto autentico.

Grazie agli amici dei lab. limitrofi compagni di pause caffè ed ottimi amici : Francesco, Carmen, Marco, Sheila, Antonio ed Annarita.

Grazie alla mia famiglia per l'infinito supporto emotivo e morale che non viene mai meno da una vita! In particolare grazie e ai miei fratelli che dal letto accanto o da migliaia di km di distanza sono i miei migliori amici: so che ci saremo sempre l'uno per l'altra! Grazie anche a te papà... perché il tuo amore è uno dei pilastri della mia vita.

Grazie alla mia famiglia intesa in senso ampio ed ai miei amici (con relativa prole) che l'arricchiscono! Vi voglio un gran bene! Tutti!

Infine grazie al mio futuro marito in cui trovo il mio completamento: grazie perché ogni giorno ci impegniamo a costruire un amore che libera.